

Quantitative theory of magnetic interactions in solids

Attila Szilva and Yaroslav Kvashnin

*Department of Physics and Astronomy, Division of Materials Theory,
Uppsala University, Box 516, SE-75120 Uppsala, Sweden*

Evgeny A. Stepanov

CPHT, CNRS, École polytechnique, Institut Polytechnique de Paris, 91120 Palaiseau, France

Lars Nordström

*Department of Physics and Astronomy, Division of Materials Theory, Uppsala University,
Box 516, SE-75120 Uppsala, Sweden
and Wallenberg Initiative Materials Science for Sustainability, Uppsala University,
75121 Uppsala, Sweden*

Olle Eriksson


*Division of Materials Theory, Uppsala University, Box 516, SE-75120 Uppsala, Sweden
and Wallenberg Initiative Materials Science for Sustainability, Uppsala University,
75121 Uppsala, Sweden*

Alexander I. Lichtenstein

*Institut für Theoretische Physik, Universität Hamburg,
Notkestraße 9, 22607 Hamburg, Germany*

Mikhail I. Katsnelson

*Institute for Molecules and Materials, Radboud University,
Heyendaalseweg 135, 6525 AJ Nijmegen, Netherlands*

 (published 11 September 2023)

This review addresses the method of explicit calculations of interatomic exchange interactions of magnetic materials. This involves exchange mechanisms normally referred to as a Heisenberg exchange, a Dzyaloshinskii-Moriya interaction, and an anisotropic symmetric exchange. The connection between microscopic theories of the electronic structure, such as density functional theory and dynamical mean-field theory, and interatomic exchange is examined. The different aspects of extracting information for an effective spin Hamiltonian that involves thousands of atoms, from electronic structure calculations considering significantly fewer atoms (1–50), is highlighted. Examples of exchange interactions of a large group of materials is presented, which involves heavy elements of the $3d$ period, alloys between transition metals, Heusler compounds, multilayer systems as well as overlayers and adatoms on a substrate, transition metal oxides, $4f$ elements, magnetic materials in two dimensions, and molecular magnets. Where possible, a comparison to experimental data is made that becomes focused on the magnon dispersion. The influence of relativity is reviewed in a few cases, as is the importance of dynamical correlations. Development to theories that handle out-of-equilibrium conditions is also described here. The review ends with a description of extensions of the theories behind explicit calculations of interatomic exchange to nonmagnetic situations, such as those that describe chemical (charge) order and superconductivity.

DOI: [10.1103/RevModPhys.95.035004](https://doi.org/10.1103/RevModPhys.95.035004)

CONTENTS

I. Introduction	2	II. Linear Response Theory of the Susceptibility	7
A. The early history of magnetism	3	III. Mapping Electronic Energies to an Effective Spin Hamiltonian	10
B. Magnetic materials and magnetic phenomena	4	A. Basic assumptions	10
C. Recent trends in magnetism	6	B. The mapping scheme	11
D. Early theories of interatomic exchange	6	C. Excitation of the spin model	11
E. Comment on nomenclature	6	IV. Basic Concepts of Electronic Structure Theory	12
		A. Grand canonical potential at zero temperature	13

B. Green's function formalism	13
C. Grand canonical potential at finite temperature	13
V. Derivation of the Exchange Formulas	14
A. Magnetic local force theorem	14
B. Energy variation from a noncollinear Kohn-Sham Hamiltonian	15
C. Perturbation to first order	16
D. The sum rule	16
E. Further decomposition of the Green's function and its physical interpretation	16
F. Bilinear interaction parameters due to one-site spin rotation	18
G. Bilinear interaction parameters due to two-site spin rotations	18
H. Explicit symmetric or asymmetric interactions	19
I. Interaction parameters obtained from one- and two-site variations	19
J. Local versus global spin models	20
K. Exchange interactions in correlated systems	21
VI. Beyond Kinetic Exchange	22
VII. Numerical Examples of Interatomic Exchange	24
A. Elemental transition metals	25
B. Itinerant magnets based on 3d metal alloys and compounds	30
C. Alloys with 4d and 5d elements	31
D. Results from the disordered local moment approximation	31
E. Multilayers and atoms on metallic surfaces	32
F. Influence of spin-orbit coupling	33
G. Clusters of atoms on surfaces	34
H. <i>f</i> -electron systems	35
I. Transition metal oxides	36
J. Novel 2D magnets	37
K. <i>sp</i> magnets	38
L. Molecular magnets	39
VIII. Out-of-Equilibrium Exchange	40
IX. Local Moment Formation and Spin Dynamics	42
A. Derivation of the bosonic action for the fermionic problem	43
B. Exchange interactions in many-body theory and relation to other approaches	46
C. Equation of motion for the local magnetic moment	48
D. Local magnetic moment formation	49
X. Nonmagnetic Analogs of Exchange Interaction	51
XI. Summary and Outlook	54
Acknowledgments	56
References	56

I. INTRODUCTION

Magnetic phenomena naturally have a quantum origin. This follows from the success that quantum theory has had in describing magnetism, but it can also be ascribed to the discovery of a theorem of Bohr and van Leeuwen that demonstrates that a classical treatment fails in describing any magnetic properties at thermal equilibrium, with the magnetic susceptibility identically equal to zero (Mohn, 2006). Quantum mechanics has offered an excellent tool to analyze and interpret magnetic materials and, since its birth nearly 100 years ago, the magnetism community has developed concepts as well as experimental and theoretical techniques to study magnetism. Many have covered the essentials

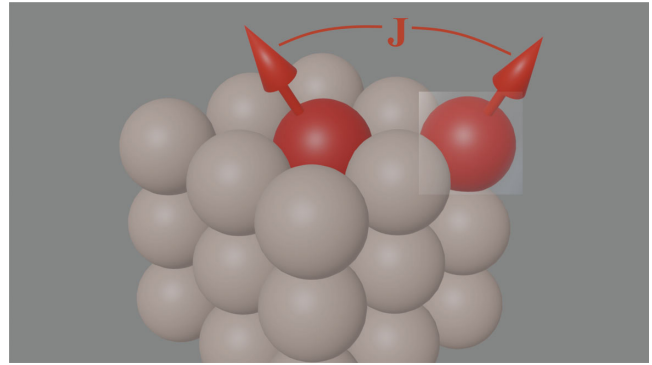


FIG. 1. Schematic illustration of the multiscale step of using information from electronic structure calculations considering the primitive unit cell (bright square) to evaluate the exchange interaction J between two atomic spin moments shown by red (dark gray) arrows. Note that atomic magnetic moments are depicted for only one pair of atoms; moments of other atoms are not shown.

of these techniques, as well as magnetic materials and magnetic phenomena (Goodenough, 1963; Vonsovskii, 1974; White and Bayne, 1983; Jensen and Mackintosh, 1991; Yosida, 1996; Fazekas, 1999; Buschow and Boer, 2003; Mohn, 2006; Stöhr and Siegmann, 2006; Getzlaff, 2008; Coey, 2010; Eriksson *et al.*, 2017; Kübler, 2017; Skomski, 2021). The purpose of this review is by no means an attempt to cover what has already been described in detail in the literature. Instead, the main ambition of this work is to describe in detail how interatomic exchange interactions can be evaluated from *ab initio* electronic structure theory in a framework based on density functional theory (DFT) (Hohenberg and Kohn, 1964; Kohn and Sham, 1965) and dynamical mean-field theory (DMFT) (Georges *et al.*, 1996; Lichtenstein and Katsnelson, 1998; Kotliar *et al.*, 2006). The pioneering work that this review focuses on was published in 1984 (Lichtenstein, Katsnelson, and Gubanov, 1984). Since then many important contributions have been made to what is now a vibrant research field; these both include fundamental questions on the nature of the interatomic exchange interaction and involve practical investigations into how to find functional materials with tailor-made properties. The latter studies involve green energy technologies, for instance, the attempt to find permanent magnets that do not contain the costly and (from a mining perspective) environmentally troublesome rare-earth metals, as well as to discover materials to be used in magneto-caloric devices (Tegus *et al.*, 2002; Gutfleisch *et al.*, 2011). As this review describes, it is possible to evaluate the interatomic exchange interaction between any pair of magnetic atoms of a solid from theoretical electronic structure calculations that consider atoms only within a primitive unit cell. This is illustrated schematically in Fig. 1, and the capability of extracting information from one scale (that of a conventional unit cell) to another scale that involves thousands or even millions of atoms is an important step in realizing approaches for an effective description of magnetism and magnetization dynamics.

This review hence describes how to calculate from electronic structure theory the interaction term \mathcal{J}_{ij} of the Heisenberg Hamiltonian,

$$\mathcal{H}_H = \sum_{\langle ij \rangle} \mathcal{J}_{ij} \vec{S}_i \cdot \vec{S}_j, \quad (1.1)$$

where the summation is made over pairs of atomic spins \vec{S}_i and where its relativistic generalization (Udvardi *et al.*, 2003) allows one to evaluate the Dzyaloshinskii-Moriya (DM) interaction (of vector form \vec{D}_{ij})¹ in

$$\mathcal{H}_{DM} = \sum_{\langle ij \rangle} \vec{D}_{ij} \cdot (\vec{S}_i \times \vec{S}_j). \quad (1.2)$$

Since this review is focused on methods to evaluate interatomic exchange interactions from electronic structure theory, a word on the nature of the electron states is relevant. In solids the electron states producing an atomic spin that is mapped to describe low-energy excitations by means of Eqs. (1.1) and (1.2) are traditionally divided into localized electron states or itinerant Bloch states. Traditionally the Heisenberg Hamiltonian was adopted primarily for the class of magnetic materials with localized electron states, but as this review outlines many investigations have also shown its success for systems where the electron states are best described as Bloch states. The key aspect for this success is described in Sec. IB, which demonstrates that magnetism (and atomic spins) can be localized in space even though the electronic structure is completely itinerant. With modern developments in the theory of electronic structure, it is in fact quite possible to describe with equal accuracy the electronic structure of localized and itinerant-electron systems, something we return to later. The key question is actually a question of not so much localized versus itinerant-electron states but rather how configuration dependent the calculated parameters of Eqs. (1.1) and (1.2) are. This is discussed in Sec. V.

The steps described in this review, which are used to derive an expression of interatomic exchange interactions, can be seen as the most robust argument (or derivation) for using the Heisenberg Hamiltonian (and its generalizations) to analyze magnetic phenomena, compared to the original argument of Heisenberg and Dirac (Dirac, 1926; Heisenberg, 1926), who considered a simple system, that of a two-electron system and the energy difference between spin-singlet and spin-triplet states (a derivation that is covered in most work in solid-state physics). In fact, the connection between electronic structure information and interatomic exchange interactions pioneered by Liechtenstein, Katsnelson, and Gubanov (1984) can be seen as the magnetic parallel to the quantum mechanical forces that are available from the Hellmann-Feynman theorem. The similarity also extends to their use; the interatomic exchange interactions can be used for torque minimization to find a ground-state magnetic configuration similar to the force minimization to obtain the geometrical minimum of the nuclear position. In addition, the use of a magnetic torque for studies of dynamics of magnets [in so-called spin-dynamics simulations (Antropov *et al.*, 1995)] is completely analogous to the use of forces for molecular dynamics simulations. Note that coupled spin-lattice dynamics simulations (Antropov *et al.*, 1995) involving both interatomic

forces and exchange have also been described and used in practical simulations (Hellsvik *et al.*, 2019).

This review outlines explicit calculations of exchange parameters, where the term *explicit* implies that the parameters are obtained explicitly and directly once the solution to an electronic structure calculation is obtained (Liechtenstein, Katsnelson, and Gubanov, 1984, 1985; Liechtenstein *et al.*, 1987). This can be compared to implicit approaches, where a Hamiltonian of the form used in Eqs. (1.1) and (1.2) is used to fit total energies obtained from electronic structure calculations for a large number of magnetic configurations. A third method that is frequently employed is to calculate in a DFT framework the total energies of spin-spiral configurations for several wavelengths of the spin spiral. In this way one can obtain information of a reciprocal space representation of the exchange, and after a Fourier transform the real-space interatomic exchange parameters are obtained (Kübler *et al.*, 1988; Mryasov *et al.*, 1991; Sandratskii, 1991, 1998; Halilov *et al.*, 1998; Sandratskii and Bruno, 2002; Jakobsson *et al.*, 2015).

The implicit, cluster expansion approach and the spin-spiral approach have both been used with success, but they are beyond the scope of this review. We do, however, note a few key references that have outlined the cluster expansion approach (Drautz and Fähnle, 2004; Singer, Dietermann, and Fähnle, 2011), and various treatises that have covered the spin-spiral approach (Kübler *et al.*, 1988; Sandratskii, 1998; Jakobsson *et al.*, 2015). The focus of this review is, as mentioned, on the explicit method of extracting intra-atomic exchange directly from a single electronic structure calculation, and details on how this is done both formally and practically are presented. We note that the method introduced by Liechtenstein, Katsnelson, and Gubanov (1984) has its strengths, in that it is a universal way to calculate exchange parameters of Eqs. (1.1) and (1.2), in the sense that systems with or without translation symmetry can be considered and that alloys and compounds can be treated on an equal footing. It also offers an orbital decomposition of the interactions that opens up for symmetry analysis from contributions between different irreducible representations of the electron states. It is also an excellent way to investigate general trends of the exchange interaction.

Note that approaches similar to the one reviewed here for the calculations of interatomic exchange have been derived and used with success in other fields of solid-state science. Examples involve, for instance, the chemical interaction between atomic species in alloys, in a method referred to as generalized perturbation theory, first presented by Ducastelle and Gautier (1976) [for a review see Ruban *et al.* (2004)], that is designed to calculate chemical interactions in alloys. We will discuss this method in Sec. X.

A. The early history of magnetism

Before continuing these introductory remarks, we provide a short expose of the early historical discoveries of magnetic phenomena. In ancient times it was known that a type of stone found in northern Greece, close to a place called Magnesia, could attract iron. Thales of Milet (a Greek philosopher living in the seventh century BCE) is documented to be aware of the mysterious and invisible force these stones could have on iron

¹See Eqs. (3.14) and (3.15) for a more precise generalization.

(Verschuur, 1996; Mohn, 2006). Other philosophers of the past that were attracted to the mysterious properties of these magnetic minerals (later named lodestone, where the magnetism stems from Fe_3O_4) involve Plinus the Elder and Lucretius, both of whom were active in the first century CE (Verschuur, 1996). The name of this first discovered magnetic mineral comes from the Lodestar (the pole star), which leads to (or marks) the northerly direction (Verschuur, 1996). The first documented magnetic device used for establishing direction, the compass, was found in a Chinese manuscript dating from the 11th century (Mohn, 2006), and it is indeed curious that this technology is used widely even today, 1000 years later. Apart from their use in navigation, these first compasses were used for construction of buildings and their alignment, in the belief that they would be in harmony with the forces of nature (Verschuur, 1996).

Other historical breakthroughs in the science of magnetism and magnetic materials involved Peter Peregrinus (13th century), who undertook several experiments with lodestone and discovered that a magnet has poles. He in fact used the term *polus* to describe the north and south ends of a magnet (Verschuur, 1996). Curiously, he is known for the quote, “experience rather than argument is the basis of certainty in science,” a principle most natural science lives by today that he realized over half a millennium ago. Some 300 years after the investigations of Peregrinus, the first treatise of magnetism was published by William Gilbert (Verschuur, 1996). In his book, with a title translated in English as “On the Lodestone and Magnetic Bodies and on the Great Magnet the Earth; a New Physiology, Demonstrated by Many Arguments and Experiments,” he presented, among many things, his greatest realization, namely, that magnetism could be found to disappear when the material was heated and that Earth itself is magnetic (Verschuur, 1996).

The final major historical leap in the science of magnetism, before the development of quantum mechanics, was the discovery of electromagnetism, one of the greatest discoveries of the 19th century. This is covered in almost all of the physics literature and thus is not further discussed here. We note, however, that, from a practical point of view, several discoveries made in the 19th century concerning magnetic materials now form a firm basis for technologies used to propel our society. As a concrete example, Faraday’s induction law, which allows the conversion of mechanical energy to electricity, is used in all power plants. In addition, the development of electrical motors, which increasingly becomes a standard technology for motorized vehicles, has performance based on the magnetic field strength (Tegus *et al.*, 2002; Gutfleisch *et al.*, 2011). A final example is that of magnetic refrigeration and the principle of adiabatic demagnetization, which is considerably less energy demanding than a compressor-based technology of cooling (Tegus *et al.*, 2002; Gutfleisch *et al.*, 2011). Hence, many technologies that rely on magnetic materials are used in our society, as they are key components to the economy and to the well-being of household and private use. The functionality of these technologies is based on the performance of the magnetic materials that they are constructed around. Hence, in a general aim of a more electrified society, and with an ambition of finding greener technologies to generate electricity, for instance, in farms of wind power

mills, the search for magnetic materials with tailored properties has become an active field of science (Tegus *et al.*, 2002; Gutfleisch *et al.*, 2011).

We end this section with a comment on the coupling of magnetism and biology. The coupling of magnetism and living matter have been discussed over the many centuries that magnetic phenomena have been known. For instance, Bartholomew the Englishman (13th century) advocated for its medicinal powers (Verschuur, 1996), and the ideas of Franz Anton Mesmer (late 18th and early 19th centuries) around “animal magnetism” have escaped few. Although the ideas of Mesmer are now regarded as nonsense, the influence of magnetic fields on biological matter is well established, for instance, as demonstrated by levitating animals or fruit when they are subjected to strong magnetic fields.² It has also been established that birds use nanoparticles of magnetite (Fe_3O_4) to navigate Earth’s magnetic field (Wiltchko *et al.*, 2006). In addition, it is well known that magnetic materials, again in the form of magnetite, can be produced by bacteria such as magnetotactic bacteria, and the bacterium GS-15 is known to produce magnetite (Snowball, Zillén, and Sandgren, 2002). It has even been speculated that this is one reason for large amounts of fine-grained magnetite found in ancient sediments. Single-domain magnetite produced in this way could then reveal the magnetic recording of the ancient geomagnetic field.

B. Magnetic materials and magnetic phenomena

Most elements have for the free atom a pairing of electron spins due to an intra-atomic exchange interaction among the electrons. This leads to atomic moments, similar to what is schematically illustrated in Fig. 1, for almost all elements in the periodic table, provided that they are isolated atoms. In solid-state materials things are more complicated since the spin-pairing energy competes with the kinetic energy, which is lowest for equal population of spin-up and spin-down electrons. Combined with the fact that band formation of electron states can make the kinetic energy rather significant, one ends up with a competition between two mechanisms, one favoring an equal population of spin states and another favoring spin pairing and local (or atom-centered) moments. Stoner theory quantifies this competition and allows one to identify a simple rule for when magnetic order is expected; see Mohn (2006). Among most elemental solids, it is in fact the kinetic energy and band formation that dominate, such that an equal amount of spin-up and spin-down electron states are populated, making these materials either Pauli paramagnetic or diamagnetic. Spontaneous magnetic order occurs for only a limited number of elements in the periodic table, and at (or just below) room temperature only four are found to have spontaneous ferromagnetic (FM) order (bcc Fe, hcp Co, fcc Ni, and hcp Gd). However, there are thousands of compounds and alloys that show significant magnetic moments, and there are plenty of materials to investigate with respect to the many interesting magnetic phenomena that have been reported.

²As can be seen at <https://www.youtube.com/watch?v=A1vyB-O5i6E>.

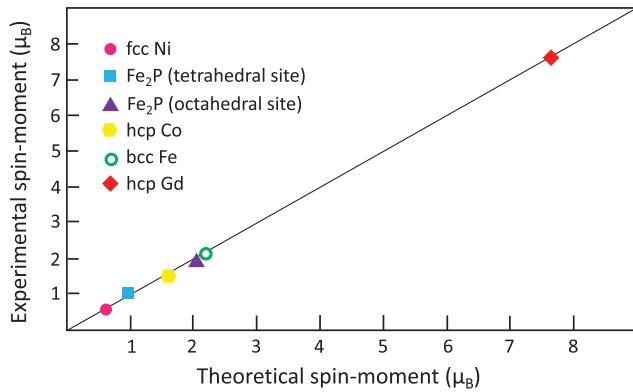


FIG. 2. Comparison between measured magnetic spin moments and results obtained from theoretical calculations based on DFT. Data are given in μ_B per atom. Data from Eriksson *et al.* (2017).

One of the more efficient ways to evaluate the delicate balance between band formation and spin pairing relies on DFT and the invention of efficient methods for solving the electronic structure of solids such that measured magnetic moments can be reproduced with good accuracy. These calculations are often referred to as *ab initio* ones, indicating that they are carried out without experimental input. Results from *ab initio* theory are shown in Fig. 2, where a comparison is made to experimental results for the four previously mentioned ferromagnetic elements, as well as for the ferromagnetic, hexagonal compound Fe_2P . This compound has Fe atoms occupying two distinct crystallographic sites, a tetrahedral and an octahedral site, and neutron scattering measurements have revealed that the magnetic moments of these sites are significantly different. As Fig. 2 shows, *ab initio* theory reproduces the measured magnetic moments with good accuracy. The moments for Fe_2P are particularly interesting since they reveal a delicate balance between band formation and interatomic exchange energy, resulting in entirely different moments for Fe atoms situated on different crystallographic sites. The results shown in Fig. 2 actually reveal a rather typical accuracy of theory based on DFT, at least when it comes to reproducing magnetic moments. Based on 2935 calculations, Huebsch *et al.* (2021) showed the predictive power of spin-polarized density functional theory (combined with cluster-multipole expansion) by reproducing the experimental magnetic configurations with an accuracy of $\pm 0.5\mu_B$.

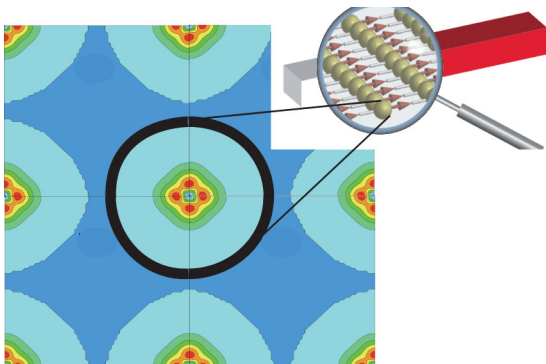


FIG. 3. Magnetization density of bcc Fe from theoretical calculations based on DFT. Adapted from Eriksson *et al.*, 2017.

Notable difficulties of DFT-based theory are, however, found for correlated electron systems, where multiconfiguration effects become important, something that we also discuss in this review.

Ab initio theory provides another important piece of information: that provided by the magnetization density. This is illustrated in Fig. 3 for bcc Fe for a plane inside the crystal, spanned by vectors parallel to the axis of the conventional unit cell of the bcc structure. Note that red (dark gray) coloration indicates high magnetization density, while blue (light gray) indicates low values for this density. As the figure shows, the magnetization density is high only in a small region that is located close to the atomic nuclei of the Fe atoms. This is a typical result and allows one, for almost all materials, to describe the magnetic state as being composed of atom-centered (or atomic) moments, as illustrated in the upper right of the figure. The results shown in Fig. 3 justify a discussion based on atomic moments and the different types of phenomena such moments display. These results also shine a light on the dynamics of magnetism, and the distinction made between fast (electrons) and slow (site-dependent magnetization directions) variables, illustrating the concept of “temporarily broken ergodicity,” which was analyzed in detail by Staunton *et al.* (1984, 1985) and Gyorffy *et al.* (1985). This is the basic principle for performing atomistic spin-dynamics simulations, as outlined by Eriksson *et al.* (2017), where the slow variables evolve under the influence of a local Weiss field.

The inset of Fig. 3 illustrates a specific arrangement of atomic moments and, as the figure shows, bcc Fe is a ferromagnet; all atomic moments point in the same direction. However, for other materials many different orderings of atomic moments have been reported, including antiferromagnetism, where every other magnetic moment shown in the inset of Fig. 3 would have its direction reversed. A majority of the materials that have finite atomic moments have one of these two types of collinear magnetic order. However, more complex magnetic orders exist in nature, where atomic moments form a noncollinear arrangement; see Kübler (2017). Among the elements, such order is found predominantly among the lanthanides (Jensen and Mackintosh, 1991). As highlighted by the Nobel Prize in Physics 2021, glasslike phenomena are also found for specific groups of magnetic materials in which one singular magnetic ground state is never realized. Instead, the magnetism can be understood to reflect a multivalley landscape, where many different configurations of the atomic moments result in similar energies (Snowball, Zillén, and Sandgren, 2002). Thermal fluctuations can make the system drift from one configuration to the next, and aging phenomena are a fingerprint of spin glasses. Dilute alloys [such as Mn impurities in a Cu matrix (Cannella and Mydosh, 1972)] and, more recently, elemental Nd (Kamber *et al.*, 2020; Verlhac *et al.*, 2022) are known spin glass systems.

Each class of magnetic materials has its own characteristic in terms of ground-state properties as well as fingerprints revealing its excited state. This involves quasiparticle properties of the collective excitations, referred to as magnons [see Mohn (2006)], the temperature dependence of the magnetic state, the value of the ordering temperature, and the critical exponents used to characterize second-order phase transitions when the magnetic state vanishes with temperature. Many (if not all) of

these phenomena are typically analyzed using Eqs. (1.1) [and (1.2)], and different forms of Heisenberg exchange interactions have been discussed to be responsible for the widespread list of magnetic properties found in nature. As reviewed here, this involves direct exchanges, super and double exchanges, Rudderman-Kittel-Kasuya-Yosida (RKKY) interactions, and interlayer exchanges. In these investigations the dimensionality of the magnetic material is a natural component of the analysis, and the celebrated Mermin-Wagner theorem describes the connection between dimensionality and finite temperature effects of spontaneously broken symmetries of magnets; see Mermin and Wagner (1966), Chakravarty, Halperin, and Nelson (1989), Irkhin, Katanin, and Katsnelson (1999), and Ruelle (1999).

C. Recent trends in magnetism

Recent trends in magnetism have often focused on systems in the nanoscale. This relates, for instance, to magnetic multilayers and trilayers, where perhaps the most celebrated finding is the giant magnetoresistance effect and its applications for sensors (Baibich *et al.*, 1988; Binasch *et al.*, 1989). Most applications in magnetic information storage currently rely on sensors based on the tunneling magnetoresistance effect (Bowen *et al.*, 2001), where the use of MgO as an optimal tunneling layer was predicted (Butler, 1985) by *ab initio* theory before experimental verification. These investigations have focused on systems that are confined to one dimension, and thin-film physics has been reviewed in many works on magnetism (Stöhr and Siegmann, 2006; Kübler, 2017). Such studies of quasi-two-dimensional systems have now been expanded to focus on topological magnetic states (such as skyrmions, merons, and hopfions) (Belavin and Polyakov, 1975) as well as investigations of purely 2D materials. The latter class is particularly interesting given its strong influence on geometrical dimensionality and magnetism, as stated by the Mermin-Wagner theorem. However, Cr trihalides have been synthesized and their magnetic properties are by now well known (Huang *et al.*, 2017). Other aspects of magnetism that are currently under investigation are coupled to questions about ultrafast dynamics, pioneered by Beaurepaire *et al.* (1996), as well as magnonics (Kruglyak, Demokritov, and Grundler, 2010) and spintronics (Wolf *et al.*, 2001). As a final remark in this section, we note the recent interest in spin-ice (Bramwell and Gingras, 2001) and spin-liquid states (Norman, 2016), as well as the so-called Kitaev systems (Kitaev, 2006).

D. Early theories of interatomic exchange

This review has as its starting point the work of Liechtenstein, Katsnelson, and Gubanov (1984), but it is clear that the work by Liechtenstein, Katsnelson, and Gubanov (1984) overlapped with earlier works that also attempted to find a formalism that allows one to extract interatomic exchange from information given by *ab initio* electronic structure theory. We specifically mention the early work of Oguchi, Terakura, and Hamada (1983) and Oguchi, Terakura, and Williams (1983), who presented a similar but not identical method. In this work an approach was used in

which the magnetic moments were rotated by 180° in order to extract the exchange interaction strength, instead of the use of infinitesimally small rotations, which is the essence of the work in Liechtenstein, Katsnelson, and Gubanov (1984). The results of Oguchi, Terakura, and Hamada (1983) and Oguchi, Terakura, and Williams (1983) were in fact similar to earlier work by Inoue and Moriya (1967) and Lacour-Gayet and Cyrot (1974). We also mention here the early work of Gyorffy and Stocks (1980) and Liu (1961), which inspired the work of Liechtenstein, Katsnelson, and Gubanov (1984) and an early work of Wang, Prange, and Korenman (1982), who studied fluctuating local band theory of itinerant-electron ferromagnetism in nickel and iron.

Note also that exchange interactions in solids have a bearing on many phenomena and theories of magnetism that, due to space limitations, cannot be fully covered here. For instance, spin-fluctuation theories have been used with great success to analyze excited-state properties of magnetic solids, including the temperature dependence of magnetism, susceptibility, and specific heat; see Mohn (2006). These theories are typically connected to Landau or Ginzburg-Landau theories, which are not the topic of this review, since they have already been covered thoroughly in the literature (White and Bayne, 1983; Mohn, 2006; Stöhr and Siegmann, 2006; Kübler, 2017).

E. Comment on nomenclature

Before discussing the main results of this review, we comment on the form of the Hamiltonian used in this text. In the derivations and the examples given, we use the following expressions:

$$\mathcal{H}_H = \sum_{\langle ij \rangle} J_{ij} \vec{e}_i \cdot \vec{e}_j \quad (1.3)$$

and

$$\mathcal{H}_{DM} = \sum_{\langle ij \rangle} \vec{D}_{ij} \cdot (\vec{e}_i \times \vec{e}_j), \quad (1.4)$$

where \vec{e}_i is a unit vector describing the direction of the magnetic moment of the atom at site i . In this review we refer to the interaction parameters in Eq. (1.3) either as interatomic exchange or as Heisenberg exchange (J_{ij}) and the DM interaction (\vec{D}_{ij}), or simply as the J_{ij} 's or \vec{D}_{ij} 's. Note also that the definition of the interatomic energy used in this work is with a plus sign in front of the summations in Eq. (1.3), where the summation is made over pairs of atoms $\langle ij \rangle$. One sometimes uses a slightly different notation in which the summation is made such that $i \neq j$, but the indices i and j run over all atoms considered in a calculation. In this case a factor 1/2 appears in front of the summations in Eq. (1.3) to ensure that each pair interaction is calculated only once. Some choose to use a minus sign in front of Eq. (1.3). We also note that in the derivation of the interatomic exchange formula a sum where the local interaction $i = j$ is also considered will be temporally needed, as shown in Eq. (5.53). In Sec. VII, where results of exchange parameters are given, the numerical values (in the main text and also in the figures) are consistent with the nomenclature given by Eq. (1.3).

A comparison between Eqs. (1.1) and (1.3) gives the result that $J_{ij} = \mathcal{J}_{ij} S_i S_j$, where S_i and S_j stand for the lengths of the vectors \vec{S}_i and \vec{S}_j . Similarly, we obtain that $\vec{D}_{ij} = \vec{\mathcal{D}}_{ij} S_i S_j$. This distinction is important when one compares interactions obtained from different theoretical methods and experiments. The different forms of Eqs. (1.1) and (1.3) [and between Eqs. (1.2) and (1.4)] also allows an important distinction between quantum and classical spin Hamiltonians. We adopt here the nomenclature that Eqs. (1.3) and (1.4) allow for infinitesimal rotations of the direction of an atomic moment, and hence \vec{e}_i can be treated as a classical vector. This differs from approaches when \vec{S}_i [as in Eqs. (1.1) and (1.2)] is considered as a quantum mechanical operator. The latter is preferable from a formal point of view, but it is in many cases impractical. In fact, all material specific examples given in this review make use of Eqs. (1.3) and (1.4). Here we describe magnetic fields that are expressed in energy units. In other words, we consider a magnetic field as $\vec{B} = (1/2)g\mu_B\vec{\tilde{B}}$, where \tilde{B} is measured in tesla, μ_B is the Bohr magneton, and g equals approximately -2 for electrons. Note also that we use bold symbols here for vectors in real and reciprocal space, while symbols with an arrow denote vectors in spin space. Finally, note that the dot symbol when components of a vector or a tensor are contracted (summed over), for instance, $\vec{A} \cdot \vec{B} = \sum_{\mu} A^{\mu} B^{\mu}$ or $\vec{D} \cdot \mathbb{C} \cdot \vec{E} = \sum_{\mu\nu} D^{\mu} C^{\mu\nu} E^{\nu}$, the cross symbol is used for a cross product (or vector product), and the star symbol is used when an equation continues on a new line.

II. LINEAR RESPONSE THEORY OF THE SUSCEPTIBILITY

In this review we present a description of magnetic interactions of many-electron systems via the separation of specific spin degrees of freedom (roughly, directions of localized magnetic moments) from a complete quantum description of all properties of the system starting with the Schrödinger equation. This cannot be done without approximations, due to a presence of strong interelectron interactions. Nevertheless, it makes sense to start with a formally rigorous scheme and then introduce these approximations step by step, something that we do here.

For equilibrium properties, there are two main practical schemes: density functional theory (DFT) based on the Hohenberg-Kohn theorem (Hohenberg and Kohn, 1964) with the associated Kohn-Sham quasiparticles (Kohn and Sham, 1965) and a Green's function formalism based on the Luttinger-Ward generating functional (Luttinger and Ward, 1960; Hedin, 1965a). Spin dynamics deal with out-of-equilibrium properties, and both of these main techniques can be generalized for this case. For the Green's function functional, this was done in the most general form by Baym and Kadanoff (1961) but in reality this method does not have any applications to the properties of real materials, since it is computationally too demanding. Only in model systems has there been any real progress (Aoki *et al.*, 2014). Since we are focused on the applications to real materials connecting

calculated results to experimental observations, we do not consider time-dependent Green's function functionals here.

On the other hand, the time-dependent generalization of density functional theory has been realized. It is based on the Runge-Gross theorem (Runge and Gross, 1984) and its generalization to spin-polarized calculations (Liu and Vosko, 1989). There are numerous examples of time-dependent density functional theory (TDDFT) having been applied to specific magnetic materials (Cooke, Blackman, and Morgan, 1985; Savrasov, 1998; Sharma *et al.*, 2007; Buczek, Ernst, and Sandratskii, 2011; Gorni, Timrov, and Baroni, 2018; Singh *et al.*, 2019). In principle, if one knows the exact time-dependent density functional and, in particular, the so-called exchange-correlation kernel (Runge and Gross, 1984), one can calculate the dynamical magnetic susceptibility and find the spin-wave spectrum as the poles of the dynamical susceptibility. A fitting of exchange parameters could even be done to the calculated spectrum. This method would be formally exact, but not practical, at least at this stage, since the successes in building of reliable expressions for the exchange-correlation kernel are still highly restrictive [note, however, that the first attempts have been made (Thiele, Gross, and Kümmel, 2008; Castro, Werschnik, and Gross, 2012)]. To proceed with practical calculations, we introduce an approximation, that is, the so-called adiabatic approximation (ADA) within TDDFT. According to this approximation, the exchange-correlation kernel is equal to its equilibrium form. This is a significant simplification. Indeed, whereas the full exchange-correlation kernel depends on two times, in the adiabatic approximation it depends on only one time, via the time dependence of the charge and spin densities only. After this approximation is made, one can proceed to the final expression for the exchange parameters (Katsnelson and Lichtenstein, 2004). We follow this derivation here, which generalizes earlier theories (Callaway, Wang, and Laurent, 1981).

We proceed with the master equation of density functional theory, the Kohn-Sham equation, which has the form of a single-particle Schrödinger equation. Within the self-consistent ADA-TDDFT approximation, it has the form

$$i \frac{\partial \psi}{\partial t} = H \psi, \\ H = -\nabla^2 + V(\mathbf{r}) - [\vec{B}_{\text{xc}}(\mathbf{r}) + \vec{B}_{\text{ext}}(\mathbf{r})] \cdot \vec{\sigma}, \quad (2.1)$$

where $V(\mathbf{r})$ is the effective potential, $\vec{B}_{\text{ext}}(\mathbf{r})$ and $\vec{B}_{\text{xc}}(\mathbf{r})$ are the external magnetic field and the exchange-correlation field, respectively, that couple to the electrons spin, and $\vec{\sigma}$ stands for the Pauli spin matrices $\{\sigma_x, \sigma_y, \sigma_z\}$. Note that we adopt the original formulation of density functional theory, which was composed at $T = 0$. The work of Mermin (1965) and subsequent other work (Eschrig, 2010; Pittalis *et al.*, 2011), showed that the power of density functional theory also extends to finite temperature. However, for the purposes of this review, it is sufficient to adopt the original formulation of density functional theory. Note also that Rydberg units are used here: $\hbar = 2m = e^2/2 = 1$.

Next we employ the adiabatic approximation while assuming that the functional dependencies of the exchange-correlation potential, and hence the field of the charge and

spin density, are the same as in the stationary case. In the local-spin-density approximation (LSDA) the effective potential depends on the values of charge and spin densities at the same spatial and temporal point only,

$$V(\mathbf{r}) = V_{\text{ext}}(\mathbf{r}) + \int d\mathbf{r}' \frac{n(\mathbf{r}')}{|\mathbf{r} - \mathbf{r}'|} + \frac{\partial}{\partial n} [n\epsilon_{\text{xc}}],$$

$$\vec{B}_{\text{xc}}(\mathbf{r}) = -\frac{\vec{m}}{m} \frac{\partial}{\partial m} [n\epsilon_{\text{xc}}], \quad (2.2)$$

where $n(\mathbf{r})$ and $\vec{m}(\mathbf{r})$ are the charge and spin density, $m(\mathbf{r})$ is the magnitude of $\vec{m}(\mathbf{r})$, ϵ_{xc} is the exchange-correlation energy density, and $V_{\text{ext}}(\mathbf{r})$ is the external potential, that is, the electrostatic potential of the nuclei. Note that the spin-orbit interaction is considered later in the review. We also note that in the previous expressions we have, in some places, omitted for simplicity the spatial argument \mathbf{r} that is present in all variables in Eq. (2.2). In some of the following equations, we also adopt this simplifying notation.

The spin susceptibility that we are interested in is the linear-response function; therefore, we consider the limit $\vec{B}_{\text{ext}}(\mathbf{r}) \rightarrow 0$. The effective complete “nonequilibrium” field contains both an external field and an additional exchange-correlation field due to redistribution of the spin density. The variation in this field can be expressed as

$$\delta B_{\text{tot}}^{\alpha} = \delta B_{\text{ext}}^{\alpha} + \frac{\delta B_{\text{xc}}^{\alpha}}{\delta m^{\beta}} \delta m^{\beta}, \quad (2.3)$$

where $\alpha\beta$ are Cartesian indices and a sum over repeated indices is assumed.

The exact, nonlocal, frequency-dependent spin susceptibility $\hat{\chi}^{\alpha\beta}$ is the kernel of the operator that connects the variation of the spin density and the external magnetic field,

$$\delta m^{\alpha} = \hat{\chi}^{\alpha\beta} \delta B_{\text{ext}}^{\beta}. \quad (2.4)$$

We use here the standard definition of the operator product,

$$(\hat{\chi}\varphi)(\mathbf{r}) = \int d\mathbf{r}' \chi(\mathbf{r}, \mathbf{r}') \varphi(\mathbf{r}'). \quad (2.5)$$

A parallel consideration for the calculation of the spin susceptibility follows from the Runge-Gross theorem (Runge and Gross, 1984) and its generalization to the spin-polarized case (Liu and Vosko, 1989), where in the time-dependent density functional theory one has the exact relation

$$\delta m^{\alpha} = \hat{\chi}_0^{\alpha\beta} \delta B_{\text{tot}}^{\beta}, \quad (2.6)$$

where $\hat{\chi}_0^{\alpha\beta}$ is the susceptibility of an auxiliary system of one-electron Kohn-Sham particles. Comparing Eqs. (2.3), (2.4), and (2.6), we arrive at the result in which

$$\hat{\chi}^{\alpha\beta} = \hat{\chi}_0^{\alpha\beta} + \hat{\chi}_0^{\alpha\gamma} \frac{\delta B_{\text{xc}}^{\gamma}}{\delta m^{\delta}} \hat{\chi}^{\delta\beta}, \quad (2.7)$$

which is a particular case of the Bethe-Salpeter equation (Salpeter and Bethe, 1951), with $\delta B_{\text{xc}}^{\gamma}/\delta m^{\delta}$ playing the role of the vertex Γ . Note that this equation turns out to be formally exact within ADA TDDFT. Actually, even if one does not assume the local-spin-density approximation, Eq. (2.7) is still exact, but the vertex Γ is then not local in spatial coordinates.

The adiabatic approximation, however, assumes its locality in time.

The local-spin-density approximation (2.2) leads to further simplifications. Indeed, one then obtains

$$\frac{\delta B_{\text{xc}}^{\gamma}}{\delta m^{\delta}} = \frac{B_{\text{xc}}}{m} \left(\delta_{\gamma\delta} - \frac{m^{\gamma} m^{\delta}}{m^2} \right) + \frac{m^{\gamma} m^{\delta}}{m^2} \frac{\partial B_{\text{xc}}}{\partial m}, \quad (2.8)$$

where the first term is purely transverse and the second one is purely longitudinal with respect to the local magnetization density (or the local magnetic moment) and B_{xc} is the length of \vec{B}_{xc} .

As a next simplification, we restrict ourselves to the case of collinear magnetic ground states with moments along the z direction. Thus, the coupling between the longitudinal and transverse components of the magnetic susceptibility vanishes. For the transverse spin susceptibility, which is commonly denoted by χ^{+-} and depends on the frequency ω , we have the following simple expression:

$$\chi^{+-}(\mathbf{r}, \mathbf{r}', \omega) = \chi_0^{+-}(\mathbf{r}, \mathbf{r}', \omega) + \int d\mathbf{r}'' \chi_0^{+-}(\mathbf{r}, \mathbf{r}'', \omega) I_{\text{xc}}(\mathbf{r}'') \chi^{+-}(\mathbf{r}'', \mathbf{r}', \omega), \quad (2.9)$$

where

$$I_{\text{xc}} = \frac{2B_{\text{xc}}}{m} \quad (2.10)$$

is an exchange correlation Stoner (or Hund) interaction. This is the standard random phase approximation (RPA) equation for the transverse susceptibility written for the spatially inhomogeneous case. This follows directly from the adiabatic local spin-density approximations of TDDFT without any further assumptions. The magnetic and charge electron densities, as well as the bare magnetic susceptibility, are related to the Kohn-Sham states in the usual way,

$$m = \sum_{\mu\sigma} \sigma f_{\mu\sigma} |\psi_{\mu\sigma}(\mathbf{r})|^2, \quad (2.11)$$

$$n = \sum_{\mu\sigma} f_{\mu\sigma} |\psi_{\mu\sigma}(\mathbf{r})|^2, \quad (2.12)$$

and

$$\chi_0^{+-}(\mathbf{r}, \mathbf{r}', \omega) = \sum_{\mu\nu} \frac{f_{\mu\uparrow} - f_{\nu\downarrow}}{\omega - \epsilon_{\mu\uparrow} + \epsilon_{\nu\downarrow}} \psi_{\mu\uparrow}^*(\mathbf{r}) \psi_{\nu\downarrow}(\mathbf{r}) \psi_{\nu\downarrow}^*(\mathbf{r}') \psi_{\mu\uparrow}(\mathbf{r}'). \quad (2.13)$$

In Eqs. (2.11),(2.12),(2.13), $\psi_{\mu\sigma}$ and $\epsilon_{\mu\sigma}$ are eigenstates and eigenenergies for the following time-independent Kohn-Sham equation:

$$(H_0 - \sigma B_{\text{xc}}) \psi_{\mu\sigma} = \epsilon_{\mu\sigma} \psi_{\mu\sigma},$$

$$H_0 = -\nabla^2 + V(\mathbf{r}). \quad (2.14)$$

In Eq. (2.14) σ (without a vector symbol) stands for the spin index $\pm 1 = \uparrow\downarrow$, $f_{\mu\sigma} = f(\epsilon_{\mu\sigma})$ is the Fermi distribution function, and μ labels the Kohn-Sham states.

The same approach leads to expressions for the longitudinal spin susceptibility, which turns out to be coupled to the charge density. Since these expressions are not necessary for the derivation of the values of the exchange parameters, we do not show them here but instead refer the interested reader to [Katsnelson and Lichtenstein \(2004\)](#).

Further transformations are needed to make the expressions for the spin-wave spectrum more explicit. When substituting Eq. (2.10) into Eq. (2.9), we have the product of the exchange-correlation field and wave functions. According to Eq. (2.14), this can be transformed as

$$2B_{xc}\psi_{\mu\uparrow}\psi_{\nu\downarrow}^* = (\varepsilon_{\nu\downarrow} - \varepsilon_{\mu\uparrow})\psi_{\nu\downarrow}^*\psi_{\mu\uparrow} + \nabla(\psi_{\mu\uparrow}\nabla\psi_{\nu\downarrow}^* - \psi_{\nu\downarrow}^*\nabla\psi_{\mu\uparrow}). \quad (2.15)$$

Substituting Eq. (2.15) into Eq. (2.13), one has

$$2(\chi_0^{+-}B_{xc})(\mathbf{r}, \mathbf{r}', \omega) = m(\mathbf{r})\delta(\mathbf{r} - \mathbf{r}') - \omega\chi_0^{+-}(\mathbf{r}, \mathbf{r}', \omega), \quad (2.16)$$

where we have used the completeness condition

$$\sum_{\mu} \psi_{\mu\sigma}^*(\mathbf{r})\psi_{\mu\sigma}(\mathbf{r}') = \delta(\mathbf{r} - \mathbf{r}'). \quad (2.17)$$

Substituting Eq. (2.16) into Eq. (2.9), we can transform the latter expression to the following form:

$$\begin{aligned} \hat{\chi}^{+-} &= \hat{\chi}_0^{+-} + \hat{\chi}_0^{+-} \frac{2B_{xc}}{m} \hat{\chi}^{+-} \\ &= \hat{\chi}_0^{+-} + \hat{\chi}^{+-} - \omega\hat{\chi}_0^{+-} \frac{1}{m} \hat{\chi}^{+-} + \frac{\hat{\Lambda}}{m} \hat{\chi}^{+-} \end{aligned} \quad (2.18)$$

or, equivalently,

$$\hat{\chi}^{+-} = m[\omega - (\hat{\chi}_0^{+-})^{-1}\hat{\Lambda}]^{-1}, \quad (2.19)$$

where

$$\begin{aligned} \Lambda(\mathbf{r}, \mathbf{r}', \omega) &= \sum_{\mu\nu} \frac{f_{\mu\uparrow} - f_{\nu\downarrow}}{\omega - \varepsilon_{\mu\uparrow} + \varepsilon_{\nu\downarrow}} \psi_{\mu\uparrow}^*(\mathbf{r})\psi_{\nu\downarrow}(\mathbf{r}) \\ &\quad \star \nabla[\psi_{\mu\uparrow}(\mathbf{r}')\nabla\psi_{\nu\downarrow}^*(\mathbf{r}') - \psi_{\nu\downarrow}^*(\mathbf{r}')\nabla\psi_{\mu\uparrow}(\mathbf{r}')]. \end{aligned} \quad (2.20)$$

Using Eqs. (2.13) and (2.19), we come to the final expression

$$\hat{\chi}^{+-} = (m + \hat{\Lambda})(\omega - I_{xc}\hat{\Lambda})^{-1}. \quad (2.21)$$

We emphasize that the transformation from Eq. (2.9) to Eq. (2.21) is exact. The latter, however, is more convenient for studying the magnon spectrum.

The susceptibility expressed in Eq. (2.21) has poles at the condition

$$\omega = \Omega(\mathbf{r}, \mathbf{r}', \omega) \equiv I_{xc}\Lambda(\mathbf{r}, \mathbf{r}', \omega). \quad (2.22)$$

Solutions to Eq. (2.22) allow us to find a real-valued expression for the magnon spectrum. The imaginary part of Ω describes Stoner damping of magnons that appear in metals. Note that there are many practical calculations of exchange

interactions and magnon dispersion of real material using the dynamical susceptibility ([Callaway, Wang, and Laurent, 1981](#); [Cooke, Blackman, and Morgan, 1985](#); [Savrasov, 1998](#); [Muniz and Mills, 2002](#); [Costa, Muniz, and Mills, 2005](#); [Lounis *et al.*, 2010](#); [Belozarov, Katanin, and Anisimov, 2017](#); [Gorni, Timrov, and Baroni, 2018](#); [Ke and Katsnelson, 2021](#)).

The last step we describe in this section, which allows a crucial result, is to restore effective exchange integrals from Eq. (2.19). This procedure cannot be made in a unique way; there are at least two different definitions of exchange integrals and both are reasonable, although not identical.

We can first try to fit interatomic exchange parameters to the poles of the susceptibility, that is, to the magnon spectrum. To do this explicitly, we need more transformations. Substituting Eq. (2.15) into Eq. (2.20), one obtains

$$\begin{aligned} \Lambda(\mathbf{r}, \mathbf{r}', \omega) &= \sum_{\mu\nu} \frac{f_{\mu\uparrow} - f_{\nu\downarrow}}{\omega - \varepsilon_{\mu\uparrow} + \varepsilon_{\nu\downarrow}} \\ &\quad \star \psi_{\mu\uparrow}^*(\mathbf{r})\psi_{\nu\downarrow} [2B_{xc}(\mathbf{r}') - \varepsilon_{\nu\downarrow} + \varepsilon_{\mu\uparrow}] \psi_{\nu\downarrow}^*(\mathbf{r}') \psi_{\mu\uparrow}(\mathbf{r}'). \end{aligned} \quad (2.23)$$

Therefore, one can write

$$\begin{aligned} \Omega(\mathbf{r}, \mathbf{r}', \omega) &= \frac{4}{m(\mathbf{r})} J(\mathbf{r}, \mathbf{r}', \omega) + I_{xc}(\mathbf{r}) \sum_{\mu\nu} \frac{f_{\mu\uparrow} - f_{\nu\downarrow}}{\omega - \varepsilon_{\mu\uparrow} + \varepsilon_{\nu\downarrow}} \\ &\quad \star (\varepsilon_{\mu\uparrow} - \varepsilon_{\nu\downarrow}) \psi_{\mu\uparrow}^*(\mathbf{r}) \psi_{\nu\downarrow}(\mathbf{r}) \psi_{\nu\downarrow}^*(\mathbf{r}') \psi_{\mu\uparrow}(\mathbf{r}'). \end{aligned} \quad (2.24)$$

It is reasonable to identify the quantity

$$\begin{aligned} J(\mathbf{r}, \mathbf{r}', \omega) &= \sum_{\mu\nu} \frac{f_{\mu\uparrow} - f_{\nu\downarrow}}{\omega - \varepsilon_{\mu\uparrow} + \varepsilon_{\nu\downarrow}} \\ &\quad \star \psi_{\mu\uparrow}^*(\mathbf{r}) B_{xc}(\mathbf{r}) \psi_{\nu\downarrow}(\mathbf{r}) \psi_{\nu\downarrow}^*(\mathbf{r}') B_{xc}(\mathbf{r}') \psi_{\mu\uparrow}(\mathbf{r}') \end{aligned} \quad (2.25)$$

as frequency-dependent interatomic exchange parameters. If one sets $\omega = 0$ in Eq. (2.25), one arrives at RKKY-type indirect interactions ([Vonsovskii, 1974](#); [Yosida, 1996](#)). As later shown, Eqs. (2.23), (2.24), (2.25) are exactly equivalent to the expressions given by [Liechtenstein, Katsnelson, and Gubanov \(1984\)](#), [Liechtenstein *et al.* \(1987\)](#), and [Liechtenstein, Anisimov, and Zaanen \(1995\)](#). In fact, Eqs. (2.23), (2.24), (2.25) are more general, since they do not assume a rigid-moment approximation and they take into account the full coordinate dependence of the wave functions. Using Eq. (2.17), one can also show that

$$\Omega(\mathbf{r}, \mathbf{r}', 0) = \frac{4}{m(\mathbf{r})} J(\mathbf{r}, \mathbf{r}', 0) - 2B_{xc}(\mathbf{r})\delta(\mathbf{r} - \mathbf{r}'). \quad (2.26)$$

The other way to evaluate interatomic exchange interactions is to connect exchange parameters to the energy of spin-spiral configurations, that is, with the static magnetic susceptibility $\hat{\chi}^{+-}(0)$. This can be rewritten as

$$\hat{\chi}^{+-}(0) = m(\hat{\Omega}^{-1} - \frac{1}{2}B_{xc}^{-1}), \quad (2.27)$$

which corresponds to the renormalized spin-wave energy

$$\hat{\Omega} = \hat{\Omega}(1 - \frac{1}{2}B_{xc}^{-1}\hat{\Omega})^{-1}. \quad (2.28)$$

Note that Eq. (2.28) corresponds to the definition of exchange parameters in terms of the energy of static spin configurations (Szczech, Tusch, and Logan, 1998; Antropov, 2003; Bruno, 2003). As we later show, this corresponds to the exchange parameters of Liechtenstein, Katsnelson, and Gubanov (1984), Liechtenstein *et al.* (1987), and Liechtenstein, Anisimov, and Zaanen (1995), normalized by taking into account constraints of the density functional (Bruno, 2003).

Thus, strictly speaking, one cannot map the density functional susceptibility onto an effective Heisenberg model with interatomic exchange parameters in a unique way. The formal reason is the renormalization of the numerator, that is, the residue of the susceptibility at the magnon pole in Eq. (2.21). There are, however, two important limits where this difference disappears.

First, if we pass to the Fourier representation with the wave vector \mathbf{q} and consider the limit $\mathbf{q} \rightarrow 0$, then, due to the Goldstone theorem ($\Omega \rightarrow 0$), the renormalization of the magnon spectrum (2.28) disappears. This means that the expression for the spin-wave stiffness constant (Liechtenstein, Katsnelson, and Gubanov, 1984) determining magnon spectrum at $\mathbf{q} \rightarrow 0$ is well defined and exact within the local-spin-density approximation. Second, if typical magnon energies are much smaller than the Stoner splitting, $B_{xc}^{-1}\hat{\Omega}$ is small and the two definitions of exchange integrals coincide. This corresponds to an adiabatic approximation for magnons (note that magnon energies are much smaller than typical electron energies) that should be clearly distinguished from the adiabatic approximation in the sense of TDDFT. This is the case where the mapping of a full quantum mechanical description to the effective spin model is possible. In the remainder of the review, we focus on this case.

In Fig. 4 we highlight the results of Wan, Yin, and Savrasov (2006) using the expressions for the previously discussed exchange parameters. The figure shows results of a calculation for NiO and, after performing a Fourier transform from real space $J(\mathbf{r}, \mathbf{r}')$ from Eq. (2.25) to reciprocal space $J(\mathbf{q})$, the

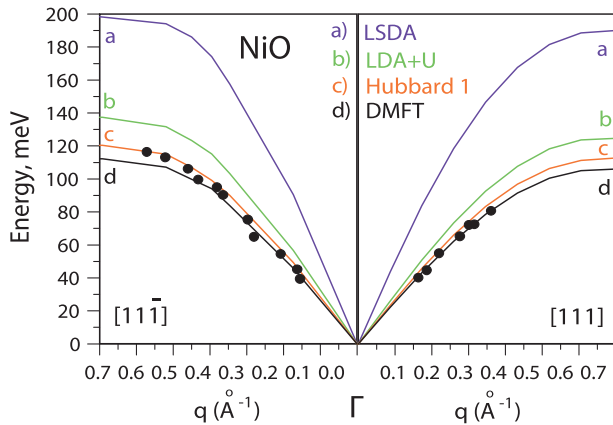


FIG. 4. Calculated and measured magnon dispersion of NiO. Note that several levels of approximation for the theory are shown (solid lines) together with experiments (solid circles). Adapted from Wan, Yin, and Savrasov, 2006.

magnon dispersion was calculated. Figure 4 also shows experimental data, and one can see that the agreement between observation and calculation is satisfactory if the correct level of approximation is used for solving the Kohn-Sham equation (2.1). For NiO dynamical mean-field theory, LDA + U , where LDA stands for local-density approximation, and the Hubbard 1 approximation are both found to reproduce experiments reasonably well. This is further discussed in Sec. VII.

III. MAPPING ELECTRONIC ENERGIES TO AN EFFECTIVE SPIN HAMILTONIAN

In Sec. I we mentioned the central aspect of this review: to extract from calculations of the electronic structure parameters that accurately describe magnetic excitations. In this section we outline the basic principles of a method to do this, as was originally proposed by Liechtenstein, Katsnelson, and Gubanov (1984). A more detailed description of this method, with an extension for noncollinear spin systems when spin-orbit coupling (SOC) is also considered, will be presented in Sec. V. We emphasize that unless explicitly stated, we are concerned only with parameters that describe the coupling between spin moments. We start with a section that contains the essential aspect of Liechtenstein, Katsnelson, and Gubanov (1984) and Liechtenstein *et al.* (1987), which involves how to connect changes of the energy of a spin Hamiltonian [such as that in Eq. (1.1)] with changes of the grand canonical potential that contains energies of the electronic subsystem.

A. Basic assumptions

We start by making a central assumption: that it is possible to identify well-defined regions of a material where the magnetization density is more or less unidirectional and sizable only close to an atomic nucleus. This implies the existence of local atomic magnetic moments (atomic spins), as illustrated in Fig. 3, with ferromagnetic, antiferromagnetic (AFM), or noncollinear interactions between atomic spin moments. As discussed in connection with Fig. 3, few if any materials are not accurately described in this way.

An atomic spin moment is chosen here to be described with a direction \vec{e}_i quantified as

$$\vec{e}_i = (\sin(\theta_i) \cos(\phi_i), \sin(\theta_i) \sin(\phi_i), \cos(\theta_i)), \quad (3.1)$$

where θ_i and ϕ_i stand for the polar and azimuthal angles, respectively, of the atomic spin moment at site i . The rigid-spin approximation (Phariseau and Gyroff, 2012) is also assumed, where upon rotation of atomic spins the length is not changed.

The method employed by Liechtenstein, Katsnelson, and Gubanov (1984) is an explicit method for calculations of interatomic exchange interactions that relies on a formalism of the Green's function of the electronic subsystem (Gyroff *et al.*, 1985; Kübler, 2017). The basic idea is that an effective spin Hamiltonian accurately describes the energy of different atomic spin configurations that are close to the magnetic ground state. We later refer to the energy of the spin

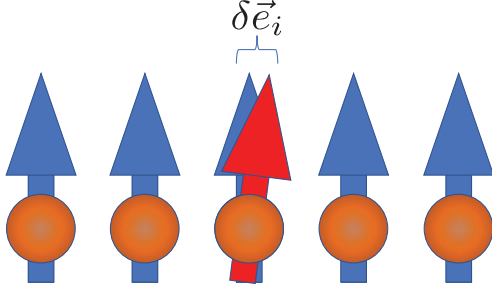


FIG. 5. Schematic for the one-site spin rotation when the unperturbed system is collinear and ferromagnetic. An atomic spin at site i is rotated with an infinitesimal vector $\delta\vec{e}_i$. This process costs the energy $\delta\mathcal{H}_i^{\text{one}}$ due to the fact that the spin interacts with every other spin in the rest of the spin system.

Hamiltonian as \mathcal{H} , and one must make sure that the variation of \mathcal{H} , when the spin configuration is modified slightly, closely follows the changes of the true total energy (the later described grand canonical potential Ω) provided by the electronic subsystem. This then allows us to map energies of the electron subsystem, as provided by, for instance, density functional theory, to energies of an effective spin Hamiltonian, as given in Eq. (1.1). Practically, this mapping is based on the magnetic force theorem, which states that the variation of total energy of the electronic subsystem can be expressed in terms of variations only of occupied single-particle energies (Andersen *et al.*, 1980; Mackintosh and Andersen, 1980; Methfessel and Kübler, 1982; Liechtenstein, Katsnelson, and Gubanov, 1984). Recently a comparison of different mapping procedures for calculation of exchange interactions in various classes of magnetic materials was presented by Solovyev (2021). More details on the argumentation and its extension for correlated systems are discussed in Secs. VA and VK, respectively.

B. The mapping scheme

In making the mapping between energies of the spin Hamiltonian and energies of the electronic subsystem, one considers as a reference state the atomic spin arrangement of the ground state with the energy \mathcal{H} . The orientation of one atomic spin moment, at site i , is then rotated at an infinitesimally small angle, keeping the length of the spin vector conserved; see Fig. 5. The variation of the direction of the spin due to this rotation is denoted $\delta\vec{e}_i$, and the new direction of the perturbed spin can be written as

$$\vec{e}'_i \rightarrow \vec{e}_i + \delta\vec{e}_i. \quad (3.2)$$

The energy of this system, which can be seen as having a small perturbation from the ground state, can be written as $\mathcal{H}' = \mathcal{H}'(\delta\vec{e}_i)$, where

$$\mathcal{H}' = \mathcal{H} + \delta\mathcal{H}_i^{\text{one}}. \quad (3.3)$$

As a second step, one considers a system with two atomic spin moments rotated, at the sites i and j . One can then express the energy of this spin arrangement as

$$\mathcal{H}'' = \mathcal{H} + \delta\mathcal{H}_i^{\text{one}} + \delta\mathcal{H}_j^{\text{one}} + \delta\mathcal{H}_{ij}^{\text{two}}, \quad (3.4)$$

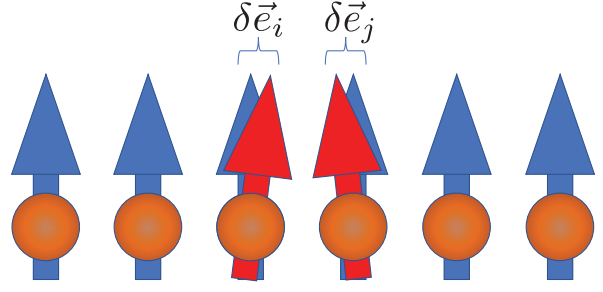


FIG. 6. Schematic for the two-site spin rotation when the unperturbed system is collinear, ferromagnetic. Atomic spins at sites i and j are rotated with the infinitesimal vector $\delta\vec{e}_i$ and $\delta\vec{e}_j$, respectively. This process costs the energy $\delta\mathcal{H}_i^{\text{one}} + \delta\mathcal{H}_j^{\text{one}} + \delta\mathcal{H}_{ij}^{\text{two}}$, where $\delta\mathcal{H}_i^{\text{one}}$ and $\delta\mathcal{H}_j^{\text{one}}$ stand for the energy cost of a one-site rotation (shown in Fig. 5), while the interacting term $\delta\mathcal{H}_{ij}^{\text{two}}$ (see the text) characterizes the exchange energy between the spins located at sites i and j .

where $\mathcal{H}'' = \mathcal{H}''(\delta\vec{e}_i, \delta\vec{e}_j)$ stands for the energy of a spin system with two atomic moments rotated an infinitesimal amount; see Fig. 6.

One can assume that the same procedure can be done for the grand canonical potential variation of the electronic system, where the value of the single-site rotated system is

$$\Omega' = \Omega + \delta\Omega_i^{\text{one}} \quad (3.5)$$

and the value of the two-site rotated system is

$$\Omega'' = \Omega + \delta\Omega_i^{\text{one}} + \delta\Omega_j^{\text{one}} + \delta\Omega_{ij}^{\text{two}}. \quad (3.6)$$

The next step is to derive explicit expressions for both $\delta\Omega_i^{\text{one}}$ and $\delta\Omega_{ij}^{\text{two}}$ and to make a comparison with $\delta\mathcal{H}_i^{\text{one}}$ and $\delta\mathcal{H}_{ij}^{\text{two}}$, respectively. The limit when the SOC is neglected and the spins are arranged collinearly along a global quantization axis (for instance, the z direction) is referred to here as the Liechtenstein-Katsnelson-Antropov-Gubanov (LKAG) limit (Liechtenstein, Katsnelson, and Gubanov, 1984; Liechtenstein *et al.*, 1987). A typical case for a small deviation from the collinear state with atomic moments along the z axis considered here is $\delta\vec{e}_i \simeq (\delta\theta_i, 0, -1/2(\delta\theta_i)^2)$.

C. Excitation of the spin model

The classical Heisenberg spin Hamiltonian was introduced in Eq. (1.3). As shown in Fig. 5, we first derive the one-site spin rotation variation $\delta\mathcal{H}_{H,i}^{\text{one}}$. We denote the nonperturbed spin configuration by the set of $\{\vec{e}_l\}$ vectors and a perturbed system by the set of $\{\vec{e}_l + \delta_{il}\delta\vec{e}_i\}$, where $\delta\vec{e}_i$ stands for an infinitesimal variation of the spin direction due to a rotation at site i with the angle $\delta\theta_i$. One then finds that

$$\begin{aligned} \mathcal{H}'_H &= \sum_{\langle lk \rangle} J_{lk} (\vec{e}_l + \delta_{il}\delta\vec{e}_i) \cdot (\vec{e}_k + \delta_{ik}\delta\vec{e}_i) \\ &= \mathcal{H}_H + \frac{1}{2} \sum_{l(\neq i)} J_{li} \vec{e}_l \cdot \delta\vec{e}_i + \frac{1}{2} \sum_{k(\neq i)} J_{ik} \delta\vec{e}_i \cdot \vec{e}_k, \end{aligned} \quad (3.7)$$

where the origin of the factor of 1/2 is as explained in Sec. I E. Note that Eq. (3.7) can be simplified to describe the energy gain due to the rotation as

$$\delta\mathcal{H}_{H,i}^{\text{one}} = \sum_{l(\neq i)} J_{li} \vec{e}_l \cdot \delta\vec{e}_i \quad (3.8)$$

since the interaction is symmetric: $J_{il} = J_{li}$. This means that the energy variation of the one-site spin rotation is an energy cost resulting from the interaction of the rotated spin and its environment formed by the nonrotated spins, as shown in Fig. 5.

If the nonperturbed configuration is now collinear ferromagnetic, i.e., $\{\vec{e}_j\} = \{(0, 0, 1)\}$ for all j in the spin system with the energy \mathcal{H}_H , one obtains $\vec{e}_j \cdot \delta\vec{e}_i = \delta e_i^z$, which is proportional to $\cos\delta\theta_i - 1$, i.e., approximately proportional to $-(1/2)(\delta\theta_i)^2$. Therefore, in the ferromagnetic limit, one can demonstrate that

$$\delta\mathcal{H}_{H,i}^{\text{one}} \simeq -\frac{1}{2} \sum_{j(\neq i)} J_{ji} (\delta\theta_i)^2. \quad (3.9)$$

Next we simultaneously rotate two spins at sites i and j with $\delta\theta_i$ and $\delta\theta_j$, respectively. As shown in Fig. 6, the perturbed system for the two-site spin rotation is given by the set of $\{\vec{e}_i + \delta_{ii}\delta\vec{e}_i + \delta_{ji}\delta\vec{e}_j\}$ and its energy is

$$\mathcal{H}_H'' = \mathcal{H}_H + \delta\mathcal{H}_{H,i}^{\text{one}} + \delta\mathcal{H}_{H,j}^{\text{one}} + J_{ij}\delta\vec{e}_i \cdot \delta\vec{e}_j. \quad (3.10)$$

Comparing Eq. (3.10) to Eq. (3.4), we obtain³

$$\delta\mathcal{H}_{H,ij}^{\text{two}} = J_{ij}\delta\vec{e}_i \cdot \delta\vec{e}_j. \quad (3.11)$$

In the LKAG limit when $\delta\vec{e}_i = (\delta\theta_i, 0, 0)$, $\delta\vec{e}_j = (\delta\theta_j, 0, 0)$, and $\delta\theta_i = -\delta\theta_j = \delta\theta$, i.e., the spins are rotated in the opposite directions, it can be shown that

$$\delta\mathcal{H}_{H,ij}^{\text{two}} = J_{ij}\delta\theta_i\delta\theta_j = -J_{ij}(\delta\theta)^2. \quad (3.12)$$

One can in a more general way consider a spin Hamiltonian with a tensorial coupling between the spins as follows:

$$\mathcal{H}_T = \sum_{\langle ij \rangle} \vec{e}_i \cdot \mathbb{J}_{ij} \cdot \vec{e}_j, \quad (3.13)$$

where $\mathbb{J}_{ij} = \{J_{ij}^{\mu\nu}; \mu, \nu \in \{x, y, z\}\}$. This is needed even in a collinear system when SOC is present (Udvardi *et al.*, 2003). Note that \mathcal{H}_T can be rewritten as

$$\mathcal{H}_T = \mathcal{H}_H + \mathcal{H}_{\text{anis}} + \mathcal{H}_{\text{DM}}, \quad (3.14)$$

where

$$\mathcal{H}_{\text{anis}} = \sum_{\langle ij \rangle} \vec{e}_i \cdot \mathbb{A}_{ij} \cdot \vec{e}_j \quad (3.15)$$

is the symmetric anisotropic interaction tensor and \mathcal{H}_H and \mathcal{H}_{DM} were introduced in Eqs. (1.3) and (1.4), respectively. More precisely, the 3×3 tensorial interaction is given by

$$\mathbb{J}_{ij} = \begin{pmatrix} J_{ij} + A_{ij}^{xx} & D_{ij}^z + A_{ij}^{xy} & -D_{ij}^y + A_{ij}^{xz} \\ -D_{ij}^z + A_{ij}^{xy} & J_{ij} + A_{ij}^{yy} & D_{ij}^x + A_{ij}^{yz} \\ D_{ij}^y + A_{ij}^{xz} & -D_{ij}^x + A_{ij}^{yz} & J_{ij} + A_{ij}^{zz} \end{pmatrix}. \quad (3.16)$$

Such a 3×3 tensor can be decomposed by symmetry into three independent tensor terms; a symmetric scalar or rank 0 \mathbb{S} , an asymmetric vector or rank 1 \mathbb{V} , and a symmetric rank 2 tensor term \mathbb{T} , respectively. These are defined as

$$\mathbb{S} = \frac{1}{3} \text{Tr} \mathbb{J}, \quad (3.17)$$

$$\mathbb{V} = \vec{D}, \quad (3.18)$$

$$\mathbb{T} = \mathbb{A} - \frac{1}{3} \text{Tr} \mathbb{A}. \quad (3.19)$$

While we have referred to the Heisenberg interaction as the term where the explicit magnetic interaction is a scalar, there is an alternative view that the Heisenberg interaction is an interaction that effectively is a scalar, i.e., \mathbb{S} . This approach ensures that the other interactions are traceless. This means that the Dzyaloshinskii-Moryia interaction is unique, but the exact Heisenberg and second rank tensor are matters of choice.

The one- and two-site energy variations of \mathcal{H}_T can be given as the sum of the variations of \mathcal{H}_H , $\mathcal{H}_{\text{anis}}$, and \mathcal{H}_{DM} , i.e.,

$$\delta\mathcal{H}_{T,i}^{\text{one}} = \sum_{j(\neq i)} [J_{ij}\delta\vec{e}_i \cdot \vec{e}_j + \vec{D}_{ij} \cdot (\delta\vec{e}_i \times \vec{e}_j) + \delta\vec{e}_i \cdot \mathbb{A}_{ij} \cdot \vec{e}_j] \quad (3.20)$$

and

$$\delta\mathcal{H}_{T,ij}^{\text{two}} = J_{ij}\delta\vec{e}_i \cdot \delta\vec{e}_j + \vec{D}_{ij} \cdot (\delta\vec{e}_i \times \delta\vec{e}_j) + \delta\vec{e}_i \cdot \mathbb{A}_{ij} \cdot \delta\vec{e}_j, \quad (3.21)$$

respectively. The expressions of energy variations of the spin Hamiltonian in Eqs. (3.20) and (3.21) must now be compared to similar expressions for the grand canonical potential variations of the electrons. Before we make this connection, we review a few important aspects of electronic structure theory in Sec. IV.

IV. BASIC CONCEPTS OF ELECTRONIC STRUCTURE THEORY

In this section we introduce a few central concepts of electronic structure theory, such as the one-electron Green's function and the integrated density of states that is needed in Sec. V, where we present the details of the derivation of the generalized interatomic exchange formulas.

We first need an expression for the electronic energy and its variations under a perturbation, such as the rotations in Figs. 5 and 6. The grand canonical ensemble is used for this purpose, where energy and particles of the system considered can be exchanged with a reservoir, implying that the chemical potential (μ) and temperature (T) are relevant thermodynamic variables. The grand canonical potential can be calculated as

³A factor of 2 would appear in the last term of Eq. (3.10), but it is canceled by a factor of 1/2; see Sec. I E for an explanation.

$$\Omega = E - TS - \mu N, \quad (4.1)$$

where E is the energy given by

$$E = \int_{-\infty}^{\infty} d\varepsilon \varepsilon f(\varepsilon) n(\varepsilon), \quad (4.2)$$

S is the entropy of the band electrons

$$S = - \int_{-\infty}^{\infty} d\varepsilon n(\varepsilon) \{ f(\varepsilon) \ln f(\varepsilon) + [1 - f(\varepsilon)] \ln [1 - f(\varepsilon)] \}, \quad (4.3)$$

and N is the number of electrons in the valence band. Note that $f(\varepsilon)$ is the Fermi-Dirac distribution function and $n(\varepsilon)$ denotes the density of states (DOS). The exact conditions, which have proven crucial in constraining and constructing accurate approximations for ground-state DFT, are generalized to finite temperature. They are based on the work of Mermin (1965) and were discussed by Pittalis *et al.* (2011).

A. Grand canonical potential at zero temperature

Considering that the Fermi energy ε_F usually is much higher than the critical Curie or Néel temperature, it is for most cases enough to work in the $T = 0$ approach [i.e., $f(\varepsilon)$ is a step function]. In this case $\Omega = E - \varepsilon_F N$, i.e.,

$$\Omega = \int_{-\infty}^{\varepsilon_F} d\varepsilon \varepsilon n(\varepsilon) - \varepsilon_F N = - \int_{-\infty}^{\varepsilon_F} d\varepsilon N(\varepsilon), \quad (4.4)$$

where partial integration has been used. In Eq. (4.4) the number of states function [or integrated density of states (IDOS)] $N(\varepsilon)$ is introduced, and one finds that the grand canonical potential can be calculated as an integral of this function. This means that one has to determine the variations of IDOS to get the variations of the grand canonical potential. A practical way to do this is to employ the so-called Lloyd formula, which is described in Sec. V. Note that the corresponding formula of Eq. (4.4) for cases when the energy argument is in the complex plane is presented in Sec. IV B.

B. Green's function formalism

Since the derivation of the interatomic exchange formulas relies on a Green's function formalism of the electronic structure, we summarize here the most central aspects needed. A full account was given by Economou (2006). The Green's function (or resolvent) of the electronic Hamiltonian H is defined as

$$G(z) = (z - H)^{-1}, \quad (4.5)$$

where $z \in \mathbb{C}$. This implies that $G(z^*) = G^\dagger(z)$. If both sides of the equation $(z_2 - H) - (z_1 - H) = z_2 - z_1$ are multiplied by $G(z_1)G(z_2)$, one stipulates that $z_2 = z + dz$ and $z_1 = z$, and one considers the limit $dz \rightarrow 0$, then

$$\frac{dG(z)}{dz} = -G^2(z) \quad (4.6)$$

can be obtained.

Next we consider an electronic Hamiltonian H with a discrete spectrum⁴ with solutions $H\varphi_\mu = \varepsilon_\mu\varphi_\mu$. Note that $\langle\varphi_\mu|\varphi_\nu\rangle = \delta_{\mu\nu}$ and the solutions to H form a complete set. The spectral resolution of the Green's function can then be obtained from the so-called Lehmann representation,

$$G(z) = \sum_{\mu} \frac{|\varphi_\mu\rangle\langle\varphi_\mu|}{z - \varepsilon_\mu}. \quad (4.7)$$

This implies that on the basis of the eigenfunction of H the Green's function could be represented as $G_{\mu\nu}(z) = \delta_{\mu\nu}[1/(z - \varepsilon_\mu)]$. In addition, $G(z)$ is undefined for $z = \varepsilon_\mu$. However, considering z in the complex plane just above or below the real axis ($z = \varepsilon \pm i\delta$) allows us to define⁵

$$G^\pm(\varepsilon) = \lim_{\delta \rightarrow 0^+} G(\varepsilon \pm i\delta). \quad (4.8)$$

Note that a lattice site-dependent Green's function $G_{ij}(z)$ is relevant here, and it is obtained as

$$G(z) = \sum_{ij\mu} \frac{|\phi_i\rangle\langle\phi_i|\varphi_\mu\rangle\langle\varphi_\mu|\phi_j\rangle\langle\phi_j|}{z - \varepsilon_\mu} = \sum_{ij} |\phi_i\rangle G_{ij}(z) \langle\phi_j| \quad (4.9)$$

with local functions $|\phi_i\rangle$ at site i .

C. Grand canonical potential at finite temperature

To derive the grand canonical potential at finite temperature, it is useful to find a relationship among the IDOS, the DOS, and the Green's function, and one may note that, in a system of independent fermions, the expectation value of a one-particle observable A is given as

$$\langle A \rangle = \sum_{\mu} p_{\mu} \langle \varphi_{\mu} | A | \varphi_{\mu} \rangle, \quad (4.10)$$

where $p_{\mu} = f(\varepsilon_{\mu})$, i.e., the Fermi-Dirac distribution function. One can evaluate Eq. (4.10) with the help of Cauchy's theorem, which states that for a closed contour oriented clockwise the integration of a function $g(z)/(z - a)$ is equal to $-2\pi ig(a)$ if a is within the contour (otherwise, the result is zero). With the help of Cauchy's theorem and Eq. (4.7), Eq. (4.10) can be given simply by $G^+(\varepsilon)$ as follows⁶:

$$\langle A \rangle = -\frac{1}{\pi} \Im \int_{-\infty}^{\infty} d\varepsilon f(\varepsilon) \text{Tr}_{L\sigma} A G^+(\varepsilon), \quad (4.11)$$

⁴Our conclusions would be the same for a continuous spectrum.

⁵Note that $G^\pm(\varepsilon) = [G^\mp(\varepsilon)]^\dagger$.

⁶For more details, see <http://newton.phy.bme.hu/~szunyogh/Elszker/Kkr-slides.pdf>.

where the trace is taken over both the orbital (L) and spin (σ) spaces. If A is the identity operator, one obtains

$$N = -\frac{1}{\pi} \Im \int_{-\infty}^{\infty} d\varepsilon f(\varepsilon) \text{Tr}_{L\sigma} G^+(\varepsilon). \quad (4.12)$$

This allows us to identify the following relationship between the DOS and the Green's function:

$$n(\varepsilon) = -\frac{1}{\pi} \Im \text{Tr}_{L\sigma} G^+(\varepsilon). \quad (4.13)$$

In the rest of the review we consider the limit of the upper part of the complex plane [Eq. (4.8)], and the plus sign is omitted for brevity for functions of real energies.

One can recognize that in Eq. (4.12) the integral is taken along the real axis, which is not always convenient, i.e., it is preferable to transform such integrals to the complex plane. We proceed with the realization that the DOS can equally well be calculated with the help of $G^-(\varepsilon)$, or since $\Re G^+(\varepsilon) = \Re G^-(\varepsilon)$ one can use

$$n(\varepsilon) = -\frac{1}{2\pi i} \text{Tr}_{L\sigma} \{G^+(\varepsilon) - G^-(\varepsilon)\}. \quad (4.14)$$

With the latter choice, the number of particles of Eq. (4.12) can be reformulated as

$$\begin{aligned} N &= -\frac{1}{2\pi i} \int_{-\infty}^{\infty} d\varepsilon f(\varepsilon) \text{Tr}_{L\sigma} \{G^+(\varepsilon) - G^-(\varepsilon)\} \\ &= -\frac{1}{2\pi i} \text{Tr}_{L\sigma} \left\{ \int_{-\infty}^{\infty} d\varepsilon f G^+ + \int_{\infty}^{-\infty} d\varepsilon f G^- \right\}. \end{aligned} \quad (4.15)$$

Referring to the two integrals as I^+ and I^- , one can view them as the two path integrals illustrated with thick blue lines in Fig. 7. A closed contour integral can be obtained by adding the two paths labeled C^+ and C^- , respectively, shown in the figure as a thin red line, that both give vanishing contributions since the energies of this part of the path can be chosen to lie

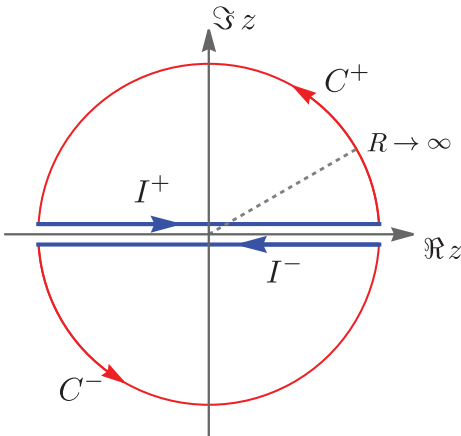


FIG. 7. Integration paths in the complex plane.

infinitely far away from the poles of the Green's functions. Since the integrand is analytical within these contours, these integrals can be evaluated by summing the residues that arise from the Fermi-Dirac distribution $\text{Res}(f, \mu + i\omega_n) = -T$ due to its poles at the Matsubara energies $z = \mu + i\omega_n$, where $\omega_n = (2n + 1)\pi T$ and T is the temperature (Auerbach, 1994). Hence,

$$\begin{aligned} N &= (I^+ + C^+) + (I^- + C^-) \\ &= -\frac{1}{2\pi i} \left\{ \oint_+ dz f G + \oint_- dz f G \right\} \\ &= -\frac{1}{2\pi i} \text{Tr}_{L\sigma} \sum_{n=-\infty}^{\infty} (2\pi i) \text{Res}(f G, \mu + i\omega_n) \\ &= T \sum_{n=-\infty}^{\infty} \text{Tr}_{L\sigma} G(\mu + i\omega_n). \end{aligned} \quad (4.16)$$

V. DERIVATION OF THE EXCHANGE FORMULAS

In this section, we present the details of the mapping of the electronic Hamiltonian to the spin Hamiltonian given by the \mathbb{J}_{ij} tensor, as shown in Eq. (3.13). The derivation is general in the sense that we consider a noncollinear spin arrangement when the SOC interaction is present. Hence, we later give explicit expressions for the Heisenberg J_{ij} , the DM vector \vec{D}_{ij} , and the symmetric anisotropic exchange term \mathbb{A}_{ij} in general, and the interpretation of the results in the LKAG limit.

A. Magnetic local force theorem

As mentioned in Sec. III, the mapping of the electronic Hamiltonian to the spin Hamiltonian is based on the magnetic force theorem, since one can always consider small variations from the ground states; i.e., a mapping to an effective Hamiltonian is locally⁷ possible (close enough to the magnetic ground state).

We now write the grand canonical potential as

$$\Omega = \Omega_{\text{sp}} - \Omega_{\text{dc}}. \quad (5.1)$$

In Eq. (5.1) the subscript sp stands for single particle and Ω_{sp} represents the integral in Eq. (4.4). In addition, Ω_{dc} stands for the interaction or “double-counting” term. One can calculate the first-order change in Ω when the system is under some perturbation. In deriving the magnetic force theorem, one can consider small rotations as perturbations. These changes are assumed to be described by a certain set of parameters (Methfessel and Kübler, 1982). As a first step, the potential is held fixed, which leads to a variation in the single-particle energy $\delta^* \Omega_{\text{sp}}$. In a second step, the parameters that characterize the changes are held constant and the potential is allowed to relax to self-consistency. This leads to variations $\delta_1 \Omega_{\text{sp}}$ and $-\delta \Omega_{\text{dc}}$ in the single-particle energies and the double-counting

⁷See the discussion of local versus global spin models later in this section.

term, respectively. However, these two contributions $\delta_1 \Omega_{sp}$ and $-\delta \Omega_{dc}$ cancel each other, as shown by Andersen *et al.* (1980), Mackintosh and Andersen (1980), Methfessel and Kübler (1982), and Liechtenstein, Katsnelson, and Gubanov (1984). In summary, the magnetic force theorem indeed shows that the variation of total energy of the electronic subsystem can be expressed in terms of variations only of occupied single-particle energies. Note that the magnetic local force theorem strictly holds only for first-order variations.

Finally, we close this section by mentioning that it is a challenge to find the ground state due to many local minima in the DFT-total-energy landscape. The problem of how to find a list of initial magnetic configurations for the practical calculations was addressed by Huebsch *et al.* (2021) and Zheng and Zhang (2021).

B. Energy variation from a noncollinear Kohn-Sham Hamiltonian

We start this section with a general noncollinear state with spin moments $\{\vec{e}_i\}$ and the Kohn-Sham Hamiltonian defined by Eq. (2.1). For simplicity we introduce $\vec{B}(\mathbf{r})$ as $\vec{B}(\mathbf{r}) = \vec{B}_{xc}(\mathbf{r}) + \vec{B}_{ext}(\mathbf{r})$, and in condensed form we can express the spin-dependent interaction as $B \equiv \vec{B}(\mathbf{r}) \cdot \vec{\sigma}$. One can then let the directions of the local moments rotate away slightly from a given magnetic configuration. Instead of the case in which only one spin is rotated in the spin system, as shown in Fig. 5 and by Eq. (3.2), we allow in principle a $\delta \vec{e}_i$ change at all possible sites. As we later see, this is more than a sum of one-site rotations because of the intersite interactions. However, the corresponding perturbation in the electronic potential δV , which is purely spin dependent, can be divided into local changes of the spin-polarized potential in a given region around the atomic sites where the moments are varied,

$$\delta V = -\sum_i \delta \vec{B}_i \cdot \vec{\sigma} = -\sum_i B_i \delta \vec{e}_i \cdot \vec{\sigma}, \quad (5.2)$$

where $\vec{B}_i \equiv B_i \vec{e}_i$. Having the perturbation δV , one can write for the perturbed Green's function G' (omitting for simplicity the energy argument) that

$$G' = G + G \delta V G', \quad G = G' - G \delta V G' = (1 - G \delta V) G', \quad (5.3)$$

where G stands for the unperturbed Green's function.

From Eq. (4.6) one can deduce that

$$G = -\frac{\partial \ln G}{\partial \varepsilon}, \quad (5.4)$$

which means that the IDOS, which is the primitive function to the DOS of Eq. (4.13), is given by

$$N = -\frac{1}{\pi} \Im \text{Tr}_{iL\sigma} (-\ln G) \quad (5.5)$$

and the change in IDOS is then given by the Lloyd formula (Lloyd, 1967), i.e.,

$$\begin{aligned} \delta N &= -\frac{1}{\pi} \Im \text{Tr}_{iL\sigma} \{-\ln G' + \ln (1 - G \delta V) G'\} \\ &= -\frac{1}{\pi} \Im \text{Tr}_{iL\sigma} \ln (1 - G \delta V). \end{aligned} \quad (5.6)$$

This means that one does not have to deal with the exact Green's function G' in order to calculate δN . One can also expand the logarithm in a series as long as δV is small, which yields

$$\delta N = \frac{1}{\pi} \Im \text{Tr}_{iL\sigma} \sum_{k=1}^{\infty} \frac{(\delta V G)^k}{k}, \quad (5.7)$$

where the order of the two factors can be altered due to the properties of the trace. Note that G is the Green's function corresponding to the electronic Hamiltonian (2.1). It can be decomposed to intersite terms G_{ij} according to Eq. (4.9), which can be further decomposed into spin components in a form where

$$G_{ij} = G_{ij}^0 + \vec{G}_{ij} \cdot \vec{\sigma}, \quad (5.8)$$

where \vec{G}_{ij} is a vector with the components of G_{ij}^x , G_{ij}^y , and G_{ij}^z . We introduce here the notation G_{ij}^η , where the index η enumerates both the scalar spin-independent Green's function and the components of the spin-dependent vector Green's function of Eq. (5.8), i.e., η can be 0, x , y , or z . Note that G_{ij} is defined in both the spin and orbital spaces, while G_{ij}^η is represented only in the orbital space. In other words, G_{ij} can be represented by an 18×18 matrix, while G_{ij}^η is a 9×9 matrix when spd orbitals are used in a practical calculation. We refer here to G_{ij}^0 as the charge part and to \vec{G}_{ij} as the spin part of the Green's function. The physical interpretation of the decomposition is discussed in Sec. V E. Note that in the LKAG limit the vector \vec{G}_{ij} has only a z component, and in Sec. V I we define the up and down spin channels with the help of G_{ij}^0 and G_{ij}^z . Note also that the trace in Eqs. (5.6) and (5.7) is over the atomic sites i , the local basis functions L , and the spin components σ .

Based on Eq. (4.4), the variation in grand canonical potential [Eq. (4.1)] due to the moment rotations is obtained through integration of the change in the number of states function, i.e.,

$$\delta \Omega = -\int_{-\infty}^{\infty} d\varepsilon \delta N(\varepsilon) f(\varepsilon), \quad (5.9)$$

where Eq. (5.7) can be used for δN . The corresponding grand canonical potential variation formula at finite temperature can be expressed as

$$\delta \Omega = T \sum_{n=-\infty}^{\infty} \pi \delta N(\mu + i\omega_n), \quad (5.10)$$

where δN [which along the real axis is given by Eq. (5.6)] is generalized to the following expression in the complex plane:

$$\delta N(z) = -\frac{1}{\pi} \text{Tr}_{iL\sigma} \ln [1 - \delta V G(z)], \quad (5.11)$$

with the limit

$$\Im \lim_{\Im z \rightarrow 0^+} \delta N(z) = \delta N(\varepsilon). \quad (5.12)$$

With Eq. (5.11) one can rewrite the sum over Matsubara frequencies in Eq. (5.10) as the trace

$$\delta \Omega = -\text{Tr} \ln (1 - \delta V G) = \text{Tr} \sum_k \frac{(\delta V G)^k}{k}, \quad (5.13)$$

which is short notation for

$$\text{Tr} = \text{Tr}_{oiL\sigma} = T \sum_{n=-\infty}^{\infty} \text{Tr}_{iL\sigma}. \quad (5.14)$$

Using analytical continuation from the Matsubara space to the real frequencies, we get the following relation (Katsnelson and Lichtenstein, 2000):

$$\text{Tr}_{oiL\sigma} = -\frac{1}{\pi} \int_{-\infty}^{\infty} d\varepsilon f(\varepsilon) \Im \text{Tr}_{iL\sigma}. \quad (5.15)$$

C. Perturbation to first order

One can directly conclude that whenever the lowest order in Eq. (5.7) is not vanishing it will dominate providing torques on some of the local moments. Therefore, we first analyze the first-order term, which can be described as a sum of one-site rotations, i.e.,

$$\delta N^{\text{one}} = \frac{1}{\pi} \Im \text{Tr}_{iL\sigma} \delta V G = \sum_i \delta N_i^{\text{one}}, \quad (5.16)$$

where the site local variation of the number of states is

$$\begin{aligned} \delta N_i^{\text{one}} &= -\frac{1}{\pi} \Im \delta \vec{e}_i \cdot \text{Tr}_{L\sigma} B_i \vec{\sigma} G_{ii} \\ &= -\frac{2}{\pi} \Im \delta \vec{e}_i \cdot \text{Tr}_L B_i \vec{G}_{ii}, \end{aligned} \quad (5.17)$$

and the factor 2 arises from the trace over spin variables. The grand canonical potential variation ($\delta \Omega_i^{\text{one}}$) due to one-site rotation (Fig. 5) is based on the expression δN_i^{one} [given by Eq. (5.17)], and the details of the derivation are presented in Sec. V F. Note that Fig. 5 shows a collinear (ferromagnetic) case. However, Eq. (5.17) also holds for cases in which the rotation $\delta \vec{e}_i$ appears in a noncollinear background of atomic moments.

D. The sum rule

While δN_i^{one} (and therefore $\delta \Omega_i^{\text{one}}$) can be obtained by direct calculation based only on on-site quantities, as shown by Eq. (5.17), we prefer to deepen the analysis by taking an

algebraic step that allows us to express this first-order term as a bilinear intersite magnetic interaction that eases the understanding of these magnetic interactions. Since the local Green's functions arise from a self-consistent solution of a magnetically ordered state, one can derive an explicit expression for it in the following way. Consider a solution obtained from a well-defined nonmagnetic system with a Hamiltonian in the form of the right-hand side of Eq. (2.1); more precisely, $V(\mathbf{r}) = V_0^{\text{nm}}$. In this case $\vec{B}_{\text{xc}}(\mathbf{r}) = \vec{B}_{\text{ext}}(\mathbf{r}) = 0$. Note that the non-spin-polarized potential V_0^{nm} for this nonmagnetic state in general will not be equivalent to the corresponding spin-independent part of the potential V_0 for a magnetic state. The Green's function of the magnetic state is related to the Green's function of the nonmagnetic state G_{nm} through Dyson's equation as follows (omitting for simplicity the energy argument):

$$G = G_{\text{nm}} + G_{\text{nm}} \Delta V G \quad (5.18)$$

or

$$(G^{-1} - G_{\text{nm}}^{-1})_{ij} = \{V_0^{\text{nm}} - V_0 + \vec{B}_j \cdot \vec{\sigma}\} \delta_{ij}, \quad (5.19)$$

where the spin-polarized fields can be written as $\vec{B}_j = B_j \vec{e}_j$ and $\Delta V = V_0 - \vec{B}_j \cdot \vec{\sigma} - V_0^{\text{nm}}$.

To arrive at a suitable expression, one makes use of the fact that this magnetic state has to be degenerate with the corresponding time reversed state, i.e., the state in which all moments are switched and the direction of a charge current is reversed. The Green's function for this time reversed problem \tilde{G} is given by

$$(\tilde{G}^{-1} - G_{\text{nm}}^{-1})_{ij} = \{V_0^{\text{nm}} - V_0 - \vec{B}_j \cdot \vec{\sigma}\} \delta_{ij}. \quad (5.20)$$

The difference between Eqs. (5.19) and (5.20) gives

$$(G^{-1} - \tilde{G}^{-1})_{ij} = 2\vec{B}_j \cdot \vec{\sigma} \delta_{ij}. \quad (5.21)$$

By letting \tilde{G} and G act on Eq. (5.21) from either side in a symmetric fashion, we arrive at the following sum rule for the local Green's functions:

$$\tilde{G}_{ii} - G_{ii} = \sum_j (G_{ij} \vec{B}_j \cdot \vec{\sigma} \tilde{G}_{ji} + \tilde{G}_{ij} \vec{B}_j \cdot \vec{\sigma} G_{ji}). \quad (5.22)$$

E. Further decomposition of the Green's function and its physical interpretation

To be able to utilize Eq. (5.22), one can further decompose the components of the Green's function in Eq. (5.8) into terms that are either even or odd under space reversal (Fransson *et al.*, 2017). This can be done by introducing $G_{ij}^{\eta\kappa}$, where the first index η was introduced and explained after Eq. (5.8), while the second index κ can be viewed as an indicator whether the terms that are space reversal invariant and those are not, i.e., κ can be 0 or 1. This decomposition of the Green's function can be summarized as

$$G_{ij}^\eta = G_{ij}^{\eta 0} + G_{ij}^{\eta 1}, \quad (5.23)$$

where it also turns out that G_{ij}^{00} and \vec{G}_{ij}^1 are time reversal invariant, while G_{ij}^{01} and \vec{G}_{ij}^0 are not, where we have written the x -, y -, or z -dependent components of the Green's function as vectors, i.e., \vec{G}^κ . This decomposition plays a useful role in how the Green's function behaves under site exchange, since in a real local basis (Fransson *et al.*, 2017) we have

$$G_{ij}^{\eta\kappa} = (-1)^\kappa G_{ji}^{\eta\kappa T}. \quad (5.24)$$

In fact, Fransson *et al.* (2017) showed that these two-index Green's functions are decomposed in terms that produce local

charge G^{00} or spin densities \vec{G}^0 and charge G^{01} and spin currents \vec{G}^1 , an aspect we later return to.

We can express both the Green's function and its time reversed version as a superposition of these two index-decomposed Green's functions as

$$G = G^{00} + G^{01} + \vec{G}^0 \cdot \vec{\sigma} + \vec{G}^1 \cdot \vec{\sigma}, \quad (5.25)$$

$$\tilde{G} = G^{00} - G^{01} - \vec{G}^0 \cdot \vec{\sigma} + \vec{G}^1 \cdot \vec{\sigma}. \quad (5.26)$$

These decomposed Green's functions are then inserted into Eq. (5.22), which leads to

$$\begin{aligned} \tilde{G}_{ii} - G_{ii} = & \sum_j \{ (G^{00} + G^{01} + \vec{G}^0 \cdot \vec{\sigma} + \vec{G}^1 \cdot \vec{\sigma})_{ij} \vec{B}_j \cdot \vec{\sigma} (G^{00} - G^{01} - \vec{G}^0 \cdot \vec{\sigma} + \vec{G}^1 \cdot \vec{\sigma})_{ji} \\ & + (G^{00} - G^{01} - \vec{G}^0 \cdot \vec{\sigma} + \vec{G}^1 \cdot \vec{\sigma})_{ij} \vec{B}_j \cdot \vec{\sigma} (G^{00} + G^{01} + \vec{G}^0 \cdot \vec{\sigma} + \vec{G}^1 \cdot \vec{\sigma})_{ji} \}, \end{aligned} \quad (5.27)$$

which for the spin-dependent and time reversal odd part \vec{G}_{ii}^0 of $(1/2)(G_{ii} - \tilde{G}_{ii}) = G_{ii}^{01} + \vec{G}_{ii}^0 \cdot \vec{\sigma}$ allows us to identify the following expression (Cardias, Bergman *et al.*, 2020):

$$\begin{aligned} \vec{G}_{ii}^0 = & - \sum_j \{ (G_{ij}^{00} \vec{B}_j G_{ji}^{00} - G_{ij}^{01} \vec{B}_j G_{ji}^{01}) + i(\vec{G}_{ij}^1 \times \vec{B}_j G_{ji}^{00} + G_{ij}^{00} \vec{B}_j \times \vec{G}_{ji}^1) \\ & - i(\vec{G}_{ij}^0 \times \vec{B}_j G_{ji}^{01} + G_{ij}^{01} \vec{B}_j \times \vec{G}_{ji}^0) + (\vec{G}_{ij}^1 \cdot \vec{B}_j \vec{G}_{ji}^1 - \vec{G}_{ij}^0 \cdot \vec{B}_j \vec{G}_{ji}^0) \\ & - [(\vec{G}_{ij}^1 \times \vec{B}_j) \times \vec{G}_{ji}^1 - (\vec{G}_{ij}^0 \times \vec{B}_j) \times \vec{G}_{ji}^0] \}. \end{aligned} \quad (5.28)$$

Note that Eq. (5.28) is general, despite the fact that we arrived at it from considerations of the Green's function of its normal and spin reversed state. Hence, Eq. (5.28) can also be used for small angle rotations of moments,⁸ which is utilized in Sec. V F.

To give a physical interpretation for the charge and spin densities and charge and spin currents, it is useful to study the decomposition of the Green's function in real space $G(\mathbf{r}, \mathbf{r}'; \varepsilon)$ into eight independent two indexed contributions, i.e., to consider

$$G(\mathbf{r}, \mathbf{r}'; \varepsilon) = \sum_{\eta \in \{0,x,y,z\}} \sum_{\kappa=0}^1 \sigma_\eta G^{\eta\kappa}(\mathbf{r}, \mathbf{r}'; \varepsilon), \quad (5.29)$$

where σ_0 represents the identity matrix. Note that the second index κ of the Green's function in Eq. (5.29) indicates whether the function is even (0) or odd (1) under the exchange of spatial coordinates ($\mathbf{r} \leftrightarrow \mathbf{r}'$)

$$G^{\eta\kappa}(\mathbf{r}', \mathbf{r}; \varepsilon) = (-1)^\kappa G^{\eta\kappa}(\mathbf{r}, \mathbf{r}'; \varepsilon), \quad (5.30)$$

where the κ decomposition is defined through

⁸Note that ΔV , which we consider in Secs. V D and V E, is not the same as δV , which stands for perturbations due to different kind of infinitesimally small spin rotations in the rest of Sec. V.

$$G^\kappa(\mathbf{r}, \mathbf{r}'; \varepsilon) = \frac{G(\mathbf{r}, \mathbf{r}'; \varepsilon) + (-1)^\kappa G(\mathbf{r}', \mathbf{r}; \varepsilon)}{2}. \quad (5.31)$$

The meaning of this two-index decomposition can be summarized by

$$G(\mathbf{r}, \mathbf{r}'; \varepsilon) = \sum_{\eta \in \{0,x,y,z\}} \sum_{\kappa=0}^1 (-1)^\kappa \sigma_\eta G^{\eta\kappa}(\mathbf{r}', \mathbf{r}; \varepsilon). \quad (5.32)$$

The four different Green's functions, two scalar and two vector valued, as previously discussed, each have a direct physical property, as in the local and nonrelativistic limit they give rise to charge and spin density (scalar and vector) and charge and spin current densities (vector and tensor), respectively, through

$$n(\mathbf{r}) = -\frac{1}{\pi} \Im \lim_{\mathbf{r}' \rightarrow \mathbf{r}} \int G^{00}(\mathbf{r}, \mathbf{r}'; \varepsilon) d\varepsilon, \quad (5.33)$$

$$\vec{m}(\mathbf{r}) = -\frac{1}{\pi} \Im \lim_{\mathbf{r}' \rightarrow \mathbf{r}} \int \vec{G}^0(\mathbf{r}, \mathbf{r}'; \varepsilon) d\varepsilon, \quad (5.34)$$

$$\mathbf{j}(\mathbf{r}) = -\frac{1}{\pi} \Re \lim_{\mathbf{r}' \rightarrow \mathbf{r}} \int \nabla G^{01}(\mathbf{r}, \mathbf{r}'; \varepsilon) d\varepsilon, \quad (5.35)$$

$$\vec{q}(\mathbf{r}) = -\frac{1}{\pi} \Re \lim_{\mathbf{r}' \rightarrow \mathbf{r}} \int \nabla \vec{G}^1(\mathbf{r}, \mathbf{r}'; \varepsilon) d\varepsilon. \quad (5.36)$$

These four independent density quantities are important in the case of magnetic materials and are known to appear in many other approaches, including general Hartree-Fock theory (Fukutome, 1981).

Expanding the Green's function represented in real space in a local basis [Eq. (4.9)] results in

$$G^{\eta\kappa}(\mathbf{r}, \mathbf{r}'; \varepsilon) = \phi_i^T(\mathbf{r}) G_{ij}^{\eta\kappa} \phi_j(\mathbf{r}'), \quad (5.37)$$

where space is divided into regions around the atomic sites such that the site i is specified by the position \mathbf{r} and the vector of basis functions $\phi_i(\mathbf{r})$ is uniquely defined. The condition of Eq. (5.30) then leads to

$$\begin{aligned} G^{\eta\kappa}(\mathbf{r}', \mathbf{r}; \varepsilon) &= \phi_j^T(\mathbf{r}') G_{ji}^{\eta\kappa} \phi_i(\mathbf{r}) \\ &= (-1)^\kappa \phi_i^T(\mathbf{r}) G_{ij}^{\eta\kappa} \phi_j(\mathbf{r}') \\ &= (-1)^\kappa [\phi_j(\mathbf{r}')^T \{G_{ij}^{\eta\kappa}\}^T \phi_i(\mathbf{r})]^T \\ &= (-1)^\kappa \phi_j(\mathbf{r}')^T \{G_{ij}^{\eta\kappa}\}^T \phi_i(\mathbf{r}), \end{aligned} \quad (5.38)$$

where the outer transpose is superfluous since it is acting on a scalar. This leads to the relation for the Green's function matrices expanded in a real basis shown in Eq. (5.24), which illustrates that the decomposed Green's functions that stem from currents ($\kappa = 1$) are asymmetric in the direction of the propagation, in contrast to those that stem from densities ($\kappa = 0$).

F. Bilinear interaction parameters due to one-site spin rotation

One can generally express the variation of the grand potential as a series of contributions coming from different orders of perturbation as

$$\delta\Omega = \delta\Omega^{\text{one}} + \delta\Omega^{\text{two}} + \dots \quad (5.39)$$

It is relevant to express the first two terms in the series in terms of bilinear interaction parameters. In the case of one-site spin rotation, one then has to express the one-site grand potential variation $\delta\Omega^{\text{one}}$ in terms of intersite Green's functions, which corresponds to inserting Eq. (5.17) into Eq. (5.9), where Eq. (5.17) is given by the on-site Green's function \vec{G}_{ii} . However, it is only the time reversal odd spin-dependent Green's function \vec{G}_{ii}^0 that will give rise to a nonzero product $\text{Tr}_L B_i \vec{G}_{ii}$ in Eq. (5.17), where \vec{G}_{ii}^0 in turn can be expressed in terms of intersite Green's functions due to the sum rule of Eq. (5.28). Hence, one can express the first-order term as a superposition of different pair interactions using

$$\begin{aligned} \delta\Omega^{\text{one}} &= \frac{2}{\pi} \Im \sum_i \delta \vec{e}_i \cdot \int \text{Tr}_L B_i \vec{G}_{ii}^0(\varepsilon) d\varepsilon \\ &= 2 \sum_{\langle ij \rangle} \delta \vec{e}_i \cdot \mathbb{J}_{ij}^{(1)} \cdot \vec{e}_j + \delta\Omega_{\text{loc}}^{\text{one}}, \end{aligned} \quad (5.40)$$

where the tensor $\mathbb{J}_{ij}^{(1)}$ has the same form as Eqs. (3.13),(3.14), (3.15),(3.16), with the exchange parameter $J_{ij}^{(1)}$, the DM vector $\vec{D}_{ij}^{(1)}$, and the symmetric anisotropic interaction tensor

$\mathbb{A}_{ij}^{(1)}$. Note that comparing Eq. (5.40) to Eq. (3.20) allows us to identify the exchange parameter $J_{ij}^{(1)}$ as

$$\begin{aligned} J_{ij}^{(1)} &= -\frac{2}{\pi} \Im \int \text{Tr}_L \left(B_i G_{ij}^{00} B_j G_{ji}^{00} - B_i G_{ij}^{01} B_j G_{ji}^{01} \right. \\ &\quad \left. + \sum_\nu B_i G_{ij}^{\nu 0} B_j G_{ji}^{\nu 0} - \sum_\nu B_i G_{ij}^{\nu 1} B_j G_{ji}^{\nu 1} \right) d\varepsilon, \end{aligned} \quad (5.41)$$

while the components of the vector $\vec{D}_{ij}^{(1)}$ and the tensor $\mathbb{A}_{ij}^{(1)}$ are given by

$$D_{ij}^{(1)\nu} = -\frac{4}{\pi} \Re \int \text{Tr}_L (B_i G_{ij}^{00} B_j G_{ji}^{\nu 1} - B_i G_{ij}^{01} B_j G_{ji}^{\nu 0}) d\varepsilon \quad (5.42)$$

and

$$A_{ij}^{(1)\nu\mu} = -\frac{4}{\pi} \Im \int \text{Tr}_L (B_i G_{ij}^{\nu 1} B_j G_{ji}^{\mu 1} - B_i G_{ij}^{\nu 0} B_j G_{ji}^{\mu 0}) d\varepsilon, \quad (5.43)$$

respectively, where μ and ν can be x , y , or z . Note that the index (1) in $J_{ij}^{(1)}$, $\vec{D}_{ij}^{(1)}$, and $\mathbb{A}_{ij}^{(1)}$ refers to the fact that these parameters are derived from one-site spin rotation. We also note that the prefactor 2 in the second line in Eq. (5.40) arises for the same reason that the one-site term is entered twice in Eq. (3.6). The second term in Eq. (5.40) is given by

$$\delta\Omega_{\text{loc}}^{\text{one}} = \sum_i \delta \vec{e}_i \cdot \mathbb{J}_i^{(1)} \cdot \vec{e}_i, \quad (5.44)$$

which may play roles for the magnetic anisotropy (Solovyev, Dederichs, and Mertig, 1995) or the longitudinal exchange couplings (Shallcross *et al.*, 2005); i.e., we have arrived at a more general model that is beyond what is usually considered in bilinear spin models such as Eq. (3.20). However, in the collinear-nonrelativistic limit, this term can be shown to be canceled by a similar local term in the second-order interaction (Liechtenstein *et al.*, 1987), which we return to in Sec. VI. Nevertheless, considering the intersite terms on the second line in Eq. (5.40), a local mapping can always be made with the Heisenberg exchange parameter $J_{ij} = J_{ij}^{(1)}$, the DM vector $\vec{D}_{ij} = \vec{D}_{ij}^{(1)}$, and the symmetric anisotropic interaction tensor $\mathbb{A}_{ij} = \mathbb{A}_{ij}^{(1)}$ around the magnetic order of the reference state.

G. Bilinear interaction parameters due to two-site spin rotations

Whenever the first-order term vanishes, the second-order perturbation plays a role. This is the case for a collinear state in the absence of SOC where the first-order contribution is identically zero. This term might also be of importance when one aims to calculate collective excitations, i.e., spin waves, in linear spin-wave theory, where the spin Hamiltonian has to be bilinear in the variations of the magnetic moments (Toth and Lake, 2015). The second-order term in Eq. (5.7) can be written as δN^{two} , which is analogous to δN^{one} as given by Eq. (5.16). Inserting δN^{two} into Eq. (5.9) leads to the grand potential variation $\delta\Omega^{\text{two}}$, which corresponds to simultaneous rotations

at sites i and j , as illustrated in Fig. 6, and is naturally bilinear. This term also contains a local term $\delta\Omega_{\text{loc}}^{\text{two}}$ that we again ignore. One can then obtain

$$\delta\Omega^{\text{two}} - \delta\Omega_{\text{loc}}^{\text{two}} = -\frac{1}{2\pi} \sum_{\langle ij \rangle} \int \Im \text{Tr}_L \delta\vec{e}_i \cdot \vec{\sigma} B_i G_{ij} \delta\vec{e}_j \cdot \vec{\sigma} B_j G_{ji} d\epsilon. \quad (5.45)$$

Note that Fig. 6 shows a collinear ferromagnetic case, but Eq. (5.45) also holds for the general noncollinear case. Note that Eq. (5.45) can be simplified in a similar fashion as the first-order contributions; first decompose the Green's functions and then sum out the spin degrees of freedom after manipulating the matrix product by means of Pauli algebra. A comparison with Eq. (3.21) leads to

$$\delta\Omega^{\text{two}} - \delta\Omega_{\text{loc}}^{\text{two}} = \sum_{\langle ij \rangle} \delta\vec{e}_i \cdot \mathbb{J}_{ij}^{(2)} \cdot \delta\vec{e}_j, \quad (5.46)$$

where $J_{ij}^{(2)}$ is defined as

$$J_{ij}^{(2)} = -\frac{2}{\pi} \Im \int \text{Tr}_L \left(B_i G_{ij}^{00} B_j G_{ji}^{00} + B_i G_{ij}^{01} B_j G_{ji}^{01} - \sum_{\nu} B_i G_{ij}^{\nu 0} B_j G_{ji}^{\nu 0} - \sum_{\nu} B_i G_{ij}^{\nu 1} B_j G_{ji}^{\nu 1} \right) d\epsilon, \quad (5.47)$$

while the components of $\vec{D}_{ij}^{(2)}$ and $\mathbb{A}_{ij}^{(2)}$ are given by

$$D_{ij}^{(2)\nu} = -\frac{4}{\pi} \Re \int \text{Tr}_L (B_i G_{ij}^{00} B_j G_{ji}^{\nu 1} + B_i G_{ij}^{01} B_j G_{ji}^{\nu 0}) d\epsilon \quad (5.48)$$

and

$$A_{ij}^{(2)\nu\mu} = -\frac{4}{\pi} \Im \int \text{Tr}_L (B_i G_{ij}^{\nu 1} B_j G_{ji}^{\mu 1} + B_i G_{ij}^{\nu 0} B_j G_{ji}^{\mu 0}) d\epsilon, \quad (5.49)$$

respectively, where the superscript (2) in $J_{ij}^{(2)}$, $\vec{D}_{ij}^{(2)}$, and $\mathbb{A}_{ij}^{(2)}$ refers to the fact that these parameters are derived from two-site spin rotations. This is an alternative mapping since $\mathbb{J}_{ij}^{(2)} \neq \mathbb{J}_{ij}^{(1)}$; i.e., the mapping procedures based on the one- and two-site spin rotations lead to different results in general. Their comparison and physical interpretations are discussed in Sec. VI.

H. Explicit symmetric or asymmetric interactions

With a relation in hand for the decomposed Green's function, we observe that the interactions are explicitly determined as symmetric or asymmetric. For example, for the Dzyaloshinskii-Moriya interaction of Eq. (5.42) we can, since the trace of the transpose of a matrix is equal to the trace of the matrix and the trace of a product is invariant under cyclic permutation of the factors, derive its asymmetric property explicitly due to the property of Eq. (5.24) as follows:

$$\begin{aligned} D_{ij}^{(1)\nu} &= -\frac{4}{\pi} \Re \int \text{Tr}_L (B_i G_{ij}^{00} B_j G_{ji}^{\nu 1} - B_i G_{ij}^{01} B_j G_{ji}^{\nu 0})^T d\epsilon \\ &= \frac{4}{\pi} \Re \int \text{Tr}_L (B_j G_{ji}^{\nu 1} B_i G_{ij}^{00} - B_j G_{ji}^{\nu 0} B_i G_{ij}^{01}) d\epsilon \\ &= -D_{ji}^{(1)\nu}. \end{aligned} \quad (5.50)$$

In general, we can conclude that pair interaction terms that include an even number of asymmetric Green's functions become symmetric, while those that include an odd number are asymmetric. It is clear then that it is only the Dzyaloshinskii-Moriya interaction that is asymmetric among the bilinear interactions of Eqs. (5.41), (5.42), (5.43). Note that the argumentation presented here holds for $D_{ij}^{(2)\nu}$; see Eq. (5.48) as well.

I. Interaction parameters obtained from one- and two-site variations

Since we have reformulated the first-order interactions into a bilinear form [Eq. (5.41)], it can be directly compared with the second-order interactions that are naturally bilinear [Eq. (5.47)]. There are clear differences between the two expressions, which might not be surprising, since they reflect different quantities. The first-order interaction describes the local torques on the magnetic moments, while the second-order interaction mainly describes the interaction of rotated moments. However, in the LKAG limit, i.e., with collinear order and negligible spin-orbit coupling, it has been observed (Liechtenstein, Katsnelson, and Gubanov, 1984) that they actually give rise to identical interaction parameters. When one studies the details of this limit, it turns out that this is slightly fortuitous. The mapping to the spin Hamiltonian \mathcal{H}_T based on one-site spin rotation resulted in the exchange parameters $J_{ij}^{(1)}$, $\vec{D}_{ij}^{(1)}$, and $\mathbb{A}_{ij}^{(1)}$, while a similar mapping based on two-site spin variations led to the parameters $J_{ij}^{(2)}$, $\vec{D}_{ij}^{(2)}$, and $\mathbb{A}_{ij}^{(2)}$. In the LKAG limit there is no spin or charge current present, and we can choose a global coordinate system in which the nonperturbed spin arrangement will point in the z direction. One has the freedom to restrict the small rotations to the x - z plane.

We start with the exchange parameters obtained from two-site variations. In this case we can see that the $J_{ij}^{(2)}$ parameter defined by Eq. (5.47) is reduced to

$$J_{ij}^{(2)} = -\frac{2}{\pi} \Im \int \text{Tr}_L (B_i G_{ij}^{00} B_j G_{ji}^{00} - B_i G_{ij}^{\pm 0} B_j G_{ji}^{\mp 0}) d\epsilon. \quad (5.51)$$

In the LKAG limit, $\vec{D}_{ij}^{(2)}$, as defined in Eq. (5.48), vanishes and the symmetric anisotropic interaction tensor $\mathbb{A}_{ij}^{(2)}$, as defined in Eq. (5.49), will only have one nonvanishing component $A_{ij}^{(2)zz}$ with a collinear magnetic order along the z direction. However, since the variation $\delta e_i^z = -(\delta\theta_i)^2/2$ is quadratic in the small rotation angle $\delta\theta_i$, this term gives a variation of fourth and not second order in the rotation angles.⁹ This means

⁹When $\delta\theta_i = -\delta\theta_j = \delta\theta$, then $\delta e_i^z \delta e_j^z$ is proportional to $(\delta\theta)^4$.

that only the first Heisenberg term of Eq. (5.46) is relevant, i.e., of second order in the variation angle. We introduce the notation $G_{ij}^\uparrow = G_{ij}^{00} + G_{ij}^{z0}$ and $G_{ij}^\downarrow = G_{ij}^{00} - G_{ij}^{z0}$. The LKAG exchange expression is then given in the following well-known form:

$$J_{ij}^{(2)} = -\frac{2}{\pi} \Im \int \text{Tr}_L(B_i G_{ij}^\uparrow B_j G_{ji}^\downarrow) d\epsilon. \quad (5.52)$$

We note here that, substituting Eq. (4.7) into Eq. (5.52) and integrating over energy, one arrives at an expression that is equivalent to Eq. (2.25) (Antropov, Katsnelson, and Liechtenstein, 1997). We also note that the leading term in the corresponding variation in the grand potential becomes

$$\delta\Omega^{\text{two}} \approx \frac{1}{2} \sum_{ij} J_{ij}^{(2)} \delta\theta_i \delta\theta_j. \quad (5.53)$$

In other words, only the on-site i - i term will have a factor 1/2 and the intersite terms will be given as shown in Eq. (3.12).

Next we focus on the parameters obtained from one-site variation in the absence of SOC. For a collinear order along z , one has to deal only with the component δe_i^z of the variation, and the second line in Eq. (5.40) is reduced to

$$\delta\Omega^{\text{one}} \approx -\sum_{ij} (J_{ij}^{(1)} + A_{ij}^{(1)zz}) (\delta\theta_i)^2 / 2. \quad (5.54)$$

In the nonrelativistic limit a global spin rotation, i.e., all $\delta\theta_i = \delta\theta$, is always a symmetry operation, which is now seen to appear as a nontrivial cancellation of the first- and second-order interactions from the consideration that

$$\begin{aligned} \delta\Omega &= \delta\Omega^{\text{one}} + \delta\Omega^{\text{two}} + \dots \\ &\approx -\frac{1}{2} \sum_{ij} (J_{ij}^{(1)} + A_{ij}^{(1)zz} - J_{ij}^{(2)}) (\delta\theta)^2 = 0, \end{aligned} \quad (5.55)$$

which is justified by inspection of Eqs. (5.40) and (5.51) considering the vanishing intersite Green's functions $\vec{G}^1 = G^{01} = 0$ in the LKAG limit. Another case in which there is a cancellation between first and second order is the case of rotation of the moment at a single site $i = 0$. We then note that in the LKAG limit the sum over all intersite exchange parameters $J_0 = \sum_{(0i)} J_{0i}^{(2)}$ is determined by a cancellation (Liechtenstein *et al.*, 1987) of $\delta\Omega_{\text{loc}}^{\text{one}}$ and $\delta\Omega_{\text{loc}}^{\text{two}}$ in the total variation of the grand potential, resulting in the following expression¹⁰:

¹⁰Note that the expressions on the first and second lines of Eq. (5.56) are proportional to $-(\delta\theta_0)^2$. This leads to a non-trivial expression for J_0 that depends exclusively on on-site Green's functions, which can be utilized in the testing of code implementations.

$$\begin{aligned} \delta\Omega^{\text{one}} + \delta\Omega_{\text{loc}}^{\text{two}} &= -\frac{2}{\pi} \Im \int \text{Tr}_L \left(B_0 \frac{G_{00}^\uparrow - G_{00}^\downarrow}{2} \frac{(\delta\theta_0)^2}{2} \right. \\ &\quad \left. + \frac{1}{2} B_0 G_{00}^\uparrow B_0 G_{00}^\downarrow (\delta\theta_0)^2 \right) d\epsilon \\ &= -\sum_{(0i)} 2(J_{0i}^{(1)} + A_{0i}^{(1)zz}) \frac{(\delta\theta_0)^2}{2} \\ &= -\sum_{(0i)} J_{0i}^{(2)} (\delta\theta_0)^2 = -J_0 (\delta\theta_0)^2. \end{aligned} \quad (5.56)$$

Note also that for a collinear state with SOC included the symmetric interactions still vanish at first order, while the asymmetric DM interaction will be finite in the absence of inversion symmetry. This nonvanishing torque leads to instabilities of collinear order such as ferromagnetic states that are unstable toward cycloidal order (Mankovsky and Ebert, 2017) or antiferromagnetic order that are unstable toward tilting, which might give rise to a weak ferromagnetic order (Solovyev, Hamada, and Terakura, 1996a; Mazurenko and Anisimov, 2005).

Finally, we note that the components of the DM vectors $\vec{D}_{ij}^{(1)}$ and $\vec{D}_{ij}^{(2)}$ are sums of two independent terms. Both terms are mediated by products of Green's functions such that one factor is density related and the other is current related, as indicated by the zero- and one-site exchange symmetry indices κ defined in Eqs. (5.24) and (5.42),(5.43),(5.44),(5.45),(5.46),(5.47),(5.48). This implies that, for a trivial topology with collinear spin arrangement, the DM term will vanish in the absence of SOC, as the current contributions are then prohibited, while for general noncollinear order these interactions are nonvanishing even in the absence of SOC. For the second term of the symmetric anisotropic interaction parameters $\mathbb{A}_{ij}^{(1)}$ and $\mathbb{A}_{ij}^{(2)}$ defined in Eqs. (5.43),(5.44),(5.45),(5.46),(5.47),(5.48),(5.49) is mediated by density-related spin-polarized Green's functions that exist for all magnetic order even in the absence of SOC. This term was investigated and discussed as an anisotropy anomaly by Lounis and Dederichs (2010).

We end this section with the comment that, for practical reasons, we give in Sec. VII numerical examples of exchange interactions that are based mostly on the equations obtained from the two-site energy variations. An exception is the results given in Fig. 13, where the first derivative of the grand potential with respect to the angle is shown.

J. Local versus global spin models

We comment here upon the distinction between local and global spin models proposed by Streib *et al.* (2021). Here we are focusing on spin models that are obtained within a generalization of the LKAG approach. This approach is still based on the fact that there is a perturbation that consists of small rotations of local moments in an already magnetic reference state. The generalization of LKAG is that the magnetic state is now allowed to have any noncollinear order and that relativistic effects, i.e., mainly spin-orbit coupling, are included, but only in a weak enough limit that the local moments are still well defined as spin moments. In such an approach the reference state will incorporate composed

Green's functions \vec{G}^0 , \vec{G}^1 , and G^0 that are directly dependent on the magnetic order. Hence, the mapped spin model is valid only locally on the energy versus configuration curve; i.e., it is relevant only for small magnetic variations around the reference state. This is in contrast to the concept of global spin models, which are supposed to be valid for all magnetically ordered states and the full curve of energy versus configuration.

The fact that the models are local implies that they do not have to fulfill global symmetry requirements. A magnetic state dependence of the interaction coefficients arises naturally for local models due to their dependence on the reference state (Cardias, Bergman *et al.*, 2020; Streib *et al.*, 2021). If the state dependence is taken into account for a local spin model, all global symmetries are recovered.

One way to avoid the reference state dependence is to start with a nonmagnetic reference state for which the Green's functions are independent of any magnetic state. In this approach (Brinker, Dias, and Lounis, 2019, 2020) there will be extensions of the formulas beyond bilinear interactions, which involve biquadratic effects with coupling terms like $\sum_{\langle ij \rangle} \mathcal{J}_{ij}^{\text{BQ}} (\vec{S}_i \cdot \vec{S}_j)^2$ and generalizations of it, i.e., $\sum_{\langle ijkl \rangle} \mathcal{J}_{ijkl}^{\text{Ring}} (\vec{S}_i \cdot \vec{S}_j)(\vec{S}_k \cdot \vec{S}_l)$, where i, j, k , and l are site indices. In such an approach the perturbations are proportional to the full spin-dependent potentials, and these larger perturbations in the series of equations (5.7) will generally be slowly convergent, so higher orders play a role.

These two approaches, with nonmagnetic and magnetic reference states, are in a sense complementary. While one approach includes the effects in terms of multispin interactions (Drautz and Fähnle, 2004; Mankovsky, Polesya, and Ebert, 2020b), the other approach includes the same effects within the composite Green's functions mediating the interaction. The first approach will have a large validity range, in favorable cases perhaps even global, but will be less accurate for any given magnetic state, while the second approach can calculate the interaction parameters accurately for any general magnetic order, but for only one local magnetic state at a time.

It is also important to realize that the existence of global spin models for itinerant-electron systems is not guaranteed, since there is no way to prove that the magnetic degrees of freedom can be globally described using a Hamiltonian dependent solely on spin operators. At the same time, at least for small frequencies and small wave vectors, any ferromagnetic system should be described by the macroscopic Landau-Lifshitz equation (Akhiezer, Bar'yakhtar, and Peletminskii, 1968; Vonsovskii, 1974; Aharoni, 2000). This means that at least the expression for the spin-wave stiffness constant based on small variations from the ferromagnetic ground state is always meaningful (Lichtenstein, Katsnelson, and Gubanov, 1984). Moreover, within local approximations such as dynamical mean-field theory (see Sec. V K) the expression for the spin-wave stiffness constant derived from magnetic force theorem becomes exact (Lichtenstein and Katsnelson, 2001).

K. Exchange interactions in correlated systems

To calculate the effective exchange interaction parameters for correlated magnetic systems, the dynamical mean-field

theory (DMFT) approach has been explored with a local frequency-dependent self-energy. The implementation of DMFT into DFT-based first-principles calculations (Lichtenstein and Katsnelson, 1998; Kotliar *et al.*, 2006) is based on the mapping to multiband Hubbard-like model. It assumes knowledge of effective parameters characterizing local Coulomb interactions (the problem involving the Hubbard U parameter). The state-of-the-art approach includes taking into account screening effects via the so-called constrained random phase approximation (cRPA) (Aryasetiawan *et al.*, 2004). Within this approach no arbitrary parameters are introduced and calculations remain fully first principles. Note that in the early days of this method U was frequently used as a fitting parameter. The historical developments of the method and its relations to the previous LDA + U formalism were discussed by Kotliar *et al.* (2006). What is important here is the statement that in principle DFT and DMFT can be combined in a fully *ab initio* way. The remaining questions on the applicability of cRPA for realistic situations were recently analyzed in detail by van Loon *et al.* (2021).

We first prove the analog of the local force theorem in DMFT-like theory (Katsnelson and Lichtenstein, 2000). Instead of working with the thermodynamic potential Ω as a density functional, we have to start with its general expression in terms of an exact Green's function (Luttinger and Ward, 1960; Kotliar *et al.*, 2006), i.e.,

$$\begin{aligned}\Omega &= \Omega_{\text{sp}} - \Omega_{\text{dc}}, \\ \Omega_{\text{sp}} &= -\text{Tr}\{\ln[\Sigma - G_0^{-1}]\}, \\ \Omega_{\text{dc}} &= \text{Tr}\Sigma G - \Phi,\end{aligned}\quad (5.57)$$

where G , G_0 , and Σ are an exact Green's function, its bare value, and its self-energy, respectively; Φ is the Luttinger generating functional (the sum of all connected skeleton diagrams without free legs); $\text{Tr} = \text{Tr}_{oiL\sigma}$ is the sum over Matsubara frequencies $\text{Tr}_{\omega} \cdots = T \sum_{\omega} \cdots$, $\omega = \pi T(2n + 1)$, and $n = 0, \pm 1, \dots$; and T is the temperature. Furthermore, $iL\sigma$ represents site numbers (i), orbital quantum numbers ($L = l, m$), and spin projections σ , respectively. The two Green's functions are related via the Dyson equation as

$$G^{-1} = G_0^{-1} - \Sigma, \quad (5.58)$$

with the important variational identity

$$\delta\Phi = \text{Tr}\Sigma\delta G. \quad (5.59)$$

We represent Eq. (5.57) as a difference of single-particle (sp) and double-counted (dc) terms, as usual in density functional theory. When quasiparticle damping is neglected, Ω_{sp} is simply the thermodynamic potential of “free” fermions but with exact quasiparticle energies. Suppose that we change the external potential by small spin rotations. The variation of the thermodynamic potential can then be written as

$$\delta\Omega = \delta^*\Omega_{\text{sp}} + \delta_1\Omega_{\text{sp}} - \delta\Omega_{\text{dc}}, \quad (5.60)$$

where δ^* is the variation without taking into account the change of the “self-consistent potential” (i.e., self-energy) and

δ_1 is the variation due to this change of Σ . When Eq. (5.59) is taken into account, it can be easily shown [see [Luttinger and Ward \(1960\)](#) and [Kotliar *et al.* \(2006\)](#)] that one can identify

$$\delta_1 \Omega_{\text{sp}} = \delta \Omega_{\text{dc}} = \text{Tr} G \delta \Sigma \quad (5.61)$$

and hence

$$\delta \Omega = \delta^* \Omega_{\text{sp}} = -\delta^* \text{Tr} \ln [\Sigma - G_0^{-1}], \quad (5.62)$$

which is an analog of the local force theorem in density functional theory ([Andersen *et al.*, 1980](#); [Mackintosh and Andersen, 1980](#); [Methfessel and Kübler, 1982](#); [Liechtenstein, Katsnelson, and Gubanov, 1984](#)).

In the DMFT scheme, the self-energy is local; i.e., it is diagonal in site indices. We write the spin-matrix structure of the self-energy and Green's function in the following form:

$$\begin{aligned} \Sigma_i &= \Sigma_i^c + \vec{\Sigma}_i^s \vec{\sigma}, \\ G_{ij} &= G_{ij}^c + \vec{G}_{ij}^s \vec{\sigma}, \end{aligned} \quad (5.63)$$

where $\Sigma_i^{(c,s)} = (1/2)(\Sigma_i^\uparrow \pm \Sigma_i^\downarrow)$ and $\vec{\Sigma}_i^s = \Sigma_i^s \vec{e}_i$, with \vec{e}_i the unit vector in the direction of the effective spin-dependent potential on site i and in the local moment approximation not depending on frequency (discussed further in [Sec. IX](#)), $G_{ij}^c = (1/2)\text{Tr}_\sigma(G_{ij})$, and $\vec{G}_{ij}^s = (1/2)\text{Tr}_\sigma(G_{ij}\vec{\sigma})$.

Following the general idea of infinitesimal rotation of local magnetic potential and self-energy, the effective exchange interactions in correlated magnetic systems can be obtained by rewriting all equations in this section with a substitution of Σ_i^s for B_i , leading to ([Katsnelson and Lichtenstein, 2000](#))

$$J_{ij} = 2\text{Tr}_{\omega L}(\Sigma_i^s G_{ij}^\uparrow \Sigma_j^s G_{ji}^\downarrow), \quad (5.64)$$

compared to [Eq. \(5.15\)](#). In the strong-coupling limit for the half-filled Hubbard model, [Eq. \(5.64\)](#) is reduced to the standard Anderson kinetic exchange t_{ij}^2/U ([Stepanov, Brener *et al.*, 2022](#)).

VI. BEYOND KINETIC EXCHANGE

We now return to a general discussion of exchange interactions within the formally rigorous scheme of the time-dependent density functional presented in [Sec. IE](#). In this approach, the entire dynamics of the many-electron system is described in terms of the time-dependent one-particle density matrix $\rho_{\alpha\beta}(\mathbf{r}, \mathbf{r}, t) = \langle \eta_\beta^\dagger(\mathbf{r}, t) \eta_\alpha(\mathbf{r}, t) \rangle$, where $\eta_\alpha(\mathbf{r}, t)$ is the annihilation operator for the electron at the point \mathbf{r} with spin projection α at the instant time t . Equivalently, one can introduce the charge $n(\mathbf{r}, t) = \text{Tr}_{L\sigma} \rho(\mathbf{r}, \mathbf{r}, t)$ and magnetization $\vec{m}(\mathbf{r}, t) = \text{Tr}_{L\sigma} \rho(\mathbf{r}, \mathbf{r}, t) \vec{\sigma}$ densities [also obtained in the time-independent case from [Eqs. \(2.11\)](#) and [\(2.12\)](#)]. In the adiabatic approximation, the spin and charge densities are expressed in terms of Kohn-Sham spinor eigenfunctions $\psi_{v\alpha}(\mathbf{r}, t)$ and the corresponding eigenenergies $\epsilon_v(t)$ satisfying the Kohn-Sham equations [\(2.1\)](#) and [\(2.14\)](#). The Kohn-Sham wave functions and the corresponding energies depend here on time due to the time dependence of the densities and

external field (the latter is supposed to be slowly varying in time compared to the characteristic electron energies).

Even in the local-density approximation there is a non-locality in the kinetic term in the total density functional, via nonlocality of the kinetic-energy term $T[\hat{\rho}]$, due to the non-locality of the Kohn-Sham states. The total effective magnetic field can be represented as

$$\vec{B}_{\text{tot}}(\mathbf{r}) = -\frac{\delta T}{\delta \vec{m}(\mathbf{r})} - \frac{\delta E_{\text{xc}}}{\delta \vec{m}(\mathbf{r})} + \vec{B}_{\text{ext}}(\mathbf{r}), \quad (6.1)$$

and the first term on the rhs of [Eq. \(6.1\)](#) depends on $\vec{m}(\mathbf{r}')$ at $\mathbf{r}' \neq \mathbf{r}$ even if the exchange-correlation term $\vec{B}_{\text{xc}}(\mathbf{r})$ is local. This leads to exchange interactions, i.e., a connection between magnetization direction in different points of space. In this sense, exchange parameters discussed thus far all correspond to kinetic, or indirect, exchange. Note that despite the fact that the GW approach formally goes beyond locality it deals with the nonlocality in charge density only, not that of the spin density. This means that within GW theory one has only kinetic exchange as well.

As discussed in [Sec. VII](#), the entire experience of calculations of exchange parameters via the LKAG formula or its extensions is that for many classes of systems it reproduces experimental data with good accuracy. This means that in most cases an indirect, that is, a kinetic, contribution to exchange interactions is dominant. There is nevertheless a natural question as to what exactly is neglected in this approach ([Katsnelson and Antropov, 2003](#)). To answer this question one needs to go beyond the local spin-density approximation and study the nonlocality of $\vec{B}_{\text{xc}}[\vec{m}]$.

There are many works on a general analysis of noncollinear magnetism within a density functional without a local spin-density approximation ([Heine and Samson, 1983](#); [Kübler *et al.*, 1988](#); [Nordström and Singh, 1996](#); [Kleinman, 1999](#); [Capelle, Vignale, and Györfy, 2001](#); [Capelle and Györfy, 2003](#); [Katsnelson and Antropov, 2003](#); [Peralta, Scuseria, and Frisch, 2007](#); [Sharma *et al.*, 2007, 2018](#); [Scalmani and Frisch, 2012](#); [Bulik *et al.*, 2013](#); [Eich and Gross, 2013](#); [Eich, Pittalis, and Vignale, 2013](#); [Kübler, 2017](#); [Ullrich, 2018](#)). Here we focus on only one aspect of this activity, namely, the applicability of the local spin-density approximation to the calculations of exchange parameters. To study this issue we need to investigate the origin of nonlocality in the exchange-correlation functionals.

At the construction of the local spin-density approximation, one starts with the calculation of the exchange-correlation energy for a homogeneous electron gas from a given charge and spin density. A natural step in studying its nonlocality is to replace this reference system with the simplest nonuniform state, namely, the electron gas in a spin-spiral state. This approach was suggested by [Kleinman \(1999\)](#) at the level of the Fock approximation, and by [Katsnelson and Antropov \(2003\)](#) at the level of the RPA. The latter was developed further and used in electronic structure calculations; see [Peralta, Scuseria, and Frisch \(2007\)](#), [Sharma *et al.* \(2007, 2018\)](#), [Scalmani and Frisch \(2012\)](#), [Bulik *et al.* \(2013\)](#), [Eich and Gross \(2013\)](#), [Eich, Pittalis, and Vignale \(2013\)](#), and [Ullrich \(2018\)](#). To illustrate the basic idea and some simple

estimations, we follow here the presentation of [Katsnelson and Antropov \(2003\)](#).

We now consider a homogeneous electron gas in the spin-density-wave (SDW) state. This is characterized by anomalous averages $s_{\mathbf{p}} = \langle c_{\mathbf{p}+\mathbf{Q}/2\uparrow}^{\dagger} c_{\mathbf{p}-\mathbf{Q}/2\downarrow} \rangle$, where $c_{\mathbf{p}\sigma}^{\dagger}$ and $c_{\mathbf{p}\sigma}$ are the creation and annihilation operators of electrons with momentum \mathbf{p} and spin projection σ . To consider a spin-density wave, it is convenient to use a spinor representation of the creation and annihilation operators similar to the Gorkov-Nambu formalism in the theory of superconductivity ([Vonsovsky, Izumov, and Kurmaev, 1982](#); [Schrieffer, 1999](#)). To this end, we introduce the spinor operator $\eta_{\mathbf{p}} = (c_{\mathbf{p}+\mathbf{Q}/2\uparrow}^{\dagger}, c_{\mathbf{p}-\mathbf{Q}/2\downarrow})$. The Hamiltonian of the homogeneous electron gas then takes the following form:

$$H = \sum_{\mathbf{p}} \eta_{\mathbf{p}} h_{\mathbf{p}} \eta_{\mathbf{p}} + \frac{1}{2} \sum_{\mathbf{q} \neq 0} \sum_{\mathbf{p}\mathbf{p}'} v_c(\mathbf{q}) (\eta_{\mathbf{p}+\mathbf{q}}^{\dagger} \eta_{\mathbf{p}}) (\eta_{\mathbf{p}'-\mathbf{q}}^{\dagger} \eta_{\mathbf{p}'}), \quad (6.2)$$

where $v_c(\mathbf{q}) = 4\pi e^2 / \mathbf{q}^2 V$, with V a volume, $h_{\mathbf{p}} = \theta_{\mathbf{p}} + \tau_{\mathbf{p}} \sigma_z - \Delta_{\mathbf{p}} \sigma_x$, and

$$\begin{aligned} \theta_{\mathbf{p}} &= \frac{1}{2}(\varepsilon_{\mathbf{p}+\mathbf{Q}/2} + \varepsilon_{\mathbf{p}-\mathbf{Q}/2}) = \mathbf{p}^2/2 + \mathbf{Q}^2/8 - \mu, \\ \tau_{\mathbf{p}} &= \frac{1}{2}(\varepsilon_{\mathbf{p}+\mathbf{Q}/2} - \varepsilon_{\mathbf{p}-\mathbf{Q}/2}) = \mathbf{p}\mathbf{Q}/2, \end{aligned} \quad (6.3)$$

where $\varepsilon_{\mathbf{p}} = \mathbf{p}^2/2 - \mu$ is the energy of the free electron and $2\Delta_{\mathbf{p}}$ is the antiferromagnetic gap related to the formation of the spin-density wave. Note that in this section we use the units $\hbar = m = 1$. In the Fock approximation the gap is equal to

$$\Delta_{\mathbf{p}} = \sum_{\mathbf{p}'} v_c(\mathbf{p} - \mathbf{p}') s_{\mathbf{p}'}. \quad (6.4)$$

To simplify the consideration as much as possible, one can replace v_c with an effective Stoner exchange splitting $I = (V_{\text{exc}}^{\uparrow} - V_{\text{exc}}^{\downarrow}) / (n_{\uparrow} - n_{\downarrow})$, where $V_{\text{exc}}^{\sigma} = \partial(n\varepsilon_{\text{exc}}) / \partial n_{\sigma}$. Equation (6.4) can then be replaced by $\Delta = I(n_{\uparrow} - n_{\downarrow})/2$, where Δ does not depend on \mathbf{p} .

To calculate the correlation contribution to the energy of the homogeneous electron gas, one can restrict oneself to the simplest meaningful approximation, namely, the RPA corresponding to the summation of all ‘‘bubble’’ diagrams ([Mahan, 2000](#); [Giuliani and Vignale, 2005](#)). The ‘‘bare’’ Green’s function in the Matsubara representation has the following form:

$$G(i\omega_m, \mathbf{p}) = \frac{1}{i\omega_m - h_{\mathbf{p}}} = \frac{i\omega_m - \theta_{\mathbf{p}} + \tau_{\mathbf{p}} \sigma_z - \Delta_{\mathbf{p}} \sigma_x}{(i\omega_m - \xi_{\mathbf{p}\uparrow})(i\omega_m - \xi_{\mathbf{p}\downarrow})}, \quad (6.5)$$

where $\xi_{\mathbf{p}\uparrow, \downarrow} = \theta_{\mathbf{p}} \mp E_{\mathbf{p}}$ is a quasiparticle spectrum for a SDW with $E_{\mathbf{p}} = \sqrt{\tau_{\mathbf{p}}^2 + \Delta^2}$. From Eq. (6.5) one can find the occupation number matrix

$$2N_{\mathbf{p}} = \left(1 + \frac{\tau_{\mathbf{p}} \sigma_z - \Delta \sigma_x}{E_{\mathbf{p}}}\right) f_{\mathbf{p}\uparrow} + \left(1 - \frac{\tau_{\mathbf{p}} \sigma_z - \Delta \sigma_x}{E_{\mathbf{p}}}\right) f_{\mathbf{p}\downarrow}, \quad (6.6)$$

where $f_{\mathbf{p}\sigma} = f(\xi_{\mathbf{p}\sigma})$ is a Fermi function. For the Fock contribution to the exchange-correlation energy one then has

$$\begin{aligned} E_{\text{Fock}} &= -\frac{1}{2} \sum_{\mathbf{p}\mathbf{p}'} v_c(\mathbf{p} - \mathbf{p}') \text{Tr}[N(\mathbf{p})N(\mathbf{p}')] \\ &= E_{\text{Fock}}^{(1)} + E_{\text{Fock}}^{(2)}, \end{aligned} \quad (6.7)$$

where

$$\begin{aligned} E_{\text{Fock}}^{(1)} &= -\frac{1}{4} \sum_{\mathbf{p}\mathbf{p}'\sigma} v_c(\mathbf{p} - \mathbf{p}') f_{\mathbf{p}\sigma} f_{\mathbf{p}'\sigma} \left(1 + \frac{\tau_{\mathbf{p}} \tau_{\mathbf{p}'} + \Delta^2}{E_{\mathbf{p}} E_{\mathbf{p}'}}\right), \\ E_{\text{Fock}}^{(2)} &= -\frac{1}{2} \sum_{\mathbf{p}\mathbf{p}'} v_c(\mathbf{p} - \mathbf{p}') f_{\mathbf{p}\uparrow} f_{\mathbf{p}'\downarrow} \left(1 - \frac{\tau_{\mathbf{p}} \tau_{\mathbf{p}'} + \Delta^2}{E_{\mathbf{p}} E_{\mathbf{p}'}}\right). \end{aligned} \quad (6.8)$$

Further, one may consider the case of small \mathbf{Q} only, which is sufficient for the calculation of the contributions to the spin-wave stiffness constant. The RPA-based calculations without this restriction were first performed by [Eich, Pittalis, and Vignale \(2013\)](#). Expansion of Eq. (6.7) up to \mathbf{Q}^2 leads to the corrections of the chemical potential (from the conservation of the number of particles),

$$\delta\tilde{\mu} = \tilde{\mu}_{\mathbf{Q}} - \tilde{\mu}_{\mathbf{Q}=0} = -\frac{\mathbf{Q}^2}{8F(n_{\uparrow}, n_{\downarrow})}, \quad (6.9)$$

and to the total energy,

$$\begin{aligned} \frac{E_{\text{Fock}}}{V} &= -\frac{e^2}{8\pi^3} \left\{ (p_{F\uparrow}^4 + p_{F\downarrow}^4) \right. \\ &\quad \left. - Q^2 \left[\left(\frac{1}{2F} - \frac{2}{3} \right) (p_{F\uparrow}^2 + p_{F\downarrow}^2) + \frac{(p_{F\uparrow} + p_{F\downarrow})^2}{12F^2} \right] \right\}, \end{aligned} \quad (6.10)$$

where $F = (p_{F\uparrow} + p_{F\downarrow})I(n_{\uparrow}, n_{\downarrow})/2\pi^2$ is a dimensionless Stoner enhancement factor, $p_{F\sigma} = (6\pi^2 n_{\sigma})^{1/3}$.

To treat the correlation effects, one may use RPA and sum up the bubble diagrams ([Mahan, 2000](#); [Giuliani and Vignale, 2005](#)). The corresponding expression is given as follows in terms of the empty-loop polarization operator:

$$\Pi(i\omega, \mathbf{q}) = -\text{Tr} \sum_{\mathbf{p}} T \sum_{\varepsilon_n} G(\mathbf{p} + \mathbf{q}, i\varepsilon_n + i\omega_n) G(\mathbf{p}, i\varepsilon_n). \quad (6.11)$$

The corresponding contribution to the Ω potential equals

$$\begin{aligned} \Omega_{\text{corr}} &= \sum_{\mathbf{q}} \int_{-\infty}^{\infty} \frac{d\omega}{4\pi} \left\{ \ln \left[\frac{1 + v_c(\mathbf{q}) \Pi(i\omega, \mathbf{q})}{1 + v_c(\mathbf{q}) \Pi_{\mathbf{Q}=0}(i\omega, \mathbf{q})} \right] \right. \\ &\quad \left. - v_c(\mathbf{q}) [\Pi(i\omega, \mathbf{q}) - \Pi_{\mathbf{Q}=0}(i\omega, \mathbf{q})] \right\}, \end{aligned} \quad (6.12)$$

where only the \mathbf{Q} -dependent part of the correlation energy was considered. Substituting Eq. (6.5) into Eq. (6.11), one finds that

$$\begin{aligned} \Pi(i\omega, \mathbf{q}) = & \frac{1}{2} \sum_{\mathbf{p}, \sigma} \left(1 + \frac{\tau_{\mathbf{p}} \tau_{\mathbf{p}+\mathbf{q}} + \Delta^2}{E_{\mathbf{p}} E_{\mathbf{p}+\mathbf{q}}} \right) \frac{f_{\mathbf{p}\sigma} - f_{\mathbf{p}+\mathbf{q}\sigma}}{i\omega + \xi_{\mathbf{p}\mathbf{q}\sigma} - \xi_{\mathbf{p}\sigma}} \\ & + 2 \sum_{\mathbf{p}} \left(1 - \frac{\tau_{\mathbf{p}} \tau_{\mathbf{p}+\mathbf{q}} + \Delta^2}{E_{\mathbf{p}} E_{\mathbf{p}+\mathbf{q}}} \right) \frac{f_{\mathbf{p}\uparrow} - f_{\mathbf{p}+\mathbf{q}\downarrow}}{i\omega + \xi_{\mathbf{p}+\mathbf{q}\downarrow} - \xi_{\mathbf{p}\uparrow}}. \end{aligned} \quad (6.13)$$

The corresponding exchange-correlation addition to the spin-wave spectrum at finite \mathbf{Q} can be written as

$$\delta\omega_{\mathbf{Q}} = \frac{4}{M} [E_{\text{SDW}}(\mathbf{Q}) - E_{\text{SDW}}(0)], \quad (6.14)$$

where $E_{\text{SDW}}(\mathbf{Q})$ is the total energy of the spin spiral and M is the magnetic moment of the unit cell.

The next step is to restore the expression of the exchange-correlation functional corresponding to Eq. (6.14). The simplest rotational invariant expression has the form

$$E_{\text{exc}} = \int d\mathbf{r} \{ n\epsilon_{\text{exc}}(n_{\uparrow}, n_{\downarrow}) + \lambda(n_{\uparrow}, n_{\downarrow})D \}, \quad (6.15)$$

where $D = (\nabla_{\alpha} e_{\beta})(\nabla_{\alpha} e_{\beta}) = (\nabla\theta)^2 + \sin^2\theta(\nabla\varphi)^2$ is the rotational invariant of lowest order. Here $\vec{e} = \vec{m}/|\vec{m}| \equiv (\sin\theta \cos\varphi, \sin\theta \sin\varphi, \cos\theta)$. More detailed analysis of the functional dependence in the general density functional was given by Sharma *et al.* (2007), Scalmani and Frisch (2012), Bulik *et al.* (2013), Eich and Gross (2013), Eich, Pittalis, and Vignale (2013), and Ullrich (2018). Based on the analysis of Fock and random phase approximation (RPA) expressions for the total energy of the spin-spiral state, the following expression for λ was suggested by Katsnelson and Antropov (2003):

$$\lambda(n_{\uparrow}, n_{\downarrow}) = -\frac{e^2}{16\pi^2} \left(\frac{1}{F} - \frac{4}{3} \right) (V_{\text{exc}}^{\uparrow} P_{F\uparrow} - V_{\text{exc}}^{\downarrow} P_{F\downarrow}) + \frac{e^2}{96\pi^3 F^2}. \quad (6.16)$$

To evaluate the importance of the nonlocality of the exchange-correlation functional for the exchange parameters, one can calculate the corresponding contribution to the spin-wave stiffness constant, which can be expressed as

$$D = \frac{4}{M} \left[\lim_{\mathbf{Q} \rightarrow 0} \frac{E_{\text{SDW}}(\mathbf{Q}) - E_{\text{SDW}}(0)}{\mathbf{Q}^2} \right]. \quad (6.17)$$

Namely, Eq. (6.15) gives

$$\delta D = \frac{4}{M} \int d\mathbf{r} \lambda(n_{\uparrow}, n_{\downarrow}), \quad (6.18)$$

with integration over the entire elementary cell. The numerical calculations for the case of Fe and Ni performed by Katsnelson and Antropov (2003) led to the following results: whereas the standard local-spin-density approximation gave the values 239 and 692 meV \AA^2 for D in bcc Fe and fcc Ni, respectively, the corrections [Eq. (6.18)] for δD were equal to 13 and 45 meV \AA^2 , respectively. Hence, the total D became

253 and 735 meV \AA^2 for bcc Fe and fcc Ni, respectively. Thus, for these materials, which serve as important systems for testing theoretical models, the indirect kinetic contributions are much larger than the direct contributions from the nonlocality of the exchange-correlation functional.

In the model approach (for instance, a tight-binding one), direct exchange enters the Hamiltonian straightforwardly via the matrix elements

$$\begin{aligned} J_{ij} = & \langle ij | v | ji \rangle \\ = & \int d\mathbf{r} d\mathbf{r}' \psi_i^*(\mathbf{r}) \psi_j^*(\mathbf{r}') v(\mathbf{r} - \mathbf{r}') \psi_j(\mathbf{r}) \psi_i(\mathbf{r}'), \end{aligned} \quad (6.19)$$

where $v(\mathbf{r} - \mathbf{r}')$ is the effective potential of the electron-electron interaction (in the simplest approximation, just Coulomb interaction). In most cases this contribution is supposed to be irrelevant, but in some cases it is claimed that this interaction is important and can even change the calculated magnetic ground state (for instance, it can transform a spin-spiral state into a ferromagnet). Examples include single-side hydrogenated graphene (Mazurenko *et al.*, 2016) and half-metallic CrO₂ (Solovyev, Kashin, and Mazurenko, 2015). The direct exchange interaction is also relevant in single-side fluorinated graphene (Mazurenko *et al.*, 2016) and fourth-group adatoms at the surface of Si(111) (Badrtdinov *et al.*, 2016) and SiC(0001) (Badrtdinov *et al.*, 2018). Whereas *sp*-bonded magnets may be considered an exotic exception, the example of CrO₂ demonstrates that this issue is not completely clear even for conventional 3*d*-electron magnets and requires a careful investigation.

VII. NUMERICAL EXAMPLES OF INTERATOMIC EXCHANGE

In this section we provide examples of numerical calculations of interatomic exchange interactions as well as magnetic moments for several classes of materials. Reviews of theoretical results of magnetic materials have previously been published, albeit with different foci than this review. However, it is noteworthy that Mohn (2006), Eriksson *et al.* (2017), and Kübler (2017) made a comparison between experiment and theory regarding bulk magnetic moments, with some of the results shown in Fig. 2. In general, DFT calculations reproduce experimental magnetic moments with an error that seldom exceeds 5%, in particular, for transition metal elements and their intermetallic compounds. Since reviews of magnetic moments have already been published, we focus in this section on results of the interatomic exchange. Kübler (2017) reviewed results of interlayer exchange interactions of magnetic multilayers, as well as magnon dispersion from spin-spiral calculations (Kübler *et al.*, 1988; Sandratskii, 1991, 1998; Halilov *et al.*, 1998; Sandratskii and Bruno, 2002; Jakobsson *et al.*, 2015). Results for thin films were reviewed by Etz *et al.* (2015), who compared magnon measurements based on spin-polarized electron energy loss spectroscopy (SPEELS) to adiabatic magnon spectra evaluated from explicit calculations of interatomic exchange. Finally, we note that Sato *et al.* (2010) conducted a full review of the magnetic properties, including explicit calculations of interatomic

exchange of diluted magnetic semiconductors. We also note here that the most direct comparison between experiment and theory of interatomic exchange interactions is likely to be the magnon dispersion. This is in contrast to estimates of the Curie temperature, which in principle also reflects the strength of the interatomic exchange. However, most of the DFT calculations of interatomic exchange are carried out at low (in fact zero) temperature, which challenges a comparison for results at finite temperature. If the exchange interaction were not dependent on temperature (or magnetic configuration), a comparison to experimental results at finite temperature, such as the ordering temperature, would not be problematic. Although most materials do have an interatomic exchange that depends on temperature, there has been progress in calculations of configuration-dependent exchanges and magnetic properties at finite temperature, as discussed in Sec. V. Before entering details of material specific results of interatomic exchange, we note that since we give examples from previously published works there will be a mixture of units presented. In particular, energy is in some works given in eV and sometimes in rydbergs. We have, however, been consistent with the definition of the spin Hamiltonian introduced in Sec. I, which means that a negative value of the interatomic exchange corresponds to a ferromagnetic coupling.

Early implementations of the explicit method, i.e., Eq. (5.52), were incorporated in the linear muffin-tin orbital (LMTO) (Andersen and Jepsen, 1984) and Korringa-Kohn-Rostoker (KKR) (Korringa, 1947; Kohn and Rostoker, 1954) electronic structure methods. Both approaches were first formulated within either the muffin-tin (MT) or the atomic sphere approximation (ASA), where the potential inside each sphere is assumed to be spherically symmetric. For close-packed systems this is a reasonable approximation, and the results were consistent. However, with the development of so-called full-potential electronic structure methods, which are free from geometrical constraints of the self-consistent density and potential, it quickly became clear that for more loosely packed, or low-dimensional, systems, this level of approximation is needed. There are several *ab initio* implementations, using different basis functions, that employ a full-potential approach. However, note that the computationally much more efficient ASA calculations are still being pursued with good accuracy, especially for close-packed systems.

The greatest advantage of ASA-based codes is the compact representation of the basis functions, which are atom centered and have a well-defined angular momentum character. This is convenient for implementation of the magnetic force theorem, which operates with quantities that have a site index i attached (Sec. V). In the full-potential codes the basis set is more extended and a minimal basis set is generally avoided. In this case, the problem of defining a good representation of the local basis [see Eq. (4.9)] becomes less obvious and generally does not have a unique solution. This issue sometimes hinders a proper quantitative comparison between the results obtained with various codes or even implementations within a given code.

When one evaluates the interatomic exchange interaction between two atoms, the resulting values may depend on the choice of orbitals that represent these atoms; see Han, Ozaki, and Yu (2004) and Yoon *et al.* (2018). This issue was

discussed in detail by Kvashnin, Grånäs *et al.* (2015) and Steenbock *et al.* (2015), where the comparison between the J_{ij} 's obtained with the projection on the muffin-tin sphere and Löwdin-orthogonalized orbitals were presented. Overall, the results for fcc Ni and hcp Gd have been consistent, but in general it is found that, depending on the system, there may be an unwanted sensitivity to the projection. Moreover, strong covalent bonding between $3d$ and ligand states also calls either for perturbing the spins of the hybrid orbitals or for explicit treatment of ligand spins as a stand-alone entity (Logemann *et al.*, 2017, 2018; Solovyev, 2021).

One commonly used choice is to use Wannier functions to obtain a localized basis for the J_{ij} calculations (Rudenko *et al.*, 2013; Korotin *et al.*, 2015; Logemann *et al.*, 2018; Zhu, Edström, and Ederer, 2020). In particular, maximally localized Wannier functions (Marzari *et al.*, 2012) form an appealing basis set that is well defined for a given set of bands and thus enables the comparison of the magnetic interactions obtained with different DFT codes. There are a couple of versatile software applications that allow one to apply the present formalism for an arbitrary tight-binding Hamiltonian independent of the chosen projection scheme (Yoon *et al.*, 2020; He *et al.*, 2021). Keeping these issues in mind, we now proceed with a discussion of calculated results of interatomic exchange for several classes of magnetic materials.

A. Elemental transition metals

One of the most important test cases for explicit calculations of interatomic exchange is the ability to quantitatively reproduce magnetic properties such as spin-wave dispersion and ordering temperature of the three ferromagnetic $3d$ elements: bcc Fe, hcp Co, and fcc Ni. The spin-wave stiffness D of bcc Fe was evaluated in the original articles with explicit calculations of interatomic exchange (Liechtenstein, Katsnelson, and Gubanov, 1984; Liechtenstein *et al.*, 1987). In these works, the interaction between the first two coordination shells was calculated for bcc Fe. The dominant, nearest-neighbor (NN) coupling was found to be FM, while the next NN coupling was found to be antiferromagnetic and much smaller. The obtained value of the spin-wave stiffness D was 294 meV Å² for bcc Fe, which is in good agreement with experimental values that range from 305 (You *et al.*, 1980) to 314 meV Å² (Stringfellow, 1968). This initial result proved the formalism described in detail in Sec. V to be highly promising. The formula for calculating the Heisenberg exchange J_{ij} also allowed Liechtenstein, Katsnelson, and Gubanov (1984) and Liechtenstein *et al.* (1987) to evaluate D as a function of the upper integration limit, which can be viewed as the position of the Fermi level; see Fig. 8. This provides valuable information on how D can be affected by doping of the material. In particular, as one changes the Fermi level to arrive at the half-filled $3d$ shell, at around -1 to -3 eV in Fig. 8, D takes negative values, indicating that the FM reference state becomes unstable.

Liechtenstein, Katsnelson, and Gubanov (1984) and Liechtenstein *et al.* (1987) argued that the NN exchange coupling primarily determines the value of spin-wave stiffness. The interactions with the neighbors beyond the second

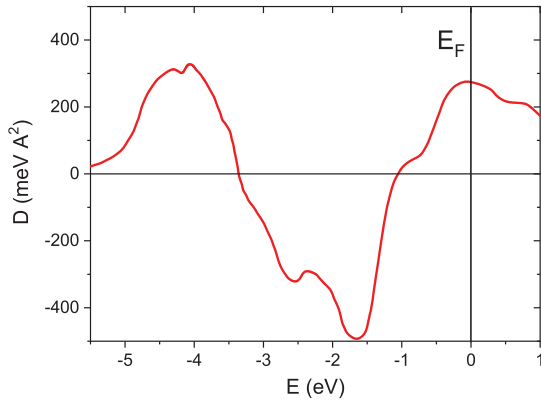


FIG. 8. Spin-wave stiffness in bcc Fe as a function of the upper integration limit. Adapted from Liechtenstein, Katsnelson, and Gubanov, 1984.

coordination shell were not computed, as their contribution to D was expected to be negligibly small due to their oscillatory sign (Oguchi, Terakura, and Hamada, 1983). However, later it was shown that the magnetic interactions in elemental transition metals are in fact extremely long range (Antropov, Harmon, and Smirnov, 1999; van Schilfgaarde and Antropov, 1999; Frota-Pessôa, Muniz, and Kudrnovský, 2000), and obtaining a well-converged value of the spin-wave stiffness was indeed found to be extremely difficult (Antropov, Harmon, and Smirnov, 1999; van Schilfgaarde and Antropov, 1999).

Pajda *et al.* (2001) made a substantial advancement in that direction by performing a thorough study of spin waves and ordering temperatures, calculated from explicit values of J_{ij} , for bcc Fe, fcc Co, and fcc Ni. Their calculations were performed using a tight-binding LMTO method (Andersen and Jepsen, 1984). This work was done using the full set of valence states (spd basis) and a fine k -point mesh. For a magnetic material with one atom per unit cell, the spin-wave dispersion is governed by the exchange couplings J_{ij} in the following manner:

$$\omega(\mathbf{q}) = \frac{4}{M} \sum_j J_{ij} [1 - \exp(i\mathbf{q} \cdot \mathbf{R}_{ij})], \quad (7.1)$$

where M is the value of the saturated magnetic moment. Since the real-space values of J_{ij} 's are involved, the summation has to be truncated. Pajda *et al.* (2001) considered interactions with 195 and 172 shells for bcc and fcc metals, respectively, in order to ensure that the spin-wave dispersions are converged. The obtained dispersion for fcc Ni is shown in Fig. 9. The experimental data obtained with inelastic neutron scattering are also shown for comparison. Since the experimental spin waves become damped for higher values of q , it is possible to compare experiments and theory only in a region around the zone center and, as Fig. 9 shows, in this regime the agreement between theory and experiment is impressive. Results of similar accuracy were obtained from spin-spiral calculations (Kübler, 2017), and it is reassuring that DFT calculations of interatomic exchange obtained from different methods give similar results. In fact, a direct comparison between the two

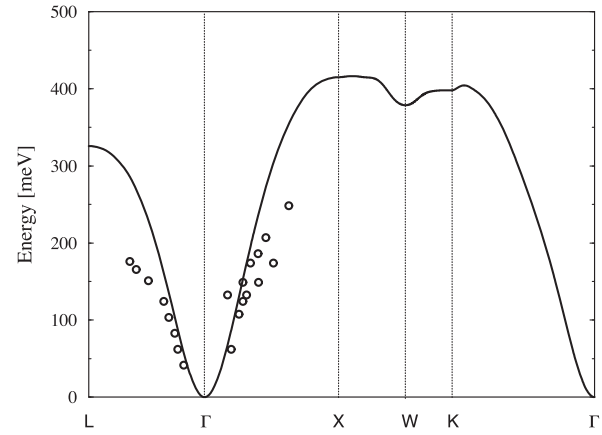


FIG. 9. Calculated spin-wave dispersion relation of fcc Ni from Pajda *et al.* (2001). Experimental data are from Mook and Paul (1985).

methods was made for bcc Fe, with similar results (Bergqvist, 2005).

In Fig. 9 experimental data are shown only for fcc Ni. This is due primarily to the fact that it is difficult to measure inelastic scattering of polarized neutrons of Co owing to the strong self-absorption effect. In addition, the crystal structure of bulk Co is hcp, not fcc. However, as reviewed by Etz *et al.* (2015), experimental results of the magnon dispersion have been published for thin films of Co (in the fcc structure) as an overlayer of, for instance, Cu (001). For these systems, one can also find good agreement between theory and experiments. The results for thin films of fcc Co were also reported by Liu *et al.* (1996), Vollmer *et al.* (2003, 2004), and Balashov *et al.* (2014), with good agreement between theory and observations.

Since this review focuses on the explicit method, in Fig. 10 we compare selected, calculated interatomic exchange parameters of bcc Fe, which is a common test material in the case of code implementations. The exchange parameters in Fig. 10 are calculated by Eq. (5.52); however, the actual electronic structure methods used, energy functionals employed, and details of the implementations differ in the different investigations reported. This causes some differences among the various investigations. The first-nearest-neighbor couplings [and here using the form of the Heisenberg Hamiltonian in Eq. (1.3)] were obtained as -1.97 (Morán, Ederer, and Fähnle, 2003), -2.86 (Pajda *et al.*, 2001), -2.40 (Frota-Pessôa, Muniz, and Kudrnovský, 2000), -2.44 (Antropov, Harmon, and Smirnov, 1999), -1.90 (Mankovsky, Polesya, and Ebert, 2020a), and -1.90 mRy (Kvashnin *et al.*, 2016). These data, together with interactions at longer distances, are shown in Fig. 10. Note from the figure that the general behavior of the interatomic exchange interaction as a function of distance between atoms is similar for all reported studies. The strongest interactions are between nearest neighbors, followed by that from next nearest neighbors, while longer range interactions are in all published studies much weaker. Figure 10 also shows that differences in the value of interatomic exchange varies between the published results, which reflects the sensitivity of this parameter with respect to computational details (basis set, energy functional, etc.). Another relevant parameter that is extracted from a set of interatomic exchange is the total

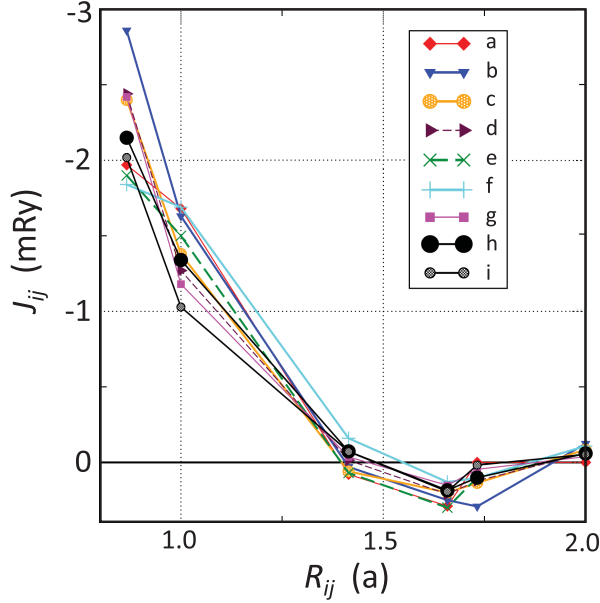


FIG. 10. Interatomic exchange parameters in bulk bcc Fe calculated from Eq. (5.52) with different code implementations. (a) Denoted by red squares, a tight-binding (TB) LMTO-ASA method was used by Morán, Ederer, and Fähnle (2003). (b) Another TB LMTO method was used by Pajda *et al.* (2001). (c) Results obtained using a real-space LMTO-ASA code by Frota-Pessôa, Muniz, and Kudrnovský (2000). Other real-space LMTO-ASA calculations made by (d) Antropov, Harmon, and Smirnov (1999) and (e) van Schilfhaarde and Antropov (1999). (f) Real-space tight-binding framework used by Spišák and Hafner (1997). (g) LDA++ approach used for the first time by Katsnelson and Lichtenstein (2000). (h) Full-potential, relativistic calculation (RSPt) was used with an extended basis and in (i) RSPt was used by with a minimal basis (unpublished). Note that $J_1 = -1.9$ mRy was found using a KKR calculation by Mankovsky, Polesya, and Ebert (2020a).

exchange value $J_0 = \sum_{(0i)} J_{0i}$ given by Eq. (5.56). Values for J_0 were found to be -10.00 (Sakuma, 1999), -11.03 (Frota-Pessôa, Muniz, and Kudrnovský, 2000), -12.20 (Katsnelson and Lichtenstein, 2000), and -13.58 mRy (Pajda *et al.*, 2001). These values vary approximately with the same amount as the values in Fig. 10, which seems natural. Note that all numerical values that we report here are adjusted¹¹ to the spin Hamiltonian of Eq. (1.3). More details on this issue are given in Sec. IE.

Pajda *et al.* (2001) discussed the long-range character of the oscillations in detail. Using stationary phase approximation and the asymptotic behavior of the intersite Green's function, the long-range character of the J_{ij} 's was shown to be of the following form:

$$J_{ij} \propto \Im \frac{\exp \{i[(\mathbf{k}_F^\uparrow + \mathbf{k}_F^\downarrow)\mathbf{R}_{ij} + \Phi^\uparrow + \Phi^\downarrow]\}}{R_{ij}^3}, \quad (7.2)$$

¹¹In many cases one can find $-(1/2)J_{ij}$ values in the literature where the nomenclature differs.

where \mathbf{k}_F is the wave vector of energy E_F having the direction such that the associated group velocity is parallel to \mathbf{R}_{ij} , Φ is an additional phase factor, and \uparrow and \downarrow denote spin projections. For weak itinerant-electron ferromagnets, which have both spin-up (majority) and spin-down (minority) bands partially occupied, the Fermi wave vectors are real and one recovers the oscillatory exchange interaction, known as the RKKY mechanism of indirect exchange (Ruderman and Kittel, 1954). At the same time, if one of the spin channels is completely empty or filled, the Fermi wave vector becomes imaginary $\mathbf{k}_F = i\kappa_F$, which in turn results in the evanescence of the J_{ij} 's. Thus, in weak ferromagnets one can expect more long-range magnetic interactions than in half metals or strong ferromagnets, which have a filled majority band. This result also provides an explanation for why bcc Fe, as a weak ferromagnet, shows much more pronounced Kohn anomalies in the spin-wave spectra than Co and Ni (Halilov *et al.*, 1998).

Pajda *et al.* (2001) demonstrated that the interactions with distant neighbors must be taken into account when one calculates the spin-wave stiffness. However, by considering interactions between distant atoms (which are more than six lattice constants apart), one finds that the value of D keeps oscillating as more coordination shells are taken in the summation. The reason for this is that the expression for D includes a term R_{ij}^2 ; see Eq. (7.3). The J_{ij} 's have at worst (from a summation point of view) an R_{ij}^{-3} dependence [Eq. (7.2)]. As a result, the numerical convergence of D is problematic. One solution to this problem was proposed by Pajda *et al.* (2001). It was suggested that the expression for spin-wave stiffness can be regularized by introducing an additional decay factor η , which ensures its convergence at large distances. Thus, the $D(\eta)$ is then defined as

$$D(\eta) = \lim_{R_{\max} \rightarrow \infty} \frac{2}{3M} \sum_{R_{ij} \leq R_{\max}} J_{ij} R_{ij}^2 e^{-\eta R_{ij}/a}, \quad (7.3)$$

and the spin-wave stiffness is finally calculated by taking the limit of η going to zero:

$$D = \lim_{\eta \rightarrow 0} D(\eta). \quad (7.4)$$

The obtained values are shown in Table I. They show systematic good agreement with experimental data measured by different techniques. In Table I we also show the experimental

TABLE I. Calculated and measured values of spin-wave stiffness in elemental ferromagnets in meV Å².

Metal	D_{theo} (Pajda <i>et al.</i> , 2001)	D_{exp}
Fe (bcc)	250 ± 7	281, ^a 266, ^b 256 ^b
Co (fcc)	663 ± 6	384, ^b 371, ^b 466, ^c 435, ^d 580 ^e
Ni (fcc)	756 ± 29	374, ^b 403, ^b 555 ^f

^aFrom Shirane, Minkiewicz, and Nathans (1968).

^bFrom Pickart *et al.* (1967) and references therein.

^cFrom Liu *et al.* (1996) (thin films).

^dhcp Co. From Liu *et al.* (1996).

^ehcp Co. From Pauthenet (1982).

^fFrom Mook, Lynn, and Nicklow (1973).

results for hcp Co. The magnetic interactions in hcp Co were calculated in several studies (van Schilfgaarde and Antropov, 1999; Turek, Kudrnovský, Drchal *et al.*, 2003; Kvashnin, Sun *et al.*, 2015). In one of the more recent works the spin-wave excitations and T_c were calculated by means of atomistic spin-dynamics simulations, and excellent agreement with experiment for both properties was reported (Chimata *et al.*, 2017).

The magnetic ordering temperatures of the three FM metals have also been calculated from several different approaches: mean-field approximation (MFA), Tiablikov's decoupling scheme [also known as RPA (Tiablikov, 2013)], classical Monte Carlo simulations, or atomistic spin dynamics (Turzhevskii, Liechtenstein, and Katsnelson, 1990; Antropov *et al.*, 1995, 1996; Evans *et al.*, 2014; Eriksson *et al.*, 2017; Shirinyan *et al.*, 2019), where the last reference uses unsupervised machine learning. The MFA values for bcc Fe and fcc Co were reported to be in reasonably good agreement with experiment. For instance, for Fe it was found to be ~ 1400 K, while the experimental value is 1045 K (Pajda *et al.*, 2001). Given the fact that MFA is known to overestimate the values by roughly 30% compared to the more accurate Monte Carlo method (Binder and Heermann, 2010), the calculated value is close to what should be expected.

The calculations for fcc Ni suggested T_c values of about 397 K in MFA and 350 K in RPA (Pajda *et al.*, 2001), which are much smaller than the experimental value of about 630 K. This underestimation was already reported by Liechtenstein *et al.* (1987) and van Schilfgaarde and Antropov (1999). On the contrary, the spin-wave stiffness is overestimated compared to the experiment. This suggests that the inconsistency of the results for Ni cannot be circumvented by a simple rescaling of the exchange integrals.

The problem related to describing magnetic excitations in fcc Ni has been addressed for a long time. Bruno (2003) suggested that the corrections to the LKAG formula due to transverse constraining fields become substantial when the exchange splitting is small and becomes comparable with magnon energies, as discussed in Sec. 1E. This is indeed the case for fcc Ni, whose saturated magnetic moment amounts to roughly $0.6\mu_B$ per atom, indicating that the splitting between spin-up and spin-down bands is the smallest among three elemental magnets, as shown by Singer, Fähnle, and Bihlmayer (2005). Using renormalized values of exchange parameters, it was shown that the MFA-based T_c estimates can be substantially improved (Bruno, 2003). At the same time, the employed corrections were shown not to modify the magnon spectrum (Katsnelson and Lichtenstein, 2004), such that the good agreement between theory and experiment remained (Fig. 9).

However, as discussed, the Ni case also raises questions as to whether the small moment of Ni can be treated classically. In addition, the values of the magnetic moments in fcc Ni significantly depend on the magnetic configuration, and this dependence is much more pronounced than in bcc Fe (Turzhevskii, Liechtenstein, and Katsnelson, 1990; Rosengaard and Johansson, 1997; Antropov, Harmon, and Smirnov, 1999). The best gauge for estimating the accuracy of an interatomic exchange of fcc Ni is to compare magnon dispersion, as opposed to the Curie temperature.

Since both the calculated magnetic moments and the interatomic exchange integrals depend on the reference state, the spin stiffness should be better described by the set of J_{ij} 's extracted from the ordered magnetic ground state, while T_c should be estimated using a magnetic configuration found at the ordering temperature (Ruban *et al.*, 2004; Shallcross *et al.*, 2005). The problem is that representing such a state in DFT calculations is not straightforward. In the so-called disordered local moment picture discussed in Sec. VII D, the magnetic moments experience a completely spin-disordered environment introduced via the coherent potential approximation (CPA) (Soven, 1967; Elliott, Krumhansl, and Leath, 1974; Kakehashi, 1992). However, in these calculations the local moment in fcc Ni collapses to zero (Shallcross *et al.*, 2005), in contrast to observations. A generalized Heisenberg model that not only takes into account the short-range order effects (Antropov, 2005) but also allows the magnetic moments to change their magnitude, i.e., introduces longitudinal spin fluctuations, was proposed by Rosengaard and Johansson (1997), Ruban *et al.* (2007), and Wysocki, Glasbrenner, and Belashchenko (2008). This model indicates that the calculated T_c values of bcc Fe and fcc Ni are in good agreement with the experimental values.

In general, interatomic exchange is a quantity that critically depends on the details of the electronic structure. The results discussed thus far were obtained employing the LSDA or the similar, spin-polarized generalized gradient approximation (GGA). Electron correlations beyond the LSDA and GGA can be captured by means of a combination of DFT and dynamical mean-field theory (Georges *et al.*, 1996; Lichtenstein and Katsnelson, 1998; Kotliar *et al.*, 2006). Katsnelson and Lichtenstein (2000) used this method to calculate interatomic exchange. It was shown that taking into account local correlations of bcc Fe will influence both the local magnetic moment and J_{ij} .

The results shown in Fig. 11 indicate that the calculation of the spin-wave stiffness in bcc Fe, obtained using the LSDA, is different from results of DFT + DMFT (by roughly 20%). We note that the starting point for these calculations was a nonmagnetic DFT solution, and therefore the local exchange splitting emerges purely from DMFT and is governed by the Hubbard U term. However, it was shown that if one starts with magnetic DFT and performs DMFT calculations in addition, then the differences between the LSDA and LSDA + DMFT results are modest (Kvashnin, Grånäs *et al.*, 2015). This is related partly to the fact that the exchange splitting is introduced by the LSDA and does not change much after U is explicitly added to consideration. In the case of moderate correlation strength, the overall differences in the total exchange interaction J_0 are related to the quasiparticle's mass renormalization, which is brought about by electron-electron interactions (Mazurenko *et al.*, 2013). However, since orbitals of different symmetries have different effective masses, the overall impact of dynamical correlations on each individual J_{ij} is more sophisticated. Borisov *et al.* (2021) showed that dynamical correlations, as described by DMFT, can produce an up to 30% variation of the leading Heisenberg and DM exchange interactions. This was exemplified by a study of intermetallic compounds such as CoPt and FePt and MnSi and

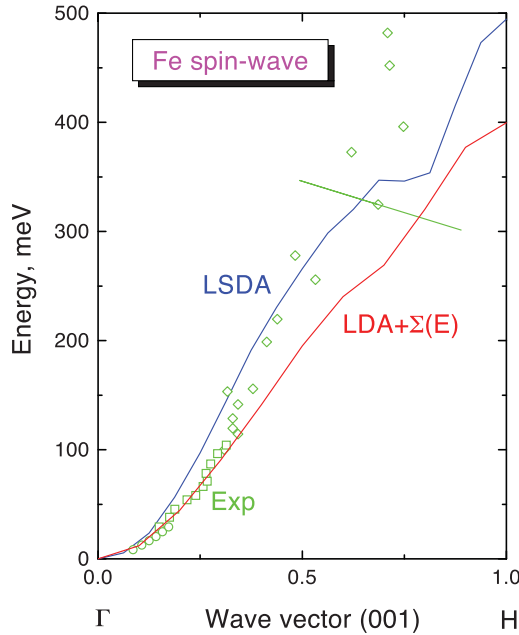


FIG. 11. Spin-wave dispersion in bcc Fe as obtained from DFT + DMFT [referred to as LDA + $\Sigma(E)$] and spin-polarized DFT (LSDA) calculations. From Katsnelson and Lichtenstein, 2000.

FeGe, as well as transition metal bilayers Co/Pt(111) and Mn/W(001). Furthermore, nonlocal correlations modeled on the *GW* level have also been made for Fe, Co, and Ni (Yoon *et al.*, 2019), albeit with marginal changes in the Heisenberg exchange.

An advantage of the formalism of explicit calculation of the J_{ij} parameters is that one can perform orbital-by-orbital decomposition of each magnetic coupling. This decomposition is possible since in the LKAG formula [given by Eq. (5.52)] Tr_L can first be taken over just a part of the orbitals, i.e., one can analyze the individual orbital contributions of the exchange parameter. In a cubic material one can then follow the coupling between different irreducible representations of the *3d* orbitals (E_g and T_{2g}). This turns out to be a powerful tool for obtaining a microscopic understanding of the nature of magnetic interactions. To be specific, if the material has cubic symmetry, the *d* orbitals split into E_g and T_{2g} manifolds. In the basis of cubic harmonics, the local exchange splitting becomes a diagonal matrix and the exchange interaction can be represented as a sum of orbital contributions $J_{ij}^{mm'}$, where an orbital m on the site i is coupled to each orbital m' on the site j . In the cubic system it is therefore natural to group these terms into three contributions,

$$J_{ij} = J_{ij}^{E_g-E_g} + J_{ij}^{E_g-T_{2g}} + J_{ij}^{T_{2g}-T_{2g}}, \quad (7.5)$$

which combine the individual orbital contributions according to the symmetry of the *d* orbitals involved. Kvashnin *et al.* (2016) performed this orbital decomposition of the NN exchange integral for a series of transition metal alloys in the bcc structure. The results, which are shown in Fig. 12, reveal that in the cases of Mn and Fe there is strong competition between different terms having opposite (FM

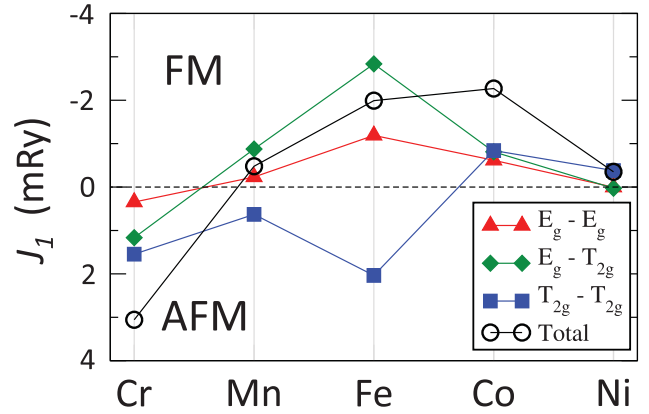


FIG. 12. Calculated orbital-decomposed first-nearest-neighbor exchange interaction in elemental *3d* metals in the bcc structure from Kvashnin *et al.* (2016). The calculations were made with the use of the real-space LMTO-ASA method.

and AFM) signs. This balance is most intricate for bcc Fe, where all three terms in Eq. (7.5) are of comparable size. It was shown that, thanks to this decomposition, it was possible to identify the microscopic exchange mechanisms for each of these three channels, revealing a combination of RKKY, double exchange, and superexchange (Kvashnin *et al.*, 2016).

Overall, the sign of the NN coupling in all elemental *3d* systems follows the well-known Bethe-Slater curve, but it is governed by a complex interplay between different orbital contributions (Cardias *et al.*, 2017). This result paves the way to designing magnetic interactions in metallic *3d* systems in general and allows for a deeper analysis of interatomic exchange interactions. One way to continue the analysis is to calculate the symmetry-decomposed interaction parameters between further neighbors, as has been done for bcc Fe (Kvashnin *et al.*, 2016) and other *3d* elements (Cardias *et al.*, 2017). One of the most important conclusions in the case of bcc Fe is that the exchange between the T_{2g} orbitals is Heisenberg-like and long range, while it is relatively short range with a substantial non-Heisenberg behavior in the case of the $E_g - E_g$ and mixed ($E_g - T_{2g}$) channels (Kvashnin *et al.*, 2016).

Note that the non-Heisenberg behavior of bcc Fe and, especially, fcc Ni has been discussed for a long time (Turzhevskii, Lichtenstein, and Katsnelson, 1990), from calculations that considered $\delta\Omega_i^{\text{one}}$ [see Eqs. (3.3), (3.4), (5.39), and (5.40)] when a spin is rotated by a finite θ_i , as shown in Fig. 13. The results of the figure are clear: a strong configuration dependence can be observed for the magnetic moment and the angular dependence of the energy variation does not follow a sine function, especially for angles far from the ground state.

Szilva *et al.* (2017) considered a similar system, i.e., one spin was rotated by a finite θ_i at site i on a bcc Fe lattice when all other spins formed a ferromagnetic background and θ_i ran from 0 to π . In the study the two-site energy variation was the main focus. Note that in general one formally gets for the two-site energy variation (in the lack of SOC)

$$\delta\Omega_{ij}^{\text{two}} = -(J_{ij}^{\text{H}} \cos \theta_i + J_{ij}^{\text{NH}} \sin \theta_i)(\delta\theta)^2, \quad (7.6)$$

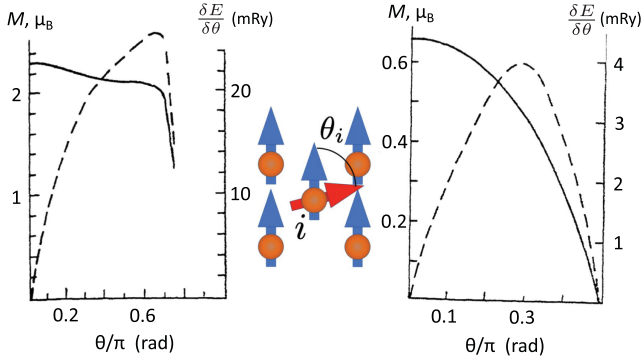


FIG. 13. Magnetic moment in μ_B (solid lines) and the first derivative of the energy (Ω) with respect to angle θ_i (dashed lines) for the cases of bcc Fe (left) and fcc Ni (right) when one spin is rotated with a finite θ_i in a ferromagnetic background (Turzhevskii, Liechtenstein, and Katsnelson, 1990), as shown in the added schematic.

where the terms that are proportional to a cosine and a sine function are referred to as the Heisenberg (H) term and non-Heisenberg (NH) terms, respectively, and $J_{ij}^H = J_{ij}^{(2)} + A_{ij}^{(2)xx}$ and $J_{ij}^{NH} = -2A_{ij}^{(2)zx}$ according to Eqs. (5.47) and (5.49). In this discussion, when the first-nearest-neighbor couplings are considered, the ij indices are replaced by the index 1. The calculated Heisenberg and non-Heisenberg results for different values of θ_i are shown by the solid black line in Fig. 14. The figure shows that in a general noncollinear case the non-Heisenberg contribution can be significant. However, the symmetry decomposition proves that in the T_{2g} channel the system is more Heisenberg-like and the non-Heisenberg behavior originates from E_g and the mixed channel. This is in good agreement with the conclusions based on the collinear

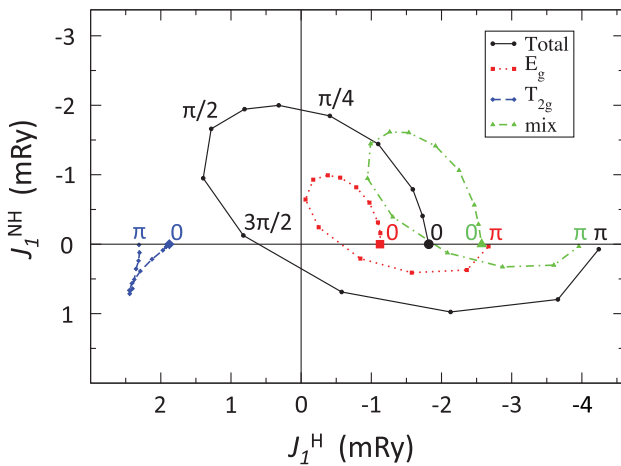


FIG. 14. First-nearest-neighbor Heisenberg and non-Heisenberg interatomic exchange parameters in bcc Fe when one spin is rotated by a finite θ_i running from zero to π at site i in a ferromagnetic background in the case of bcc Fe (Szilva *et al.*, 2017). $J_1^H = J_1^{(2)} + A_1^{(2)xx}$ and $J_1^{NH} = -2A_1^{(2)zx}$; see Eqs. (5.47) and (5.49). The black (solid) curve stands for the total value while the red (dotted), blue (dashed), and green (dash-dotted) lines show its symmetry decomposition in the d channel defined by Eq. (7.5).

formalism presented by Kvashnin *et al.* (2016) and Cardias *et al.* (2017).

B. Itinerant magnets based on 3d metal alloys and compounds

The explicit method for calculating exchange has been widely applied to study 3d-based alloys and compounds (Turek *et al.*, 2006; Ebert, Ködderitzsch, and Minár, 2011), and we describe in this section some examples. According to the Slater-Pauling curve, the maximal magnetization per atom in 3d metal alloys is achieved for the $\text{Fe}_{1-x}\text{Co}_x$ family. In the entire composition range, these alloys are ferromagnetic (Ležaić, Mavropoulos, and Blügel, 2007). Ležaić, Mavropoulos, and Blügel (2007) suggested that all pairs of Fe-Fe, Fe-Co, and Co-Co interactions are FM and that the NN $J^{\text{Fe-Co}}$ have the highest value. The latter result was reported earlier for an ordered B2-FeCo system (MacLaren *et al.*, 1999), highlighting the fact that the efficient hybridization between the Fe and Co states results in the enhancement of both the saturated magnetization and T_c . For $x > 0.17$, an experimental value of T_c of the bcc phase is unknown since the structural bcc-fcc transition occurs before the bcc structure reaches a Curie temperature. The temperature of the bcc-fcc transition sets a lower value of the expected T_c of the bcc structure, and it is high. In fact, MFA-based estimates predict a value of 1600 K for $x = 0.5$ (Ležaić, Mavropoulos, and Blügel, 2007), which is consistent with expectations. An interesting feature of this family of alloys is that by changing concentration one gradually transforms the electronic structure to achieve a transition from weak to strong ferromagnetism. As a result, depending on Co concentration, the magnetic interactions (and hence the T_c 's) have substantially different sensitivities to volume changes (Ležaić, Mavropoulos, and Blügel, 2007).

Iron-nickel alloys form in the fcc crystal structure and are celebrated thanks to the Invar effect: a vanishing thermal expansion at room temperature that is in an intrinsic relation with the temperature dependence of the magnetic configuration (van Schilfgaarde, Abrikosov, and Johansson, 1999). Ruban *et al.* (2005) calculated the magnetic interactions in $\text{Fe}_{0.5}\text{Ni}_{0.5}$ and $\text{Fe}_{0.65}\text{Ni}_{0.35}$. They were compared with those in fcc γ -Fe, and it was found that although both types of systems are frustrated, the physical picture is drastically different. In fcc Fe, the frustration comes from the competition between FM NN exchange coupling and that of more distant neighbors, which have a long-range oscillatory character. In contrast, the Fe-Ni alloys are already characterized by highly dispersive interactions with the first coordination shell, as shown in Fig. 15. Although CPA-based results agree well with the averaged J_{ij} 's obtained from the supercell approach, the latter captures more details and reveals strong influence of the local environment, which infers why the magnetic order of these alloys is so complex. Note that fcc-based Fe-Mn alloys have a tendency similar to AFM coupling and noncollinearity (Sakuma, 2000). Generally, for Ni-based alloys it was found that the renormalized (Bruno, 2003) J_{ij} 's provide better estimates of the T_c 's (Kudrnovský, Drchal, and Bruno, 2008), which is again related to the relatively small exchange splitting of its 3d states.

Heusler alloys have been intensely studied with the explicit formalism of exchange interactions (Kurtulus *et al.*, 2005;

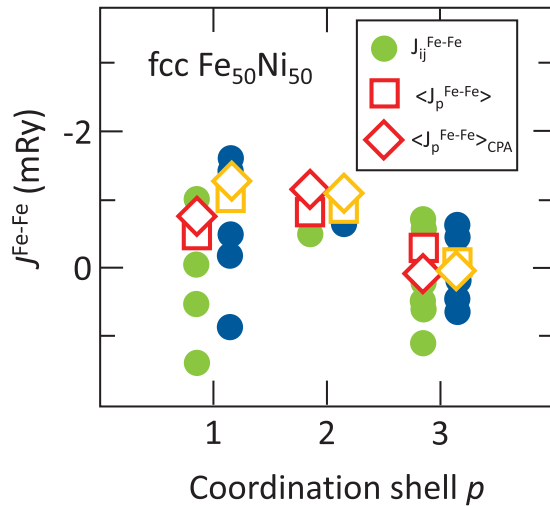


FIG. 15. Calculated Fe-Fe exchange interactions with first three coordination shells in fcc $\text{Fe}_{50}\text{Ni}_{50}$ for two different unit cell volumes (V) (Ruban *et al.*, 2005). The 16-atom supercell-based results for $V = 73.6 \text{ a.u.}^3$ and $V = 70.3 \text{ a.u.}^3$ are shown with blue (dark gray) and green (light gray) circles, respectively. Supercell- and CPA-averaged J_{ij} 's are shown for comparison.

Rusz *et al.*, 2006; Buchelnikov *et al.*, 2008, 2010; Thoene *et al.*, 2009; Comtesse *et al.*, 2014; Wollmann *et al.*, 2014; Khmelevskiy, Simon, and Szunyogh, 2015; Simon *et al.*, 2015; Chico *et al.*, 2016). For instance, Thoene *et al.* (2009) conducted a systematic study of magnetic interactions, spin-wave dispersion, and T_c for the series of Heusler compounds with $L2_1$ structure. The results shown in Fig. 16 demonstrate that T_c 's calculated from J_{ij} 's combined with a MFA estimate of the ordering temperature are in excellent overall agreement with experiment. Given all the approximations of their work, such as a MFA for T_c estimation and the neglect of local correlations, one may regard this excellent result as somewhat fortuitous. However, it is still impressive that the theory is able to correctly reproduce the experimental trend so well.

Heusler alloys attract significant attention partially due to the half-metallic character that is observed in some of them. However, there are many other half metals, such as Cr and

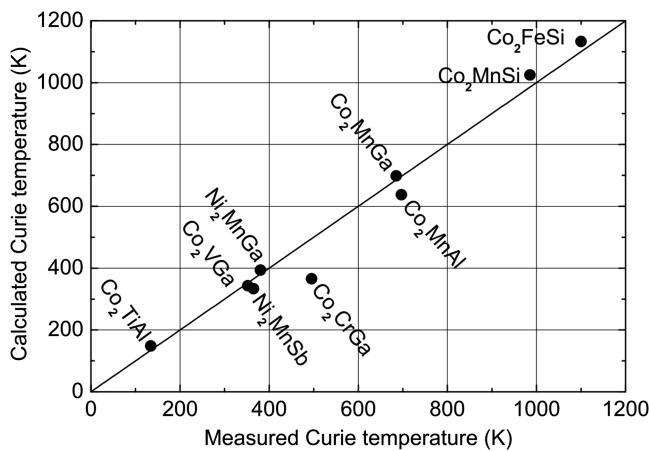


FIG. 16. Calculated vs measured T_c 's in the series of $L2_1$ Heusler alloys. From Thoene *et al.*, 2009.

Mn compounds, with a zinc blende structure that were also successfully modeled using the formalism presented here (Sanyal, Bergqvist, and Eriksson, 2003; Bose and Kudrnovský, 2010; Liu, Bose, and Kudrnovský, 2010). An overall review of the calculated J_{ij} 's in half-metallic magnets was given by Katsnelson *et al.* (2008). As expected from the earlier considerations [Eq. (7.2)], the J_{ij} 's in half metals are relatively short range.

C. Alloys with 4d and 5d elements

The 4d and 5d metals are typically nonmagnetic due to relatively more pronounced band dispersion, which makes it difficult for the Stoner criterion to get satisfied. However, when placed in proximity to 3d metals, these elements can have substantial induced magnetic moments (Mohn and Schwarz, 1993). The problem regarding coexisting intrinsic and induced moments was addressed in several works on FePt and CoPt alloys with $L1_0$ structure (Mryasov, 2004, 2005). It was suggested that the size of the induced moments of 5d elements is defined by an effective Weiss field that is produced by the surrounding 3d magnetic moments. This idea was later elaborated on when a generalized Monte Carlo-based scheme was suggested that dynamically updates the induced magnetic moments for each magnetic configuration during the simulation (Polesya *et al.*, 2010). Application of this scheme to the series of $\text{Fe}_x\text{Pd}_{1-x}$ and $\text{Co}_x\text{Pt}_{1-x}$ alloys was shown to deliver a systematically good agreement with experimental values of T_c . Polesya *et al.* (2016) pointed out that such treatment of the induced moments effectively leads to the emergence of higher-order biquadratic exchange interactions between 3d metal moments. Indeed, such interactions were suggested (Mryasov, 2005) to play a key role in explaining the metamagnetism of FeRh (Barker and Chantrell, 2015). In ordered FePd_3 , the biquadratic interactions were suggested to stabilize the noncollinear $3Q$ phase under pressure (Kvashnin *et al.*, 2012), and they were needed to get a consistent model of magnetism in ferropnictides (Wysocki, Belashchenko, and Antropov, 2011).

Alloying 3d metals with heavier elements can also boost the effective strength of the spin-orbit coupling. The SOC constant of Pt 5d states is 1 order of magnitude larger than that of Fe 3d states, and can therefore be used to enhance anisotropic magnetic interactions and the magnetocrystalline anisotropy (MAE). Indeed, the results for Pt-doped 3d metals (Solov'ev, Dederichs, and Mertig, 1995) showed that the MAE is to a large extent defined by nonlocal scattering of electrons from the SOC potential of Pt states. We later see how these ideas become particularly useful for inducing large magnetocrystalline anisotropy and DM interactions in low-dimensional systems.

D. Results from the disordered local moment approximation

Thus far we have focused most of our discussion on theoretical calculations of the electronic structure, and the mapping of these results to the Hamiltonians (1.3) and (1.4). However, the electronic structure can have a strong configuration dependence, which was demonstrated in a sequence of papers (Staunton *et al.*, 1984, 1985; Gyorffy *et al.*, 1985).

In these works finite temperature effects were introduced by separating the variables into slow and fast, and the concept of temporarily broken ergodicity was introduced, as mentioned in connection to Fig. 3. A central aspect of these works was the description of the electronic structure above an ordering temperature by means of the disordered local moment (DLM) model (Hasegawa, 1979a; Hubbard, 1979b; Edwards, 1982; Oguchi, Terakura, and Hamada, 1983; Pindor *et al.*, 1983; Staunton *et al.*, 1984, 1985; Gyorffy *et al.*, 1985), in which the electronic structure is evaluated from a single-site approximation of the coherent potential approximation. This implies that the electronic structure at finite temperature is represented by an atom with a potentially finite magnetic moment in an environment with “spin-average” scattering properties. Hence, there is no short-range order in this model, which seems at variance with experimental results from, for instance, muon-spin resonance, with a significant amount of short-range order also at elevated temperatures. The fluctuating local band (FLB) model (Korenman, Murray, and Prange, 1977a; Capellmann, 1979; Moriya, 1981) also builds on short-range magnetic order at or even above the ordering temperature, and in fact the early works of the FLB model express the basic principles behind noncollinear electronic structure theory. In this discussion it becomes relevant to note some early works of Hubbard, who argued for a theory that builds on itinerant-electron states, but with a local exchange field that varies in direction and strength from atom to atom; see Hubbard (1981a, 1981b). The probability of finding a system in a given configuration of a local exchange field was evaluated by an energy expression together with a Boltzmann factor, allowing for calculations of magnetism at finite temperature. This theory resulted in a Curie temperature of 1840 K for Fe and 1200 K for Ni. Both values are significantly larger than the experimental values.

Although many materials show short-range order above the ordering temperature, the DLM approach, which neglects short-range order, has given encouraging result; see Khmelevskiy *et al.* (2007), Delczeg-Czirjak *et al.* (2012), Ruban and Razumovskiy (2012), and Dong *et al.* (2017). As an example of this method, we show in Fig. 17 the inverse of the susceptibility of bcc Fe, evaluated as a function of temperature, in a calculation that builds on the DLM model (Staunton *et al.*, 1984). As seen in the figure, the susceptibility diverges at 1260 K, corresponding to the ordering temperature, which is in good agreement with the experimental Curie temperature of 1040 K. There are several examples of calculations of Heisenberg exchange from the DLM approach, e.g., the works quoted earlier in this section, and the relativistic extension of the DLM approach it makes possible to calculate the temperature dependence of magnetic anisotropy as well (Staunton *et al.*, 2006). We also note that a notable review of critical dynamics of magnets above and below the transition temperature was given by Frey and Schwabl (1994).

E. Multilayers and atoms on metallic surfaces

With the development of epitaxial growth techniques, it is now possible to produce extremely thin layers of magnetic materials with good control of the structural homogeneity. The

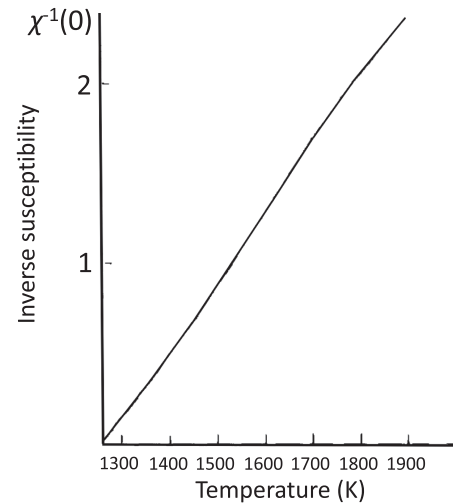


FIG. 17. Calculated inverse susceptibility of bcc Fe in units of $10^{-2}\mu_B^{-2}[\text{Ry}/(a_0/2\pi)^2]$ (where $a_0 = 2.789 \text{ \AA}$), from DLM electronic structure theory (see the text), evaluated as a function of temperature. Adapted from Staunton *et al.*, 1984.

magnetic interactions in such low-dimensional magnets bring many surprises and opportunities for applications, such as spintronics and magnonics.

For thin-film systems, SPEELS serves as an accurate experimental tool for observing magnon excitations (Vollmer *et al.*, 2003). In a number of works, the adiabatic magnon spectra, calculated using J_{ij} 's, are directly compared against measured spectra, with a generally good agreement (Chuang *et al.*, 2014; Meng *et al.*, 2014; Zakeri, Qin, and Ernst, 2021). To incorporate finite temperatures into the theory, atomistic spin-dynamics simulations have also been widely used to model the surface magnons; for a review, see Etz *et al.* (2015). Among the studied materials one observes the Co/Cu(111), Co/Cu(001), Fe/Cu(001), and Fe/W(110) systems (Bergqvist *et al.*, 2013).

Exchange interactions in multilayers of elemental transition metals have been investigated in many studies. Vaz, Bland, and Lauhoff (2008) provided a comprehensive overview of calculated spin-wave stiffnesses that were obtained using different electronic structure methods. An interesting result was obtained by Pajda *et al.* (2000) and Bruno *et al.* (2002), where Fe and Co monolayers on Cu(001) were considered. Depending on the thickness of the capping Cu layer, the T_c 's were shown to have an oscillatory character. This result, also shown in Fig. 18, was suggested to be caused by the interference effects in the capping layer. Such oscillations have actually been observed in Co/Cu/Ni trilayers (Ney *et al.*, 1999) and also explained using the explicit approach of calculating exchange interactions (Isaev *et al.*, 2001).

Multilayers of 3d metals on the substrates of heavier elements get even more unpredictable behavior. This is partially related to substantial exerted strain as well as a modification of the bandwidth of electron states. For instance, Meng *et al.* (2014) studied Fe/Rh(001) and found a pronounced softening of acoustic magnons at the M point, shown as a dip in the dispersion in Fig. 19. Usually in layered systems the lowest magnon branch originates from the spins subject to

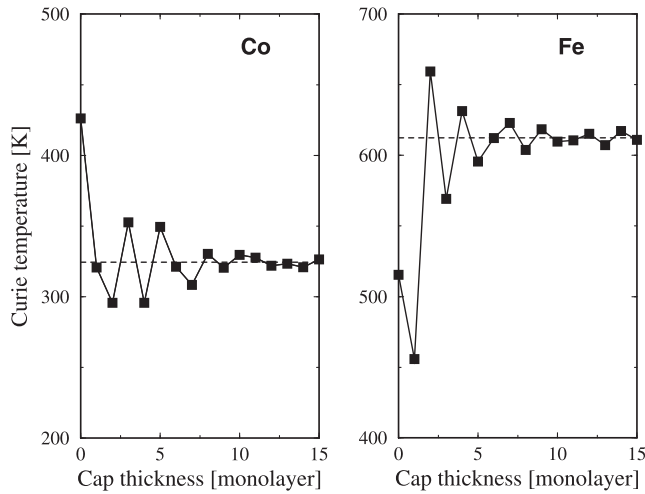


FIG. 18. RPA-derived estimates of the T_c of (left panel) Co and (right panel) Fe monolayers on a Cu(001) substrate, covered by a Cu layer of varying thickness. From Pajda *et al.*, 2000.

the smallest effective Weiss field (defined by the total exchange interaction). Meng *et al.* (2014) demonstrated that Fe atoms at the interface have a strong tendency to AFM coupling and therefore give the main contribution to the lowest acoustic magnon mode. This is an unexpected result, given that bulk bcc Fe has such a pronounced NN and next NN FM interaction. In fact, this tendency was also reported for a pure Fe surface (Keshavarz *et al.*, 2015) and is related to the changes of density of states of the surface Fe atoms. A tendency similar to AFM Fe-Fe interactions was reported for Fe/Ir(001) (Kudrnovský *et al.*, 2009; Zakeri *et al.*, 2013; Chuang *et al.*, 2014). We note that in a similar system, a monolayer Fe on Rh(111), an up-up-down-down double-row-wise antiferromagnetic magnetic ground state was directly observed by Krönlein *et al.* (2018). Note also that the occurrence of a novel type of atomic-scale spin lattice in an Fe monolayer on the Ir(001) surface was predicted by Hoffmann *et al.* (2015).

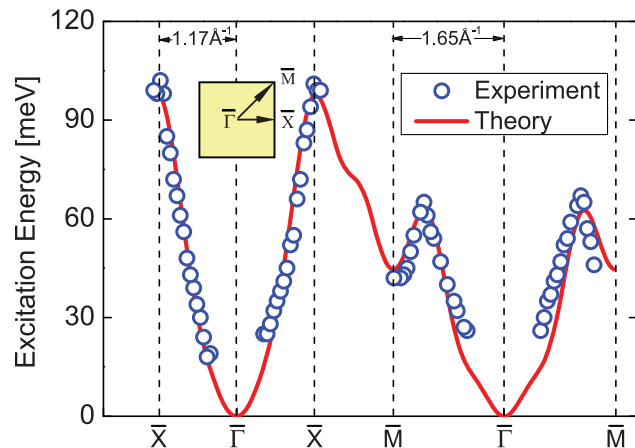


FIG. 19. Computed and measured acoustic magnon dispersions in Fe/Rh(001). Inset shows the parts of the Brillouin zone used in the plot. From Meng *et al.*, 2014.

F. Influence of spin-orbit coupling

Although several LKAG-inspired approaches for calculating relativistic interactions have been proposed, DM interactions have attracted the most attention (Solovyev, Hamada, and Terakura, 1996a; Udvardi *et al.*, 2003; Mazurenko and Anisimov, 2005; Ebert and Mankovsky, 2009; Katsnelson *et al.*, 2010; Secchi *et al.*, 2013; Mankovsky and Ebert, 2017; Ebert, Mankovsky, and Wimmer, 2021). As described here, DM parameters can be extracted using a first-order or second-order variation in the spin rotation angles, depending on the situation.

The first-order approach was utilized to calculate the instability of a ferromagnetic state toward a formation of a cycloid configuration by Mankovsky and Ebert (2017), as well as of the so-called weak ferromagnets [which are weakly ferromagnetic due to uncompensated antiferromagnetism, in contrast to the weak itinerant-electron ferromagnets (Mazurenko and Anisimov, 2005; Katsnelson *et al.*, 2010) discussed in Sec. VII A]. In regard to weak ferromagnets, this leads to good agreement with experimentally observed canting angles for both La_2CuO_4 (Katsnelson *et al.*, 2010) and FeBO_3 (Dmitrienko *et al.*, 2014). This approach relies on the fact that the canting angle is small and a collinear magnetic state, subject to a finite torque acting on the magnetic moments, is not far from the true one. In this approach one can rotate spin and orbital momenta separately, and for both studied systems the latter contributed significantly to the total DM interaction value. Similar calculations of finite torques on collinear magnetic moments due to symmetry allowed DM interactions are the calculation of the small tiltings due to lattice distortions in LaMnO_3 (Solovyev, Hamada, and Terakura, 1996a) and the instability of the ferromagnetic state of the B20 alloy $\text{Fe}_{1-x}\text{Co}_x\text{Ge}$ toward a cycloidal spin-density wave (Mankovsky and Ebert, 2017). The latter instability is the origin of the formation of skyrmion lattices in this system (Heinze *et al.*, 2011).

The second-order approach is most appropriate for DM interactions that are used for spin-wave spectra. Udvardi *et al.* (2003) demonstrated the relativistic effects on the excitation spectra through a systematic comparison of relativistic exchange couplings calculated for Fe/Cu(001) and Fe/Au(001). They showed that strong SOC of Au-5d states gives rise to substantially different magnon spectra for the in-plane and out-of-plane orientation of the magnetization. Currently experimental efforts are concentrated on the studies of DM interactions in such systems (Zakeri *et al.*, 2010). Indeed, DM interactions can be effectively enhanced on the surfaces of heavy elements due to the combined effect of narrow surface states and substrate-induced, large SOC. By means of explicit calculations, it was shown that a sizable DM interaction exists between Fe atoms on a W(110) surface (Udvardi and Szunyogh, 2009). The so-obtained DM vectors are shown in Fig. 20. Owing to the symmetry of the system, the DM vectors are oriented strictly in the plane of the surface such that the z component of the DM vector is zero.

Moreover, Udvardi and Szunyogh (2009) predicted these interactions to give rise to an asymmetry of the magnon dispersion, i.e., a preferred chirality, with an asymmetry energy defined as $\Delta E = E(\mathbf{q}) - E(-\mathbf{q})$. This asymmetry

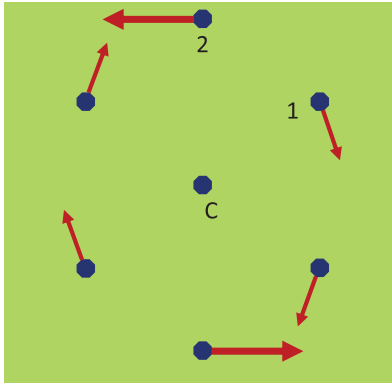


FIG. 20. Schematic representation of the calculated DM interactions in Fe/W(110) between the central iron atom (C) and its NN and next NN, denoted as 1 and 2, respectively. The DM vectors are seen to obey twofold rotational symmetry. From Udvardi and Szunyogh, 2009.

was later confirmed experimentally by Zakeri *et al.* (2010). The comparison between computed and measured asymmetry energy for the Fe/W(110) system, also shown in Fig. 21, was made by Bergqvist *et al.* (2013). Without DM interactions, ΔE is strictly zero for all q vectors. Thus, ΔE can be effectively used for quantifying DM couplings in this class of systems, partially due to the high resolution of SPEELS-based experiments and partially due to the theory of evaluating D_{ij} . In this respect, the relativistic interactions between transition metals deposited on Pt(111) have particularly attracted attention (Mankovsky *et al.*, 2009; Vida *et al.*, 2016; Simon *et al.*, 2018; Zimmermann *et al.*, 2019).

As demonstrated by Udvardi and Szunyogh (2009), a Hamiltonian with a 3×3 tensorial coupling between the spins can be considered where the x component of the moment on atomic site i can interact with the y component of the moment on atomic site j , as shown in Eqs. (3.13) and (3.14). These interactions come in a form that is antisymmetric under

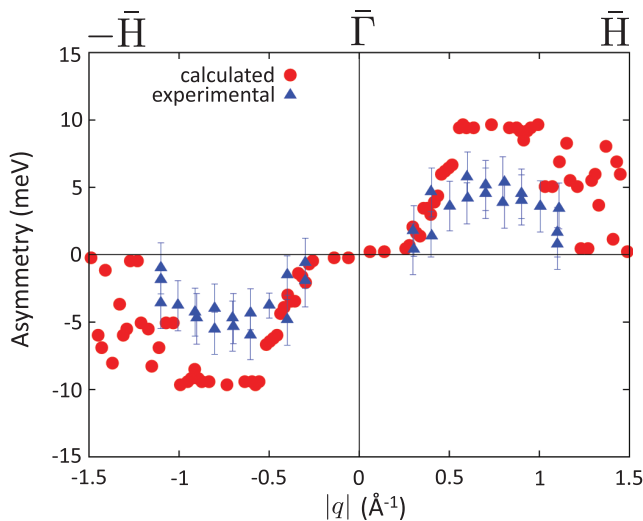


FIG. 21. Experimental (Zakeri *et al.*, 2010) and theoretical (Udvardi and Szunyogh, 2009) chiral asymmetry of the magnon spectrum of bilayer Fe/W(110). From Bergqvist *et al.*, 2013.

an interchange of the x and y indices, which leads to the previously discussed DM interaction. However, there is also a symmetric component to the anisotropic exchange interaction, as shown in Eq. (3.15), that in some cases is significant. An example is a recent calculation of symmetric and antisymmetric exchanges of CoPt, where the two interactions were found to be of similar size (Borisov *et al.*, 2021). As a final remark in this section, we note that more references on calculations of DM interactions by various first-principles methods were included in a recent review focused on this topic (Yang, Liang, and Cui, 2023).

G. Clusters of atoms on surfaces

With the invention of real-space methods for calculations of electronic structures (Haydock, Heine, and Kelly, 1975; Andersen and Jepsen, 1984), it has become possible to study magnetic exchange interactions of systems without periodic boundary conditions. This is the case when clusters or defects are embedded into a solid or at a surface with the use of LMTO (Andersen and Jepsen, 1984) or KKR methods (Korringa, 1947; Kohn and Rostoker, 1954). In Fig. 22 we give an example in which the real-space LMTO-ASA method was used (Igarashi *et al.*, 2012), since its implementation is built on a Green's function formalism and the expressions of interatomic exchange (Sec. V) are more or less straightforward to implement. This has been discussed in a series of works (Frota-Pessôa, Muniz, and Kudrnovský, 2000; Bergman *et al.*, 2007; Ribeiro *et al.*, 2011; Igarashi *et al.*, 2012; Bezerra-Neto *et al.*, 2013; Szilva *et al.*, 2013, 2017; Cardias *et al.*, 2016; Carvalho *et al.*, 2021). The results shown

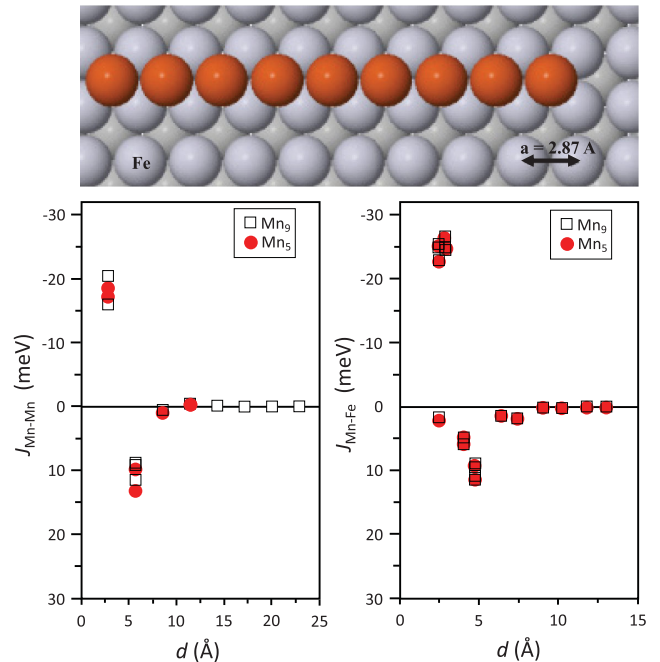


FIG. 22. Upper panel: geometry of Mn chain shown by orange (dark gray) spheres on a bcc Fe surface [(001) orientation] with Fe atoms as light gray spheres. Lower panels: calculated exchange interactions between Mn-Mn pairs and between Fe-Mn pairs. Data from Igarashi *et al.* (2012).

in Fig. 22 were obtained from a calculation based on the LSDA, for an isolated chain of Mn atoms (five and nine Mn atoms in the chain were considered) on top of a bcc Fe(001) surface. The results of Fig. 22 show that interactions are dominantly short range between all atom types. In addition, the interactions between Mn-Mn pairs and between Mn-Fe pairs can be either ferromagnetic or antiferromagnetic, depending on the distance between the atoms. This competition between interactions is responsible for the complex, noncollinear magnetic structures found in this system.

H. *f*-electron systems

Unpaired electrons of transition metal *d* states is the most common source of magnetism, but not the only one. Many elements with partially filled electronic *f* shells also exhibit intrinsic magnetic ordering. Modeling magnetism of such systems is challenging since the *f* electrons are governed by a sophisticated interplay among strong local correlations, spin-orbit coupling, crystal field effects, and hybridization. Capturing all these ingredients on equal footing is a great challenge for first-principles electronic structure calculations.

An advantage of the rare-earth elements is that their 4*f* wave functions are extremely localized and hybridization effects can be neglected (with two exceptions: La and Ce) (Jensen and Mackintosh, 1991). Indeed, although 4*f* electrons are responsible for the formation of the local magnetic moments, they do not explicitly participate in the formation of magnetic interactions (Ruderman and Kittel, 1954). Instead, the 4*f* electrons locally spin polarize the valence 6*s*6*p*5*d* orbitals, which mediate the exchange couplings; see Perlov, Halilov, and Eschrig (2000).

Turek, Kudrnovský, Bihlmayer, and Blügel (2003) showed that, by treating the 4*f* electrons as a noninteracting spin-polarized core, a good description of magnetic interaction can be achieved for hcp Gd from calculations of a ferromagnetic (FM) state. Gadolinium orders ferromagnetically with an observed total magnetic moment of about $7.6\mu_B$ per atom, where $7\mu_B$ come from half-filled *f* shell ($S = 7/2$) (Jensen and Mackintosh, 1991). This was reproduced by theory (Colarieti-Tosti *et al.*, 2003). Turek, Kudrnovský, Bihlmayer, and Blügel (2003) determined the MFA-based estimate of the T_c as 334 K, which is in excellent agreement with experiment (293 K) (Jensen and Mackintosh, 1991). Subsequent studies treated the paramagnetic phase of Gd by means of the DLM approach (Khmelevskiy *et al.*, 2007). Although the calculated values of NN J_{ij} were different from the FM-derived ones, a similar T_c estimate was obtained.

A systematic study of the entire series of late rare-earth elements was conducted by Locht *et al.* (2016). They showed that the calculations incorporating local 4*f* correlations on Hubbard I level of approximation (HIA) (Lichtenstein and Katsnelson, 1998) are capable of reproducing both electronic valence band excitation spectra, showing well pronounced atomic multiplets, and magnetic interactions of these systems. In addition, full charge self-consistency in DMFT was shown to be of utter importance for correctly describing the exchange couplings. The interaction terms J_{ij} can already be well described with the 4*f*-as-core approach, which is much less computationally demanding.

As Locht *et al.* (2016) showed, the best possible approach to the electronic structure of the rare-earth elements is the HIA approximation. It reproduces measured electronic structures (both occupied and unoccupied states) and results in realistic magnetic properties. As Locht *et al.* (2016) discussed, LDA + *U* has a significantly worse performance for elemental rare-earth elements. This was explicitly shown in Fig. 14 of Locht *et al.* (2016), where the valence band of HIA calculations was compared to LDA + *U* calculations. The latter is seen to not capture experiments, while the former does. In addition, for compounds such as TbN, HIA gives a much better description of the total energy, equilibrium lattice constant, and bulk modulus than LDA + *U* (Peters *et al.*, 2014). At the same time, as Locht *et al.* (2016) argued, a poor-man's treatment of the 4*f* electrons is to consider them as nonhybridizing core states with a spin moment constrained according to *LS* coupling, an approach also considered by Turek, Kudrnovský, Bihlmayer, and Blügel (2003) that successfully reproduced experimental moments and exchange interactions. In the case where nonlocal interaction effects are important, that is, intersite Coulomb interactions, a reasonable alternative could be the self-interaction-corrected approximation (SIC LSDA) (Temmerman, Szotek, and Winter, 1993; Temmerman *et al.*, 2007).

The Fourier transform of the obtained J_{ij} of the heavy rare-earth elements, which was calculated by Locht *et al.* (2016), is shown in Fig. 23 [as $J(\vec{q}) - J(0)$]. The minimum value of this curve indicates the ground-state magnetic ordering *q* vector. The results show that Er and Tm have a tendency to have noncollinear magnetic order [similar to Eu (Turek, Kudrnovský, Diviš *et al.*, 2003)]. Holmium also borders on having a finite-*q* maximum, which is compatible with experiments (Jensen and Mackintosh, 1991). In fact, Ho just passed the border between ferromagnetism and noncollinearity, and measurements demonstrate a finite spin-spiral vector. Calculations based on nonhybridizing core states with a 4*f* spin moment constrained according to *LS* coupling have

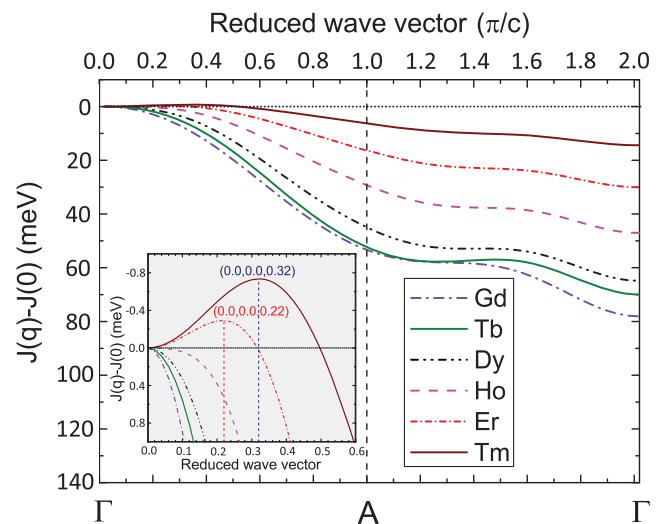


FIG. 23. Fourier transform of the exchange interaction $J(\vec{q}) - J(0)$ in heavy elemental lanthanides (Locht *et al.*, 2016). If the minimum corresponds to the Γ point, the ferromagnetic order is preferable.

reproduced this experimental finding accurately (Nordström and Mavromaras, 2000).

Locht *et al.* (2016) calculated the ordering temperatures from the spin Hamiltonian [Eq. (1.3)] using explicit calculations of the obtained J_{ij} . This combined with Monte Carlo simulations allowed for estimates of the ordering temperature, which was shown to be in good agreement with experiments for all studied, heavy rare-earth elements. Overall, the ordering temperature was found to decrease linearly with the number of electrons in the $4f$ shell. In addition, an interesting self-induced spin glass state was recently experimentally observed for elemental Nd (Kamber *et al.*, 2020; Verlhac *et al.*, 2022). *Ab initio* calculations of the exchange parameters of this element have revealed that this is related to the unique exchange interactions of the crystal structure of Nd (double hcp), with competing FM and AFM interactions of equal strength.

Numerous lanthanide-based systems (Rusz, Turek, and Diviš, 2005; Liu and Altounian, 2010; Khmelevskiy, 2012; Söderlind *et al.*, 2017; Gong *et al.*, 2019) were successfully modeled using the methods reviewed here to calculate the interatomic exchange by treating the $4f$ electrons as core states. Alternatively, HIA (which also neglects the hybridization effects) was also used in some works (Han, Wan, and Savrasov, 2008; Wan, Dong, and Savrasov, 2011). Both theoretical methods to treat the $4f$ shell have been used to analyze the magnetism of intermetallic compounds containing $4f$ elements. This class of materials, often referred to as hard magnets, is of particular importance for electromagnetic applications, such as the conversion of mechanical energy to electricity or as a key component in electrical engines; see Skomski and Coey (1993, 1999), Coey (2010), and Skomski (2021). The most established permanent magnet is $\text{Nd}_2\text{Fe}_{14}\text{B}$ [see Croat *et al.* (1984), Herbst *et al.* (1984), and Sagawa *et al.* (1984)], a material that has had its electronic structure and magnetic properties investigated with DFT (Jaswal, 1990; Nordström, Johansson, and Brooks, 1993). In these earlier theories of the electronic structure of compounds containing lanthanides, the $4f$ shell was treated as a nonhybridized part of a spin-polarized core, where the magnetic state was confined to follow LS coupling, and in general good agreement between theory and observations was found. Calculations using the HIA have also been published for hard magnets, for instance, for SmCo_5 (Grånäs *et al.*, 2012), where the electronic structure and magnetic properties were found to be in good agreement with experiments (Tie-song *et al.*, 1991). The reason why calculations based on “ $4f$ as core” and HIA reproduce the experimental magnetic properties is connected to the fact that both are faithful to the standard model of the lanthanides (Jensen and Mackintosh, 1991), in which the $4f$ shell basically is an atomlike, nonhybridized entity. In more recent years the theory connected to HIA has been developed to also enable calculations of crystal field splittings of the $4f$ shell (Pourovskii *et al.*, 2020; Boust *et al.*, 2022), an important achievement in the field, since the $4f$ crystal field splitting is connected to the magnetocrystalline anisotropy of these systems (Jensen and Mackintosh, 1991; Skomski and Coey, 1999; Coey, 2010; Skomski, 2021), and therefore for their excellent magnetic performance. When it comes to calculations of interatomic exchange using the LKAG formalism,

fewer examples have been published. A notable recent exception, however, is calculations of the Heisenberg exchange of the compound $\text{Ce}_2\text{Fe}_{17}$ (Vishina *et al.*, 2021), a material that is considered an alternative to $\text{Nd}_2\text{Fe}_{14}\text{B}$ for applications as a hard magnet. Its peculiar magnetic properties were explained from electronic structure calculations coupled to the LKAG formalism of interatomic exchange (Vishina *et al.*, 2021).

The magnetic interactions of $5f$ -based compounds are much more complicated due to more pronounced hybridization and the stronger spin-orbit coupling. This situation often leads to strong spin-orbital mixing, which in turn gives rise to high anisotropy of the spin density, so approximating spins with dipoles no longer applies. Instead, higher-order multipoles come into play that have been extensively discussed in the context of actinide oxides (Santini *et al.*, 2009) as well as other actinide compounds (Bultmark *et al.*, 2009; Cricchio, Grånäs, and Nordström, 2011). A new methodology has recently been applied to investigate the magnetism of UO_2 (Pourovskii and Khmelevskiy, 2019) and NpO_2 (Pourovskii and Khmelevskiy, 2021). In the former case, calculated quadrupolar exchange interactions have successfully predicted stabilization of the $3Q$ magnetic order in the cubic phase, which previously could be explained only by the presence of lattice distortions. To calculate these multipoles, a generalized many-body force theorem was proposed by Pourovskii (2016). It relies on the assumption that the correlated states (responsible for magnetism) can be well projected onto atomic wave functions (calculated via HIA). Another general approach valid for less correlated actinide compounds adopts the DFT + U method, which treats the correlation in mean-field level (Bultmark *et al.*, 2009). This type of approach is in agreement by large with experiments regarding magnitudes of actinide magnetic moments, with substantial orbital moments and reduced spin moments. The effect behind these calculated magnetic moments can be explained as due to the presence of large high rank magnetic multipoles (Cricchio, Grånäs, and Nordström, 2011).

I. Transition metal oxides

Transition metal oxides (TMOs) are a class of materials that show a wide variety of different magnetic orders and interesting physical and chemical properties. The magnetism of these materials can usually be explained in terms of superexchange (Kramers, 1934; Goodenough, 1955, 1963; Anderson, 1959; Kanamori, 1959) or double-exchange processes (Zener, 1951). The competition between them is responsible for a particularly rich phase diagram of doped manganites (Schiffer *et al.*, 1995).

Oguchi, Terakura, and Hamada (1983) and Oguchi, Terakura, and Williams (1983) calculated magnetic interactions in transition metal monoxides MnO and NiO from first principles at an early stage. The obtained values were too high compared with experiment, which was most likely related to the absence of strong local correlations in the calculation. Indeed, later it was shown that taking a Hubbard U term into account for the transition metal $3d$ states substantially improves the situation (Solovyev and Terakura, 1998; Fischer *et al.*, 2009; Logemann *et al.*, 2017; Keshavarz *et al.*, 2018). As demonstrated by Fischer *et al.* (2009), a systematic, good description of

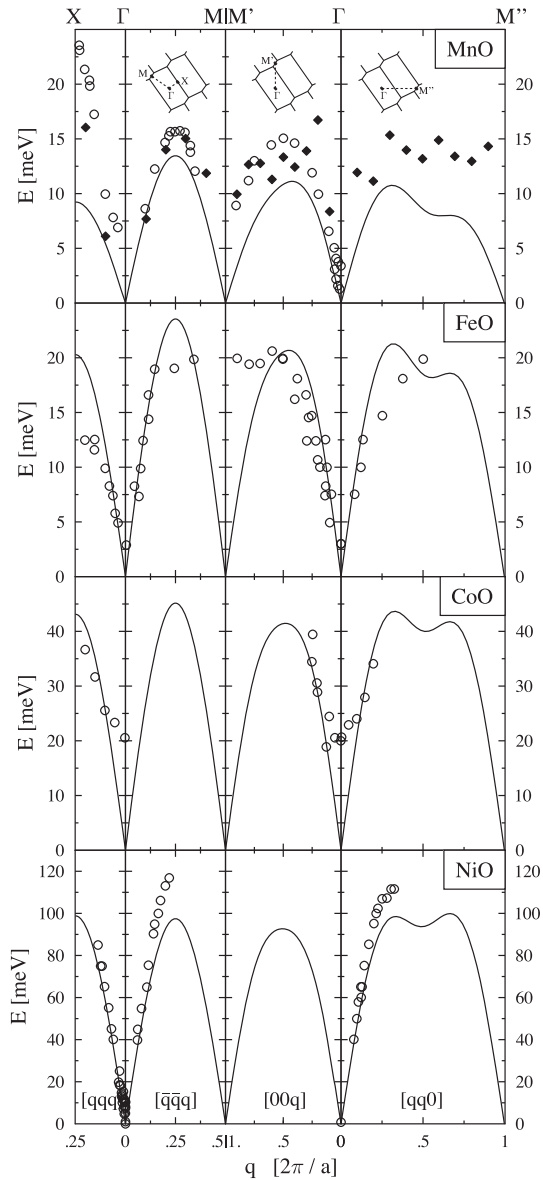


FIG. 24. Calculated spin-wave dispersion in MnO, FeO, CoO, and NiO (solid lines). Experimental results are shown with symbols. From Fischer *et al.*, 2009.

the Néel temperatures can be obtained in the entire series of transition metal monoxides using a SIC version of DFT, although the valence band spectrum of these types of calculations does not agree with observations. The magnon spectra calculated from SIC theory of MnO, FeO, CoO, and NiO (Fischer *et al.*, 2009) is shown in Fig. 24, and there is excellent agreement with experimental data. Furthermore, the impact of dynamical correlations (treated in DMFT) on J_{ij} of the transition metal monoxides was considered by Wan, Yin, and Savrasov (2006) and Kvashnin, Grånäs *et al.* (2015). Although there are some quantitative differences, the results of DMFT are close to the LDA + U results, SIC data, and values from the HIA; see Fig. 4. This result might seem counterintuitive since the electronic structure resulting from the different approaches is substantially different (Grånäs *et al.*, 2012). The likely reason is probably due to the fact that wide-gap TMOs are close to the $U \gg t$ limit, where the exchange integrals are roughly defined

as t^2/U , which is similar in the various approaches. The interatomic exchange extracted from a calculation of the susceptibility using the GW approximation provides results of similar quality (Kotani and Schilfgaarde, 2008).

Perovskite 3d oxides were intensely studied by Solovyev, Hamada, and Terakura (1996a, 1996b), Solovyev and Terakura (1999a, 1999b), and Solovyev (2006). Despite the large variety of magnetic phases found in these materials, J_{ij} 's are usually consistent with experimental ground-state magnetic orders. This is a rewarding result. Treating the electron interactions beyond DFT usually results in better values of the interatomic exchange interactions of these materials. LaMnO₃ may be an interesting exception to this rule. Solovyev, Hamada, and Terakura (1996b) suggested that the Hubbard U acting on the e_g and t_{2g} orbitals of this compound are different due to differences in the screening of the two sets of orbitals. It was thus suggested that having no U is a better choice than adding the same U on the entire set of Mn-3d orbitals for LaMnO₃. However, this result depends on details of the implementation, as discussed by Jang *et al.* (2018).

Generally, TMOs are regarded as good Heisenberg magnets, in the sense that the spins are localized around 3d ions and the interactions are of a bilinear kind without strong configuration dependence. However, the total energies of different magnetic orders are not always consistent with the Heisenberg model of Eq. (1.3), as previously reported (Solovyev, 2009; Logemann *et al.*, 2017). Oxygen polarization is suggested to be responsible for this inconsistency (Keshavarz *et al.*, 2018). Moreover, for certain oxides, like LiCu₂O₂, which have a 90° superexchange, direct exchange also plays a crucial role (Mazurenko *et al.*, 2007). Direct exchange interactions were introduced in the original Heitler-London scheme (Heitler and London, 1927). Oxides with more complex crystal structures (Mazurenko, Mila, and Anisimov, 2006; Jodlauk *et al.*, 2007; Mazurenko *et al.*, 2008; Barker, Pashov, and Jackson, 2020; Gorbatov *et al.*, 2021), including the ones with 4d and 5d elements (Solovyev, 2002; Etz *et al.*, 2012; Panda *et al.*, 2016) have also been successfully analyzed with respect to the interatomic exchange using the method reviewed here. We also note that multispin interactions have been found to be important in magnetic oxides (Fedorova *et al.*, 2015).

As a final point of this section, we point out that, for heavy transition metals of the 5d series, the large spin-orbit coupling leads to strong spin-orbital mixing as in the $j = 1/2$ pseudospin relevant for Ir oxides (Moon *et al.*, 2008). The arguments in Sec. VII H for the case where the pure spin moment has less meaning is also valid for 5d oxides.

J. Novel 2D magnets

Magnetism in layered van der Waals-bonded materials was reported in the 1960s (Tsubokawa, 1960; Dillon and Olson, 1965). For a long time, these materials were not the focus of researchers, but in recent years they have attracted significant attention (Gong *et al.*, 2017; Huang *et al.*, 2017). The discovery of intrinsic 2D magnetic order not only challenges well-established preconceptions about 2D magnetism (Mermin and Wagner, 1966) but also offers prospects for building ultrathin spintronic devices by combining these types

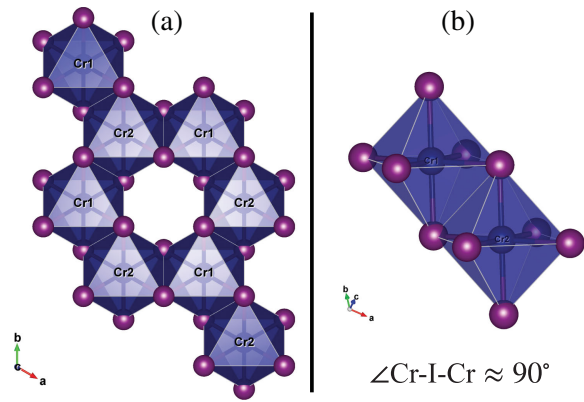


FIG. 25. Left panel: crystal structure of a CrI_3 monolayer with I atoms shown as spheres with a light part in their center and Cr shown as homogeneously colored spheres. The Cr atoms form a honeycomb lattice. Right panel: local structure of the Cr–I–Cr bond.

of layered materials (Burch, Mandrus, and Park, 2018; Gibertini *et al.*, 2019).

CrI_3 is the most well-studied example of 2D magnets. It is ferromagnetic and the T_c of its monolayer form is 45 K, which is slightly smaller than that of the bulk form (61 K) (Huang *et al.*, 2017). The crystal structure of the monolayer of CrI_3 is shown in Fig. 25. Here Cr atoms are seen to form a honeycomb lattice, and each of them is surrounded by six iodine atoms forming an octahedron. Two I octahedra of the NN Cr atoms are sharing an edge, as illustrated in Fig. 25(b), which results in the Cr–I–Cr bond angle being close to 90° . The material is an insulator, so the magnetic interactions are expected to be defined by a superexchange process that also involves the I $5p$ states. Nominally the Cr^{3+} ions should be characterized by a d^3 configuration, with a half-filled t_{2g} shell and with the e_g states completely empty. Besbes *et al.* (2019) showed that the e_g states form strong covalent bonds with I $5p$ orbitals and become effectively occupied by hybridization and band broadening. As a result, the NN J_{ij} 's between Cr atoms are affected by two competing contributions, namely, the AFM superexchange between half-filled t_{2g} orbitals and the FM superexchange between t_{2g} and e_g states. The latter dominates and results in the overall FM sign of the NN exchange. The same physics was confirmed to also take place in the case of monolayer CrI_3 (Kashin *et al.*, 2020; Soriano *et al.*, 2021). Since the structure is the same in all three chromium halides CrX_3 ($X = \{\text{Cl}, \text{Br}, \text{I}\}$), the complex nature of the NN coupling in these materials explains why its sign is so sensitive to lattice distortions and strain (Webster and Yan, 2018; Dupont *et al.*, 2021; Sadhukhan *et al.*, 2022). A similar orbital analysis for the interlayer coupling (Jang *et al.*, 2019) provided a microscopic description of the theoretically predicted stacking-dependent magnetic order in bilayer CrI_3 (Sivadas *et al.*, 2018), which was also confirmed experimentally (Li *et al.*, 2019; Song *et al.*, 2019). The calculated magnetic interactions in trilayer CrI_3 were suggested to exhibit similar features (Wang and Sanyal, 2021).

One interesting aspect of bulk CrI_3 is a large gap (≈ 4 meV) between the two magnon branches, which was observed

experimentally (Chen *et al.*, 2018). There are mainly two mechanisms that have been proposed to explain this, namely, a large next NN DM interaction (Chen *et al.*, 2018) or a NN Kitaev interaction (Lee *et al.*, 2020). Relativistic exchange interactions in bulk and monolayer CrI_3 were studied by Kvashnin *et al.* (2020). Using both conventional DFT and two different flavors (Anisimov, Zaanen, and Andersen, 1991; Czyżyk and Sawatzky, 1994) of LDA + U calculations, they found that calculated DM interaction and Kitaev terms were both found too small to induce a substantial gap in the magnon spectrum at the K point. Ke and Katsnelson (2021) suggested that CrI_3 is a moderately correlated material with strong nonlocal interaction effects and GW approximation combined with a Hubbard U are needed to reproduce the magnon spectrum and, most importantly, that the ≈ 4 meV magnon gap is open by correlation enhanced interlayer coupling. More elaborate discussions on the role of nonlocal correlation effects and on the importance of charge self-consistency in CrX_3 were conducted by Acharya, Pashov, Cunningham *et al.* (2021) and Acharya, Pashov, Rudenko *et al.* (2021). Given the relatively young age of this field of magnetic materials, it is likely that other mechanisms will be discussed in the future.

Other 2D magnets such as $\text{Cr}_2\text{Ge}_2\text{Te}_6$ (Wang *et al.*, 2019), Fe_3GeTe_2 (Jang *et al.*, 2020), CrOX ($X = \{\text{Cl}, \text{Br}\}$) (Jang *et al.*, 2021), and FeX_2 (Ghosh, Jose, and Kumari, 2021) have been studied with the help of explicit calculations of interatomic exchange. The class of 2D versions of $\text{Cr}_2\text{X}_2\text{Te}_6$ ($X = \text{Ge}$ and Si) systems was predicted from *ab initio* electronic structure theory (Lebègue *et al.*, 2013) before the experimental realization. A common feature of magnetic 2D materials is that they are characterized by relatively strong hybridization of $3d$ orbitals of the transition metals and the p orbitals of the ligand states. In this case, the choice of electronic states that should be used in the expressions of interatomic exchange (Sec. V), i.e., the projection scheme, becomes particularly nontrivial. This issue was raised by Besbes *et al.* (2019) and Wang *et al.* (2019).

K. *sp* magnets

Another class of systems where the magnetism emerges from highly covalent states is *sp* magnets. One example of such materials is semihydrogenated or fluorinated graphene (Mazurenko *et al.*, 2016). Another example is systems of X adatoms ($X = \{\text{Sn}, \text{C}, \text{Si}, \text{Pb}\}$) deposited periodically on silicon $\text{Si}(111)$ (Slezák, Mutombo, and Cháb, 1999; Lobo *et al.*, 2003; Upton, Miller, and Chiang, 2005; Modesti *et al.*, 2007; Zhang *et al.*, 2010; Li *et al.*, 2013; Tresca *et al.*, 2018), germanium $\text{Ge}(111)$ (Carpinelli *et al.*, 1997; Floreano *et al.*, 2001; Tresca and Calandra, 2021), or $\text{SiC}(0001)$ surfaces (Glass *et al.*, 2015). These systems are characterized by the presence of a single relatively narrow half-filled band crossing Fermi level, which is subject to strong local and nonlocal electron correlations; see Hansmann, Ayrál *et al.* (2013), Hansmann, Vaugier *et al.* (2013), and Badrtdinov *et al.* (2016). Although this band originates from the *sp* electrons of adatoms, its wave function is highly delocalized and has tails well inside the Si slab, as seen in Fig. 26. It has been proposed that this band leads to a magnetic instability and various exotic magnetic orders can be realized in these

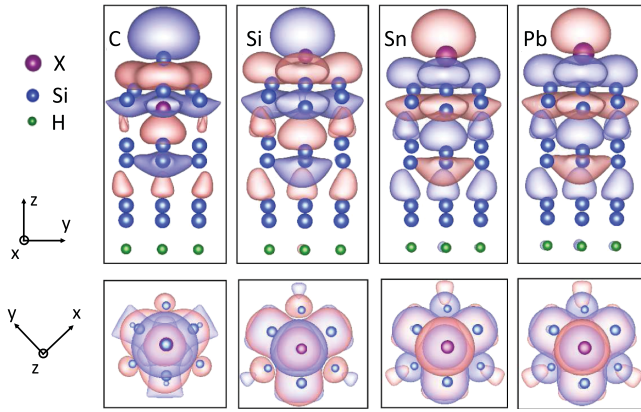


FIG. 26. Maximally localized Wannier functions representing the band crossing of the Fermi level in Si(111):X, where $X = \{\text{Sn, C, Si, Pb}\}$. Large (violet) spheres denote adatoms, while isosurfaces indicate the different parts of the Wannier functions. From Badrtdinov *et al.*, 2016.

materials. For instance, the low-temperature ground state of Si(111):X systems ranging from a 120° Néel temperature (Schuwalow, Grieger, and Lechermann, 2010) to a collinear row-wise state (Li *et al.*, 2011) and different noncollinear chiral magnetic orders (Tresca *et al.*, 2018; Vandelli *et al.*, 2023). Moreover, formation of skyrmions is suggested to emerge upon application of a high magnetic field (Badrtdinov *et al.*, 2016) or high-frequency laser field (Stepanov, Dutreix, and Katsnelson, 2017).

Owing to the delocalized nature of the orbitals carrying the magnetic moments, the influence of direct exchange mechanism is extremely pronounced. It gives rise to a ferromagnetic exchange (as expected for wave functions with small overlap), and its magnitude is so strong that it may compensate for indirect exchange contributions (Badrtdinov *et al.*, 2016). As a result, the isotropic exchange can be effectively suppressed, which results in a relatively large $|\vec{D}|/J$ ratio, where $|\vec{D}|$ is the size of the DM interaction (Badrtdinov *et al.*, 2016; Vandelli *et al.*, 2023). Since this ratio defines the period of magnetic texture, the suppression of J has led to the proposition that extremely compact skyrmions can be realized (Badrtdinov *et al.*, 2018). Ultimately, it has been envisaged that exchange-free skyrmions can also potentially emerge (Stepanov, Nikolaev *et al.*, 2019).

L. Molecular magnets

Single molecular magnets are a class of systems where transition metal atoms are embedded in an organic environment (Gatteschi *et al.*, 1994). The chemical formulas of these systems are complicated. One of them is $\text{K}_6[\text{V}_{15}\text{As}_6\text{O}_{42}(\text{H}_2\text{O})] \cdot 8\text{H}_2\text{O}$, which is most often referred to as V_{15} for brevity. The coupling between the $3d$ magnetic moments often results in a total magnetization that is uncompensated, where the net moment is regarded as a total molecular spin. Since the interactions between these molecular complexes are weak, their collective behavior is similar to that of an ensemble of noninteracting pointlike magnetic entities. Thus, molecular magnets allow one to not only address fundamental aspects of magnetism on the mesoscale (Chiorescu *et al.*, 2000; Dobrovitski, Katsnelson,

and Harmon, 2000) but also find their applications in spintronics (Bogani and Wernsdorfer, 2008; Mannini *et al.*, 2009).

DFT calculations have been widely used to understand the basic electronic and magnetic properties of molecular magnets; for a review, see Postnikov, Kortus, and Pederson (2006). The formalism of Sec. V has been widely applied to model magnetic interactions and excitation spectra in the systems like V_{15} (Boukhvalov *et al.*, 2004), Mn_4 (Kampert *et al.*, 2009), and Mn_{12} (Boukhvalov *et al.*, 2002; Mazurenko *et al.*, 2014). This work has shown that a good description of both electron spectroscopy and magnetic excitations is possible only if the correlation effects of the $3d$ states are taken into account via application of the LDA + U approach, which is similar to the situation involving $3d$ oxides. Note that the total energy difference method has also been widely used to extract the J_{ij} parameters for these systems; see Park, Pederson, and Stephen Hellberg (2004) and Ruiz, Cano, and Alvarez (2005).

The most complete description of exchange interactions in molecular magnets was done for Mn_{12} acetate by Mazurenko *et al.* (2014). The structure of this complex, shown in Fig. 27, contains two inequivalent types of Mn atoms having different oxidation states. Eight Mn^{3+} and four Mn^{4+} ions are coupled antiferromagnetically, which results in a total uncompensated spin $S = 10$. Contrary to previous works, which addressed only isotropic interactions, Mazurenko *et al.* (2014) added relativistic exchange interactions and single-ion anisotropy to the picture. The following spin Hamiltonian was considered by Mazurenko *et al.* (2014):

$$\hat{\mathcal{H}} = \mathcal{H}_{\text{DM}} + \mathcal{H}_H + \sum_{i\mu\nu} \hat{S}_i^\mu A_i^{\mu\nu} \hat{S}_i^\nu, \quad (7.7)$$

where $\{\mu, \nu\} \in \{x, y, z\}$ and $A_i^{\mu\nu}$ is the single-site anisotropy tensor. Hence, this is a generalization of the sum of Eqs. (1.1) and (1.2) since magnetic crystalline anisotropy is included.

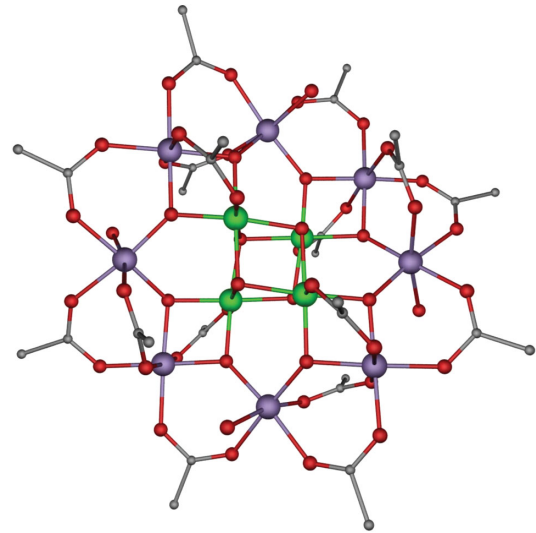


FIG. 27. Crystal structure of Mn_{12} acetate. Purple atoms (large dark gray spheres) represent Mn^{3+} ($S = 2$) ions, and green atoms (large light gray) correspond to Mn^{4+} ($S = 3/2$). Carbon and oxygen are shown as small light gray and small dark gray red, respectively; hydrogen atoms were omitted for clarity. From Zabala-Lekuona, Seco, and Colacio, 2021.

Since transition metal ions in such molecular complexes have a relatively low-symmetric environment, the Dzyaloshinskii-Moriya interactions can take relatively large values (more than typically encountered in bulk 3d oxides). This was the case for a Mn₁₂ complex, where the calculations using spin-orbit coupling revealed that the ferrimagnetic arrangement of Mn spins is canted due to the presence of DM interaction. Combining Heisenberg exchange, DM interaction, and magnetocrystalline anisotropy, Mazurenko *et al.* (2014) performed an exact diagonalization study of the complete 12-spin Hamiltonian given by Eq. (7.7) while treating all constituent spins as quantum operators. Thanks to an efficient realization of a parallel Lanczos algorithm, it was possible to calculate the 50 lowest eigenvalues of the system, which allowed for a qualitative comparison with inelastic neutron scattering data and to assign different measured peaks to the transitions from the lowest ($S = 10$) to the excited ($S = 9$) multiplets.

VIII. OUT-OF-EQUILIBRIUM EXCHANGE

Femtosecond laser sources provide a unique possibility of manipulating magnetism at ultrafast timescales (Kirilyuk, Kimel, and Rasing, 2010; Mentink, 2017). In particular, the light irradiation of magnetic materials allows one to modify the value of the exchange interaction (Melnikov *et al.*, 2003; Subkhangulov *et al.*, 2014; Mikhaylovskiy *et al.*, 2015). The idea of small spin rotations as a way to derive effective exchange interactions can be generalized to the case of time-dependent electron Hamiltonians (Secchi *et al.*, 2013). Secchi *et al.* (2013) applied the approach to the time-dependent multiorbital Hubbard model, that is, only on-site interaction was taken into account. The Hamiltonian has the form

$$\hat{H}(t) \equiv \hat{H}_T(t) + \hat{H}_V, \quad (8.1)$$

where $\hat{H}_T(t)$ is the time-dependent single-particle Hamiltonian

$$\begin{aligned} \hat{H}_T(t) &\equiv \sum_{i_a \lambda_a} \sum_{i_b \lambda_b} T_{i_a \lambda_a, i_b \lambda_b}(t) \sum_{\sigma} \hat{\phi}_{i_a \lambda_a \sigma}^{\dagger} \hat{\phi}_{i_b \lambda_b \sigma} \\ &= \sum_a \sum_b T_{ab}(t) \hat{\phi}_a^{\dagger} \cdot \hat{\phi}_b, \end{aligned} \quad (8.2)$$

where we have grouped the site and orbital indices according to $a \equiv (i_a, \lambda_a)$ and $b \equiv (i_b, \lambda_b)$ and introduced the spinor fermionic operators

$$\hat{\phi}_a^{\dagger} = \begin{pmatrix} \hat{\phi}_{a\uparrow}^{\dagger} & \hat{\phi}_{a\downarrow}^{\dagger} \end{pmatrix}, \quad \hat{\phi}_b = \begin{pmatrix} \hat{\phi}_{b\uparrow} \\ \hat{\phi}_{b\downarrow} \end{pmatrix}. \quad (8.3)$$

The interaction Hubbard-like Hamiltonian \hat{H}_V is assumed to be time independent:

$$\hat{H}_V \equiv \frac{1}{2} \sum_i \sum_{\lambda_1 \lambda_2 \lambda_3 \lambda_4} \sum_{\sigma \sigma'} V_{\lambda_1 \lambda_2 \lambda_3 \lambda_4} \hat{\phi}_{i \lambda_1 \sigma}^{\dagger} \hat{\phi}_{i \lambda_2 \sigma'}^{\dagger} \hat{\phi}_{i \lambda_3 \sigma} \hat{\phi}_{i \lambda_4 \sigma'}. \quad (8.4)$$

The spinor field operators $\hat{\phi}_a$ describe both spin and charge dynamics of the interacting itinerant-electron system. To separate supposedly slow spin dynamics from fast charge dynamics, one can introduce the rotational matrices

$$R_i(t) \equiv \begin{pmatrix} \sqrt{1 - |\xi_i(t)|^2} & \xi_i^*(t) \\ -\xi_i(t) & \sqrt{1 - |\xi_i(t)|^2} \end{pmatrix}, \quad (8.5)$$

where we have introduced the bosonic fields

$$\xi_i(t) \equiv -e^{i\varphi_i(t)} \sin[\theta_i(t)/2], \quad (8.6)$$

with $\theta_i \in [0, \pi[$, $\varphi_i \in [0, 2\pi[$ the polar angles that determine the spin axis on site i at time t . It holds that $R_i^{\dagger}(t) \cdot R_i(t) = 1$.

The matrix \hat{R} provides a transition to the new field operators $\hat{\psi}_a$ via the transformation

$$\begin{aligned} \hat{\phi}_a^{\dagger}(t) &= \hat{\psi}_a^{\dagger}(t) R_a^{\dagger}(t), \\ \hat{\phi}_a(t) &= R_a(t) \hat{\psi}_a(t), \end{aligned} \quad (8.7)$$

and we assume that in the new coordinate frame the average spin at site i at time instant t , $\langle 0 | \hat{\psi}_{a\sigma}^{\dagger} \hat{\sigma}_a \hat{\psi}_{a\sigma} | 0 \rangle$, is directed along the z axis. Thus, all information about the instant direction of the local spin $\langle 0 | \hat{\phi}_{a\sigma}^{\dagger} \hat{\sigma}_a \hat{\phi}_{a\sigma} | 0 \rangle$ is passed to the bosonic field $\xi_i(t)$.

Secchi *et al.* (2013) reformulated the problem at the Baym-Kadanoff-Keldysh contour (Kadanoff and Baym, 1962; Rammer and Smith, 1986; Kamenev, 2011; Stefanucci and Leeuwen, 2013), which is a common way to proceed in nonequilibrium quantum statistical mechanics. The effective action of the system is expanded up to the second order in the angles of spin rotations $\theta_i(t)$, and the result is compared to the effective action of the time-dependent classical Heisenberg model. As a result, we have expressions for the time-dependent exchange parameters that are expressed in terms of single-particle Green's functions and electron self-energies. Both the derivation and the final expressions are cumbersome; see Secchi *et al.* (2013) for the original paper. The procedure can be dramatically simplified if we consider electron correlations at the level of a time-dependent mean-field approximation (Secchi, Lichtenstein, and Katsnelson, 2016a). In this case one can derive relatively compact expressions for the time-dependent magnetic susceptibility and extract the exchange parameters from them, which is similar to the method used in Sec. IE. The corresponding expression has the following form (Secchi, Lichtenstein, and Katsnelson, 2016a):

$$\begin{aligned} J_{ij}(t) &= i \Sigma_{iS}(t) \lim_{\epsilon \rightarrow 0^+} \int_0^{\infty} d\tau e^{-\epsilon\tau} \Sigma_{jS}(t - \tau/2) \\ &\times \left[\left(G_{\downarrow}^< \right)_{j,t-\tau/2}^{i,t+\tau/2} \left(G_{\uparrow}^> \right)_{i,t+\tau/2}^{j,t-\tau/2} - \left(G_{\downarrow}^> \right)_{j,t-\tau/2}^{i,t+\tau/2} \left(G_{\uparrow}^< \right)_{i,t+\tau/2}^{j,t-\tau/2} \right]. \end{aligned} \quad (8.8)$$

In Eq. (8.8) $\Sigma_{iS}(t) = (1/2)[\Sigma_{i\uparrow}(t) - \Sigma_{i\downarrow}(t)]$ is the spin part of the local self-energy that is dependent only on one time t in the mean-field approximation and $(G_{\sigma}^{<})_{j,t}^{i,t}$ are the corresponding components of the Keldysh two-time Green's functions.

The theoretical description of interacting electronic systems under different time-dependent perturbations, such as an applied electric field, generally requires the use of advanced many-body numerical techniques. However, there is a particular type of perturbation, namely, an off-resonant periodic driving, that can be addressed in a relatively simple way.

Indeed, this type of driving brings the system to a non-equilibrium steady state, and the corresponding many-body problem can therefore be solved using existing time-independent approaches. The standard theoretical framework to describe the periodically driven system is the Floquet formalism (Bukov, D'Alessio, and Polkovnikov, 2015; Eckardt, 2017). This method relies on an effective time-independent Hamiltonian description of the nonequilibrium system at stroboscopic times. In the limiting case of a high-frequency driving, this effective Hamiltonian can be derived analytically. The key idea is to take advantage of a high-frequency feature of the light and use a Magnus-like perturbation expansion that allows one to reduce the time evolution of a quantum state to a time-independent eigenvalue problem with respect to the effective Hamiltonian (Itin and Neishtadt, 2014; Itin and Katsnelson, 2015). This can be done as follows: The time-periodic Hamiltonian $H(t)$ of the initial problem obeys the time-dependent Schrödinger equation

$$i\partial_t\Psi(\lambda, t) = H(t)\Psi(\lambda, t). \quad (8.9)$$

One can introduce a dimensionless parameter $\lambda = \delta E/\Omega$ that compares a certain energy scale δE of the system to the frequency Ω of the applied field. One then tries to find a unitary transformation $\Psi(\lambda, \tau) = \exp\{-i\Delta(\tau)\}\psi(\lambda, \tau)$ that removes the time dependence of the Hamiltonian. Here we introduce $\tau = \Omega t$ and also impose the condition that $\Delta(\tau) = \sum_{n=1}^{+\infty} \lambda^n \Delta_n(\tau)$, with $\Delta_n(\tau)$ a 2π periodic function. The Schrödinger equation (8.9) can then be rewritten as

$$i\partial_t\psi(\lambda, \tau) = \lambda\bar{\mathcal{H}}\psi(\lambda, \tau) \quad (8.10)$$

with an effective Hamiltonian

$$\bar{\mathcal{H}} = e^{i\Delta(\tau)}\bar{H}(\tau)e^{-i\Delta(\tau)} - i\lambda^{-1}e^{i\Delta(\tau)}\partial_\tau e^{-i\Delta(\tau)}. \quad (8.11)$$

In Eqs. (8.10) and (8.11) the bar over the Hamiltonian indicates a normalization on the energy scale δE : $\bar{H}(\tau) = H(\tau)/\delta E$. Using the series representation $\bar{\mathcal{H}} = \sum_{n=1}^{+\infty} \lambda^n \tilde{H}_n$, one can determine operators \tilde{H}_n and $\Delta_n(\tau)$ iteratively in all orders in λ . The zeroth-order term in this representation is given by the time average over the period of the driving $\tilde{H}_0 = \langle \bar{H}(\tau) \rangle = \bar{H}_0$ defined as $\bar{H}_m = \int_{-\pi}^{+\pi} (d\tau/2\pi) e^{im\tau} \bar{H}(\tau)$. The first- and second-order terms λ in the effective Hamiltonian are given by the following equations:

$$\tilde{H}_1 = -\frac{1}{2} \sum_{m \neq 0} \frac{[\bar{H}_m, \bar{H}_{-m}]}{m}, \quad (8.12)$$

$$\begin{aligned} \tilde{H}_2 = & \frac{1}{2} \sum_{m \neq 0} \frac{[[\bar{H}_m, \bar{H}_0], \bar{H}_{-m}]}{m^2} \\ & + \frac{1}{3} \sum_{m \neq 0} \sum_{n \neq 0, m} \frac{[[\bar{H}_m, \bar{H}_{n-m}], \bar{H}_{-n}]}{mn}, \end{aligned} \quad (8.13)$$

where the square brackets stand for a commutator. The resulting effective time-independent Hamiltonian describes the stroboscopic dynamics of the system, whereas its evolution between

two stroboscopic times is encoded in the time-dependent function $\Delta_n(\tau)$. This approach allows one to explore interesting phases of matter and to control different properties of materials through a direct tuning of model parameters (hopping amplitudes and electronic interactions) that in Floquet theory become explicitly dependent on characteristics of the applied perturbation; see Itin and Katsnelson (2015), Bukov, Kolodrubetz, and Polkovnikov (2016), Dutreix, Stepanov, and Katsnelson (2016), Kitamura and Aoki (2016), Dutreix and Katsnelson (2017), Stepanov, Dutreix, and Katsnelson (2017), Peronaci, Parcollet, and Schiró (2020), and Valmispild *et al.* (2020).

The introduced formalism can also be used for calculating magnetic exchange interactions under the effect of high-frequency light irradiation (Itin and Katsnelson, 2015; Mentink, Balzer, and Eckstein, 2015; Claassen *et al.*, 2017; Mentink, 2017; Stepanov, Dutreix, and Katsnelson, 2017; Barbeau *et al.*, 2019). In particular, in a strong-coupling limit $U \gg t$, where U is the Coulomb interaction and t is the hopping amplitude, one can make a Schrieffer-Wolff transformation in order to map the derived effective Hamiltonian onto a Heisenberg Hamiltonian (Chao, Spalek, and Oleś, 1977a, 1977b; MacDonald, Girvin, and Yoshioka, 1988; Spalek, 2007). In the presence of an external time-dependent perturbation, transformation was performed by Bukov, Kolodrubetz, and Polkovnikov (2016), Stepanov, Dutreix, and Katsnelson (2017), and Valmispild *et al.* (2020). The resulting isotropic symmetric exchange interaction $J = J^K - J^D$ contains two contributions. The kinetic exchange interaction corresponds to a usual AFM superexchange $J^K = \tilde{t}^2/U$ that exists in equilibrium. However, out-of-equilibrium J^K contains the hopping amplitude $\tilde{t} = t\mathcal{J}_0(\mathcal{E})$, which is renormalized by the m th-order Bessel function of the first kind $\mathcal{J}_m(\mathcal{E})$ due to the effect of high-frequency light irradiation. The dimensionless parameter $\mathcal{E} = eE_0a/\Omega$ contains the strength of the laser field E_0 , the elementary charge e , and the lattice constant a_0 . The AFM exchange J^K competes with the direct FM exchange interaction $J^D = J_{\text{bare}}^D + J_{\text{ind}}^D$. The bare part of the direct exchange J_{bare}^D stems from nonlocal electronic interactions and is already present in equilibrium; see Mazurenko *et al.* (2007, 2008, 2016), Rudenko *et al.* (2013), and Badrtdinov *et al.* (2016). The second part corresponds to the contribution that is induced by the high-frequency light irradiation (Itin and Katsnelson, 2015; Bukov, Kolodrubetz, and Polkovnikov, 2016),

$$J_{\text{ind}}^D = 2t^2U \sum_{m=1}^{+\infty} \frac{\mathcal{J}_m^2(\mathcal{E})}{m^2\Omega^2 - U^2}. \quad (8.14)$$

In the case of a nearly resonant driving $\Omega \simeq U/m$ (Itin and Katsnelson, 2015; Mentink, Balzer, and Eckstein, 2015) or when the bare direct exchange is sufficiently large (Stepanov, Dutreix, and Katsnelson, 2017), the total isotropic symmetric exchange interaction can be substantially modified by high-frequency light and can even change sign under certain conditions. The introduced formalism can also be extended to other types of magnetic exchange interactions, such as Dzyaloshinskii-Moriya (Stepanov, Dutreix, and Katsnelson, 2017), chiral three-spin (Claassen *et al.*, 2017), and biquadratic exchange interactions (Barbeau *et al.*, 2019), which can all be

tuned by high-frequency laser pulses. In particular, the light control of magnetic interactions may dynamically induce chiral spin liquids in frustrated Mott insulators (Claassen *et al.*, 2017). This may also allow for creation, stabilization, and modification of the shape of skyrmions in materials where these topological spin textures do not exist at equilibrium conditions (Stepanov, Dutreix, and Katsnelson, 2017). Moreover, when the isotropic symmetric exchange interaction J is completely suppressed by the light irradiation, one can access a unique phase where magnetic properties of the system are governed solely by the Dzyaloshinskii-Moriya interaction (Stepanov, Nikolaev *et al.*, 2019).

IX. LOCAL MOMENT FORMATION AND SPIN DYNAMICS

Historically, the density functional theory became the standard language for the theory of magnetism and magnetic interactions. As previously discussed, in this framework exchange interactions can be obtained considering variations of the total energy with respect to small rotations of magnetic moments starting from equilibrium ground states. Despite the success of this approach in describing many magnetic materials, there are several important problems that cannot be addressed using this language. Indeed, realistic models for magnetic materials that are derived within DFT are interacting electronic problems. However, finding a possibility of mapping these electronic models onto Heisenberg-like spin problems is a highly nontrivial task that remains unsolved in the framework of DFT. In addition, calculating the exchange interactions using the magnetic force theorem is based on the assumption that the variation of the magnetization from the ground-state magnetic configuration is small, which is frequently not the case, especially for itinerant-electron systems.

The most common way to introduce an effective spin model for an interacting electronic problem is based on a Schrieffer-Wolff transformation (Chao, Spátek, and Oleś, 1977a, 1977b; MacDonald, Girvin, and Yoshioka, 1988; Spátek, 2007), which, strictly speaking, is justified only at integer filling in the limiting case of a large interaction between electrons. Already t - J or s - d exchange models (Vonsovskii, 1974) that are frequently used to describe the physics of a doped Mott insulator cannot be easily mapped onto a pure spin Hamiltonian. Moreover, spin degrees of freedom in the transformed problem are described in terms of composite fermionic variables and not in terms of physical bosonic fields as would be desirable for pure spin models. This results in a need to introduce artificial constraints in order to conserve the length of the total spin. In addition, one also has to assume that the average value of these composite fermionic variables that defines the local magnetization is nonzero. The latter is hard to justify in a paramagnetic regime, where, generally speaking, it should also be possible to introduce a Heisenberg-like spin model.

Even though deriving an effective spin problem for interacting electrons is not an easy task, one must do more than that and find a way to introduce a correct equation of motion for spin degrees of freedom. For localized spins, the classical equation for the spin precession can be obtained by evaluating path integrals over spin-coherent states in the saddle-point

approximation (Schapere and Wilczek, 1989; Inomata, Kuratsui, and Gerry, 1992; Auerbach, 1994). In this approach, the kinetic term that describes the rotational dynamics of spins originates from the topological Berry phase, for which the conservation of the length of the total spin on each site is a necessary condition. For this reason, generalizing the formalism of spin-coherent states to itinerant-electron problems is mathematically a highly nontrivial task. Nevertheless, finding a way to derive the equation of motion for the local magnetic moment in the framework of electronic problems is crucial for a correct description of the full spin dynamics of the system. Indeed, studying classical spin Hamiltonians allows one to describe only a uniform precession of the local magnetic moment. Taking into account dissipation effects, e.g., Gilbert damping, requires one to couple classical spins to itinerant electrons (Sayad and Potthoff, 2015; Sayad, Rausch, and Potthoff, 2016). In addition, considering classical spins disregards quantum fluctuations of the modulus of the local magnetic moment (Pekker and Varma, 2015) that were observed in recent experiments (Rüegg *et al.*, 2008; Merchant *et al.*, 2014; Hong *et al.*, 2017; Jain *et al.*, 2017; Souliou *et al.*, 2017; Ying, Schmidt, and Wessel, 2019). In analogy with high-energy physics, these fast fluctuations are usually described in terms of a massive Higgs mode (Englert and Brout, 1964; Guralnik, Hagen, and Kibble, 1964; Higgs, 1964a, 1964b), while slow spin rotations are associated with Goldstone modes that originate from the broken rotational invariance in spin space.

The problem of describing the physics of the local magnetic moment in the framework of interacting electronic models was intensively studied in the late 1970s and early 1980s (Korenman, Murray, and Prange, 1977a, 1977b, 1977c; Hasegawa, 1979b; Hubbard, 1979a, 1979b; Hasegawa, 1980a, 1980b, 1983; Edwards, 1982, 1983). In these works the local moments were formally introduced into the Hubbard model using the Hubbard-Stratonovich transformation and making use of a static approximation for the introduced decoupling fields. Note that the static approximation in the Hubbard model is closed conceptually to the disordered local moment approach (Oguchi, Terakura, and Hamada, 1983; Pindor *et al.*, 1983; Gyorffy *et al.*, 1985; Staunton *et al.*, 1986; Staunton and Gyorffy, 1992; Niklasson *et al.*, 2003) within density functional theory. As a result, the initial translationally invariant system of interacting electrons is replaced by a single-particle problem involving electrons moving in a random magnetic field acting on spins. Fluctuations in the direction of these fields are taken into account, thus allowing one to go beyond a mean-field approach. For the case of the Hubbard or s - d exchange models at Bethe lattices, one can build the effective classical spin Hamiltonian, taking into account both Anderson superexchange and Zener double exchange of essentially a non-Heisenbergian character (Auslender and Katsnel'son, 1982; Auslender and Katsnelson, 1982). This approach allows one to go far beyond the Stoner picture of itinerant-electron magnetism and clarifies several important questions, such as the origin of Curie-Weiss law for magnetic susceptibility above Curie temperature, but it does not result in a complete quantitative theory of magnetism of itinerant electrons. In particular, it does not work at low temperatures where magnonlike dynamical excitations play a

crucial role. An attempt to add these effects and to come to a unified picture in a phenomenological way was made by [Moriya \(2012\)](#). Several important questions have remained unsolved; for instance, the role of dynamical fluctuations that are known to be responsible for the Kondo effect ([Hamann, 1967](#)) was not clarified.

There have also been many attempts to address the problem involving the spin dynamics of interacting electrons. To get the Berry phase, one usually follows a standard route that consists in introducing rotation angles for a quantization axis of electrons ([Schulz, 1990](#); [Weng, Ting, and Lee, 1991](#); [Dupuis and Pairault, 2000](#); [Dupuis, 2001](#)). These angles are considered as path-integral variables to fulfill rotational invariance in the spin space. In this case, the Berry phase term appears as an effective gauge field that, however, is coupled to fermionic variables instead of a spin bosonic field. Considering purely electronic problems makes it difficult to disentangle spin and electronic degrees of freedom. For this reason, until recently it was not possible to connect the Berry phase to a proper bosonic variable that describes the modulus of the local magnetic moment. For the same reason, it was also not possible to introduce a proper Higgs field to describe fluctuations of the modulus of the magnetization. Indeed, in electronic problems this field is usually introduced by decoupling the interaction term ([Sachdev, 2008](#); [Scheurer *et al.*, 2018](#); [Thomson and Sachdev, 2018](#); [Wu *et al.*, 2018](#); [Gazit, Assaad, and Sachdev, 2020](#)). First, this decoupling field does not have a clear physical meaning and its dynamics does not necessarily correspond to the dynamics of the local magnetic moment. Second, in actual calculations this effective Higgs field is usually treated in a mean-field approximation, assuming that it has a nonzero average value, which is nontrivial to justify in a paramagnetic phase. Keep in mind that although the decoupling of the interaction term is a mathematically exact procedure, it can be performed in many different ways. In particular, this fact leads to a famous Fierz ambiguity problem ([Jaeckel, 2002](#); [Jaeckel and Wetterich, 2003](#); [Baier, Bick, and Wetterich, 2004](#)) if the decoupling field is further treated in a mean-field approximation.

The aim of this section is to collect all previous achievements in describing spin degrees of freedom of interacting electrons and unify them in a general theory of spin dynamics and effective exchange interactions in strongly correlated systems. In this section we discuss how an effective quantum spin action written in terms of physical bosonic variables can be rigorously derived starting with a pure electronic problem. We show that this derivation can be performed without assuming that the average magnetization is nonzero and without imposing any constraints, such as artificial magnetic fields. We illustrate that the introduced effective spin problem allows one to obtain all kinds of exchange interactions between spins, and thus to establish relations between the magnetic local force approach and the standard language of response functions. Further, we show that the corresponding equation of motion for this action correctly describes the dissipative rotational dynamics of the local magnetic moment via the Berry phase and the Gilbert damping term and also takes into account the Higgs fluctuations of the modulus of the magnetic moment. At the end, we introduce a physical criterion for the formation of the local magnetic moment in

the system and show that this approach is applicable even in the paramagnetic regime. As a whole, this section provides a solid and mathematically consistent background for a complete description of spin dynamics in strongly correlated electron systems.

A. Derivation of the bosonic action for the fermionic problem

To introduce a consistent theory of spin dynamics, we follow the route presented by [Stepanov *et al.* \(2018\)](#) and [Stepanov, Brener *et al.* \(2022\)](#) and use the action formalism based on the Feynman path-integral technique as a more appropriate language for treating many-body quantum problems. We start with the following general action for a multi-orbital extended Hubbard model as a particular example of the strongly correlated electronic problem that possesses spin dynamics:

$$\begin{aligned} \mathcal{S}_{\text{latt}}[c^{(*)}] = & - \int_0^\beta d\tau \sum_{jj',\sigma\sigma',ll'} c_{j\tau\sigma l}^* [\mathcal{G}^{-1}]_{jj'\sigma\sigma'}^{\tau\tau ll'} c_{j'\tau\sigma' l'} \\ & + \frac{1}{2} \int_0^\beta d\tau \left\{ \sum_{j,\sigma\sigma',\{l\}} U_{l_1 l_2 l_3 l_4} c_{j\tau\sigma l_1}^* c_{j\tau\sigma l_2} c_{j\tau\sigma' l_3}^* c_{j\tau\sigma' l_4} \right. \\ & \left. + \sum_{jj',\zeta,\{l\}} V_{l_1 l_2 l_3 l_4}^{jj'\zeta} \rho_{j\tau l_1 l_2}^\zeta \rho_{j'\tau l_3 l_4}^\zeta \right\}. \end{aligned} \quad (9.1)$$

Equation (9.1) is written in terms of annihilation (creation) fermionic Grassmann variables $c_{j\tau\sigma l}^{(*)}$ and is considered in the lattice j , imaginary time τ , spin $\sigma = \{\uparrow, \downarrow\}$, and orbital l space. The bare (noninteracting) Green's function is defined by the inverse of the matrix

$$[\mathcal{G}^{-1}]_{jj'\sigma\sigma'}^{\tau\tau ll'} = \delta_{\tau\tau'} [\delta_{jj'} \delta_{\sigma\sigma'} \delta_{ll'} (-\partial_\tau + \mu) - \epsilon_{jj'\sigma\sigma'}^{\tau\tau ll'}]. \quad (9.2)$$

It contains the chemical potential μ and the hopping matrix $\epsilon_{jj'\sigma\sigma'}^{\tau\tau ll'}$. The latter has the following form in the spin space: $\epsilon_{jj'\sigma\sigma'}^{\tau\tau ll'} = \epsilon \delta_{\sigma\sigma'} + i \vec{k} \cdot \vec{\sigma}_{\sigma\sigma'}$, where the diagonal part ϵ of this matrix corresponds to the usual hopping amplitude of the electrons. The nondiagonal part \vec{k} accounts for the spin-orbit coupling in the Rashba form ([Bychkov and Rashba, 1984](#); [Yildirim *et al.*, 1995](#)). The interacting part of the model action (9.1) consists of the local Coulomb potential $U_{l_1 l_2 l_3 l_4}$ and the nonlocal interaction $V_{l_1 l_2 l_3 l_4}^{jj'\zeta}$ ($V_{jj} = 0$) between electrons in the charge ($\zeta = c$) and spin ($\zeta = s = \{x, y, z\}$) channels. Composite fermionic variables $\rho_{j\tau ll'}^\zeta = n_{j\tau ll'}^\zeta - \langle n_{ll'}^\zeta \rangle$ describe fluctuations of charge and spin densities $n_{j\tau ll'}^\zeta = \sum_{\sigma\sigma'} c_{j\tau\sigma l}^* \sigma_{\sigma\sigma'}^\zeta c_{j\tau\sigma' l'}$ around their average values.

We note that the exchange interactions between spins in the bosonic problem that we aim to derive are nonlocal, while the dynamics of the magnetic moment is usually described by local Berry and Higgs terms. For this reason, it would be useful to explicitly decouple local and nonlocal correlations in the system. [Stepanov *et al.* \(2018\)](#) and [Stepanov, Brener *et al.* \(2022\)](#) proposed performing this decoupling by considering the local site-independent reference problem that accounts for the local part of the lattice action (9.1),

$$\begin{aligned} \mathcal{S}_{\text{imp}}^{(j)}[c^{(*)}] = & - \iint_0^\beta d\tau d\tau' \sum_{\sigma, l'l'} c_{j\tau\sigma l}^* [g_0^{-1}]_{\tau\tau'}^{ll'} c_{j\tau'\sigma l'} \\ & + \frac{1}{2} \int_0^\beta d\tau \sum_{\sigma\sigma', \{l\}} U_{l_1 l_2 l_3 l_4} c_{j\tau\sigma l_1}^* c_{j\tau\sigma l_2} c_{j\tau\sigma' l_3}^* c_{j\tau\sigma' l_4}, \end{aligned} \quad (9.3)$$

where

$$[g_0^{-1}]_{\tau\tau'}^{ll'} = \delta_{\tau\tau'} \delta_{ll'} (-\partial_\tau + \mu) - \Delta_{\tau\tau'}^{ll'} \quad (9.4)$$

is the inverse of the bare Green's function of the reference system. Equation (9.3) has the form of the impurity problem of dynamical mean-field theory (Georges *et al.*, 1996) and is intended to describe the local correlation effects of the initial lattice action (9.1). This is achieved by introducing a non-stationary hybridization function $\Delta_{\tau\tau'}^{ll'} = \Delta^{ll'}(\tau - \tau')$ that aims at capturing the effect of surrounding electrons on a given impurity site. In general, the impurity problem (9.3) can be considered either in a polarized (Stepanov *et al.*, 2018) or in a nonpolarized form (Stepanov, Brener *et al.*, 2022), which corresponds to an ordered or paramagnetic solution for the problem, respectively. At present we stick to a nonpolarized local reference system, which allows one to describe a regime of the system where the average local magnetization is identically zero $\langle n_{ll'}^s \rangle_{\text{imp}} = 0$. In this case, the hybridization function $\Delta_{\tau\tau'}^{ll'}$ is spin independent and can be determined from the self-consistent condition $(1/2) \sum_\sigma G_{jj\sigma\sigma}^{\tau\tau' ll'} = g_{\tau\tau'}^{ll'}$ (Stepanov, Brener *et al.*, 2022), which equates the spin diagonal, local part of the interacting lattice Green's function $G_{jj\sigma\sigma}^{\tau\tau' ll'}$ and the interacting Green's function of the local reference problem $g_{\tau\tau'}^{ll'}$. A DMFT-like form of the reference system [Eq. (9.3)] allows for the exact solution of this local problem using, for example, the continuous-time quantum Monte Carlo method (Rubtsov, Savkin, and Lichtenstein, 2005; Werner *et al.*, 2006; Werner and Millis, 2010; Gull *et al.*, 2011). This implies that the corresponding local many-body correlation functions including the full interacting Green's function $g_{\tau\tau'}^{ll'}$ and the susceptibility $\chi_{l_1 l_2 l_3 l_4}^{\tau\tau'}$ can be obtained numerically exact. This drastically simplifies the investigation of many physical effects that are directly related to local electronic correlations, which, in particular, includes formation of the local magnetic moment (Stepanov, Brener *et al.*, 2022). We discuss this point in more detail in Sec. IX D.

After isolating the local reference system, the nonlocal correlations are contained in the remaining part of the lattice action $\mathcal{S}_{\text{rem}}[c^{(*)}] = \mathcal{S}_{\text{latt}}[c^{(*)}] - \sum_j \mathcal{S}_{\text{imp}}^{(j)}[c^{(*)}]$. However, the local and nonlocal correlation effects are not yet disentangled, because $\mathcal{S}_{\text{imp}}[c^{(*)}]$ and $\mathcal{S}_{\text{rem}}[c^{(*)}]$ are written in terms of the same fermionic Grassmann variables. Calculating any physical observable using the present form of the lattice action will immediately mix these correlations up. After that, a separation of them is possible only with a complex resummation of corresponding contributions to a Feynman diagrammatic expansion (Li, 2015; Brener *et al.*, 2020). As an alternative, there is a simpler way to completely disentangle local and nonlocal correlation effects. The idea consists in integrating

out the reference system, as proposed in the dual fermion (Rubtsov, Katsnelson, and Lichtenstein, 2008; Hafermann *et al.*, 2009; Rubtsov *et al.*, 2009) and dual boson theories (Rubtsov, Katsnelson, and Lichtenstein, 2012; van Loon *et al.*, 2014; Stepanov, Huber *et al.*, 2016; Stepanov, van Loon *et al.*, 2016; Peters *et al.*, 2019). To this aim, we first rewrite the nonlocal part of the action in terms of new fermionic $c^{(*)} \rightarrow f^{(*)}$ and bosonic $\rho^\sigma \rightarrow \phi^\sigma$ variables by means of the Hubbard-Stratonovich transformation (Stratonovich, 1957; Hubbard, 1959). After this transformation, the lattice action $\mathcal{S}_{\text{latt}}[c^*, f^*, \phi^\sigma]$ depends on two fermionic and one bosonic variables. Original Grassmann variables $c^{(*)}$ are contained only in the local part of the lattice action, which includes the impurity problem [Eq. (9.3)], and thus can be integrated out.

Before making this integration, one should recall that isolating local correlation effects should help one to correctly describe the dynamics of spin degrees of freedom. In general, spin dynamics might have a nontrivial form since it involves a combination of a slow spin precession and fast Higgs fluctuations of the modulus of the local magnetic moment. For this reason, it is more convenient to treat these two contributions separately. In electronic systems, the Berry phase term that describes the uniform spin precession is commonly obtained by transforming original electronic variables to a rotating frame (Schulz, 1990; Weng, Ting, and Lee, 1991; Dupuis and Pairault, 2000; Dupuis, 2001). This can be achieved by introducing a unitary matrix in the spin space,

$$R_{j\tau} = \begin{pmatrix} \cos(\theta_{j\tau}/2) & -e^{-i\varphi_{j\tau}} \sin(\theta_{j\tau}/2) \\ e^{i\varphi_{j\tau}} \sin(\theta_{j\tau}/2) & \cos(\theta_{j\tau}/2) \end{pmatrix}, \quad (9.5)$$

and making the corresponding change of variables $c_{j\tau l} \rightarrow R_{j\tau} c_{j\tau l}$, where $c_{j\tau l} = (c_{j\tau l\uparrow}, c_{j\tau l\downarrow})^T$. Rotation angles $\Omega_R = \{\theta_{j\tau}, \varphi_{j\tau}\}$ are considered as site j and time τ dependent variables. Introducing an additional functional integration over them allows one to preserve the rotational invariance in the spin space. As a consequence, the modified lattice action takes the following form: $\mathcal{S}_{\text{latt}}[c^*, f^*, \phi^\sigma, \Omega_R]$.

The Berry phase arises from the local impurity problem that upon rotation becomes (Stepanov, Brener *et al.*, 2022)

$$\mathcal{S}_{\text{imp}}^{(j)}[c^{(*)}] \rightarrow \mathcal{S}_{\text{imp}}^{(j)}[c^{(*)}] + \int_0^\beta d\tau \sum_{s,l} \mathcal{A}_{j\tau}^s \rho_{j\tau ll}^s. \quad (9.6)$$

The z component of an effective gauge field $\mathcal{A}_{j\tau}^s$ has the desired form of the Berry phase term $\mathcal{A}_{j\tau}^z = (i/2) \dot{\varphi}_{j\tau} (1 - \cos \theta_{j\tau})$. To exclude other components of the gauge field from consideration, one usually assumes that the rotation angles Ω_R correspond to the spin-quantization axis of the electrons. In this case, the composite fermionic variable in the spin channel ρ^s is replaced by its z component ρ^z which is coupled to the ‘‘correct’’ component of the gauge field $\mathcal{A}_{j\tau}^z$. Proceeding in this direction leads to several problems. Associating rotation angles with the spin-quantization axis is nontrivial to formulate in a strict mathematical sense. Dupuis and Pairault (2000) and Dupuis (2001) introduced the slave boson approximation. However, there is no guarantee that the average magnetization on a given lattice site will also point in the z direction. Indeed, the

spin-quantization axes on different sites may point in different directions, which may induce an effective mean magnetic field that will change the direction of the magnetization on a given site. In particular, this does not allow one to replace the composite fermionic variable ρ^z by its average value in the Berry phase term (9.6). Moreover, in the paramagnetic phase this replacement does not make sense, because the average magnetization in this case is identically zero. Finally, in Eq. (9.6) the effective gauge field $\mathcal{A}_{j\tau}^z$ is coupled to a composite fermionic variable ρ^s instead of a proper vector bosonic field that describes fluctuations of the local magnetic moment. This representation of spin degrees of freedom does not conserve the length of the total spin, which is a necessary condition for a correct description of a spin precession.

We emphasize that the rotation angles cannot be associated with the direction of the newly introduced bosonic field for spin degrees of freedom ϕ^s . This field enters the lattice action as an effective quantum magnetic field that polarizes the electrons (Stepanov *et al.*, 2018; Stepanov, Brener *et al.*, 2022) and is frequently associated with the Higgs field (Sachdev, 2008; Scheurer *et al.*, 2018; Thomson and Sachdev, 2018; Wu *et al.*, 2018; Gazit, Assaad, and Sachdev, 2020). However, this effective bosonic field is introduced as the result of a Hubbard-Stratonovich transformation and does not have a clear physical meaning. Moreover, even if it would be possible to associate ϕ^s with the physical Higgs field, its dynamics would not necessarily correspond to the dynamics of the local magnetic moment. All these observations suggest that the idea of describing the spin precession in terms of rotation angles is appealing, but one has to find a way to relate these angles to the direction of the local magnetic moment and not to the spin-quantization axis or to the effective Higgs field.

After the original electronic variables $c^{(*)}$ are transformed to a rotating frame, they can finally be integrated out, which results in the so-called dual boson action $\mathcal{S}_{\text{latt}}[f^{(*)}, \phi^s, \Omega_R]$ (Rubtsov, Katsnelson, and Lichtenstein, 2012; van Loon *et al.*, 2014; Stepanov, van Loon *et al.*, 2016). In this action, bare propagators for the fermionic $f^{(*)}$ and bosonic ϕ^s variables are purely nonlocal and explicitly depend on rotation angles Ω_R (Stepanov, Brener *et al.*, 2022). All local correlations are absorbed in the interaction part of the fermion-boson action $\tilde{\mathcal{F}}[f^{(*)}, \phi^s, \Omega_R]$, which consists of all possible fermion-fermion, fermion-boson, and boson-boson vertex functions of the local reference problem (9.3). To proceed further, we truncate the interaction at the two-particle level and keep only the four-point (fermion-fermion) Γ and three-point (fermion-boson) Λ^s vertices. This approximation is widely used in the dual fermion approach (Rubtsov, Katsnelson, and Lichtenstein, 2008; Hafermann *et al.*, 2009; Rubtsov *et al.*, 2009), the dual boson method (Rubtsov, Katsnelson, and Lichtenstein, 2012; van Loon *et al.*, 2014; Stepanov, Huber *et al.*, 2016; Stepanov, van Loon *et al.*, 2016; Peters *et al.*, 2019), and the recently introduced dual triply irreducible local expansion (Stepanov, Harkov, and Lichtenstein, 2019; Harkov *et al.*, 2021; Vandelli *et al.*, 2022), including their diagrammatic Monte Carlo realizations (Iskakov, Antipov, and Gull, 2016; Gukelberger, Kozik, and Hafermann, 2017; Vandelli *et al.*, 2020), which provide results that are in good agreement with the exact benchmark methods (Iskakov, Antipov, and Gull, 2016; Gukelberger,

Kozik, and Hafermann, 2017; Iskakov, Terletska, and Gull, 2018; Vandelli *et al.*, 2020; Harkov *et al.*, 2021; Schäfer *et al.*, 2021).

Integrating out the reference system not only disentangles local and nonlocal correlations but also allows one to get rid of composite fermionic variables ρ^s that are no longer present in the dual boson action $\mathcal{S}_{\text{latt}}[f^{(*)}, \phi^s, \Omega_R]$. Charge and spin degrees of freedom are now described by a proper bosonic field ϕ^s that has a well-defined propagator and a functional integration over them. Moreover, in this action the gauge field $\mathcal{A}_{j\tau}^z$ is coupled up to a certain multiplier to the spin component of this bosonic field ϕ^s (Stepanov, Brener *et al.*, 2022). However, as previously discussed, the bosonic variable ϕ^s does not have a clear physical meaning. The way to introduce a physical bosonic variable was proposed by Stepanov *et al.* (2018) and was inspired by Dupuis and Pairault (2000) and Dupuis (2001), who performed a similar transformation for fermionic fields. The idea consists in introducing a source field η^s for the original composite fermionic variable ρ^s that describes fluctuations of charge and spin densities. After obtaining the dual boson action one then performs an additional Hubbard-Stratonovich transformation $\phi^s \rightarrow \bar{\rho}^s$ that makes η^s the source field for the resulting physical bosonic field $\bar{\rho}^s$. Further, unphysical bosonic fields ϕ^s are integrated out, which leads to the fermion-boson action $\mathcal{S}_{\text{latt}}[f^{(*)}, \bar{\rho}^s, \Omega_R]$.

The derived fermion-boson action has a simpler form than the dual boson action $\mathcal{S}_{\text{latt}}[f^{(*)}, \phi^s, \Omega_R]$. Indeed, the interaction part of the fermion-boson action contains only the three-point vertex function Λ^s . The four-point vertex Γ that is present in the dual boson action is approximately canceled by the counterterm that is generated during the last Hubbard-Stratonovich transformation (Stepanov *et al.*, 2018; Stepanov, Harkov, and Lichtenstein, 2019). As a result, the fermion-boson action $\mathcal{S}_{\text{latt}}[f^{(*)}, \bar{\rho}^s, \Omega_R]$ takes the form of an effective t - J or s - d exchange model (Vonsovskii, 1974) that describes local charge and spin moments $\bar{\rho}^s$ coupled to itinerant electrons $f^{(*)}$ via the local fermion-boson vertex function Λ^s . Moreover, in this action the gauge field $\mathcal{A}_{j\tau}^z$ is coupled to the spin component of the physical bosonic field $\bar{\rho}^s$, as desired for a correct description of the rotational dynamics of the local magnetic moment (Stepanov, Brener *et al.*, 2022).

We note that at this point all parameters of the fermion-boson action, including the coupling of the gauge field $\mathcal{A}_{j\tau}^z$ to the bosonic field $\bar{\rho}^s$, explicitly depend on the rotation angles Ω_R . From the beginning, these angles are introduced to account for the spin precession explicitly. For this reason, Ω_R should be related to the direction of the local magnetic moment, which in the fermion-boson action is defined by a bosonic vector field $\bar{\rho}^s$. It is convenient to rewrite the latter in spherical coordinates as $\rho_{j\tau l l'}^s = M_{j\tau l l'} e_{j\tau}^s$, where $M_{j\tau l l'}$ is a scalar field that describes fluctuations of the modulus of the orbitally resolved local magnetic moment. In this expression we assume that the multiorbital system that exhibits a well-developed magnetic moment is characterized by a strong Hund's exchange coupling that orders spins of electrons at each orbital in the same direction. Therefore, the direction of the local magnetic moment in the system is defined by the orbital-independent unit vector $\vec{e}_{j\tau}$, as described by a set of

polar angles $\Omega_M = \{\theta'_{j\tau}, \phi'_{j\tau}\}$ associated with this vector. Stepanov, Brener *et al.* (2022) showed that taking the path integral over rotation angles Ω_R in the saddle-point approximation allows one to equate these two sets of angles $\Omega_R = \Omega_M$, which from now on define the direction of the local magnetic moment. After that, the remaining dependence on rotation angles can be eliminated from fermionic parts of the fermion-boson action. This can be achieved in the adiabatic approximation that assumes that characteristic times

for electronic degrees of freedom are much faster than those for spin ones.

The bosonic problem that describes the behavior of charge and spin densities can be obtained by integrating out fermionic fields $f^{(*)}$. The fermion-boson action is Gaussian in terms of these fields, so this integration can be performed exactly. The resulting bosonic action takes the following final form (Stepanov, Brener *et al.*, 2022):

$$\begin{aligned} \mathcal{S}_{\text{latt}} = & -\text{Tr} \ln \left[\tilde{\mathcal{G}}^{-1} \Big|_{jj'\sigma\sigma'}^{\tau\tau' l l'} - \delta_{jj'} \int_0^\beta d\tau_1 \sum_{\xi, l_1 l'_1} \sigma_{\sigma\sigma'}^\xi \Lambda_{ll'l_1 l'_1}^{\xi\tau\tau' \tau_1} \bar{\rho}_{j\tau_1 l'_1 l_1}^\xi \right] + \frac{1}{2} \int_0^\beta d\tau \sum_{jj', \xi, \{l\}} \bar{\rho}_{j\tau l l'}^\xi V_{ll'l_1 l'_1}^{jj'\xi} \bar{\rho}_{j\tau l'_1 l_1}^\xi \\ & - \frac{1}{2} \iint_0^\beta d\tau d\tau' \sum_{j, \{l\}} \{ \bar{\rho}_{j\tau l l'}^c [\chi^{c-1}]_{ll'l_1 l'_1}^{\tau\tau'} \bar{\rho}_{j\tau' l'_1 l_1}^c + M_{j\tau l l'} [\chi^{z-1}]_{ll'l_1 l'_1}^{\tau\tau'} M_{j\tau' l'_1 l_1} \} + \int_0^\beta d\tau \sum_j \mathcal{A}_{j\tau}^z \mathcal{M}_{j\tau}. \end{aligned} \quad (9.7)$$

In this action the modulus of the total magnetic moment $\mathcal{M}_{j\tau} = \sum_l M_{j\tau l}$ is coupled only to the z component of the effective gauge field $\mathcal{A}_{j\tau}^z$, which gives exactly the desired Berry phase term. Other components of the gauge field disappear upon associating rotation angles with the direction of the local magnetic moment.

B. Exchange interactions in many-body theory and relation to other approaches

Before introducing the explicit expression for the exchange interaction, we note that an unambiguous definition for this quantity does not exist. The exchange interactions are internal parameters of the model and thus depend on the particular form of the considered Hamiltonian. In its turn, the latter crucially depends on the downfolding scheme used to map the interacting electronic problem onto an effective bosonic (i.e., spin) model. For instance, it has been shown that considering small local variations from the ordered magnetic state leads to a bilinear exchange interaction that depends on the magnetic configuration, and the resulting spin Hamiltonian also contains higher-order nonlinear exchange interactions that are non-negligible *a priori* (Auslender and Katsnel'son, 1982; Auslender and Katsnelson, 1982). On the other hand, one can try to map the interacting electronic problem onto a global Heisenberg-like spin model with only a bilinear exchange interaction. In this case, the value of the bilinear exchange might differ from the one of the nonlinear spin model.

However, both forms of the spin Hamiltonian are useful. The form that contains nonlinear exchange interactions better reproduces the spectrum of spin waves (Pajda *et al.*, 2001). On the other hand, the Heisenberg Hamiltonian is a standard model for atomistic spin simulations and gives reasonable thermodynamic properties of the system (Eriksson *et al.*, 2017). To establish connection between different definitions for the exchange interaction, we start with the previously derived bosonic action (9.7). In this action local and nonlocal correlation effects are completely disentangled by construction of the theory. The first line in Eq. (9.7) describes nonlocal exchange interactions between charge $\bar{\rho}^c$ and spin $\bar{\rho}^s$ densities. The first term in Eq. (9.7) is responsible for all possible kinetic

exchange processes (including higher-order ones) mediated by electrons. This can be illustrated by directly expanding the logarithm function to all orders in $\bar{\rho}^s$ variables. Since this expansion is performed in terms of the bosonic variables that correspond to charge and magnetic densities, the resulting bilinear and nonlinear exchange interactions are well defined. This expansion is essentially different from the one performed in terms of rotation angles in DFT-based formalisms. Indeed, the latter is based on the magnetic force theorem (see Sec. VA), which, however, cannot be used for the discussion of higher-order expansion terms in the rotation angle. The situation is similar to that in the problem involving calculations of elastic moduli of solids in density functional: Whereas the first-order variations with respect to deformation are simple and can be calculated according to the local force theorem, the second-order variations contain a lot of additional terms related to the differentiation of the double-counting contributions (Zein, 1984). At the same time, the effective bosonic action discussed here is based on formally exact transformations.

The bilinear exchange interaction $J_{jj'}^{\xi\xi'}$ is given by the second order of the expansion

$$\begin{aligned} J_{jj'}^{\xi\xi' \tau\tau' l l'} = & \int_0^\beta \{d\tau_i\} \sum_{\{\sigma_i\}, \{l_i\}} \\ & \star \Lambda_{ll'l_1 l'_1}^{*\xi\xi' \tau_1 \tau_2} \tilde{\mathcal{G}}_{jj'\sigma_1 \sigma_3}^{\tau_1 \tau_3 l_1 l_3} \tilde{\mathcal{G}}_{j'\sigma_2 \sigma_4}^{\tau_2 \tau_4 l_2 l_4} \Lambda_{l_3 l_4 l'' l'''}^{\xi' \tau_3 \tau_4 \tau'}, \end{aligned} \quad (9.8)$$

where a ‘‘transposed’’ three-point vertex function $\Lambda_{l_1 l_2 l_3 l_4}^{*\xi\xi' \tau_1 \tau_2 \tau_3} = \Lambda_{l_4 l_3 l_2 l_1}^{\xi\xi' \tau_3 \tau_2 \tau_1}$ is introduced to simplify notations and $\tilde{\mathcal{G}}$ stands for the nonlocal Green's function given by the difference between DMFT G and impurity g Green's functions

$$\tilde{\mathcal{G}}_{jj'\sigma\sigma'}^{\tau\tau' l l'} = G_{jj'\sigma\sigma'}^{\tau\tau' l l'} - \delta_{jj'} \delta_{\sigma\sigma'} g_{\tau\tau'}^{ll'}. \quad (9.9)$$

The DMFT Green's function corresponds to the bare lattice Green's function (9.2) dressed in the exact self-energy Σ^{imp} of the local reference problem (9.3) (Georges *et al.*, 1996). According to the self-consistency condition, the local part of

the DMFT Green's function is identically equal to the exact local Green's function g of the reference problem.

The diagonal part of the bilinear exchange interaction is given by the Heisenberg exchange $J_{jj'}^{ss}$ for the spin density (Stepanov *et al.*, 2018; Stepanov, Brener *et al.*, 2022) and the Ising interaction $J_{jj'}^{cc}$ for the charge density (Stepanov, Huber *et al.*, 2019). The latter is discussed in detail in Sec. X. The nondiagonal $J_{jj'}^{s\neq s'}$ components give rise to the Dzyaloshinskii-Moriya and the symmetric anisotropic interactions [see Yildirim *et al.* (1995)] that may appear in the system due to spin-orbit coupling. These kinetic exchange interactions compete with the bare nonlocal electron-electron interaction $V_{jj'}^c$, which plays the role of a direct exchange between the charge and spin densities. This makes the total nonlocal bilinear exchange interaction have the form

$$\mathcal{I}_{jj'}^{cc'} = J_{jj'}^{cc'} + \delta_{cc'} V_{jj'}^c. \quad (9.10)$$

The nonlocal interaction $V_{jj'}^c$ enters the bosonic problem as it was introduced in the initial lattice action (9.1). We also note that the direct spin-spin interaction $V_{jj'}^s$ usually has the opposite sign to the kinetic interaction $J_{jj'}^{ss}$. More involved interactions (Auslender and Katsnel'son, 1982; Auslender and Katsnelson, 1982), for example, the ring (Honda, Kuramoto, and Watanabe, 1993; Eroles *et al.*, 1999; Lorenzana, Eroles, and Sorella, 1999), chiral three-spin (Pachos and Plenio, 2004; Bauer *et al.*, 2014; Owerre, 2017; Grytsiuk *et al.*, 2020; Zhang *et al.*, 2020; Sotnikov *et al.*, 2021), and four-spin exchange interactions (Sato, 2007; Heinze *et al.*, 2011; Paul *et al.*, 2020) can be obtained by expanding the first term in Eq. (9.7) to higher orders in the ρ^s variable. For calculations of the bilinear exchange interactions (9.8) in a realistic material context, see Vandelli *et al.* (2023).

At this step we can already establish relation between bilinear exchange interactions derived using a magnetic force theorem and a quantum many-body path-integral technique. In this case it is convenient to work in the Matsubara fermionic ν and bosonic ω frequency representation. To simplify expressions we further omit orbital indices that can be restored trivially. We first note that the three-point vertex function Λ^c for the zeroth bosonic frequency can be obtained from single-particle quantities,

$$\Lambda_{\nu,\omega=0}^s = \Delta_{\nu}^s + \chi_{\omega=0}^{s-1}, \quad (9.11)$$

by varying the self-energy of the local reference problem (9.3) with respect to the magnetization (Stepanov, Brener *et al.*, 2022)

$$\Delta_{\nu}^s = \partial \Sigma_{\nu}^{\text{imp}} / \partial M_{\omega=0}. \quad (9.12)$$

In the ordered phase, where the spin rotational invariance is broken, this variation can be given as

$$\Delta_{\nu}^s = \frac{\Sigma_{\nu\uparrow}^{\text{imp}} - \Sigma_{\nu\downarrow}^{\text{imp}}}{2\langle M \rangle}. \quad (9.13)$$

Equation (9.13) is justified by local Ward identities and the fact that in the regime of a well-developed magnetic moment the renormalized fermion-fermion interaction (four-point vertex function) does not depend on fermionic frequencies (Stepanov *et al.*, 2018). Therefore, in Eq. (9.11) the Δ_{ν}^s term describes the spin splitting of the self-energy due to polarization of the system. In turn, $\chi_{\omega=0}^{s-1}$ can be seen as a kinetic self-splitting effect because $\chi_{\omega}^s = -\langle \rho_{\omega}^s \rho_{-\omega}^s \rangle_{\text{imp}}$ is the exact spin susceptibility of the reference system. In magnetic materials with a relatively large value of the magnetic moment, the kinetic contribution can be neglected. Indeed, in this case the spin splitting of the self-energy is determined by the Hund's exchange coupling. The latter is much larger than the inverse of the spin susceptibility, for which the estimation $\chi_{\omega=0}^s \sim T^{-1}$ holds due to the Curie-Weiss law (Moriya, 2012). The static exchange interaction $J_{jj'}^{s's'}(\omega=0) = \int dt' J_{jj'}^{s's'}(\tau - \tau')$ [see Stepanov, Brener *et al.* (2022) for a discussion] then reduces to the form

$$J_{jj',\omega=0}^{s's'} = \sum_{\nu, \{\sigma\}} \Delta_{j\nu}^s \tilde{\mathcal{G}}_{jj'\nu}^{\sigma_1\sigma_3} \Delta_{j'\nu}^{s'} \tilde{\mathcal{G}}_{j'\nu}^{\sigma_4\sigma_2}, \quad (9.14)$$

which under the approximation (9.13) coincides with Eq. (5.64), which for the ordered phase was derived in Sec. VK using the magnetic force theorem (Liechtenstein, Katsnelson, and Gubanov, 1984, 1985; Liechtenstein *et al.*, 1987; Katsnelson and Lichtenstein, 2000; Cardias, Bergman *et al.*, 2020). Note that Eq. (9.14) contains the sum over spin indices $\{\sigma\}$ and, for this reason, does not contain the prefactor 2 that is present in Eq. (5.64). The magnetic force theorem can also be applied in a paramagnetic phase. In the HIA this was done by Pourovskii (2016), and the result coincides with Eq. (9.14), where Eq. (9.12) is calculated numerically exactly. We emphasize that in Eq. (9.8), and consequently in Eq. (9.14), the vertex function (9.11), and thus the self-energy (9.12), are given by the local reference system (9.3). Moreover, the Green's function (9.9) that enters the expression for the exchange interaction is also dressed only in the local self-energy. The spin splitting Δ^s obtained from the nonlocal self-energy was introduced by Secchi, Lichtenstein, and Katsnelson (2016b). However, the corresponding exchange interaction is formulated in terms of bare noninteracting Green's functions and can be derived considering only the density-density approximation for the interaction between electrons. For these reasons, the limit of applicability of this approach and the relation to other methods remain unclear.

In addition, if the fermionic frequency dependence in Eq. (9.11) is fully neglected, the vertex function can be approximated by the inverse of the local bare polarization $\Lambda^s \simeq \chi_{\omega=0}^{0-1}$, where $\chi_{\omega}^0 = \sum_{\nu} g_{\nu} g_{\nu+\omega}$. The exchange interaction (9.8) then reduces to the form of an effective bare nonlocal susceptibility, as derived by Antropov (2003),

$$J_{jj',\omega=0}^{s's'} = \chi_{\omega=0}^{0-1} \tilde{\mathcal{X}}_{jj',\omega=0}^0 \chi_{\omega=0}^{0-1}, \quad (9.15)$$

where $\tilde{\mathcal{X}}_{jj'\omega}^0 = \sum_{\nu} \tilde{\mathcal{G}}_{jj'\nu} \tilde{\mathcal{G}}_{j'\nu+\omega}$.

One can also establish a relation between the results of the introduced many-body theory result and the bilinear exchange

interaction that can be deduced from the lattice susceptibility $X_{jj'}^{\zeta\zeta'}$ using the following expression:

$$\bar{J}_{jj'}^{\zeta\zeta'} = \delta_{jj'} \delta_{\zeta\zeta'} [\chi^\zeta]^{-1} - [X^{-1}]_{jj'}^{\zeta\zeta'}. \quad (9.16)$$

Equation (9.16) was used by Antropov (2003), Igoshev, Efremov, and Katanin (2015), Belozero, Katanin, and Anisimov (2017), and Otsuki *et al.* (2019) to estimate the magnetic exchange interaction based on the DMFT approximation for the spin susceptibility (Georges *et al.*, 1996). One can find that this form for the bilinear exchange interaction (9.16) can also be obtained from the previously derived many-body theory if the nonlinear action (9.7) is approximated by the Gaussian form

$$\bar{S} = -\frac{1}{2} \int \int_0^\beta d\tau d\tau' \sum_{jj', \zeta\zeta'} \bar{\rho}_{j\tau}^\zeta [X^{-1}]_{jj'}^{\zeta\zeta', \tau\tau'} \bar{\rho}_{j'\tau'}^{\zeta'}. \quad (9.17)$$

Since the bosonic variables $\bar{\rho}^\zeta$ correspond to the charge and magnetic densities, the quantity $X_{jj'}^{\zeta\zeta', \tau\tau'}$ is simply the lattice susceptibility (Stepanov *et al.*, 2018; Stepanov, Huber *et al.*, 2019; Stepanov, Brener *et al.*, 2022). More accurately this approximation can be done using Peierls-Feynman-Bogoliubov variational principle (Peierls, 1938; Bogolyubov, 1958; Feynman, 1972). Comparing the two actions (9.7) and (9.17) shows that in this case the bilinear exchange interaction should indeed be given by Eq. (9.16).

Effectively, this procedure corresponds to the mapping of the spin problem (9.7), which contains all possible exchange interactions, to an effective Heisenberg problem that accounts only for the bilinear exchange. We emphasize that for this reason it would be incorrect to relate two expressions for the bilinear exchange introduced in Eqs. (9.8) and (9.16). Indeed, equating these two quantities corresponds to truncating the expansion of the logarithm in the bosonic action (9.7) at the second order in terms of $\bar{\rho}$ variables. In other words, it means neglecting the effect of the higher-order exchange interactions on the lattice susceptibility and, consequently, on the bilinear exchange interaction \bar{J} . Taking this effect into account will modify Eq. (9.8) for the bilinear exchange interaction. In particular, it will result in dressing the Green's functions \bar{G} with the nonlocal self-energy and in the renormalization of one of the two vertex functions (Λ) by collective nonlocal fluctuations in the fashion of Hedin (1965b).

These observations confirm the statement that we made at the beginning of this section, namely, that the expression for the exchange interaction strongly depends on the form of the considered spin model. If one is limited to the simplest approximation with only the bilinear form of the exchange interaction, then the latter should be calculated via Eq. (9.16) provided that consistent calculation for the lattice susceptibility is possible. For instance, using the DMFT form of the susceptibility might already be questionable because it accounts for the renormalization of the vertex function (in the ladder approximation) but disregards the nonlocal self-energy. At the same time, if a more accurate model that contains the bilinear and nonlinear exchange interactions is considered, these interactions should be computed in the form

given by the action (9.7). In this case, the bilinear interaction is given by Eq. (9.8) or its approximation (9.14). Calculating it via the lattice susceptibility (9.16) would be incorrect because it would lead to a double-counting problem for the higher-order interactions since some contribution from them is already taken into account in the lattice susceptibility. The difference between the two forms for the bilinear exchange interaction can also serve as a measure of the importance of the nonlinear exchange processes in the system.

C. Equation of motion for the local magnetic moment

The second line in the bosonic action (9.7) contains only local contributions that describe dynamics of charge and spin degrees of freedom. The first term in this line accounts for the Higgs fluctuations of the modulus of the charge ρ^c and spin M moments around their average value. This can be seen by formally expanding the time dependence of the moments in powers of $\tau - \tau'$. For the local magnetic moment this gives

$$\begin{aligned} \mathcal{S}_{\text{Higgs}} &= -\frac{1}{2} \int \int_0^\beta d\tau d\tau' \sum_j M_{j\tau} [\chi^{z-1}]_{\tau\tau'} M_{j\tau'} \\ &\simeq -\frac{1}{2} \int_0^\beta d\tau \sum_j \left\{ \chi_{\omega=0}^{z-1} M_{j\tau}^2 + \left. \frac{\partial^2 \chi_\omega^{z-1}}{2\partial\omega^2} \right|_{\omega=0} \dot{M}_{j\tau}^2 \right\}. \end{aligned} \quad (9.18)$$

The first-order difference in time vanishes because the exact local susceptibility χ_ω^z is the even function of the frequency ω . The Lagrangian equation for this action immediately gives the standard equation of motion for a simple harmonic oscillator $\ddot{M}_{j\tau} + \lambda^2 M_{j\tau} = 0$, where $\lambda^2 = -2\chi_{\omega=0}^{z-1} / (\partial_\omega^2 \chi_\omega^{z-1})|_{\omega=0}$. Note that in our definition the susceptibility χ_ω^z is negative. However, this expansion has to be performed with ultimate care. Indeed, Higgs fluctuations of the modulus of the local magnetic moment are fast, and the spin susceptibility is strongly nonlocal in time (Stepanov, Brener *et al.*, 2022). For this reason, there is no uniform justification that the Higgs fluctuations can be accurately described using an equal-time term [the second line of Eq. (9.18)] instead of the full nonstationary in time local part of the lattice action [the first line of Eq. (9.18)].

The last term in the bosonic action (9.7) that contains the effective gauge field $\mathcal{A}_{j\tau}^z$ accounts for the rotational spin dynamics. Stepanov, Brener *et al.* (2022) showed that after averaging over fast Higgs fluctuations the equation of motion for the bosonic action reduces to the standard Landau-Lifshitz-Gilbert form. To illustrate this, we replace the scalar field $M_{j\tau}$ with its constant nonzero average value $\langle M_{j\tau} \rangle = 2S$ and introduce $\vec{S}_{j\tau} = S\vec{e}_{j\tau}$. The spin part of the action becomes

$$\mathcal{S}_{\text{spin}} = \int_0^\beta d\tau \sum_j [i\dot{\varphi}_{j\tau} (1 - \cos \theta_{j\tau}) S - \vec{S}_{j\tau} \cdot \vec{h}_{j\tau}], \quad (9.19)$$

where we have explicitly rewritten the gauge field in terms of rotation angles. Components of the effective magnetic field $\vec{h}_{j\tau}$ can be expressed via the bilinear exchange interaction and the effective magnetic field that appears due to spin-orbit coupling (Stepanov, Brener *et al.*, 2022),

$$h_{j\tau}^s = -4 \int_0^\beta d\tau' \sum_{j',s'} \mathcal{I}_{jj'}^{ss'}(\tau - \tau') S_{j'\tau'}^{s'} + h_{j\tau}^{\text{SOC},s}. \quad (9.20)$$

In the general case, the equation of motion for the nonstationary spin action (9.19) is a complex set of integrodifferential equations. However, one can make use of the fact that the interaction between spins is determined by the superexchange processes mediated by electrons [Eq. (9.8)] and thus decays fast on the timescales of the inverse bandwidth. Instead, the time dependence of the angle variables $\varphi_{j\tau}$ and $\theta_{j\tau}$ is slow because the spin precession is slow in time (Sayad and Potthoff, 2015; Sayad, Rausch, and Potthoff, 2016; Watznböck *et al.*, 2020). Unlike the case of Higgs fluctuations, this allows one to expand the time dependence of the spin variable $S_{j'\tau'}^{s'}$ in Eq. (9.20) up to the first order in powers of $\tau - \tau'$, which allows one to write

$$h_j^s(t) = -4 \sum_{j',s'} I_{jj'}^{\text{R},ss'}(\Omega = 0) S_{j'}^{s'}(t) + h_j^{\text{SOC},s}(t) - 4 \sum_{j',s'} \frac{\partial}{\partial \Omega} \text{Im} I_{jj'}^{\text{R},ss'}(\Omega) \Big|_{\Omega=0} \dot{S}_{j'}^{s'}(t). \quad (9.21)$$

With Eq. (9.21) for the effective magnetic field the spin problem (9.19) becomes stationary in time, and the corresponding equation of motion for this action takes the standard Landau-Lifshitz-Gilbert form

$$\dot{\vec{S}}_j(t) = -\vec{h}_j(t) \times \vec{S}_j(t). \quad (9.22)$$

Equation (9.22) can be derived by making an analytical continuation that transforms the imaginary-time exchange interaction $\mathcal{I}_{jj'}^{ss'}(\tau - \tau')$ to a retarded function $I_{jj'}^{\text{R},ss'}(t - t')$ in real time t . In turn, $I_{jj'}^{\text{R},ss'}(\Omega)$ is a Fourier transform of the retarded exchange interaction to real frequency Ω . This transformation allows one to obtain the Gilbert damping, which is described by the last term in the effective magnetic field (9.21). A similar expression for the Gilbert damping was derived by Sayad and Potthoff (2015) and Sayad, Rausch, and Potthoff (2016) for the case of a classical spin coupled to the system of conduction electrons. Note that the Gilbert damping cannot be obtained in the imaginary-time representation, because the exchange $\mathcal{I}_{jj'}^{ss'}(\tau - \tau')$ is an even function of time. Physically, this means that dissipation effects cannot be visible in the equilibrium formalism.

There are several restrictions for the derived Landau-Lifshitz-Gilbert equation of motion that have to be discussed. Equation (9.22) describes the spin precession, which is assumed to be slow in time compared to the electronic processes in the system. The corresponding effective magnetic field (9.21) thus takes into account only the low-frequency part of the exchange interaction. In general, the exchange term (9.8) has a nontrivial frequency dependence, and even diverges at high frequencies, because it is given by a nonlocal part of the inverse of the lattice susceptibility (9.16). Nonadiabatic effects that correspond to high-frequency behavior of the exchange interaction are not taken into account by

Eq. (9.22). The latter can only be described using the derived bosonic action (9.7), which has no restriction on the regime of frequencies but is nonstationary in time.

Another important point is that the Higgs and Berry phase terms, in the form in which they enter the bosonic action (9.7), can be obtained only after associating the rotation angles with the direction of the local magnetic moment. As discussed, this can be done taking the path integral over rotation angles in the saddle-point approximation. However, this approximation can be justified only in the case of a large magnetic moment (Stepanov, Brener *et al.*, 2022). In practice, it means that the classical Landau-Lifshitz-Gilbert equation of motion is applicable only in the multiorbital case, where the large value of the local magnetic moment is provided by a strong Hund's coupling. If the magnetic moment is small, the spin dynamics in the system is governed by quantum fluctuations. In this case, the local magnetic moment can still be well defined, but its behavior can no longer be described in terms of classical equations of motion.

D. Local magnetic moment formation

The Landau-Lifshitz-Gilbert equation of motion (9.22) makes physical sense only for a nonzero value of the average magnetic moment $\langle M \rangle$. In the ordered phase this is ensured by a nonzero average value of the magnetization. Defining $\langle M \rangle$ in a paramagnetic regime is much more problematic because, in this case, the average magnetization is identically zero. For this reason, the value of $\langle M \rangle$ is commonly estimated from the static equal-time spin susceptibility as

$$3\chi_{\tau\tau}^z = \langle M^2 \rangle \simeq \langle M \rangle (\langle M \rangle + 2). \quad (9.23)$$

However, Eq. (9.23) gives a large and almost temperature-independent value for the magnetic moment even in the high-temperature regime, where the moment is not yet formed (Stepanov, Brener *et al.*, 2022). Taking into account dynamical screening effects changes the value of the average moment, but it still remains substantially larger than the one measured experimentally (Hansmann *et al.*, 2010; Toschi *et al.*, 2012; Watznböck *et al.*, 2020). This result can be explained by the fact that the local spin susceptibility simultaneously accounts for correlations of the local magnetic moment and for spin fluctuations of itinerant electrons. These two contributions to the susceptibility cannot be easily disentangled.

Stepanov, Brener *et al.* (2022) proposed the average value of the magnetic moment to obtain from the free energy of the local problem that describes the behavior of the magnetic moment. The action of this local problem

$$\mathcal{S}_{\text{loc}} = -\text{Tr} \ln \left[[g^{-1}]_{\tau\tau'} \delta_{\sigma\sigma'} + \int_0^\beta d\tau_1 \sum_{\xi} \sigma_{\sigma\sigma'}^{\xi} \Lambda_{\tau\tau_1}^{\xi} \rho_{\tau_1}^{\xi} \right] - \frac{1}{2} \iint_0^\beta d\tau d\tau' \sum_{\xi} \rho_{\tau}^{\xi} [\chi^{\xi-1}]_{\tau\tau'} \rho_{\tau'}^{\xi} \quad (9.24)$$

can be derived by excluding the contribution of itinerant electrons from the local reference system (9.3). The resulting problem is reminiscent of the bosonic action (9.7), where the nonlocal Green's function $\tilde{\mathcal{G}}$ is replaced by the full local

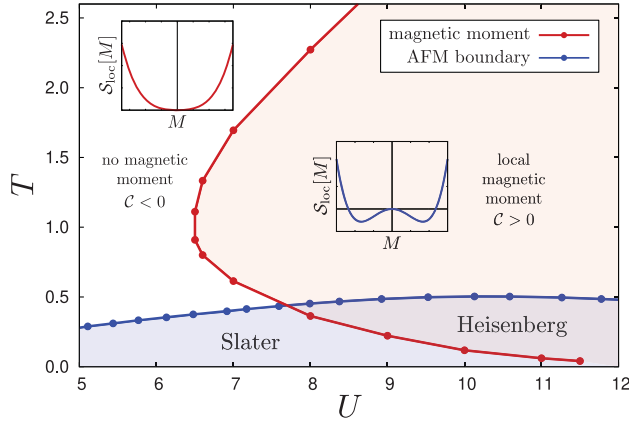


FIG. 28. Phase diagram for the 3D Hubbard model as a function of temperature T and local Coulomb interaction U . The red (light gray) line corresponds to the criterion (9.27) for the formation of the local magnetic moment. The blue (dark gray) line depicts the Néel phase boundary obtained by Hirschmeier *et al.* (2015). Insets: local free energy (9.24) as a function of the magnetic moment in two regimes when it does not exist to the left of the red (light gray) line and where it is already formed shown by the red (light gray) shaded area. Adapted from Stepanov, Brener *et al.*, 2022.

Green's function g . In the introduced local problem (9.24) the magnetic moment appears as a result of a spontaneous symmetry breaking. According to Landau phenomenology (Landau and Lifshitz, 1980), the latter corresponds to the change of the free energy from a paraboloidlike form with a minimum at $\langle M \rangle = 0$ to a Mexican-hat potential characterized by a continuous set of minima at $\langle M \rangle \neq 0$; see the insets in Fig. 28. The resulting value for the average local magnetic moment appears to be substantially smaller than the one deduced from the local spin susceptibility (9.23).

The change of the form of the free energy can be captured by the sign change of its second variation with respect to the local magnetic moment,

$$-\frac{\partial^2 \mathcal{S}_{\text{loc}}[\rho^s]}{\partial \rho_{\tau}^s \partial \rho_{\tau'}^s} = [\chi^{s-1}]_{\tau\tau'} - J_{\tau\tau'}^{\text{loc}}. \quad (9.25)$$

The right-hand side of Eq. (9.25) can be seen as a self-exchange between the local magnetic moments because it is given by the inverse of the local susceptibility with subtracted contribution of itinerant electrons. The latter is described by the following local analog of the kinetic exchange interaction (9.8):

$$J_{\tau\tau'}^{\text{loc}} = \int_0^\beta \{d\tau_i\} \sum_{\sigma} \Lambda_{\tau\tau_1\tau_2}^{*s} g_{\tau_1\tau_3}^{\sigma} g_{\tau_4\tau_2}^{\sigma} \Lambda_{\tau_3\tau_4\tau'}^s. \quad (9.26)$$

We emphasize that the local magnetic moment exists only at relatively long times compared to single-electron processes. In the static limit the moment is screened by the Kondo effect or by intersite exchange-induced spin flips. For this reason, formation of the local magnetic moment in the system corresponds to the symmetry breaking at intermediate time-scales. Consequently, as shown by Stepanov, Brener *et al.*

(2022), the second variation of the local free energy (9.25) changes sign at any time except $\tau = \tau'$. Therefore, the formation of the local moment is not a real physical transition and should be considered as a crossover effect. The static contribution to the local problem (9.24) is contained in the inverse of the local susceptibility $\chi_{\tau\tau'}^{s-1} = (\Pi_{\tau\tau'}^{s,\text{imp}})^{-1} - \delta_{\tau\tau'} U^s$. It is given by the bare local interaction in the spin channel $U^s = -U/2$. In this expression $\Pi_{\tau\tau'}^{s,\text{imp}}$ is the exact polarization operator of the reference system (9.3). The criterion for the local magnetic moment formation can thus be obtained by explicitly excluding this static contribution from Eqs. (9.24) and (9.25). The corresponding condition written in the frequency space is that

$$C = (\Pi_{\omega=0}^{s,\text{imp}})^{-1} - J_{\omega=0}^{\text{loc}} = 0. \quad (9.27)$$

Equation (9.27) illustrates that when the effective self-exchange becomes diamagnetic ($C > 0$) the system acquires a magnetic moment. The derived criterion (9.27) can be approximately related to the first variation of the local electronic self-energy with respect to the magnetization. This fact suggests that the formation of the local magnetic moment is energetically favorable when this variation is negative, which minimizes the energy of the electrons.

Applying the derived criterion (9.27) to interacting electronic systems shows that the local magnetic moment develops at temperatures well above the phase transition to the ordered state (Stepanov, Brener *et al.*, 2022). At the same time, the moment can be formed only above a relatively large critical value of the local Coulomb interaction U , which for the case of a half-filled single-orbital cubic lattice exceeds half of the bandwidth. The corresponding result is shown in Fig. 28, where the blue (dark gray) line corresponds to the Néel phase boundary and the red (light gray) line is obtained from the condition (9.27). At low temperatures the red (light gray) line determines the point at which the local magnetic moment disappears. In the regime of large interactions this is related to Kondo screening (Hewson, 1993; Chalupa *et al.*, 2021). At small U , the local magnetic moment is destroyed by local spin fluctuations, which corresponds to the regime of valence fluctuations of the Anderson model (Hewson, 1993). The low-temperature branch of the red (light gray) line splits the ordered phase into two parts, which allows one to distinguish between the Slater (Slater, 1951; Rohringer and Toschi, 2016) and Heisenberg regimes of spin fluctuations.

To summarize, the path-integral formalism allows us to derive the bosonic problem (9.7) that describes the spin dynamics of itinerant-electron systems. The nonlocal part of this problem gives a general form for all kinds of magnetic exchange interactions. Upon certain approximations, the derived expression for the bilinear exchange (9.8) reduces to the result that was originally introduced in a completely different framework of DFT. These approximations are justified by the existence of a well-developed magnetic moment in the system and determine the limit of applicability of the DFT result. Apart from deriving the magnetic interactions, the path-integral formalism makes it possible to introduce the equation of motion for spin degrees of freedom. It was shown that for a relatively large value of the magnetic

moment its slow rotational dynamics is described by a standard Landau-Lifshitz-Gilbert equation, and fast Higgs fluctuations can be taken into account by the local nonstationary in time contribution to the bosonic problem. Deriving the criterion for the formation of the local magnetic moment completes the path-integral formulation of the theory of magnetism and magnetic interactions.

X. NONMAGNETIC ANALOGS OF EXCHANGE INTERACTION

The basic idea presented and discussed in this review is an idea of a coarse-grained description of collective behavior in a system of strongly interacting electrons in solids. The prototype example is magnetism, and “gross” variables in the coarse-grained description of spin degrees of freedom are angles determining directions of individual local magnetic moments. Technically, the main tool is the magnetic force theorem, in which we express the variation of the total thermodynamic potential under small spin rotations in terms of variations of single-electron Green’s function. This approach is general and can be applied to collective phenomena other than magnetism. Here we consider two examples, namely, superconductors and charge-ordered systems. Since these subjects are auxiliary to the main aim of the review, we restrict ourselves to the presentation of main ideas and some illustrative results emphasizing similarities with the discussed approach to magnetic exchange interactions.

We start with the case of superconductors; our presentation in this part will mostly follow [Harland *et al.* \(2019\)](#). The superconductor is characterized, in the simplest case of singlet Cooper pairing, by a complex-valued order parameter, meaning a wave function of condensate of the Cooper pairs. There is an extensive literature on the subject; for a basic introduction, see [Abrikosov \(1988\)](#), [Schrieffer \(1999\)](#), and [Mahan \(2000\)](#).

We now consider a model of a strong-coupling superconductor with Cooper pairs relatively well localized in real space, an analog of a magnet with well-defined local magnetic moments. This is a poor model for conventional superconductors with a typical diameter of Cooper pairs in thousands of interatomic distances ([Abrikosov, 1988](#); [Schrieffer, 1999](#)) but it can apply reasonably well to cuprate high-temperature superconductors, assuming that we consider the lattice of copper plaquettes rather than individual sites ([Lichtenstein and Katsnelson, 2000](#); [Harland *et al.*, 2019](#)). Therefore, the macroscopic superconductivity in the system can be described in terms of a coherence of the phase of the local Cooper pairs θ_i , which are all supposed to be equal in the ground state (without the loss of generality, this ground-state value of the phase can be chosen as zero). The model that can address the issue of superconducting phase ordering, and thus macroscopic quantum properties of the superconductor, is the Josephson lattice model,

$$\mathcal{H}_{\text{eff}} = \sum_{\langle ij \rangle} J_{ij} \cos(\theta_i - \theta_j), \quad (10.1)$$

where i and j are supersite indices (such as plaquette indices for the two-dimensional Hubbard model used in the theory of superconducting cuprates). The Josephson coupling

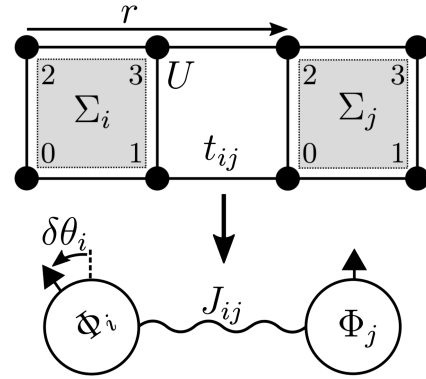


FIG. 29. Illustration of the Hubbard-plaquette lattice (t_{ij} , U) with lattice vector r , self-energies Σ_i , and plaquette sites 0–3. It is mapped to the Josephson lattice model with effective coupling J_{ij} of plaquettes due to phase fluctuations $\delta\theta_i$ of the d -wave superconducting order parameter Φ_i . Adapted from [Harland *et al.*, 2019](#).

parameters J_{ij} determine, in particular, superfluid density and London penetration depth ([Abrikosov, 1988](#); [Schrieffer, 1999](#); [Mahan, 2000](#)).

Instead of magnetic systems where we deal with the local rotational [or $SU(2)$] symmetry, for singlet superconductors we deal with the $U(1)$ symmetry; see Fig. 29. Following the general approach accepted in this review, we have to calculate the variation of the thermodynamic potential under small phase variations, and the answer will be expressed in terms of a single-particle Green’s function. In the superconducting state, the latter is a supermatrix with normal and anomalous parts (the so-called Nambu-Gorkov representation) ([Schrieffer, 1999](#)),

$$\begin{pmatrix} G^{p\uparrow} & F \\ F & G^{h\downarrow} \end{pmatrix}_{ij}^{-1} = \begin{pmatrix} G_0^{p\uparrow} & 0 \\ 0 & G_0^{h\downarrow} \end{pmatrix}_{ij}^{-1} - \delta_{ij} \begin{pmatrix} \Sigma^{p\uparrow} & S \\ S & \Sigma^{h\downarrow} \end{pmatrix}_i, \quad (10.2)$$

where $G_0^{a\sigma}$ and $G^{a\sigma}$ are the normal parts of the bare (G_0) and interacting (G) Green’s functions for an electron ($a = p$) and a hole ($a = h$) with the spin projection $\sigma \in \{\uparrow, \downarrow\}$. F is the anomalous part of the interacting Green’s function, which is considered to be local in the supersite, as done by [Lichtenstein and Katsnelson \(2000\)](#) and [Harland *et al.* \(2019\)](#). $\Sigma^{a\sigma}$ and S are the normal and anomalous parts of the self-energy, respectively.

To obtain explicit expressions for the Josephson couplings J_{ij} , we have to calculate the variation of the thermodynamic potential Ω under small variations of the superconducting phases and compare the result to Eq. (10.1). Following the consideration of the exchange interactions within dynamical mean-field theory discussed in Sec. V K, we start with a general representation of the thermodynamic potential in terms of single-particle and double-counted contribution with the Luttinger-Ward functional Φ and use the local force theorem. The result is ([Harland *et al.*, 2019](#))

$$\delta\Omega \simeq \sum_{ij} \text{Tr}(\delta_{ij} G_{ii} \delta^* \Sigma_i + \frac{1}{2} G_{ij} \delta^* \Sigma_j G_{ji} \delta^* \Sigma_i), \quad (10.3)$$

where δ^* denotes the local variation of the self-energy Σ without taking into account its variation due to the

self-consistency procedure. We omit here for simplicity matrix indices of intraplaquette and Nambu spaces.

The variation of the self-energy under an infinitesimal change of the local phase $\delta\theta_i$ entering Eq. (10.3) in a homogeneous environment reads

$$\begin{aligned} \delta^* \Sigma_i &= e^{i\delta\theta_i \sigma_z / 2} \Sigma_i e^{-i\delta\theta_i \sigma_z / 2} - \Sigma_i \\ &= \begin{pmatrix} \Sigma_i^{p\uparrow} & e^{i\delta\theta_i} S_i \\ e^{-i\delta\theta_i} S_i & \Sigma_i^{h\downarrow} \end{pmatrix} - \Sigma_i \\ &\simeq \begin{pmatrix} 0 & \{i\delta\theta_i - [(\delta\theta_i)^2/2]\} S_i \\ \{-i\delta\theta_i - [(\delta\theta_i)^2/2]\} S_i & 0 \end{pmatrix}, \end{aligned} \quad (10.4)$$

where $\Sigma_i^{p\uparrow}$, $\Sigma_i^{h\downarrow}$, and S_i are electron-up, hole-down, and anomalous parts of the supersite self-energy, respectively, and the third Pauli matrix σ_z acts in the Nambu space.

A straightforward calculation up to second order in $\delta\theta$ results in

$$\begin{aligned} \delta\Omega &= \sum_{ij} \text{Tr}_{\omega\alpha} (G_{ij}^{p\uparrow} S_j G_{ji}^{h\downarrow} S_i - \delta_{ij} F_{ii} S_i - F_{ij} S_j F_{ji} S_i) \delta\theta_i^2 \\ &\quad + \frac{1}{2} \sum_{ij} \text{Tr}_{\omega\alpha} (F_{ij} S_j F_{ji} S_i - G_{ij}^{p\uparrow} S_j G_{ji}^{h\downarrow} S_i) \delta\theta_{ij}^2. \end{aligned} \quad (10.5)$$

The trace goes over Matsubara frequencies and over the sites within the supersite (α).

The term $\propto \delta\theta_i^2$ vanishes, reflecting the gauge invariance of the theory, which can be checked using the direct calculation (Harland *et al.*, 2019). The remaining nonlocal term is proportional to $\delta\theta_{ij}^2$, i.e.,

$$\delta\Omega \equiv -\frac{1}{2} \sum_{(ij)} J_{ij} \delta\theta_{ij}^2. \quad (10.6)$$

Equation (10.6) should be compared with Eq. (10.1) to find the coupling constants J_{ij} . The answer is an expression where

$$J_{ij} = 2 \text{Tr}_{\omega\alpha} (G_{ij}^{p\uparrow} S_j G_{ji}^{h\downarrow} S_i - F_{ij} S_j F_{ji} S_i). \quad (10.7)$$

To study macroscopic observables of the Josephson lattice model, we take the continuum, long-wavelength limit of Eq. (10.1). In this limit, the interaction becomes the superconducting stiffness,

$$\begin{aligned} I_{ab} &= -\frac{1}{(2\pi)^d} \int d^d k \text{Tr}_{\omega\alpha} \\ &\quad \star \left(\frac{\partial G^{p\uparrow}(k)}{\partial k_a} S \frac{\partial G^{h\downarrow}(k)}{\partial k_b} S - \frac{\partial F(k)}{\partial k_a} S \frac{\partial F(k)}{\partial k_b} S \right), \end{aligned} \quad (10.8)$$

with the effective Hamiltonian

$$H_{\text{eff}} = \frac{1}{2} \sum_{ab} I_{ab} \int d^d r \frac{\partial \theta}{\partial r_a} \frac{\partial \theta}{\partial r_b}. \quad (10.9)$$

If we assume that the discussed lattice is isotropic (in two or three dimensions), we have $I_{ab} = I \delta_{ab}$, where the constant I is related to the London penetration depth (Abrikosov, 1988; Schrieffer, 1999),

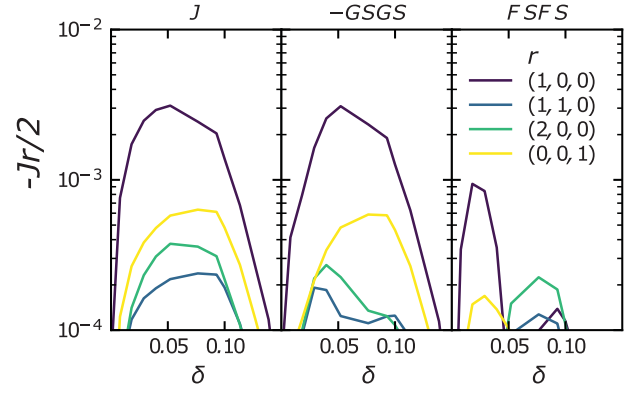


FIG. 30. Josephson coupling J_r (left panel) and its constituents $GSGS$ (center panel) and $FSFS$ (right panel) as functions of doping δ and for different plaquette translations r at $T = 1/52 \sim 0.02$ and $t_{\perp} = 0.15$. Adapted from Harland *et al.*, 2019.

$$\frac{1}{\lambda^2} = \frac{16\pi e^2}{\hbar^2 c^2} I. \quad (10.10)$$

We present an example of the calculated Josephson couplings J_r for plaquette translations r in Fig. 30. The figure shows that J_r reduces sharply with increasing plaquette-translation length $|r|$, and thus the short-range components of J_r alone can give a complete description. The strongest coupling is J_{100} , followed by the interlayer coupling J_{001} . They have their maxima around $\delta = 0.05$ and 0.1 , respectively. All couplings diminish at large dopings ($\delta > 0.1$). The first term of Eq. (10.7) ($GSGS$) is negative, and the second ($FSFS$) is positive. $GSGS$ is a mixed term with normal (G) and anomalous (S) contributions. This term provides the main contribution to J , which can be finite only if there is a superconducting gap and therefore a finite anomalous self-energy S . Regarding the largest contributions to the nearest-neighbor Josephson coupling $J_{(1,0,0)}$, $GSGS$ is about 3 times as large as $FSFS$.

Another interesting feature of correlated materials that can potentially be described by a corresponding bosonic model is charge ordering. In electronic systems this phenomenon attracts considerable attention since the discovery of the Verwey transition in magnetite (Fe_3O_4) (Verwey and Haayman, 1941; Verwey, Haayman, and Romeijn, 1947; Mott, 1974). Further, effects similar to the Verwey transition have been observed in many other materials, such as the rare-earth compound Yb_4As_3 (Fulde, Schmidt, and Thalmeier, 1995; Goto and Lüthi, 2003; Staub *et al.*, 2005), transition metal MX_2 (Arguello *et al.*, 2014; Ritschel *et al.*, 2015; Ugeda *et al.*, 2016), and rare-earth R_3X_4 (Wachter, 1980; Furuno *et al.*, 1988; Irkhin and Katsnelson, 1990) chalcogenides ($M = \text{V, Nb, Ta, R} = \text{Eu, Sm, and X} = \text{S, Se}$), Magnéli phase Ti_4O_7 (Chakraverty, 1980; Schlenker and Marezio, 1980; Eyert, Schwingschögl, and Eckern, 2004; Leonov *et al.*, 2006), vanadium bronzes $\text{Na}_x\text{V}_2\text{O}_5$, and $\text{Li}_x\text{V}_2\text{O}_5$ (Dumas, Schlenker, and Buder, 1980; Goto and Lüthi, 2003). In these materials the charge ordering is driven by the strong nonlocal Coulomb interaction and/or the electron-phonon mechanism. Both these interactions effectively reduce the strength of the local Coulomb repulsion (Berger, Valášek, and von der

Linden, 1995; Sangiovanni *et al.*, 2005; Werner and Millis, 2007; Schüler *et al.*, 2013; van Loon *et al.*, 2016) and may even result in an effective attraction between electrons. Describing these effects in the framework of *ab initio* electronic models requires one to use advanced many-body approaches, such as the quantum Monte Carlo technique (Hohenadler *et al.*, 2014; Wu and Tremblay, 2014; Buividovich *et al.*, 2017), the *GW* method combined with the extended dynamical mean-field theory (Aryal, Biermann, and Werner, 2013; Aryal *et al.*, 2017), the dynamical cluster approximation (Terletska, Chen, and Gull, 2017; Terletska *et al.*, 2018; Paki *et al.*, 2019), or the dual theories (van Loon *et al.*, 2014, 2018; Stepanov, Huber *et al.*, 2016; Vandelli *et al.*, 2020; Stepanov, Harkov *et al.*, 2022). These theoretical calculations require significant numerical efforts, which provides additional motivation for reformulating the original electronic problem in terms of effective bosonic variables.

Like magnetism, charge ordering is characterized by the local order parameter: the on-site electronic density. This ordering appears as the result of a spontaneous symmetry breaking of a discrete lattice symmetry contrary to the case of a magnetic ordering, which is associated with breaking of a continuous $SU(2)$ symmetry. For this reason, effective models formulated in terms of scalar bosonic variables are more suitable for addressing this problem. In particular, Ising-like models are frequently used for describing the ordering in alloys (Ruban *et al.*, 2004; Shallcross *et al.*, 2005; Korzhavii *et al.*, 2009; Ekholm *et al.*, 2010; Alling *et al.*, 2011). In this framework, one deals with a configuration energy written in terms of effective interactions $V_\alpha^{(n)}$ for clusters of the order of n and type α . For the case of a binary alloy $A_c B_{1-c}$ with the concentration c , the configuration energy can be written as

$$H_{\text{conf}} = \sum_p V_p^{(2)} \sum_{i,j \in p} \sigma_i \sigma_j + \sum_t V_t^{(3)} \sum_{i,j,k \in t} \sigma_i \sigma_j \sigma_k + \sum_q V_q^{(4)} \sum_{i,j,k,l \in q} \sigma_i \sigma_j \sigma_k \sigma_l + \dots, \quad (10.11)$$

where scalar variables σ_i take the value -1 or $+1$, depending on whether the A or B atom occupies the site i . Parameters for this microscopic model can be derived from *ab initio* energy calculations within the framework of density functional theory (Connolly and Williams, 1983; Hennion, 1983; Ducastelle, 1991; Ruban and Abrikosov, 2008). To this aim, one can apply a generalized perturbation theory (Gautier, Ducastelle, and Giner, 1975; Gautier, van der Rest, and Brouers, 1975; Ducastelle and Gautier, 1976; Giner *et al.*, 1976; Treglia, Ducastelle, and Gautier, 1978; Ducastelle and Treglia, 1980; Gonis *et al.*, 1987; Monnier, 1997). In this approach effective cluster interactions $V_\alpha^{(n)}$ can be obtained either by calculating the corresponding n -point correlation functions [see Ruban *et al.* (2002) and Alling *et al.* (2011)] or from the single-electron energy using the force theorem (Mackintosh and Andersen, 1980). In the latter case, the variation of the concentration of atoms of a given kind is considered a perturbation. This seems to differ significantly from a consideration of small spin rotations, the primary topic of this review, which have been used successfully in the case of magnetism. Nevertheless, the resulting pair interaction between sites j and j' is given by

$$V_{jj'}^{(2)} = -\frac{2}{\pi} \Im \int_{-\infty}^{E_F} dE \Delta t_j \tilde{G}_{jj'}(E) \Delta t_{j'} \tilde{G}_{j'j}(E), \quad (10.12)$$

which closely resembles the magnetic exchange interaction derived using the magnetic force theorem; see Sec. V. In Eq. (10.12) $\Delta t_j = (t_j^A - t_j^B)/2$ is the difference between single-site scattering matrices for A and B types of atoms and $\tilde{G}_{jj'}(E)$ is the partial interatomic Green's function of the reference system provided by a random alloy.

As in the case of magnetism, using the force theorem does not allow one to rigorously determine limits of applicability of the theory. In this regard, deriving effective Ising-like models in the many-body framework should be beneficial. In the context of interacting electronic problems, this was achieved by Stepanov, Huber *et al.* (2019) and Stepanov, Brener *et al.* (2022). The corresponding derivation was discussed in Sec. IX leading to the effective bosonic problem (9.7). Note that introducing the bosonic model for charge degrees of freedom does not require the adiabatic approximation that separates timescales and energy scales of single- and two-particle fluctuations in the magnetic case to be imposed (Stepanov, Huber *et al.*, 2019).

All possible interactions between the electronic densities at different lattice sites can be obtained by expanding the logarithm in Eq. (9.7) in terms of the bosonic field ρ^c that describes fluctuations of the charge densities n around their average values. The explicit form for the pair interaction is given by Eqs. (9.8) and (9.10). The three-point vertex function Λ^c that enters the kinetic exchange (9.8) represents a renormalized local coupling between electronic and charge degrees of freedom. Thus, this vertex can be seen as a single-site scattering matrix, which makes the many-body expression for the exchange interaction (9.8) similar to the pair cluster interaction derived in the context of alloys (10.12).

Mapping the quantum bosonic problem for electronic densities (9.7) onto a classical Ising-like model can be justified only in the regime of well-developed charge fluctuations. In a broken symmetry, charge-ordered phase, the electronic density at a given lattice site strongly differs from the average density of the system. This allows one to replace the bosonic variable ρ_j^c at each site j by its average value $\langle \rho_j^c \rangle$, which reduces the quantum bosonic action (9.7) to a classical Ising-like Hamiltonian. In the normal phase the average density on each lattice site is uniform, which makes it difficult to introduce the corresponding classical problem and complicates the determination of the regime of applicability of this approach.

Stepanov, Huber *et al.* (2019) proposed the double occupancy $d = \langle n_\uparrow n_\downarrow \rangle$ of the lattice site as a measure of the strength of the charge fluctuations in the normal phase. The double occupancy for a particular case of the extended Hubbard model on a square lattice is shown in Fig. 31. The result is obtained at half filling, where the maximum value of the double occupancy is $d_{\text{max}} = 0.25$. In this model the charge-ordered phase (light gray area) is driven by the nearest-neighbor Coulomb interaction V . If the latter defeats the on-site Coulomb repulsion U , the electronic density forms a checkerboard pattern on the lattice made of alternating doubly occupied and empty sites. For a given value of U , the maximum value of the double occupancy appears at the

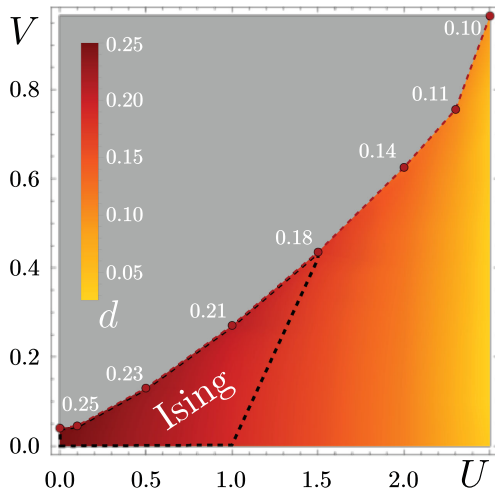


FIG. 31. Double occupancy of the extended Hubbard model shown on the $U - V$ phase diagram. Calculations are performed in the normal phase, where the value of the double occupancy d is depicted in color. The charge-ordered phase is depicted in (light) gray. The black dashed line surrounds the area of the large double occupancy $d \gtrsim 70\%d_{\max}$, where charge excitations can be described by an effective Ising model. Values of Coulomb interactions U and V are given in units of half of the bandwidth $4t = 1$, where t is the nearest-neighbor hopping amplitude. The inverse temperature for this calculation was set to $T^{-1} = 50$. From Stepanov, Huber *et al.*, 2019.

boundary between the normal and ordered phases, which is depicted by a dashed red line. This fact confirms that the strongest charge fluctuations in the normal phase emerge in the region close to the phase transition to the ordered state. However, the value of the double occupancy is not uniformly distributed along the phase boundary and decreases with an increase of the local Coulomb interaction. Stepanov, Huber *et al.* (2019) showed that strong charge fluctuations drastically suppress the frequency dependence of the effective local electron-electron interaction (the two-particle irreducible four-point vertex function). The value of the double occupancy at which the effective local interaction is nearly frequency independent and coincides with the actual Coulomb interaction U was estimated as $d \gtrsim 70\%d_{\max}$. This condition defines the Ising regime of the system, depicted by the black dashed line in Fig. 31, where charge fluctuations are indeed well developed. Note that this regime is not limited to small values of the local interaction U , which for some values of V exceed half of the bandwidth.

In the Ising regime of the normal phase, the quantum action (9.7) can be mapped onto an effective classical Hamiltonian. This can be achieved by replacing the corresponding bosonic variable by an effective charge density, which is given by the square root of the double occupancy $\rho^c \rightarrow \sqrt{d}$. Note that determining the effective charge density can be performed more accurately by finding the minimum of the local free energy in the same way that it is done for estimating the value of the local magnetic moment; see the discussion in Sec. IX. However, using the two-particle correlation function (the double occupancy) to define the average density in the case of charge degrees of freedom is also well justified, contrary to the case of magnetism, where

the magnetic phase corresponds to the ordering of single-particle quantities (local magnetizations). Since charge ordering is realized through the formation of double occupations, one needs to characterize this state from two-particle observables. Stepanov, Huber *et al.* (2019) showed that the effective Ising model introduced in such a simple way is able to predict the transition temperature between the normal- and charge-ordered phases in good agreement with much more elaborate methods, even though the calculations are performed in the unbroken symmetry phase.

XI. SUMMARY AND OUTLOOK

The developments that began with Liu (1961), Inoue and Moriya (1967), Lacour-Gayet and Cyrot (1974), Gyorffy and Stocks (1980), Oguchi, Terakura, and Hamada (1983), and Oguchi, Terakura, and Williams (1983) culminated in the work of Liechtenstein, Katsnelson, and Gubanov (1984) with a practical and efficient scheme of extracting exchange interactions between atomic magnetic moments of solids and molecules. This has opened up a field of research where a deeper understanding of magnetic interactions is possible. These early works on explicit calculations of interatomic exchange enabled new dimensions of DFT and DMFT calculations, and it is now routine to extract from electronic structure calculations on one scale (involving a few atoms per unit cell) information about exchange interactions on a much larger scale (involving pair interactions between thousands of atoms), which if needed can be used to evaluate parameters of micromagnetic simulations (Poluektov, Eriksson, and Kreiss, 2016, 2018). This represents multiscale transitions between three length scales and enables simulations of magnetic phenomena on scales equal to that of experimental sample sizes without the use of experimental information as input. In addition to offering a deeper understanding of basic magnetic exchange between atoms, the method of Liechtenstein, Katsnelson, and Gubanov (1984) has thus far been used to calculate ordering temperatures of materials and to map out magnon dispersions [via adiabatic approaches or in spin-dynamics simulations via the dynamic structure factor, as reviewed by Eriksson *et al.* (2017)]. It has also been used to address ultrafast magnetization phenomena observed in pump probe measurements (Evans, Atxitia, and Chantrell, 2015), as well as to analyze topological magnetic states (Pereiro *et al.*, 2014) and spin glass formation (Kamber *et al.*, 2020; Verlhac *et al.*, 2022), to name a few.¹²

¹²Developments in electronic structure theory in Uppsala with can be found at <https://www.physics.uu.se/research/code-development/developments-in-electronic-structure-theory/>. In addition, OpenMX from Tokyo (<https://www.openmx-square.org>), AMULET from Ekaterinburg, Russia (<http://www.amulet-code.org>), ARTAIOS from Hamburg (<https://github.com/molspintron>), and TB2J, a PYTHON package for computing magnetic interaction parameters (<https://github.com/mailhexu/TB2J>) should be mentioned here. The exchange using interaction parameters can be calculated using KKR codes as well. A corresponding link of the group of Samir Lounis can be found at <https://iffgit.fzjuelich.de/kkr/jukkr>. Assuming that calculations with the code dealing with periodic structures are intended, one can find the wiki page for the calculation of exchange coupling constants at <https://iffgit.fzjuelich.de/kkr/jukkr/-/wikis/jumu/jijdj>.

It is foreseeable that the method of [Liechtenstein, Katsnelson, and Gubanov \(1984\)](#) will continue to be developed to enable a more detailed and deeper understanding of the mechanisms that govern the properties of a magnetic material. An example here is the coupling of spin and lattice degrees of freedom, where initial steps have been taken. In a recent work ([Mankovsky *et al.*, 2022](#)) spin-lattice parameters were calculated from an extension of the formalism of [Liechtenstein, Katsnelson, and Gubanov \(1984\)](#). Hence, coupled motion, such as that involving magnons and phonons, is now possible to consider in combined spin-lattice simulations ([Antropov *et al.*, 1995](#); [Hellsvik *et al.*, 2019](#)). These developments will continue to be developed such that a natural output from electronic structure calculations is a set of interaction parameters that enable simulations of all relevant collective modes and the coupling between them.

The theories reviewed here have focused on bilinear effects, such as those expressed in Eq. (1.1). This is natural in the spirit of the LKAG approach, with perturbations corresponding to small rotations of the local moments. As the perturbations can all be considered infinitesimal, orders higher than 2 make little sense. However, in perturbational approaches ([Brinker, Dias, and Lounis, 2019](#)) that start with a nonmagnetic reference state and where the perturbations then have to be larger, the convergence is slower and higher-order terms do play a large role ([Brinker, Dias, and Lounis, 2020](#); [Grytsiuk *et al.*, 2020](#)). These multispin and multisite interactions become cumbersome to calculate systematically in general, so in most cases the interaction parameters are instead determined through a fitting of the total energies. As these two perturbational approaches lead to different descriptions and interpretation, one hopes that their complementarity, discussed in Sec. V J, will be utilized in the future to increase the understanding of complex magnetic systems.

In these extensions, which one can expect to come into focus in the approaching years, it would be of interest to analyze the interaction terms in an orbital-composed fashion, in the same way as was done for bilinear exchange ([Kvashnin *et al.*, 2016](#)), as shown in Fig. 12. In connection with this analysis, we mention that a similar analysis of the DM interaction is not straightforward since spin-orbit coupling mixes orbitals that otherwise would belong to separate irreducible representations. Orbital-decomposed DM interaction hence becomes an issue of which basis is the most natural to use, which most likely will vary from material to material, given that spin-orbit coupling is either the weakest (for the $3d$ transition metals) or equal in size to other interactions of the electronic Hamiltonian (such as for the actinides).

The primary focus of this review is on the magnetic dipole of an atom, as calculated from the expectation value of a spin operator. This is natural since for the majority of materials it is the most commonly observed order parameter. However, for some solids other order parameters are of relevance, for instance, the rank 5 or triakontadipole order that has been observed in NpO_2 ([Santini *et al.*, 2009](#)). It would be valuable if this method could be generalized from calculations of interactions between rank 1 spin moments to the case of calculations of interactions of multipoles of rank r . This would require extensions. For instance, the method of small rotations, as shown in Figs. 5 and 6, would have to be generalized

to be appropriate for these multipoles. Instead of the three independent types of interaction parameters of Eq. (5.40), one has derived expressions for $2r + 1$ independent types of interaction parameters.

To illustrate the fact that the research field reviewed here is a living, developing activity, we note a set of recent publications regarding details of the spin Hamiltonian in Eq. (1.4). [Cardias, Bergman *et al.* \(2020\)](#) and [Cardias, Szilva *et al.* \(2020\)](#) suggested that DM-like interaction terms can be realized for noncollinear magnetic structures, even if spin-orbit interactions are neglected (or are vanishingly small). This interpretation was criticized by [dos Santos Dias *et al.* \(2021\)](#), who suggested that fundamental interactions of DM character have to rely on an electronic Hamiltonian with spin-orbit coupling included. Further elaborations on nonrelativistic DM interaction were published by [Cardias *et al.* \(2022\)](#) and [dos Santos Dias *et al.* \(2022\)](#) without a firm consensus being reached.

Alternative ways to extract exchange parameters have recently been suggested ([Streib *et al.*, 2022](#)), for instance, from tight-binding electronic structure theory and adiabatic spin-dynamics simulations, where the local Weiss field is evaluated from the so-called constraining field. In this work it was suggested that effective interatomic exchange can be evaluated (dynamically) from the energy curvature tensor of any magnetic configuration. [Streib *et al.* \(2022\)](#) demonstrated that both moment lengths and effective exchange interactions can strongly depend on the magnetic configuration. Terms obtained from such an approach, which goes beyond the weak relativistic limit, contribute to isotropic exchange ([Secchi *et al.*, 2013](#)), and their relation to nonlocal crystal field excitations can be the subject of further studies.

Apart from magnetism of electrons in solids, there are some interesting magnetic phenomena related to ordering of nuclear spins in solid ^3He ([Roger, Hetherington, and Delrieu, 1983](#)). In this case, the exchange interactions cannot be described by bilinear spin Hamiltonians, and three- and four-spin exchange interactions turn out to be highly important ([Roger, Hetherington, and Delrieu, 1983](#); [Ceperley, 1995](#)). Along with solid ^3He , monolayers of ^3He on graphite are the other example of a system with complicated nuclear-spin-based magnetism ([Fukuyama, 2008](#)). Applications of the methods presented here to such systems seem to be an interesting direction for further development.

Sections VIII–X present an alternative approach to the theory of exchange interactions in light of contemporary quantum many-body theory, with its mathematically more advanced tools like path integrals and Feynman diagrams. Changing the language allows one to go much further than the initial formulation, considering the systems out of equilibrium (Sec. VIII) and nonmagnetic collective phenomena such as charge ordering and superconductivity (Sec. X), and gives a full derivation of equations of spin dynamics for itinerant-electron systems, including not only exchange-interaction-related terms but also dynamical, spin-precession terms (Sec. IX). These new developments are relatively recent, and their potential for applications is far from completely unveiled. In particular, a systematic study of laser-induced nonlinear magnetic phenomena within the developed formalism is an extremely promising prospect.

As a final remark in this section, we note that equations of the form of Eq. (1.3) (and extensions of it) have been used for research outside of materials science, or even natural science. In the Ising approximation of the classical Heisenberg Hamiltonian, the atomic spins are arranged in a z graph, usually a lattice, that can be in one of two states (+1 or -1) (Ising, 1925), and the strength of the interaction is given by J_{ij} in Eq. (1.3). This inspired the so-called classical voter model, and its extensions, which represents an idealized description for the evolution of opinions in a population (Clifford and Sudbury, 1973; Holley and Liggett, 1975; Gleeson, 2013). In the classic voter model, as in the Ising model, each voter can assume one of two states, -1 or +1. A voter at site i is selected at random and copies the state of a randomly chosen neighbor voter j . Another example where the Ising model (and percolation theory) can be used is epidemics as it is shown in a comprehensive review focused on COVID-19 (Mello *et al.*, 2021). We mention the work of Giorgio Parisi on the hidden patterns in spin glasses (Mézard, Parisi, and Virasoro, 1987) since it gave an extremely important contribution to the theory of complex system, which is a quantitative, predictive, and experimentally verifiable science (Thurner, Hanel, and Klimek, 2018). In the case of complex systems a macroscopic pattern can emerge of the mutual influence of a large number of individuals (Anderson, 1972; Principi and Katsnelson, 2016; Bagrov *et al.*, 2020), which makes it possible to understand phenomena not only in physics but also in other, significantly different areas such as mathematics, biology, neuroscience, and machine learning (Castellano, Fortunato, and Loreto, 2009; Wolf, Katsnelson, and Koonin, 2018; Baity-Jesi *et al.*, 2019).

ACKNOWLEDGMENTS

Valuable discussions with V. Antropov, A. Bergman, V. Borisov, R. Cardias, A. Delin, E. Delzceg, I. Di Marco, J. Fransson, O. Grånäs, J. Hellsvik, H. Herper, J. Jonsson, A. Katanin, A. Klautau, V. Mazurenko, I. Miranda, C. S. Ong, M. Pereiro, L. Pourovskii, A. Ruban, B. Sanyal, S. Savrasov, I. Solovyev, S. Streib, D. Thonig, P. Thunström, R. Vieira, and A. Vishina are acknowledged. In particular, the critical reading and the many useful comments by A. Ruban are acknowledged. E. A. S. acknowledges support from the European Union's Horizon 2020 research and innovation program under the Marie Skłodowska Curie Grant Agreement No. 839551-2DMAGICS. O. E., A. I. L., and M. I. K. acknowledge support from the European Research Council via Synergy Grant No. 854843 (the FASTCORR project). O. E. and L. N. acknowledge support from the Swedish Research Council (VR), and O. E. also acknowledges support from the Swedish Foundation for Strategic Research (SSF), the Swedish Energy Agency (STEM), the Wallenberg Initiative Materials Science for Sustainability (WISE) funded by the Knut and Alice Wallenberg Foundation (KAW), eSENCE, and STandUP. A. I. L. acknowledges support from the German Research Foundation through the research unit QUAST, FOR 5249, Project No. 449872909.

REFERENCES

- Abrikosov, A. A., 1988, *Fundamentals of the Theory of Metals* (North-Holland, Amsterdam).
- Acharya, Swagata, Dimitar Pashov, Brian Cunningham, Alexander N. Rudenko, Malte Rösner, Myrta Grüning, Mark van Schilfgaarde, and Mikhail I. Katsnelson, 2021, "Electronic structure of chromium trihalides beyond density functional theory," *Phys. Rev. B* **104**, 155109.
- Acharya, Swagata, Dimitar Pashov, Alexander N. Rudenko, Malte Rösner, Mark van Schilfgaarde, and Mikhail I. Katsnelson, 2021, "Importance of charge self-consistency in first-principles description of strongly correlated systems," *npj Comput. Mater.* **7**, 208.
- Aharoni, A., 2000, *Introduction to the Theory of Ferromagnetism* (Clarendon Press, Oxford).
- Akhiezer, A. I., V. G. Bar'yakhtar, and S. V. Peletminskii, 1968, *Spin Waves* (North-Holland, Amsterdam).
- Alling, B., A. V. Ruban, A. Karimi, L. Hultman, and I. A. Abrikosov, 2011, "Unified cluster expansion method applied to the configurational thermodynamics of cubic $Ti_{1-x}Al_xN$," *Phys. Rev. B* **83**, 104203.
- Andersen, O. K., and O. Jepsen, 1984, "Explicit, First-Principles Tight-Binding Theory," *Phys. Rev. Lett.* **53**, 2571-2574.
- Andersen, O. K., H. L. Skriver, H. Nohl, and B. Johansson, 1980, "Electronic structure of transition metal compounds; ground-state properties of the 3d-monoxides in the atomic sphere approximation," *Pure Appl. Chem.* **52**, 93-118.
- Anderson, P. W., 1959, "New approach to the theory of super-exchange interactions," *Phys. Rev.* **115**, 2-13.
- Anderson, Philip W., 1972, "More is different," *Science* **177**, 393-396.
- Anisimov, Vladimir I., Jan Zaanen, and Ole K. Andersen, 1991, "Band theory and Mott insulators: Hubbard U instead of Stoner I ," *Phys. Rev. B* **44**, 943-954.
- Antropov, V. P., 2003, "The exchange coupling and spin waves in metallic magnets: Removal of the long-wave approximation," *J. Magn. Magn. Mater.* **262**, L192-L197.
- Antropov, V. P., B. N. Harmon, and A. N. Smirnov, 1999, "Aspects of spin dynamics and magnetic interactions," *J. Magn. Magn. Mater.* **200**, 148-166.
- Antropov, V. P., M. I. Katsnelson, B. N. Harmon, M. van Schilfgaarde, and D. Kusnezov, 1996, "Spin dynamics in magnets: Equation of motion and finite temperature effects," *Phys. Rev. B* **54**, 1019-1035.
- Antropov, V. P., M. I. Katsnelson, and A. I. Liechtenstein, 1997, "Exchange interactions in magnets," *Physica (Amsterdam)* **237B-238B**, 336-340.
- Antropov, V. P., M. I. Katsnelson, M. van Schilfgaarde, and B. N. Harmon, 1995, "Ab Initio Spin Dynamics in Magnets," *Phys. Rev. Lett.* **75**, 729-732.
- Antropov, Vladimir, 2005, "Magnetic short-range order above the Curie temperature of Fe and Ni," *Phys. Rev. B* **72**, 140406.
- Aoki, Hideo, Naoto Tsuji, Martin Eckstein, Marcus Kollar, Takashi Oka, and Philipp Werner, 2014, "Nonequilibrium dynamical mean-field theory and its applications," *Rev. Mod. Phys.* **86**, 779-837.
- Arguello, C. J., *et al.*, 2014, "Visualizing the charge density wave transition in $2H-NbSe_2$ in real space," *Phys. Rev. B* **89**, 235115.
- Aryasetiawan, F., M. Imada, A. Georges, G. Kotliar, S. Biermann, and A. I. Liechtenstein, 2004, "Frequency-dependent local interactions and low-energy effective models from electronic structure calculations," *Phys. Rev. B* **70**, 195104.

- Auerbach, Assa, 1994, *Interacting Electrons and Quantum Magnetism* (Springer, New York).
- Auslender, M. I., and M. I. Katsnel'son, 1982, "Effective spin Hamiltonian and phase separation in the almost half-filled Hubbard model and the narrow-band *s-f* model," *Theor. Math. Phys.* **51**, 601–607.
- Auslender, M. I., and M. I. Katsnelson, 1982, "The effective spin Hamiltonian and phase separation instability of the almost half-filled Hubbard model and the narrow-band *s-f* model," *Solid State Commun.* **44**, 387–389.
- Ayral, T., S. Biermann, and P. Werner, 2013, "Screening and nonlocal correlations in the extended Hubbard model from self-consistent combined *GW* and dynamical mean field theory," *Phys. Rev. B* **87**, 125149.
- Ayral, T., S. Biermann, P. Werner, and L. Boehnke, 2017, "Influence of Fock exchange in combined many-body perturbation and dynamical mean field theory," *Phys. Rev. B* **95**, 245130.
- Badrtdinov, D. I., S. A. Nikolaev, M. I. Katsnelson, and V. V. Mazurenko, 2016, "Spin-orbit coupling and magnetic interactions in Si(111):{C, Si, Sn, Pb}," *Phys. Rev. B* **94**, 224418.
- Badrtdinov, Danis I., Sergey A. Nikolaev, Alexander N. Rudenko, Mikhail I. Katsnelson, and Vladimir V. Mazurenko, 2018, "Nanoskyrmion engineering with *sp*-electron materials: Sn monolayer on a SiC(0001) surface," *Phys. Rev. B* **98**, 184425.
- Bagrov, Andrey A., Ilia A. Iakovlev, Askar A. Iliasov, Mikhail I. Katsnelson, and Vladimir V. Mazurenko, 2020, "Multiscale structural complexity of natural patterns," *Proc. Natl. Acad. Sci. U.S.A.* **117**, 30241–30251.
- Baibich, M. N., J. M. Broto, A. Fert, F. Nguyen Van Dau, F. Petroff, P. Etienne, G. Creuzet, A. Friederich, and J. Chazelas, 1988, "Giant Magnetoresistance of (001)Fe/(001)Cr Magnetic Superlattices," *Phys. Rev. Lett.* **61**, 2472–2475.
- Baier, Tobias, Eike Bick, and Christof Wetterich, 2004, "Temperature dependence of antiferromagnetic order in the Hubbard model," *Phys. Rev. B* **70**, 125111.
- Baity-Jesi, Marco, Levent Sagun, Mario Geiger, Stefano Spigler, Gérard Ben Arous, Chiara Cammarota, Yann LeCun, Matthieu Wyart, and Giulio Biroli, 2019, "Comparing dynamics: Deep neural networks versus glassy systems," in *J. Stat. Mech.* 124013.
- Balashov, T., P. Buczek, L. Sandratskii, A. Ernst, and W. Wulfhekel, 2014, "Magnon dispersion in thin magnetic films," *J. Phys. Condens. Matter* **26**, 394007.
- Barbeau, M. M. S., M. Eckstein, M. I. Katsnelson, and J. H. Mentink, 2019, "Optical control of competing exchange interactions and coherent spin-charge coupling in two-orbital Mott insulators," *SciPost Phys.* **6**, 27.
- Barker, Joseph, and Roy W. Chantrell, 2015, "Higher-order exchange interactions leading to metamagnetism in FeRh," *Phys. Rev. B* **92**, 094402.
- Barker, Joseph, Dimitar Pashov, and Jerome Jackson, 2020, "Electronic structure and finite temperature magnetism of yttrium iron garnet," *Electron. Struct.* **2**, 044002.
- Bauer, Bela, Lukasz Cincio, Brendan P. Keller, Michele Dolfi, Guifre Vidal, Simon Trebst, and Andreas W. W. Ludwig, 2014, "Chiral spin liquid and emergent anyons in a kagome lattice Mott insulator," *Nat. Commun.* **5**, 5137.
- Baym, Gordon, and Leo P. Kadanoff, 1961, "Conservation laws and correlation functions," *Phys. Rev.* **124**, 287–299.
- Beaurepaire, E., J.-C. Merle, A. Daunois, and J.-Y. Bigot, 1996, "Ultrafast Spin Dynamics in Ferromagnetic Nickel," *Phys. Rev. Lett.* **76**, 4250–4253.
- Belavin, A. A., and A. M. Polyakov, 1975, "Metastable states of two-dimensional isotropic ferromagnets," *Pis'ma Zh. Eksp. Teor. Fiz.* **22**, 503–506 [*JETP Lett.* **22**, 245–248 (1975)], <https://inspirehep.net/literature/107068>.
- Belozarov, A. S., A. A. Katanin, and V. I. Anisimov, 2017, "Momentum-dependent susceptibilities and magnetic exchange in bcc iron from supercell dynamical mean-field theory calculations," *Phys. Rev. B* **96**, 075108.
- Berger, E., P. Valášek, and W. von der Linden, 1995, "Two-dimensional Hubbard-Holstein model," *Phys. Rev. B* **52**, 4806–4814.
- Bergman, Anders, Lars Nordström, Angela Burlamaqui Klautau, Sonia Frota-Pessôa, and Olle Eriksson, 2007, "Magnetic structures of small Fe, Mn, and Cr clusters supported on Cu(111): Noncollinear first-principles calculations," *Phys. Rev. B* **75**, 224425.
- Bergqvist, Lars, 2005, "Electronic structure and statistical methods applied to nanomagnetism, diluted magnetic semiconductors and spintronics," Ph.D. thesis (Acta Universitatis Upsaliensis).
- Bergqvist, Lars, Andrea Taroni, Anders Bergman, Corina Etz, and Olle Eriksson, 2013, "Atomistic spin dynamics of low-dimensional magnets," *Phys. Rev. B* **87**, 144401.
- Besbes, Omar, Sergey Nikolaev, Noureddine Meskini, and Igor Solovyev, 2019, "Microscopic origin of ferromagnetism in the trihalides CrCl₃ and CrI₃," *Phys. Rev. B* **99**, 104432.
- Bezerra-Neto, Manoel M., Marcelo S. Ribeiro, Biplab Sanyal, Anders Bergman, Roberto B. Muniz, Olle Eriksson, and Angela B. Klautau, 2013, "Complex magnetic structure of clusters and chains of Ni and Fe on Pt(111)," *Sci. Rep.* **3**, 3054.
- Binasch, G., P. Grünberg, F. Saurenbach, and W. Zinn, 1989, "Enhanced magnetoresistance in layered magnetic structures with antiferromagnetic interlayer exchange," *Phys. Rev. B* **39**, 4828(R).
- Binder, Kurt, and Dieter W. Heermann, 2010, "Theoretical foundations of the Monte Carlo method and its applications in statistical physics," in *Monte Carlo Simulation in Statistical Physics*, Graduate Texts in Physics (Springer, New York), pp. 5–67.
- Bogani, Lapo, and Wolfgang Wernsdorfer, 2008, "Molecular spintronics using single-molecule magnets," *Nat. Mater.* **7**, 179–186.
- Bogolyubov, N. N., 1958, "On a variational principle in the many-body problem," *Sov. Phys. Dokl.* **3**, 292–294, <https://ui.adsabs.harvard.edu/abs/1958SPhD....3..292B/abstract>.
- Borisov, Vladislav, *et al.*, 2021, "Heisenberg and anisotropic exchange interactions in magnetic materials with correlated electronic structure and significant spin-orbit coupling," *Phys. Rev. B* **103**, 174422.
- Bose, S. K., and J. Kudrnovský, 2010, "Exchange interactions and Curie temperatures in Cr-based alloys in the zinc blende structure: Volume- and composition-dependence from first-principles calculations," *Phys. Rev. B* **81**, 054446.
- Boukhalov, D. W., V. V. Dobrovitski, M. I. Katsnelson, A. I. Lichtenstein, B. N. Harmon, and P. Kögerler, 2004, "Electronic structure and exchange interactions in V₁₅ magnetic molecules: LDA + *U* results," *Phys. Rev. B* **70**, 054417.
- Boukhalov, D. W., A. I. Lichtenstein, V. V. Dobrovitski, M. I. Katsnelson, B. N. Harmon, V. V. Mazurenko, and V. I. Anisimov, 2002, "Effect of local Coulomb interactions on the electronic structure and exchange interactions in Mn₁₂ magnetic molecules," *Phys. Rev. B* **65**, 184435.
- Boust, James, Alex Aubert, Bahar Fayyazi, Konstantin P. Skokov, Yurii Skourski, Oliver Gutfleisch, and Leonid V. Pourovskii, 2022, "Ce and Dy substitutions in Nd₂Fe₁₄B: Site-specific magnetic anisotropy from first principles," *Phys. Rev. Mater.* **6**, 084410.
- Bowen, M., *et al.*, 2001, "Large magnetoresistance in Fe/MgO/FeCo(001) epitaxial tunnel junctions on GaAs(001)," *Appl. Phys. Lett.* **79**, 1655–1657.

- Bramwell, Steven T., and Michel J.P. Gingras, 2001, “Spin ice state in frustrated magnetic pyrochlore materials,” *Science* **294**, 1495–1501.
- Brener, Sergey, Evgeny A. Stepanov, Alexey N. Rubtsov, Mikhail I. Katsnelson, and Alexander I. Lichtenstein, 2020, “Dual fermion method as a prototype of generic reference-system approach for correlated fermions,” *Ann. Phys. (Amsterdam)* **422**, 168310.
- Brinker, Sascha, Manuel dos Santos Dias, and Samir Lounis, 2019, “The chiral biquadratic pair interaction,” *New J. Phys.* **21**, 083015.
- Brinker, Sascha, Manuel dos Santos Dias, and Samir Lounis, 2020, “Prospecting chiral multisite interactions in prototypical magnetic systems,” *Phys. Rev. Res.* **2**, 033240.
- Bruno, P., 2003, “Exchange Interaction Parameters and Adiabatic Spin-Wave Spectra of Ferromagnets: A ‘Renormalized Magnetic Force Theorem,’” *Phys. Rev. Lett.* **90**, 087205.
- Bruno, P., J. Kudrnovský, M. Pajda, V. Drchal, and I. Turek, 2002, “Oscillatory Curie temperature of 2D-ferromagnets,” *J. Magn. Magn. Mater.* **240**, 346–348.
- Buchelnikov, V. D., P. Entel, S. V. Taskaev, V. V. Sokolovskiy, A. Hucht, M. Ogura, H. Akai, M. E. Gruner, and S. K. Nayak, 2008, “Monte Carlo study of the influence of antiferromagnetic exchange interactions on the phase transitions of ferromagnetic Ni-Mn-X alloys ($X = \text{In, Sn, Sb}$),” *Phys. Rev. B* **78**, 184427.
- Buchelnikov, V. D., *et al.*, 2010, “First-principles and Monte Carlo study of magnetostructural transition and magnetocaloric properties of $\text{Ni}_{2+x}\text{Mn}_{1-x}\text{Ga}$,” *Phys. Rev. B* **81**, 094411.
- Buczek, Paweł, Arthur Ernst, and Leonid M. Sandratskii, 2011, “Different dimensionality trends in the Landau damping of magnons in iron, cobalt, and nickel: Time-dependent density functional study,” *Phys. Rev. B* **84**, 174418.
- Buividovich, Pavel, Dominik Smith, Maksim Ulybyshev, and Lorenz von Smekal, 2017, “Competing order in the fermionic Hubbard model on the hexagonal graphene lattice,” *Proc. Sci. LATTICE2016*, 244.
- Bukov, Marin, Luca D’Alessio, and Anatoli Polkovnikov, 2015, “Universal high-frequency behavior of periodically driven systems: From dynamical stabilization to Floquet engineering,” *Adv. Phys.* **64**, 139–226.
- Bukov, Marin, Michael Kolodrubetz, and Anatoli Polkovnikov, 2016, “Schrieffer-Wolff Transformation for Periodically Driven Systems: Strongly Correlated Systems with Artificial Gauge Fields,” *Phys. Rev. Lett.* **116**, 125301.
- Bulik, Ireneusz W., Giovanni Scalmani, Michael J. Frisch, and Gustavo E. Scuseria, 2013, “Noncollinear density functional theory having proper invariance and local torque properties,” *Phys. Rev. B* **87**, 035117.
- Bultmark, Fredrik, Francesco Cricchio, Oscar Grånäs, and Lars Nordström, 2009, “Multipole decomposition of LDA + U energy and its application to actinide compounds,” *Phys. Rev. B* **80**, 035121.
- Burch, Kenneth S., David Mandrus, and Je-Geun Park, 2018, “Magnetism in two-dimensional van der Waals materials,” *Nature (London)* **563**, 47–52.
- Buschow, Kurt Heinz Jürgen, and Frank R. Boer, 2003, *Physics of Magnetism and Magnetic Materials*, Vol. 7 (Springer, New York).
- Butler, W. H., 1985, “Theory of electronic transport in random alloys: Koringa-Kohn-Rostoker coherent-potential approximation,” *Phys. Rev. B* **31**, 3260–3277.
- Bychkov, Y. A., and E. I. Rashba, 1984, “Properties of a 2D electron gas with lifted spectral degeneracy,” *Pis’ma Zh. Eksp. Teor. Fiz.* **39**, 66–69 [*JETP Lett.* **39**, 78 (1984)], http://jetpletters.ru/ps/1264/article_19121.pdf.
- Callaway, J., C. S. Wang, and D. G. Laurent, 1981, “Magnetic susceptibility and spin waves in ferromagnetic metals,” *Phys. Rev. B* **24**, 6491–6496.
- Cannella, V., and J. A. Mydosh, 1972, “Magnetic ordering in gold-iron alloys,” *Phys. Rev. B* **6**, 4220–4237.
- Capelle, K., and B. L. Gyorffy, 2003, “Exploring dynamical magnetism with time-dependent density-functional theory: From spin fluctuations to Gilbert damping,” *Europhys. Lett.* **61**, 354–360.
- Capelle, K., G. Vignale, and B. L. Gyorffy, 2001, “Spin Currents and Spin Dynamics in Time-Dependent Density-Functional Theory,” *Phys. Rev. Lett.* **87**, 206403.
- Capellmann, H., 1979, “Theory of itinerant ferromagnetism in the 3- d transition metals,” *Z. Phys. B* **34**, 29–35.
- Cardias, R., M. M. Bezerra-Neto, M. S. Ribeiro, A. Bergman, A. Szilva, O. Eriksson, and A. B. Klautau, 2016, “Magnetic and electronic structure of Mn nanostructures on Ag(111) and Au(111),” *Phys. Rev. B* **93**, 014438.
- Cardias, R., A. Szilva, A. Bergman, I. Di Marco, M. I. Katsnelson, A. I. Lichtenstein, L. Nordström, A. B. Klautau, O. Eriksson, and Y. O. Kvashnin, 2017, “The Bethe-Slater curve revisited; new insights from electronic structure theory,” *Sci. Rep.* **7**, 4058.
- Cardias, Ramon, Anders Bergman, Attila Szilva, Yaroslav O. Kvashnin, Jonas Fransson, Angela B. Klautau, Olle Eriksson, and Lars Nordström, 2020, “Dzyaloshinskii-Moriya interaction in absence of spin-orbit coupling,” *arXiv:2003.04680*.
- Cardias, Ramon, Attila Szilva, M. M. Bezerra-Neto, M. S. Ribeiro, Anders Bergman, Yaroslav O. Kvashnin, Jonas Fransson, A. B. Klautau, Olle Eriksson, and Lars Nordström, 2020, “First-principles Dzyaloshinskii-Moriya interaction in a non-collinear framework,” *Sci. Rep.* **10**, 1–13.
- Cardias, Ramon, *et al.*, 2022, “Comment on ‘Proper and improper chiral magnetic interactions,’” *Phys. Rev. B* **105**, 026401.
- Carpinelli, J. M., H. H. Weitering, M. Bartkowiak, R. Stumpf, and E. W. Plummer, 1997, “Surface Charge Ordering Transition: α Phase of Sn/Ge(111),” *Phys. Rev. Lett.* **79**, 2859–2862.
- Carvalho, P. C., I. P. Miranda, A. B. Klautau, A. Bergman, and H. M. Petrilli, 2021, “Complex magnetic textures in Ni/Ir_n/Pt(111) ultrathin films,” *Phys. Rev. Mater.* **5**, 124406.
- Castellano, Claudio, Santo Fortunato, and Vittorio Loreto, 2009, “Statistical physics of social dynamics,” *Rev. Mod. Phys.* **81**, 591–646.
- Castro, A., J. Werschnik, and E. K. U. Gross, 2012, “Controlling the Dynamics of Many-Electron Systems from First Principles: A Combination of Optimal Control and Time-Dependent Density-Functional Theory,” *Phys. Rev. Lett.* **109**, 153603.
- Ceperley, D. M., 1995, “Path integrals in the theory of condensed helium,” *Rev. Mod. Phys.* **67**, 279–355.
- Chakravarty, Sudip, Bertrand I. Halperin, and David R. Nelson, 1989, “Two-dimensional quantum Heisenberg antiferromagnet at low temperatures,” *Phys. Rev. B* **39**, 2344–2371.
- Chakraverty, B. K., 1980, “Charge ordering in Fe_3O_4 , Ti_4O_7 and bipolarons,” *Philos. Mag. B* **42**, 473–478.
- Chalupa, P., T. Schäfer, M. Reitner, D. Springer, S. Andergassen, and A. Toschi, 2021, “Fingerprints of the Local Moment Formation and Its Kondo Screening in the Generalized Susceptibilities of Many-Electron Problems,” *Phys. Rev. Lett.* **126**, 056403.
- Chao, K. A., J. Spátek, and A. M. Oleś, 1977a, “Degenerate perturbation theory and its application to the Hubbard model,” *Phys. Lett.* **64A**, 163–166.
- Chao, K. A., J. Spátek, and A. M. Oleś, 1977b, “Kinetic exchange interaction in a narrow S -band,” *J. Phys. C* **10**, L271–L276.
- Chen, Lebing, Jae-Ho Chung, Bin Gao, Tong Chen, Matthew B. Stone, Alexander I. Kolesnikov, Qingzhen Huang, and Pengcheng

- Dai, 2018, “Topological Spin Excitations in Honeycomb Ferromagnet CrI_3 ,” *Phys. Rev. X* **8**, 041028.
- Chico, Jonathan, Samara Keshavarz, Yaroslav Kvashnin, Manuel Pereira, Igor Di Marco, Corina Etz, Olle Eriksson, Anders Bergman, and Lars Bergqvist, 2016, “First-principles studies of the Gilbert damping and exchange interactions for half-metallic Heuslers alloys,” *Phys. Rev. B* **93**, 214439.
- Chimata, R., *et al.*, 2017, “Magnetism and ultrafast magnetization dynamics of Co and CoMn alloys at finite temperature,” *Phys. Rev. B* **95**, 214417.
- Chiorescu, I., W. Wernsdorfer, A. Müller, H. Bögge, and B. Barbara, 2000, “Butterfly Hysteresis Loop and Dissipative Spin Reversal in the $S = 1/2$, V_{15} Molecular Complex,” *Phys. Rev. Lett.* **84**, 3454–3457.
- Chuang, T.-H., Kh. Zakeri, A. Ernst, Y. Zhang, H. J. Qin, Y. Meng, Y.-J. Chen, and J. Kirschner, 2014, “Magnetic properties and magnon excitations in $\text{Fe}(001)$ films grown on $\text{Ir}(001)$,” *Phys. Rev. B* **89**, 174404.
- Claassen, Martin, Hong-Chen Jiang, Brian Moritz, and Thomas P. Devereaux, 2017, “Dynamical time-reversal symmetry breaking and photo-induced chiral spin liquids in frustrated Mott insulators,” *Nat. Commun.* **8**, 1–9.
- Clifford, Peter, and Aidan Sudbury, 1973, “A model for spatial conflict,” *Biometrika* **60**, 581–588.
- Coe, John M. D., 2010, *Magnetism and Magnetic Materials* (Cambridge University Press, Cambridge, England).
- Colarieti-Tosti, M., S. I. Simak, R. Ahuja, L. Nordström, O. Eriksson, D. Åberg, S. Edvardsson, and M. S. S. Brooks, 2003, “Origin of Magnetic Anisotropy of Gd Metal,” *Phys. Rev. Lett.* **91**, 157201.
- Comtesse, Denis, Benjamin Geisler, Peter Entel, Peter Kratzer, and László Szunyogh, 2014, “First-principles study of spin-dependent thermoelectric properties of half-metallic Heusler thin films between platinum leads,” *Phys. Rev. B* **89**, 094410.
- Connolly, J. W. D., and A. R. Williams, 1983, “Density-functional theory applied to phase transformations in transition-metal alloys,” *Phys. Rev. B* **27**, 5169–5172.
- Cooke, J. F., J. A. Blackman, and T. Morgan, 1985, “New Interpretation of Spin-Wave Behavior in Nickel,” *Phys. Rev. Lett.* **54**, 718–721.
- Costa, A. T., R. B. Muniz, and D. L. Mills, 2005, “Ground State of Magnetic Dimers on Metal Surfaces,” *Phys. Rev. Lett.* **94**, 137203.
- Cricchio, F., O. Grånäs, and L. Nordström, 2011, “Polarization of an open shell in the presence of spin-orbit coupling,” *Europhys. Lett.* **94**, 57009.
- Croat, John J., Jan F. Herbst, Robert W. Lee, and Frederick E. Pinkerton, 1984, “High-energy product Nd-Fe-B permanent magnets,” *Appl. Phys. Lett.* **44**, 148–149.
- Czyżyk, M. T., and G. A. Sawatzky, 1994, “Local-density functional and on-site correlations: The electronic structure of La_2CuO_4 and LaCuO_3 ,” *Phys. Rev. B* **49**, 14211–14228.
- Delczeg-Czirjak, E. K., L. Bergqvist, O. Eriksson, Z. Gercsi, P. Nordblad, L. Szunyogh, B. Johansson, and L. Vitos, 2012, “Microscopic theory of magnetism in the magnetocaloric material $\text{Fe}_2\text{P}_{1-x}\text{T}_x$ ($T = \text{B}$ and Si),” *Phys. Rev. B* **86**, 045126.
- Dillon, J. F., and C. E. Olson, 1965, “Magnetization, resonance, and optical properties of the ferromagnet CrI_3 ,” *J. Appl. Phys.* **36**, 1259–1260.
- Dirac, P. A. M., 1926, “On the theory of quantum mechanics,” *Proc. R. Soc. A* **112**, 661–677.
- Dmitrienko, V. E., E. N. Ovchinnikova, S. P. Collins, G. Nisbet, G. Beutier, Y. O. Kvashnin, V. V. Mazurenko, A. I. Lichtenstein, and M. I. Katsnelson, 2014, “Measuring the Dzyaloshinskii-Moriya interaction in a weak ferromagnet,” *Nat. Phys.* **10**, 202–206.
- Dobrovitski, V. V., M. I. Katsnelson, and B. N. Harmon, 2000, “Mechanisms of Decoherence in Weakly Anisotropic Molecular Magnets,” *Phys. Rev. Lett.* **84**, 3458–3461.
- Dong, Zhihua, Stephan Schönecker, Dengfu Chen, Wei Li, Mujun Long, and Levente Vitos, 2017, “Elastic properties of paramagnetic austenitic steel at finite temperature: Longitudinal spin fluctuations in multicomponent alloys,” *Phys. Rev. B* **96**, 174415.
- dos Santos Dias, Manuel, Sascha Brinker, András Lászlóffy, Bendegúz Nyári, Stefan Blügel, László Szunyogh, and Samir Lounis, 2021, “Proper and improper chiral magnetic interactions,” *Phys. Rev. B* **103**, L140408.
- dos Santos Dias, Manuel, Sascha Brinker, András Lászlóffy, Bendegúz Nyári, Stefan Blügel, László Szunyogh, and Samir Lounis, 2022, “Reply to ‘Comment on “Proper and improper chiral magnetic interactions,”’” *Phys. Rev. B* **105**, 026402.
- Drautz, R., and M. Fähnle, 2004, “Spin-cluster expansion: Parametrization of the general adiabatic magnetic energy surface with *ab initio* accuracy,” *Phys. Rev. B* **69**, 104404.
- Ducastelle, F., 1991, *Order and Phase Stability in Alloys* (North-Holland, Amsterdam).
- Ducastelle, F., and F. Gautier, 1976, “Generalized perturbation theory in disordered transitional alloys: Applications to the calculation of ordering energies,” *J. Phys. F* **6**, 2039.
- Ducastelle, F., and G. Treglia, 1980, “Thermodynamic derivation of the coherent potential approximation and ordering processes in transition alloys,” *J. Phys. F* **10**, 2137–2146.
- Dumas, J., C. Schlenker, and R. Buder, 1980, “The vanadium bronzes $\text{Na}_x\text{V}_2\text{O}_5\text{-}\beta$,” *Philos. Mag. B* **42**, 485–486.
- Dupont, M., Y. O. Kvashnin, M. Shiranzai, J. Fransson, N. Laflorencie, and A. Kantian, 2021, “Monolayer CrCl_3 as an Ideal Test Bed for the Universality Classes of 2D Magnetism,” *Phys. Rev. Lett.* **127**, 037204.
- Dupuis, N., 2001, “A new approach to strongly correlated fermion systems: The spin-particle-hole coherent-state path integral,” *Nucl. Phys. B* **618**, 617–649.
- Dupuis, N., and S. Pairault, 2000, “A strong-coupling expansion for the Hubbard model,” *Int. J. Mod. Phys. B* **14**, 2529–2560.
- Dutreix, C., and M. I. Katsnelson, 2017, “Dynamical control of electron-phonon interactions with high-frequency light,” *Phys. Rev. B* **95**, 024306.
- Dutreix, C., E. A. Stepanov, and M. I. Katsnelson, 2016, “Laser-induced topological transitions in phosphorene with inversion symmetry,” *Phys. Rev. B* **93**, 241404(R).
- Ebert, H., D. Ködderitzsch, and J. Minár, 2011, “Calculating condensed matter properties using the KKR–Green’s function method—Recent developments and applications,” *Rep. Prog. Phys.* **74**, 096501.
- Ebert, H., and S. Mankovsky, 2009, “Anisotropic exchange coupling in diluted magnetic semiconductors: *Ab initio* spin-density functional theory,” *Phys. Rev. B* **79**, 045209.
- Ebert, Hubert, Sergiy Mankovsky, and Sebastian Wimmer, 2021, in *Handbook of Magnetism and Magnetic Materials*, edited by J. M. D. Coey and Stuart S. P. Parkin (Springer International Publishing, Cham, Switzerland).
- Eckardt, André, 2017, “Colloquium: Atomic quantum gases in periodically driven optical lattices,” *Rev. Mod. Phys.* **89**, 011004.
- Economou, Eleftherios N., 2006, *Green’s Functions in Quantum Physics*, Vol. 7 (Springer Science+Business Media, New York).
- Edwards, D. M., 1982, “The paramagnetic state of itinerant electron systems with local magnetic moments. I. Static properties,” *J. Phys. F* **12**, 1789–1810.
- Edwards, D. M., 1983, “Iron above the Curie temperature,” *J. Magn. Magn. Mater.* **36**, 213–216.

- Eich, F. G., and E. K. U. Gross, 2013, “Transverse Spin-Gradient Functional for Noncollinear Spin-Density-Functional Theory,” *Phys. Rev. Lett.* **111**, 156401.
- Eich, F. G., S. Pittalis, and G. Vignale, 2013, “Transverse and longitudinal gradients of the spin magnetization in spin-density-functional theory,” *Phys. Rev. B* **88**, 245102.
- Ekhholm, M., H. Zapolsky, A. V. Ruban, I. Vernyhora, D. Ledue, and I. A. Abrikosov, 2010, “Influence of the Magnetic State on the Chemical Order-Disorder Transition Temperature in Fe-Ni Permalloy,” *Phys. Rev. Lett.* **105**, 167208.
- Elliott, R. J., J. A. Krumhansl, and P. L. Leath, 1974, “The theory and properties of randomly disordered crystals and related physical systems,” *Rev. Mod. Phys.* **46**, 465–543.
- Englert, F., and R. Brout, 1964, “Broken Symmetry and the Mass of Gauge Vector Mesons,” *Phys. Rev. Lett.* **13**, 321–323.
- Eriksson, Olle, Anders Bergman, Lars Bergqvist, and Johan Hellsvik, 2017, *Atomistic Spin Dynamics: Foundations and Applications* (Oxford University Press, New York).
- Eroles, J., C. D. Batista, S. B. Bacci, and E. R. Gagliano, 1999, “Magnetic Raman scattering of insulating cuprates,” *Phys. Rev. B* **59**, 1468–1473.
- Eschrig, Helmut, 2010, “ $T > 0$ ensemble-state density functional theory via Legendre transform,” *Phys. Rev. B* **82**, 205120.
- Etz, C., I. V. Maznichenko, D. Böttcher, J. Henk, A. N. Yaresko, W. Hergert, I. I. Mazin, I. Mertig, and A. Ernst, 2012, “Indications of weak electronic correlations in SrRuO₃ from first-principles calculations,” *Phys. Rev. B* **86**, 064441.
- Etz, Corina, Lars Bergqvist, Anders Bergman, Andrea Taroni, and Olle Eriksson, 2015, “Atomistic spin dynamics and surface magnons,” *J. Phys. Condens. Matter* **27**, 243202.
- Evans, R. F. L., U. Atxitia, and R. W. Chantrell, 2015, “Quantitative simulation of temperature-dependent magnetization dynamics and equilibrium properties of elemental ferromagnets,” *Phys. Rev. B* **91**, 144425.
- Evans, R. F. L., W. J. Fan, P. Churemart, T. A. Ostler, M. O. A. Ellis, and R. W. Chantrell, 2014, “Atomistic spin model simulations of magnetic nanomaterials,” *J. Phys. Condens. Matter* **26**, 103202.
- Eyert, V., and U. Schwingenschlögl, and U. Eckern, 2004, “Charge order, orbital order, and electron localization in the Magnéli phase Ti₄O₇,” *Chem. Phys. Lett.* **390**, 151–156.
- Fazekas, Patrik, 1999, *Lecture Notes on Electron Correlation and Magnetism*, Vol. 5 (World Scientific, Singapore).
- Fedorova, Natalya S., Claude Ederer, Nicola A. Spaldin, and Andrea Scaramucci, 2015, “Biquadratic and ring exchange interactions in orthorhombic perovskite manganites,” *Phys. Rev. B* **91**, 165122.
- Feynman, R. P., 1972, *Statistical Mechanics: A Set of Lectures* (Benjamin Cummings, Reading, MA).
- Fischer, Guntram, Markus Däne, Arthur Ernst, Patrick Bruno, Martin Lüders, Zdzisława Szotek, Walter Temmerman, and Wolfram Hergert, 2009, “Exchange coupling in transition metal monoxides: Electronic structure calculations,” *Phys. Rev. B* **80**, 014408.
- Floreano, L., D. Cvetko, G. Bavdek, M. Benes, and A. Morgante, 2001, “Order-disorder transition of the (3 × 3) Sn/Ge(111) phase,” *Phys. Rev. B* **64**, 075405.
- Fransson, J., D. Thonig, P. F. Bessarab, S. Bhattacharjee, J. Hellsvik, and L. Nordström, 2017, “Microscopic theory for coupled atomistic magnetization and lattice dynamics,” *Phys. Rev. Mater.* **1**, 074404.
- Frey, E., and F. Schwabl, 1994, “Critical dynamics of magnets,” *Adv. Phys.* **43**, 577–683.
- Frota-Pessôa, S., R. B. Muniz, and J. Kudrnovský, 2000, “Exchange coupling in transition-metal ferromagnets,” *Phys. Rev. B* **62**, 5293–5296.
- Fukutome, Hideo, 1981, “Unrestricted Hartree-Fock theory and its applications to molecules and chemical reactions,” *Int. J. Quantum Chem.* **20**, 955–1065.
- Fukuyama, Hiroshi, 2008, “Nuclear magnetism in two-dimensional solid helium three on graphite,” *J. Phys. Soc. Jpn.* **77**, 111013.
- Fulde, P., B. Schmidt, and P. Thalmeier, 1995, “Theoretical model for the semi-metal Yb₄As₃,” *Europhys. Lett.* **31**, 323.
- Furuno, T., K. Ando, S. Kunii, A. Ochiai, H. Suzuki, M. Fujioka, T. Suzuki, W. Sasaki, and T. Kasuya, 1988, “Physical properties of Sm₃Se₄ at low temperatures,” *J. Magn. Magn. Mater.* **76–77**, 117–118.
- Gatteschi, Dante, Andrea Caneschi, Luca Pardi, and Roberta Sessoli, 1994, “Large clusters of metal ions: The transition from molecular to bulk magnets,” *Science* **265**, 1054–1058.
- Gautier, F., F. Ducastelle, and J. Giner, 1975, “Ordering and segregation processes in transition metal alloys in relation to their electronic structures,” *Philos. Mag.* **31**, 1373–1390.
- Gautier, F., J. van der Rest, and F. Brouers, 1975, “Energy of formation, band structure and local environment effects in transitional binary alloys,” *J. Phys. F* **5**, 1884–1894.
- Gazit, Snir, Fakher F. Assaad, and Subir Sachdev, 2020, “Fermi Surface Reconstruction without Symmetry Breaking,” *Phys. Rev. X* **10**, 041057.
- Georges, Antoine, Gabriel Kotliar, Werner Krauth, and Marcelo J. Rozenberg, 1996, “Dynamical mean-field theory of strongly correlated fermion systems and the limit of infinite dimensions,” *Rev. Mod. Phys.* **68**, 13–125.
- Getzlaff, Mathias, 2008, “Magnetism in reduced dimensions—Nanoparticles,” in *Fundamentals of Magnetism* (Springer, New York), pp. 175–210.
- Ghosh, Ram Krishna, Ashna Jose, and Geetu Kumari, 2021, “Intrinsic spin-dynamical properties of two-dimensional half-metallic FeX₂ (X = Cl, Br, I) ferromagnets: Insight from density functional theory calculations,” *Phys. Rev. B* **103**, 054409.
- Gibertini, M., M. Koperski, A. F. Morpurgo, and K. S. Novoselov, 2019, “Magnetic 2D materials and heterostructures,” *Nat. Nanotechnol.* **14**, 408–419.
- Giner, J., J. van der Rest, F. Brouers, and F. Gautier, 1976, “Charge transfer and ordering energy in a model binary alloy,” *J. Phys. F* **6**, 1281–1296.
- Giuliani, G., and G. Vignale, 2005, *Quantum Theory of the Electron Liquid* (Cambridge University Press, Cambridge, England).
- Glass, S., G. Li, F. Adler, J. Aulbach, A. Fleszar, R. Thomale, W. Hanke, R. Claessen, and J. Schäfer, 2015, “Triangular Spin-Orbit-Coupled Lattice with Strong Coulomb Correlations: Sn Atoms on a SiC(0001) Substrate,” *Phys. Rev. Lett.* **114**, 247602.
- Gleeson, James P., 2013, “Binary-State Dynamics on Complex Networks: Pair Approximation and Beyond,” *Phys. Rev. X* **3**, 021004.
- Gong, Cheng, *et al.*, 2017, “Discovery of intrinsic ferromagnetism in two-dimensional van der Waals crystals,” *Nature (London)* **546**, 265–269.
- Gong, Qihua, Min Yi, Richard F. L. Evans, Bai-Xiang Xu, and Oliver Gutfleisch, 2019, “Calculating temperature-dependent properties of Nd₂Fe₁₄B permanent magnets by atomistic spin model simulations,” *Phys. Rev. B* **99**, 214409.
- Gonis, A., X. G. Zhang, A. J. Freeman, P. Turchi, G. M. Stocks, and D. M. Nicholson, 1987, “Configurational energies and effective cluster interactions in substitutionally disordered binary alloys,” *Phys. Rev. B* **36**, 4630–4646.
- Goodenough, John B., 1955, “Theory of the role of covalence in the perovskite-type manganites [La, M(II)]MnO₃,” *Phys. Rev.* **100**, 564–573.

- Goodenough, John B., 1963, “Magnetism and the chemical bond,” *J. Phys. Chem. Solids* **10**, 87, <https://cir.nii.ac.jp/crid/1130282269282379776>.
- Gorbatov, O. I., G. Johansson, A. Jakobsson, S. Mankovsky, H. Ebert, I. Di Marco, J. Minár, and C. Etz, 2021, “Magnetic exchange interactions in yttrium iron garnet: A fully relativistic first-principles investigation,” *Phys. Rev. B* **104**, 174401.
- Gorni, Tommaso, Iurii Timrov, and Stefano Baroni, 2018, “Spin dynamics from time-dependent density functional perturbation theory,” *Eur. Phys. J. B* **91**, 1–13.
- Goto, T., and B. Lüthi, 2003, “Charge ordering, charge fluctuations and lattice effects in strongly correlated electron systems,” *Adv. Phys.* **52**, 67–118.
- Grånäs, Oscar, Igor Di Marco, Patrik Thunström, Lars Nordström, Olle Eriksson, Torbjörn Björkman, and J. M. Wills, 2012, “Charge self-consistent dynamical mean-field theory based on the full-potential linear muffin-tin orbital method: Methodology and applications,” *Comput. Mater. Sci.* **55**, 295–302.
- Grytsiuk, Sergii, J.-P. Hanke, Markus Hoffmann, Juba Bouaziz, Olena Gomonyay, Gustav Bihlmayer, Samir Lounis, Yuriy Mokrousov, and Stefan Blügel, 2020, “Topological-chiral magnetic interactions driven by emergent orbital magnetism,” *Nat. Commun.* **11**, 511.
- Gukelberger, Jan, Evgeny Kozik, and Hartmut Hafermann, 2017, “Diagrammatic Monte Carlo approach for diagrammatic extensions of dynamical mean-field theory: Convergence analysis of the dual fermion technique,” *Phys. Rev. B* **96**, 035152.
- Gull, Emanuel, Andrew J. Millis, Alexander I. Lichtenstein, Alexey N. Rubtsov, Matthias Troyer, and Philipp Werner, 2011, “Continuous-time Monte Carlo methods for quantum impurity models,” *Rev. Mod. Phys.* **83**, 349–404.
- Guralnik, G. S., C. R. Hagen, and T. W. B. Kibble, 1964, “Global Conservation Laws and Massless Particles,” *Phys. Rev. Lett.* **13**, 585–587.
- Gutfleisch, Oliver, Matthew A. Willard, Ekkes Brück, Christina H. Chen, S. G. Sankar, and J. Ping Liu, 2011, “Magnetic materials and devices for the 21st century: Stronger, lighter, and more energy efficient,” *Adv. Mater.* **23**, 821–842.
- Gyorffy, B. L., A. J. Pindor, J. Staunton, G. M. Stocks, and H. Winter, 1985, “A first-principles theory of ferromagnetic phase transitions in metals,” *J. Phys. F* **15**, 1337–1386.
- Gyorffy, B. L., and G. M. Stocks, 1980, “Momentum distribution of electrons in concentrated random alloys,” *J. Phys. F* **10**, L321.
- Hafermann, H., G. Li, A. N. Rubtsov, M. I. Katsnelson, A. I. Lichtenstein, and H. Monien, 2009, “Efficient Perturbation Theory for Quantum Lattice Models,” *Phys. Rev. Lett.* **102**, 206401.
- Halilov, S. V., H. Eschrig, A. Y. Perlov, and P. M. Oppeneer, 1998, “Adiabatic spin dynamics from spin-density-functional theory: Application to Fe, Co, and Ni,” *Phys. Rev. B* **58**, 293–302.
- Hamann, D. R., 1967, “New solution for exchange scattering in dilute alloys,” *Phys. Rev.* **158**, 570–580.
- Han, Myung Joon, Taisuke Ozaki, and Jaeyun Yu, 2004, “Electronic structure, magnetic interactions, and the role of ligands in Mn_n ($n = 4, 12$) single-molecule magnets,” *Phys. Rev. B* **70**, 184421.
- Han, Myung Joon, Xiangang Wan, and Sergej Y. Savrasov, 2008, “Competition between Kondo and RKKY exchange couplings in $Pu_{1-x}Am_x$ alloys: Density functional theory with static Hartree-Fock and dynamic Hubbard-I approximations,” *Phys. Rev. B* **78**, 060401(R).
- Hansmann, P., R. Arita, A. Toschi, S. Sakai, G. Sangiovanni, and K. Held, 2010, “Dichotomy between Large Local and Small Ordered Magnetic Moments in Iron-Based Superconductors,” *Phys. Rev. Lett.* **104**, 197002.
- Hansmann, P., T. Ayrál, L. Vaugier, P. Werner, and S. Biermann, 2013, “Long-Range Coulomb Interactions in Surface Systems: A First-Principles Description within Self-Consistently Combined *GW* and Dynamical Mean-Field Theory,” *Phys. Rev. Lett.* **110**, 166401.
- Hansmann, Philipp, Loïg Vaugier, Hong Jiang, and Silke Biermann, 2013, “What about *U* on surfaces? Extended Hubbard models for adatom systems from first principles,” *J. Phys. Condens. Matter* **25**, 094005.
- Harkov, V., M. Vandelli, S. Brener, A. I. Lichtenstein, and E. A. Stepanov, 2021, “Impact of partially bosonized collective fluctuations on electronic degrees of freedom,” *Phys. Rev. B* **103**, 245123.
- Harland, Malte, Sergey Brener, Alexander I. Lichtenstein, and Mikhail I. Katsnelson, 2019, “Josephson lattice model for phase fluctuations of local pairs in copper oxide superconductors,” *Phys. Rev. B* **100**, 024510.
- Hasegawa, H., 1983, “A spin fluctuation theory of degenerate narrow bands-finite-temperature magnetism of iron,” *J. Phys. F* **13**, 1915–1929.
- Hasegawa, Hideo, 1979a, “Single-site functional-integral approach to itinerant-electron ferromagnetism,” *J. Phys. Soc. Jpn.* **46**, 1504–1514.
- Hasegawa, Hideo, 1979b, “Single-site functional-integral approach to itinerant-electron ferromagnetism,” *J. Phys. Soc. Jpn.* **46**, 1504–1514.
- Hasegawa, Hideo, 1980a, “Single-site spin fluctuation theory of itinerant-electron systems with narrow bands,” *J. Phys. Soc. Jpn.* **49**, 178–188.
- Hasegawa, Hideo, 1980b, “Single-site spin fluctuation theory of itinerant-electron systems with narrow bands. II. Iron and nickel,” *J. Phys. Soc. Jpn.* **49**, 963–971.
- Haydock, R., V. Heine, and M. J. Kelly, 1975, “Electronic structure based on the local atomic environment for tight-binding bands. II,” *J. Phys. C* **8**, 2591–2605.
- He, Xu, Nicole Helbig, Matthieu J. Verstraete, and Eric Bousquet, 2021, “TB2J: A PYTHON package for computing magnetic interaction parameters,” *Comput. Phys. Commun.* **264**, 107938.
- Hedin, Lars, 1965a, “New method for calculating the one-particle Green’s function with application to the electron-gas problem,” *Phys. Rev.* **139**, A796–A823.
- Hedin, Lars, 1965b, “New method for calculating the one-particle Green’s function with application to the electron-gas problem,” *Phys. Rev.* **139**, A796–A823.
- Heine, V., and J. H. Samson, 1983, “Magnetic, chemical and structural ordering in transition metals,” *J. Phys. F* **13**, 2155–2168.
- Heinze, Stefan, Kirsten von Bergmann, Matthias Menzel, Jens Brede, André Kubetzka, Roland Wiesendanger, Gustav Bihlmayer, and Stefan Blügel, 2011, “Spontaneous atomic-scale magnetic skyrmion lattice in two dimensions,” *Nat. Phys.* **7**, 713–718.
- Heisenberg, W., 1926, “Mehrkörperproblem und Resonanz in der Quantenmechanik,” *Z. Phys.* **38**, 411–427.
- Heitler, W., and F. London, 1927, “Wechselwirkung neutraler Atome und homöopolare Bindung nach der Quantenmechanik [Interaction of neutral atoms and homeopolar bonding according to quantum mechanics],” *Z. Phys.* **44**, 455–472.
- Hellsvik, Johan, Danny Thonig, Klas Modin, and Diana Iuşan, Anders Bergman, Olle Eriksson, Lars Bergqvist, and Anna Delin, 2019, “General method for atomistic spin-lattice dynamics with first-principles accuracy,” *Phys. Rev. B* **99**, 104302.
- Hennion, M., 1983, “Chemical SRO effects in ferromagnetic Fe alloys in relation to electronic band structure,” *J. Phys. F* **13**, 2351.

- Herbst, J. F., J. J. Croat, F. E. Pinkerton, and W. B. Yelon, 1984, "Relationships between crystal structure and magnetic properties in $\text{Nd}_2\text{Fe}_{14}\text{B}$," *Phys. Rev. B* **29**, 4176–4178.
- Hewson, A. C., 1993, *The Kondo Problem to Heavy Fermions* (Cambridge University Press, Cambridge, England).
- Higgs, P. W., 1964a, "Broken symmetries, massless particles and gauge fields," *Phys. Lett.* **12**, 132–133.
- Higgs, Peter W., 1964b, "Broken Symmetries and the Masses of Gauge Bosons," *Phys. Rev. Lett.* **13**, 508–509.
- Hirschmeier, Daniel, Hartmut Hafermann, Emanuel Gull, Alexander I. Lichtenstein, and Andrey E. Antipov, 2015, "Mechanisms of finite-temperature magnetism in the three-dimensional Hubbard model," *Phys. Rev. B* **92**, 144409.
- Hoffmann, M., J. Weischenberg, B. Dupé, F. Freimuth, P. Ferriani, Y. Mokrousov, and S. Heinze, 2015, "Topological orbital magnetization and emergent Hall effect of an atomic-scale spin lattice at a surface," *Phys. Rev. B* **92**, 020401(R).
- Hohenadler, M., F. Parisen Toldin, I. F. Herbut, and F. F. Assaad, 2014, "Phase diagram of the Kane-Mele-Coulomb model," *Phys. Rev. B* **90**, 085146.
- Hohenberg, P., and W. Kohn, 1964, "Inhomogeneous electron gas," *Phys. Rev.* **136**, B864–B871.
- Holley, Richard A., and Thomas M. Liggett, 1975, "Ergodic theorems for weakly interacting infinite systems and the voter model," *Ann. Probab.* **3**, 643–663.
- Honda, Y., Y. Kuramoto, and T. Watanabe, 1993, "Effects of cyclic four-spin exchange on the magnetic properties of the CuO_2 plane," *Phys. Rev. B* **47**, 11329–11336.
- Hong, Tao, *et al.*, 2017, "Higgs amplitude mode in a two-dimensional quantum antiferromagnet near the quantum critical point," *Nat. Phys.* **13**, 638–642.
- Huang, Bevin, *et al.*, 2017, "Layer-dependent ferromagnetism in a van der Waals crystal down to the monolayer limit," *Nature (London)* **546**, 270–273.
- Hubbard, J., 1959, "Calculation of Partition Functions," *Phys. Rev. Lett.* **3**, 77–78.
- Hubbard, J., 1979a, "The magnetism of iron," *Phys. Rev. B* **19**, 2626–2636.
- Hubbard, J., 1979b, "Magnetism of iron. II," *Phys. Rev. B* **20**, 4584–4595.
- Hubbard, J., 1981a, "The magnetism of iron and nickel," *J. Appl. Phys.* **52**, 1654–1657.
- Hubbard, J., 1981b, "Magnetism of nickel," *Phys. Rev. B* **23**, 5974–5977.
- Huebsch, M.-T., T. Nomoto, M.-T. Suzuki, and R. Arita, 2021, "Benchmark for *Ab Initio* Prediction of Magnetic Structures Based on Cluster-Multipole Theory," *Phys. Rev. X* **11**, 011031.
- Igarashi, R. N., A. B. Klautau, R. B. Muniz, B. Sanyal, and H. M. Petrilli, 2012, "First-principles studies of complex magnetism in Mn nanostructures on the $\text{Fe}(001)$ surface," *Phys. Rev. B* **85**, 014436.
- Igoshev, P. A., A. V. Efremov, and A. A. Katanin, 2015, "Magnetic exchange in α -iron from *ab initio* calculations in the paramagnetic phase," *Phys. Rev. B* **91**, 195123.
- Inomata, A., H. Kuratsui, and C. C. Gerry, 1992, *Path Integrals and Coherent States of $SU(2)$ and $SU(1,1)$* (World Scientific, Singapore).
- Inoue, Michiko, and Tôru Moriya, 1967, "Interaction between localized moments in metals," *Prog. Theor. Phys.* **38**, 41–60.
- Irkhin, V. Yu., A. A. Katanin, and M. I. Katsnelson, 1999, "Self-consistent spin-wave theory of layered Heisenberg magnets," *Phys. Rev. B* **60**, 1082–1099.
- Irkhin, V. Yu., and M. I. Katsnelson, 1990, "RVB-type states in systems with charge and spin degrees of freedom: Sm_3Se_4 , $\text{Y}_{1-x}\text{Sc}_x\text{Mn}_2$ etc.," *Phys. Lett. A* **150**, 47–50.
- Isaev, E. I., L. V. Pourovskii, A. M. N. Niklasson, Yu. Kh. Vekilov, B. Johansson, and I. A. Abrikosov, 2001, "Magnetic properties of a Co/Cu/Ni trilayer on the $\text{Cu}(100)$ surface," *Phys. Rev. B* **65**, 024435.
- Ising, Ernst, 1925, "Contribution to the theory of ferromagnetism," *Z. Phys.* **31**, 253–258.
- Iskakov, Sergei, Andrey E. Antipov, and Emanuel Gull, 2016, "Diagrammatic Monte Carlo for dual fermions," *Phys. Rev. B* **94**, 035102.
- Iskakov, Sergei, Hanna Terletska, and Emanuel Gull, 2018, "Momentum-space cluster dual-fermion method," *Phys. Rev. B* **97**, 125114.
- Itin, A. P., and M. I. Katsnelson, 2015, "Effective Hamiltonians for Rapidly Driven Many-Body Lattice Systems: Induced Exchange Interactions and Density-Dependent Hoppings," *Phys. Rev. Lett.* **115**, 075301.
- Itin, A. P., and A. I. Neishtadt, 2014, "Effective Hamiltonians for fastly driven tight-binding chains," *Phys. Lett. A* **378**, 822–825.
- Jaekel, Joerg, 2002, "Understanding the Fierz ambiguity of partially bosonized theories," [arXiv:hep-ph/0205154](https://arxiv.org/abs/hep-ph/0205154).
- Jaekel, Joerg, and Christof Wetterich, 2003, "Flow equations without mean field ambiguity," *Phys. Rev. D* **68**, 025020.
- Jain, A., *et al.*, 2017, "Higgs mode and its decay in a two-dimensional antiferromagnet," *Nat. Phys.* **13**, 633.
- Jakobsson, A., P. Mavropoulos, E. Şaşıoğlu, S. Blügel, M. Ležaić, B. Sanyal, and I. Galanakis, 2015, "First-principles calculations of exchange interactions, spin waves, and temperature dependence of magnetization in inverse-Heusler-based spin gapless semiconductors," *Phys. Rev. B* **91**, 174439.
- Jang, Seung Woo, Min Yong Jeong, Hongkee Yoon, Siheon Ryee, and Myung Joon Han, 2019, "Microscopic understanding of magnetic interactions in bilayer CrI_3 ," *Phys. Rev. Mater.* **3**, 031001.
- Jang, Seung Woo, Do Hoon Kiem, Juhyeok Lee, Yoon-Gu Kang, Hongkee Yoon, and Myung Joon Han, 2021, "Hund's physics and the magnetic ground state of CrOX ($X = \text{Cl}, \text{Br}$)," *Phys. Rev. Mater.* **5**, 034409.
- Jang, Seung Woo, Siheon Ryee, Hongkee Yoon, and Myung Joon Han, 2018, "Charge density functional plus U theory of LaMnO_3 : Phase diagram, electronic structure, and magnetic interaction," *Phys. Rev. B* **98**, 125126.
- Jang, Seung Woo, Hongkee Yoon, Min Yong Jeong, Siheon Ryee, Heung-Sik Kim, and Myung Joon Han, 2020, "Origin of ferromagnetism and the effect of doping on Fe_3GeTe_2 ," *Nanoscale* **12**, 13501–13506.
- Jaswal, S. S., 1990, "Electronic structure and magnetism of $R_2\text{Fe}_{14}\text{B}$ ($R = \text{Y}, \text{Nd}$) compounds," *Phys. Rev. B* **41**, 9697–9700.
- Jensen, Jens, and Allan R. Mackintosh, 1991, *Rare Earth Magnetism* (Clarendon Press, Oxford).
- Jodlauk, S., P. Becker, J. A. Mydosh, D. I. Khomskii, T. Lorenz, S. V. Streltsov, D. C. Hezel, and L. Bohatý, 2007, "Pyroxenes: A new class of multiferroics," *J. Phys. Condens. Matter* **19**, 432201.
- Kadanoff, L. P., and G. Baym, 1962, *Quantum Statistical Mechanics: Green's Function Methods in Equilibrium and Nonequilibrium Problems*, 1st ed. (CRC Press, Boca Raton).
- Kakehashi, Y., 1992, "Monte Carlo approach to the dynamical coherent-potential approximation in metallic magnetism," *Phys. Rev. B* **45**, 7196–7204.
- Kamber, Umut, *et al.*, 2020, "Self-induced spin glass state in elemental and crystalline neodymium," *Science* **368**, eaay6757.

- Kamenev, Alex, 2011, *Field Theory of Non-Equilibrium Systems* (Cambridge University Press, Cambridge, England).
- Kampert, Erik, *et al.*, 2009, “Ligand-controlled magnetic interactions in Mn_4 clusters,” *Inorg. Chem.* **48**, 11903–11908.
- Kanamori, Junjiro, 1959, “Superexchange interaction and symmetry properties of electron orbitals,” *J. Phys. Chem. Solids* **10**, 87–98.
- Kashin, I. V., V. V. Mazurenko, M. I. Katsnelson, and A. N. Rudenko, 2020, “Orbitally-resolved ferromagnetism of monolayer CrI_3 ,” *2D Mater.* **7**, 025036.
- Katsnelson, M. I., and V. P. Antropov, 2003, “Spin angular gradient approximation in the density functional theory,” *Phys. Rev. B* **67**, 140406.
- Katsnelson, M. I., Y. O. Kvashnin, V. V. Mazurenko, and A. I. Lichtenstein, 2010, “Correlated band theory of spin and orbital contributions to Dzyaloshinskii-Moriya interactions,” *Phys. Rev. B* **82**, 100403.
- Katsnelson, M. I., and A. I. Lichtenstein, 2000, “First-principles calculations of magnetic interactions in correlated systems,” *Phys. Rev. B* **61**, 8906–8912.
- Katsnelson, M. I., and A. I. Lichtenstein, 2004, “Magnetic susceptibility, exchange interactions and spin-wave spectra in the local spin density approximation,” *J. Phys. Condens. Matter* **16**, 7439–7446.
- Katsnelson, M. I., V. Yu. Irkhin, L. Chioncel, A. I. Lichtenstein, and R. A. de Groot, 2008, “Half-metallic ferromagnets: From band structure to many-body effects,” *Rev. Mod. Phys.* **80**, 315–378.
- Ke, Liqin, and Mikhail I. Katsnelson, 2021, “Electron correlation effects on exchange interactions and spin excitations in 2D van der Waals materials,” *npj Comput. Mater.* **7**, 4.
- Keshavarz, S., Y. O. Kvashnin, I. Di Marco, A. Delin, M. I. Katsnelson, A. I. Lichtenstein, and O. Eriksson, 2015, “Layer-resolved magnetic exchange interactions of surfaces of late $3d$ elements: Effects of electronic correlations,” *Phys. Rev. B* **92**, 165129.
- Keshavarz, Samara, Johan Schött, Andrew J. Millis, and Yaroslav O. Kvashnin, 2018, “Electronic structure, magnetism, and exchange integrals in transition-metal oxides: Role of the spin polarization of the functional in DFT + U calculations,” *Phys. Rev. B* **97**, 184404.
- Khmelevskiy, S., T. Khmelevska, A. V. Ruban, and P. Mohn, 2007, “Magnetic exchange interactions in the paramagnetic state of hcp Gd,” *J. Phys. Condens. Matter* **19**, 326218.
- Khmelevskiy, Sergii, 2012, “Antiferromagnetic ordering on the frustrated fcc lattice in the intermetallic compound $GdPtBi$,” *Phys. Rev. B* **86**, 104429.
- Khmelevskiy, Sergii, Eszter Simon, and László Szunyogh, 2015, “Antiferromagnetism in Ru_2MnZ ($Z = Sn, Sb, Ge, Si$) full Heusler alloys: Effects of magnetic frustration and chemical disorder,” *Phys. Rev. B* **91**, 094432.
- Kirilyuk, Andrei, Alexey V. Kimel, and Theo Rasing, 2010, “Ultrafast optical manipulation of magnetic order,” *Rev. Mod. Phys.* **82**, 2731–2784.
- Kitaev, Alexei, 2006, “Anyons in an exactly solved model and beyond,” *Ann. Phys. (Amsterdam)* **321**, 2–111.
- Kitamura, Sota, and Hideo Aoki, 2016, “ η -pairing superfluid in periodically-driven fermionic Hubbard model with strong attraction,” *Phys. Rev. B* **94**, 174503.
- Kleinman, Leonard, 1999, “Density functional for noncollinear magnetic systems,” *Phys. Rev. B* **59**, 3314–3317.
- Kohn, W., and N. Rostoker, 1954, “Solution of the Schrödinger equation in periodic lattices with an application to metallic lithium,” *Phys. Rev.* **94**, 1111–1120.
- Kohn, W., and L. J. Sham, 1965, “Self-consistent equations including exchange and correlation effects,” *Phys. Rev.* **140**, A1133–A1138.
- Korenman, V., J. L. Murray, and R. E. Prange, 1977a, “Local-band theory of itinerant ferromagnetism. I. Fermi-liquid theory,” *Phys. Rev. B* **16**, 4032–4047.
- Korenman, V., J. L. Murray, and R. E. Prange, 1977b, “Local-band theory of itinerant ferromagnetism. II. Spin waves,” *Phys. Rev. B* **16**, 4048–4057.
- Korenman, V., J. L. Murray, and R. E. Prange, 1977c, “Local-band theory of itinerant ferromagnetism. III. Nonlinear Landau-Lifshitz equations,” *Phys. Rev. B* **16**, 4058–4062.
- Korotin, Dm. M., V. V. Mazurenko, V. I. Anisimov, and S. V. Streltsov, 2015, “Calculation of exchange constants of the Heisenberg model in plane-wave-based methods using the Green’s function approach,” *Phys. Rev. B* **91**, 224405.
- Korringa, J., 1947, “On the calculation of the energy of a Bloch wave in a metal,” *Physica (Amsterdam)* **13**, 392–400.
- Korzavyi, P. A., A. V. Ruban, J. Odqvist, J.-O. Nilsson, and B. Johansson, 2009, “Electronic structure and effective chemical and magnetic exchange interactions in bcc Fe-Cr alloys,” *Phys. Rev. B* **79**, 054202.
- Kotani, Takao, and Mark van Schilfgaarde, 2008, “Spin wave dispersion based on the quasiparticle self-consistent GW method: NiO, MnO and α -MnAs,” *J. Phys. Condens. Matter* **20**, 295214.
- Kotliar, G., S. Y. Savrasov, K. Haule, V. S. Oudovenko, O. Parcollet, and C. A. Marianetti, 2006, “Electronic structure calculations with dynamical mean-field theory,” *Rev. Mod. Phys.* **78**, 865–951.
- Kramers, H. A., 1934, “L’interaction entre les atomes magnétogènes dans un cristal paramagnétique [The interaction between magnetic atoms in a paramagnetic crystal],” *Physica (Amsterdam)* **1**, 182–192.
- Krönlein, Andreas, *et al.*, 2018, “Magnetic Ground State Stabilized by Three-Site Interactions: Fe/Rh(111),” *Phys. Rev. Lett.* **120**, 207202.
- Kruglyak, V. V., S. O. Demokritov, and D. Grundler, 2010, “Magnonics,” *J. Phys. D* **43**, 264001.
- Kübler, J., K.-H. Hock, J. Sticht, and A. R. Williams, 1988, “Density functional theory of non-collinear magnetism,” *J. Phys. F* **18**, 469.
- Kübler, Jürgen, 2017, *Theory of Itinerant Electron Magnetism*, International Series of Monographs on Physics Vol. 106 (Oxford University Press, New York).
- Kudrnovský, J., V. Drchal, and P. Bruno, 2008, “Magnetic properties of fcc Ni-based transition metal alloys,” *Phys. Rev. B* **77**, 224422.
- Kudrnovský, Josef, František Máca, Ilja Turek, and Josef Redinger, 2009, “Substrate-induced antiferromagnetism of a Fe monolayer on the Ir(001) surface,” *Phys. Rev. B* **80**, 064405.
- Kurtulus, Yasemin, Richard Dronskowski, German D. Samolyuk, and Vladimir P. Antropov, 2005, “Electronic structure and magnetic exchange coupling in ferromagnetic full Heusler alloys,” *Phys. Rev. B* **71**, 014425.
- Kvashnin, Y. O., A. Bergman, A. I. Lichtenstein, and M. I. Katsnelson, 2020, “Relativistic exchange interactions in CrX_3 ($X = Cl, Br, I$) monolayers,” *Phys. Rev. B* **102**, 115162.
- Kvashnin, Y. O., R. Cardias, A. Szilva, I. Di Marco, M. I. Katsnelson, A. I. Lichtenstein, L. Nordström, A. B. Klautau, and O. Eriksson, 2016, “Microscopic Origin of Heisenberg and Non-Heisenberg Exchange Interactions in Ferromagnetic bcc Fe,” *Phys. Rev. Lett.* **116**, 217202.
- Kvashnin, Y. O., O. Grånäs, I. Di Marco, M. I. Katsnelson, A. I. Lichtenstein, and O. Eriksson, 2015, “Exchange parameters of strongly correlated materials: Extraction from spin-polarized density functional theory plus dynamical mean-field theory,” *Phys. Rev. B* **91**, 125133.
- Kvashnin, Y. O., S. Khmelevskiy, J. Kudrnovský, A. N. Yaresko, L. Genovese, and P. Bruno, 2012, “Noncollinear magnetic ordering in

- compressed FePd₃ ordered alloy: A first principles study,” *Phys. Rev. B* **86**, 174429.
- Kvashnin, Y. O., W. Sun, I. Di Marco, and O. Eriksson, 2015, “Electronic topological transition and noncollinear magnetism in compressed hcp Co,” *Phys. Rev. B* **92**, 134422.
- Lacour-Gayet, P., and M. Cyrot, 1974, “Magnetic properties of the Hubbard model,” *J. Phys. C* **7**, 400.
- Landau, L. D., and E. M. Lifshitz, 1980, *Statistical Physics* (Pergamon, Oxford).
- Lebègue, S., T. Björkman, M. Klintonberg, R. M. Nieminen, and O. Eriksson, 2013, “Two-Dimensional Materials from Data Filtering and *Ab Initio* Calculations,” *Phys. Rev. X* **3**, 031002.
- Lee, Inhee, Franz G. Utermohlen, Daniel Weber, Kyusung Hwang, Chi Zhang, Johan van Tol, Joshua E. Goldberger, Nandini Trivedi, and P. Chris Hammel, 2020, “Fundamental Spin Interactions Underlying the Magnetic Anisotropy in the Kitaev Ferromagnet CrI₃,” *Phys. Rev. Lett.* **124**, 017201.
- Leonov, I., A. N. Yaresko, V. N. Antonov, U. Schwingenschlögl, V. Eyert, and V. I. Anisimov, 2006, “Charge order and spin-singlet pair formation in Ti₄O₇,” *J. Phys. Condens. Matter* **18**, 10955.
- Ležaić, M., Ph. Mavropoulos, and S. Blügel, 2007, “First-principles prediction of high Curie temperature for ferromagnetic bcc-Co and bcc-FeCo alloys and its relevance to tunneling magnetoresistance,” *Appl. Phys. Lett.* **90**, 082504.
- Li, Gang, 2015, “Hidden physics in the dual-fermion approach: A special case of a nonlocal expansion scheme,” *Phys. Rev. B* **91**, 165134.
- Li, Gang, Philipp Höpfner, Jörg Schäfer, Christian Blumenstein, Sebastian Meyer, Aaron Bostwick, Eli Rotenberg, Ralph Claessen, and Werner Hanke, 2013, “Magnetic order in a frustrated two-dimensional atom lattice at a semiconductor surface,” *Nat. Commun.* **4**, 1620.
- Li, Gang, Manuel Laubach, Andrzej Fleszar, and Werner Hanke, 2011, “Geometrical frustration and the competing phases of the Sn/Si(111) $\sqrt{3} \times \sqrt{3}R30^\circ$ surface systems,” *Phys. Rev. B* **83**, 041104(R).
- Li, Tingxin, *et al.*, 2019, “Pressure-controlled interlayer magnetism in atomically thin CrI₃,” *Nat. Mater.* **18**, 1303–1308.
- Lichtenstein, A. I., and M. I. Katsnelson, 1998, “*Ab initio* calculations of quasiparticle band structure in correlated systems: LDA ++ approach,” *Phys. Rev. B* **57**, 6884–6895.
- Lichtenstein, A. I., and M. I. Katsnelson, 2000, “Antiferromagnetism and *d*-wave superconductivity in cuprates: A cluster dynamical mean-field theory,” *Phys. Rev. B* **62**, R9283–R9286.
- Lichtenstein, A. I., and M. I. Katsnelson, 2001, “Magnetism of correlated systems: Beyond LDA,” in *Band-Ferromagnetism*, edited by Klaus Baberschke, Wolfgang Nolting, and Markus Donath (Springer, Berlin), pp. 75–93.
- Lichtenstein, A. I., V. I. Anisimov, and J. Zaanen, 1995, “Density-functional theory and strong interactions: Orbital ordering in Mott-Hubbard insulators,” *Phys. Rev. B* **52**, R5467–R5470.
- Lichtenstein, A. I., M. I. Katsnelson, V. P. Antropov, and V. A. Gubanov, 1987, “Local spin density functional approach to the theory of exchange interactions in ferromagnetic metals and alloys,” *J. Magn. Magn. Mater.* **67**, 65–74.
- Lichtenstein, A. I., M. I. Katsnelson, and V. A. Gubanov, 1984, “Exchange interactions and spin-wave stiffness in ferromagnetic metals,” *J. Phys. F* **14**, L125.
- Lichtenstein, A. I., M. I. Katsnelson, and V. A. Gubanov, 1985, “Local spin excitations and Curie temperature of iron,” *Solid State Commun.* **54**, 327–329.
- Liu, K. L., and S. H. Vosko, 1989, “A time-dependent spin density functional theory for the dynamical spin susceptibility,” *Can. J. Phys.* **67**, 1015–1021.
- Liu, S. H., 1961, “Exchange interaction between conduction electrons and magnetic shell electrons in rare-earth metals,” *Phys. Rev.* **121**, 451–455.
- Liu, X., M. M. Steiner, R. Sooryakumar, G. A. Prinz, R. F. C. Farrow, and G. Harp, 1996, “Exchange stiffness, magnetization, and spin waves in cubic and hexagonal phases of cobalt,” *Phys. Rev. B* **53**, 12166–12172.
- Liu, X. B., and Z. Altounian, 2010, “Exchange interaction in GdT₂ (*T* = Fe, Co, Ni) from first-principles,” *J. Appl. Phys.* **107**, 09E117.
- Liu, Y., S. K. Bose, and J. Kudrnovský, 2010, “First-principles theoretical studies of half-metallic ferromagnetism in CrTe,” *Phys. Rev. B* **82**, 094435.
- Lloyd, P., 1967, “Wave propagation through an assembly of spheres: II. The density of single-particle eigenstates,” *Proc. Phys. Soc. London* **90**, 207.
- Lobo, J., A. Tejada, A. Mugarza, and E. G. Michel, 2003, “Electronic structure of Sn/Si(111) – ($\sqrt{3} \times \sqrt{3}$)R30° as a function of Sn coverage,” *Phys. Rev. B* **68**, 235332.
- Locht, I. L. M., *et al.*, 2016, “Standard model of the rare earths analyzed from the Hubbard I approximation,” *Phys. Rev. B* **94**, 085137.
- Logemann, R., A. N. Rudenko, M. I. Katsnelson, and A. Kirilyuk, 2017, “Exchange interactions in transition metal oxides: The role of oxygen spin polarization,” *J. Phys. Condens. Matter* **29**, 335801.
- Logemann, R., A. N. Rudenko, M. I. Katsnelson, and A. Kirilyuk, 2018, “Non-Heisenberg covalent magnetism in iron oxide clusters,” *Phys. Rev. Mater.* **2**, 073001.
- Lorenzana, J., J. Eroles, and S. Sorella, 1999, “Does the Heisenberg Model Describe the Multimagnon Spin Dynamics in Antiferromagnetic CuO Layers?,” *Phys. Rev. Lett.* **83**, 5122–5125.
- Lounis, S., A. T. Costa, R. B. Muniz, and D. L. Mills, 2010, “Dynamical Magnetic Excitations of Nanostructures from First Principles,” *Phys. Rev. Lett.* **105**, 187205.
- Lounis, Samir, and Peter H. Dederichs, 2010, “Mapping the magnetic exchange interactions from first principles: Anisotropy anomaly and application to Fe, Ni, and Co,” *Phys. Rev. B* **82**, 180404.
- Luttinger, J. M., and J. C. Ward, 1960, “Ground-state energy of a many-fermion system. II,” *Phys. Rev.* **118**, 1417–1427.
- MacDonald, A. H., S. M. Girvin, and D. Yoshioka, 1988, “*t/U* expansion for the Hubbard model,” *Phys. Rev. B* **37**, 9753–9756.
- Mackintosh, A. R., and O. K. Andersen, 1980, *Electrons at the Fermi Surface* (Cambridge University Press, London).
- MacLaren, J. M., T. C. Schulthess, W. H. Butler, Roberta Sutton, and Michael McHenry, 1999, “Electronic structure, exchange interactions, and Curie temperature of FeCo,” *J. Appl. Phys.* **85**, 4833–4835.
- Mahan, G. D., 2000, *Many-Particle Physics* (Springer Science+Business Media, New York).
- Mankovsky, S., S. Bornemann, J. Minár, S. Polesya, H. Ebert, J. B. Staunton, and A. I. Lichtenstein, 2009, “Effects of spin-orbit coupling on the spin structure of deposited transition-metal clusters,” *Phys. Rev. B* **80**, 014422.
- Mankovsky, S., and H. Ebert, 2017, “Accurate scheme to calculate the interatomic Dzyaloshinskii-Moriya interaction parameters,” *Phys. Rev. B* **96**, 104416.
- Mankovsky, S., S. Polesya, and H. Ebert, 2020a, “Exchange coupling constants at finite temperature,” *Phys. Rev. B* **102**, 134434.
- Mankovsky, S., S. Polesya, and H. Ebert, 2020b, “Extension of the standard Heisenberg Hamiltonian to multispin exchange interactions,” *Phys. Rev. B* **101**, 174401.

- Mankovsky, Sergiy, Svitlana Polesya, Hannah Lange, Markus Weißenhofer, Ulrich Nowak, and Hubert Ebert, 2022, “Angular Momentum Transfer via Relativistic Spin-Lattice Coupling from First Principles,” *Phys. Rev. Lett.* **129**, 067202.
- Mannini, Matteo, *et al.*, 2009, “Magnetic memory of a single-molecule quantum magnet wired to a gold surface,” *Nat. Mater.* **8**, 194–197.
- Marzari, Nicola, Arash A. Mostofi, Jonathan R. Yates, Ivo Souza, and David Vanderbilt, 2012, “Maximally localized Wannier functions: Theory and applications,” *Rev. Mod. Phys.* **84**, 1419–1475.
- Mazurenko, V. V., and V. I. Anisimov, 2005, “Weak ferromagnetism in antiferromagnets: α -Fe₂O₃ and La₂CuO₄,” *Phys. Rev. B* **71**, 184434.
- Mazurenko, V. V., S. N. Isakov, A. N. Rudenko, I. V. Kashin, O. M. Sotnikov, M. V. Valentyuk, and A. I. Lichtenstein, 2013, “Correlation effects in insulating surface nanostructures,” *Phys. Rev. B* **88**, 085112.
- Mazurenko, V. V., Y. O. Kvashnin, Fengping Jin, H. A. De Raedt, A. I. Lichtenstein, and M. I. Katsnelson, 2014, “First-principles modeling of magnetic excitations in Mn₁₂,” *Phys. Rev. B* **89**, 214422.
- Mazurenko, V. V., F. Mila, and V. I. Anisimov, 2006, “Electronic structure and exchange interactions of Na₂V₃O₇,” *Phys. Rev. B* **73**, 014418.
- Mazurenko, V. V., A. N. Rudenko, S. A. Nikolaev, D. S. Medvedeva, A. I. Lichtenstein, and M. I. Katsnelson, 2016, “Role of direct exchange and Dzyaloshinskii-Moriya interactions in magnetic properties of graphene derivatives: C₂F and C₂H,” *Phys. Rev. B* **94**, 214411.
- Mazurenko, V. V., S. L. Skornyakov, V. I. Anisimov, and F. Mila, 2008, “First-principles investigation of symmetric and antisymmetric exchange interactions of SrCu₂(BO₃)₂,” *Phys. Rev. B* **78**, 195110.
- Mazurenko, V. V., S. L. Skornyakov, A. V. Kozhevnikov, F. Mila, and V. I. Anisimov, 2007, “Wannier functions and exchange integrals: The example of LiCu₂O₂,” *Phys. Rev. B* **75**, 224408.
- Mello, Isys F., Lucas Squillante, Gabriel O. Gomes, Antonio C. Seridonio, and Mariano de Souza, 2021, “Epidemics, the Ising-model and percolation theory: A comprehensive review focused on COVID-19,” *Physica (Amsterdam)* **573A**, 125963.
- Melnikov, A., I. Radu, U. Bovensiepen, O. Krupin, K. Starke, E. Matthias, and M. Wolf, 2003, “Coherent Optical Phonons and Parametrically Coupled Magnons Induced by Femtosecond Laser Excitation of the Gd(0001) Surface,” *Phys. Rev. Lett.* **91**, 227403.
- Meng, Y., Kh. Zakeri, A. Ernst, T.-H. Chuang, H. J. Qin, Y.-J. Chen, and J. Kirschner, 2014, “Direct evidence of antiferromagnetic exchange interaction in Fe(001) films: Strong magnon softening at the high-symmetry \bar{M} point,” *Phys. Rev. B* **90**, 174437.
- Mentink, J. H., 2017, “Manipulating magnetism by ultrafast control of the exchange interaction,” *J. Phys. Condens. Matter* **29**, 453001.
- Mentink, J. H., Karsten Balzer, and Martin Eckstein, 2015, “Ultrafast and reversible control of the exchange interaction in Mott insulators,” *Nat. Commun.* **6**, 6708.
- Merchant, P., B. Normand, K. W. Krämer, M. Boehm, D. F. McMorrow, and Ch. Rüegg, 2014, “Quantum and classical criticality in a dimerized quantum antiferromagnet,” *Nat. Phys.* **10**, 373–379.
- Mermin, N. D., and H. Wagner, 1966, “Absence of Ferromagnetism or Antiferromagnetism in One- or Two-Dimensional Isotropic Heisenberg Models,” *Phys. Rev. Lett.* **17**, 1133–1136.
- Mermin, N. David., 1965, “Thermal properties of the inhomogeneous electron gas,” *Phys. Rev.* **137**, A1441–A1443.
- Methfessel, M., and J. Kübler, 1982, “Bond analysis of heats of formation: Application to some group VIII and IB hydrides,” *J. Phys. F* **12**, 141–161.
- Mézard, Marc, Giorgio Parisi, and Miguel Angel Virasoro, 1987, *Spin Glass Theory and Beyond: An Introduction to the Replica Method and Its Applications*, Vol. 9 (World Scientific, Singapore).
- Mikhaylovskiy, R. V., *et al.*, 2015, “Ultrafast optical modification of exchange interactions in iron oxides,” *Nat. Commun.* **6**, 8190.
- Modesti, S., L. Petaccia, G. Ceballos, I. Vobornik, G. Panaccione, G. Rossi, L. Ottaviano, R. Larciprete, S. Lizzit, and A. Goldoni, 2007, “Insulating Ground State of Sn/Si(111) – ($\sqrt{3} \times \sqrt{3}$)R30°,” *Phys. Rev. Lett.* **98**, 126401.
- Mohn, P., and K. Schwarz, 1993, “Supercell calculations for transition metal impurities in palladium,” *J. Phys. Condens. Matter* **5**, 5099.
- Mohn, Peter, 2006, *Magnetism in the Solid State: An Introduction*, Springer Series in Solid-State Sciences Vol. 134 (Springer Science+Business Media, New York).
- Monnier, R., 1997, “First-principles approaches to surface segregation,” *Philos. Mag. B* **75**, 67–144.
- Mook, H. A., J. W. Lynn, and R. M. Nicklow, 1973, “Temperature Dependence of the Magnetic Excitations in Nickel,” *Phys. Rev. Lett.* **30**, 556–559.
- Mook, H. A., and D. McK. Paul, 1985, “Neutron-Scattering Measurement of the Spin-Wave Spectra for Nickel,” *Phys. Rev. Lett.* **54**, 227–229.
- Moon, S. J., *et al.*, 2008, “Dimensionality-Controlled Insulator-Metal Transition and Correlated Metallic State in 5d Transition Metal Oxides Sr_{n+1}Ir_nO_{3n+1} ($n = 1, 2$, and ∞),” *Phys. Rev. Lett.* **101**, 226402.
- Morán, S., C. Ederer, and M. Fähnle, 2003, “*Ab initio* electron theory for magnetism in Fe: Pressure dependence of spin-wave energies, exchange parameters, and Curie temperature,” *Phys. Rev. B* **67**, 012407.
- Moriya, T., 1981, Ed., *Magnetism in Narrow Band System*, Springer Series in Solid-State Sciences Vol. 29 (Springer, Berlin), pp. 2197–4179.
- Moriya, Toru, 2012, *Spin Fluctuations in Itinerant Electron Magnetism*, Springer Series in Solid-State Sciences Vol. 56 (Springer Science+Business Media, New York).
- Mott, N. F., 1974, *Metal-Insulator Transitions* (Taylor & Francis, London).
- Mryasov, O. N., A. I. Liechtenstein, L. M. Sandratskii, and V. A. Gubanov, 1991, “Magnetic structure of fcc iron,” *J. Phys. Condens. Matter* **3**, 7683–7690.
- Mryasov, Oleg N., 2004, “Magnetic interactions in 3d-5d layered ferromagnets,” *J. Magn. Magn. Mater.* **272–276**, 800–801.
- Mryasov, Oleg N., 2005, “Magnetic interactions and phase transformations in FeM, $M = (\text{Pt, Rh})$ ordered alloys,” *Phase Transitions* **78**, 197–208.
- Muniz, R. B., and D. L. Mills, 2002, “Theory of spin excitations in Fe(110) monolayers,” *Phys. Rev. B* **66**, 174417.
- Ney, A., F. Wilhelm, M. Farle, P. Pouloupoulos, P. Srivastava, and K. Baberschke, 1999, “Oscillations of the Curie temperature and interlayer exchange coupling in magnetic trilayers,” *Phys. Rev. B* **59**, R3938–R3940.
- Niklasson, Anders M. N., John M. Wills, Mikhail I. Katsnelson, Igor A. Abrikosov, Olle Eriksson, and Börje Johansson, 2003, “Modeling the actinides with disordered local moments,” *Phys. Rev. B* **67**, 235105.
- Nordström, L., B. Johansson, and M. S. S. Brooks, 1993, “Calculation of the electronic structure and the magnetic moments of Nd₂Fe₁₄B,” *J. Phys. Condens. Matter* **5**, 7859.

- Nordström, L., and A. Mavromaras, 2000, “Magnetic ordering of the heavy rare earths,” *Europhys. Lett.* **49**, 775.
- Nordström, Lars, and David J. Singh, 1996, “Noncollinear Intra-atomic Magnetism,” *Phys. Rev. Lett.* **76**, 4420–4423.
- Norman, M. R., 2016, “Colloquium: Herbertsmithite and the search for the quantum spin liquid,” *Rev. Mod. Phys.* **88**, 041002.
- Oguchi, T., K. Terakura, and A. R. Williams, 1983, “Band theory of the magnetic interaction in MnO, MnS, and NiO,” *Phys. Rev. B* **28**, 6443–6452.
- Oguchi, Tamio, Kiyoyuki Terakura, and Noriaki Hamada, 1983, “Magnetism of iron above the Curie temperature,” *J. Phys. F* **13**, 145.
- Otsuki, Junya, Kazuyoshi Yoshimi, Hiroshi Shinaoka, and Yusuke Nomura, 2019, “Strong-coupling formula for momentum-dependent susceptibilities in dynamical mean-field theory,” *Phys. Rev. B* **99**, 165134.
- Owerre, S. A., 2017, “Topological thermal Hall effect in frustrated Kagome antiferromagnets,” *Phys. Rev. B* **95**, 014422.
- Pachos, Jiannis K., and Martin B. Plenio, 2004, “Three-Spin Interactions in Optical Lattices and Criticality in Cluster Hamiltonians,” *Phys. Rev. Lett.* **93**, 056402.
- Pajda, M., J. Kudrnovský, I. Turek, V. Drchal, and P. Bruno, 2000, “Oscillatory Curie Temperature of Two-Dimensional Ferromagnets,” *Phys. Rev. Lett.* **85**, 5424–5427.
- Pajda, M., J. Kudrnovský, I. Turek, V. Drchal, and P. Bruno, 2001, “*Ab initio* calculations of exchange interactions, spin-wave stiffness constants, and Curie temperatures of Fe, Co, and Ni,” *Phys. Rev. B* **64**, 174402.
- Paki, Joseph, Hanna Terletska, Sergei Isakov, and Emanuel Gull, 2019, “Charge order and antiferromagnetism in the extended Hubbard model,” *Phys. Rev. B* **99**, 245146.
- Panda, S. K., Y. O. Kvashnin, B. Sanyal, I. Dasgupta, and O. Eriksson, 2016, “Electronic structure and exchange interactions of insulating double perovskite $\text{La}_2\text{CuRuO}_6$,” *Phys. Rev. B* **94**, 064427.
- Park, Kyungwha, Mark R. Pederson, and C. Stephen Hellberg, 2004, “Properties of low-lying excited manifolds in Mn_{12} acetate,” *Phys. Rev. B* **69**, 014416.
- Paul, Souvik, Soumyajyoti Haldar, Stephan von Malottki, and Stefan Heinze, 2020, “Role of higher-order exchange interactions for skyrmion stability,” *Nat. Commun.* **11**, 1–12.
- Pauthenet, R., 1982, “Experimental verification of spin-wave theory in high fields,” *J. Appl. Phys.* **53**, 8187–8192.
- Peierls, R., 1938, “On a minimum property of the free energy,” *Phys. Rev.* **54**, 918–919.
- Pekker, David, and C. M. Varma, 2015, “Amplitude/Higgs modes in condensed matter physics,” *Annu. Rev. Condens. Matter Phys.* **6**, 269–297.
- Peralta, Juan E., Gustavo E. Scuseria, and Michael J. Frisch, 2007, “Noncollinear magnetism in density functional calculations,” *Phys. Rev. B* **75**, 125119.
- Pereiro, Manuel, Dmitry Yudin, Jonathan Chico, Corina Etz, Olle Eriksson, and Anders Bergman, 2014, “Topological excitations in a Kagome magnet,” *Nat. Commun.* **5**, 4815.
- Perlov, A. Y., S. V. Halilov, and H. Eschrig, 2000, “Rare-earth magnetism and adiabatic magnon spectra,” *Phys. Rev. B* **61**, 4070–4081.
- Peronaci, Francesco, Olivier Parcollet, and Marco Schiró, 2020, “Enhancement of local pairing correlations in periodically driven Mott insulators,” *Phys. Rev. B* **101**, 161101(R).
- Peters, L., I. Di Marco, P. Thunström, M. I. Katsnelson, A. Kirilyuk, and O. Eriksson, 2014, “Treatment of $4f$ states of the rare earths: The case study of TbN,” *Phys. Rev. B* **89**, 205109.
- Peters, L., E. G. C. P. van Loon, A. N. Rubtsov, A. I. Lichtenstein, M. I. Katsnelson, and E. A. Stepanov, 2019, “Dual boson approach with instantaneous interaction,” *Phys. Rev. B* **100**, 165128.
- Pariseau, Pierre, and B. L. Gyorffy, 2012, Eds., *Electrons in Disordered Metals and at Metallic Surfaces*, NATO Advanced Study Institutes, Ser. B, Vol. 42 (Springer Science+Business Media, New York).
- Pickart, S. J., H. A. Alperin, V. J. Minkiewicz, R. Nathans, G. Shirane, and O. Steinsvoll, 1967, “Spin-wave dispersion in ferromagnetic Ni and fcc Co,” *Phys. Rev.* **156**, 623–626.
- Pindor, A. J., J. Staunton, G. M. Stocks, and H. Winter, 1983, “Disordered local moment state of magnetic transition metals: A self-consistent KKR CPA calculation,” *J. Phys. F* **13**, 979–989.
- Pittalis, S., C. R. Proetto, A. Floris, A. Sanna, C. Bersier, K. Burke, and E. K. U. Gross, 2011, “Exact Conditions in Finite-Temperature Density-Functional Theory,” *Phys. Rev. Lett.* **107**, 163001.
- Polesya, S., S. Mankovsky, D. Ködderitzsch, J. Minár, and H. Ebert, 2016, “Finite-temperature magnetism of FeRh compounds,” *Phys. Rev. B* **93**, 024423.
- Polesya, S., S. Mankovsky, O. Siper, W. Meindl, C. Strunk, and H. Ebert, 2010, “Finite-temperature magnetism of $\text{Fe}_x\text{Pd}_{1-x}$ and $\text{Co}_x\text{Pt}_{1-x}$ alloys,” *Phys. Rev. B* **82**, 214409.
- Poluektov, Mikhail, Olle Eriksson, and Gunilla Kreiss, 2016, “Scale transitions in magnetisation dynamics,” *Commun. Comput. Phys.* **20**, 969–988.
- Poluektov, Mikhail, Olle Eriksson, and Gunilla Kreiss, 2018, “Coupling atomistic and continuum modelling of magnetism,” *Comput. Methods Appl. Mech. Eng.* **329**, 219–253.
- Postnikov, Andrei V, Jens Kortus, and Mark R. Pederson, 2006, “Density functional studies of molecular magnets,” *Phys. Status Solidi (b)* **243**, 2533–2572.
- Pourovskii, L. V., 2016, “Two-site fluctuations and multipolar intersite exchange interactions in strongly correlated systems,” *Phys. Rev. B* **94**, 115117.
- Pourovskii, L. V., J. Boust, R. Ballou, G. Gomez Eslava, and D. Givord, 2020, “Higher-order crystal field and rare-earth magnetism in rare-earth- Co_5 intermetallics,” *Phys. Rev. B* **101**, 214433.
- Pourovskii, Leonid V., and Sergii Khmelevskiy, 2019, “Quadrupolar superexchange interactions, multipolar order, and magnetic phase transition in UO_2 ,” *Phys. Rev. B* **99**, 094439.
- Pourovskii, Leonid V., and Sergii Khmelevskiy, 2021, “Hidden order and multipolar exchange striction in a correlated f -electron system,” *Proc. Natl. Acad. Sci. U.S.A.* **118**, e2025317118.
- Principi, Alessandro, and Mikhail I. Katsnelson, 2016, “Self-Induced Glassiness and Pattern Formation in Spin Systems Subject to Long-Range Interactions,” *Phys. Rev. Lett.* **117**, 137201.
- Rammer, J., and H. Smith, 1986, “Quantum field-theoretical methods in transport theory of metals,” *Rev. Mod. Phys.* **58**, 323–359.
- Ribeiro, M. S., G. B. Corrêa, A. Bergman, L. Nordström, O. Eriksson, and A. B. Klautau, 2011, “From collinear to vortex magnetic structures in Mn corrals on Pt(111),” *Phys. Rev. B* **83**, 014406.
- Ritschel, T., J. Trinckauf, K. Koepf, B. Büchner, M. v. Zimmermann, H. Berger, Y. I. Joe, P. Abbamonte, and J. Geck, 2015, “Orbital textures and charge density waves in transition metal dichalcogenides,” *Nat. Phys.* **11**, 328.
- Roger, M., J. H. Hetherington, and J. M. Delrieu, 1983, “Magnetism in solid ^3He ,” *Rev. Mod. Phys.* **55**, 1–64.
- Rohringer, G., and A. Toschi, 2016, “Impact of nonlocal correlations over different energy scales: A dynamical vertex approximation study,” *Phys. Rev. B* **94**, 125144.
- Rosengaard, N. M., and Börje Johansson, 1997, “Finite-temperature study of itinerant ferromagnetism in Fe, Co, and Ni,” *Phys. Rev. B* **55**, 14975–14986.

- Ruban, A. V., and I. A. Abrikosov, 2008, “Configurational thermodynamics of alloys from first principles: Effective cluster interactions,” *Rep. Prog. Phys.* **71**, 046501.
- Ruban, A. V., M. I. Katsnelson, W. Olovsson, S. I. Simak, and I. A. Abrikosov, 2005, “Origin of magnetic frustrations in Fe-Ni Invar alloys,” *Phys. Rev. B* **71**, 054402.
- Ruban, A. V., S. Khmelevskiy, P. Mohn, and B. Johansson, 2007, “Temperature-induced longitudinal spin fluctuations in Fe and Ni,” *Phys. Rev. B* **75**, 054402.
- Ruban, A. V., and V. I. Razumovskiy, 2012, “Spin-wave method for the total energy of paramagnetic state,” *Phys. Rev. B* **85**, 174407.
- Ruban, A. V., S. Shallcross, S. I. Simak, and H. L. Skriver, 2004, “Atomic and magnetic configurational energetics by the generalized perturbation method,” *Phys. Rev. B* **70**, 125115.
- Ruban, A. V., S. I. Simak, P. A. Korzhavyi, and H. L. Skriver, 2002, “Screened Coulomb interactions in metallic alloys. II. Screening beyond the single-site and atomic-sphere approximations,” *Phys. Rev. B* **66**, 024202.
- Rubtsov, A. N., M. I. Katsnelson, and A. I. Lichtenstein, 2008, “Dual fermion approach to nonlocal correlations in the Hubbard model,” *Phys. Rev. B* **77**, 033101.
- Rubtsov, A. N., M. I. Katsnelson, and A. I. Lichtenstein, 2012, “Dual boson approach to collective excitations in correlated fermionic systems,” *Ann. Phys. (Amsterdam)* **327**, 1320–1335.
- Rubtsov, A. N., M. I. Katsnelson, A. I. Lichtenstein, and A. Georges, 2009, “Dual fermion approach to the two-dimensional Hubbard model: Antiferromagnetic fluctuations and Fermi arcs,” *Phys. Rev. B* **79**, 045133.
- Rubtsov, A. N., V. V. Savkin, and A. I. Lichtenstein, 2005, “Continuous-time quantum Monte Carlo method for fermions,” *Phys. Rev. B* **72**, 035122.
- Rudenko, A. N., F. J. Keil, M. I. Katsnelson, and A. I. Lichtenstein, 2013, “Exchange interactions and frustrated magnetism in single-side hydrogenated and fluorinated graphene,” *Phys. Rev. B* **88**, 081405.
- Ruderman, M. A., and C. Kittel, 1954, “Indirect exchange coupling of nuclear magnetic moments by conduction electrons,” *Phys. Rev.* **96**, 99–102.
- Rüegg, Ch., B. Normand, M. Matsumoto, A. Furrer, D. F. McMorrow, K. W. Krämer, H. U. Güdel, S. N. Gvasaliya, H. Mutka, and M. Boehm, 2008, “Quantum Magnets under Pressure: Controlling Elementary Excitations in TiCuCl_3 ,” *Phys. Rev. Lett.* **100**, 205701.
- Ruelle, David, 1999, *Statistical Mechanics: Rigorous Results* (World Scientific, Singapore).
- Ruiz, Eliseo, Joan Cano, and Santiago Alvarez, 2005, “Density functional study of exchange coupling constants in single-molecule magnets: The Fe_8 complex,” *Chem. Eur. J.* **11**, 4767–4771.
- Runge, Erich, and E. K. U. Gross, 1984, “Density-Functional Theory for Time-Dependent Systems,” *Phys. Rev. Lett.* **52**, 997–1000.
- Rusz, J., L. Bergqvist, J. Kudrnovský, and I. Turek, 2006, “Exchange interactions and Curie temperatures in $\text{Ni}_{2-x}\text{MnSb}$ alloys: First-principles study,” *Phys. Rev. B* **73**, 214412.
- Rusz, J., I. Turek, and M. Diviš, 2005, “Random-phase approximation for critical temperatures of collinear magnets with multiple sublattices: GdX compounds ($X = \text{Mg}, \text{Rh}, \text{Ni}, \text{Pd}$),” *Phys. Rev. B* **71**, 174408.
- Sachdev, Subir, 2008, “Quantum magnetism and criticality,” *Nat. Phys.* **4**, 173–185.
- Sadhukhan, Banasree, Anders Bergman, Yaroslav O. Kvashnin, Johan Hellsvik, and Anna Delin, 2022, “Spin-lattice couplings in two-dimensional CrI_3 from first-principles computations,” *Phys. Rev. B* **105**, 104418.
- Sagawa, Masato, Setsuo Fujimura, Norio Togawa, Hitoshi Yamamoto, and Yutaka Matsuura, 1984, “New material for permanent magnets on a base of Nd and Fe,” *J. Appl. Phys.* **55**, 2083–2087.
- Sakuma, Akimasa, 1999, “First principles study on the exchange constants of the $3d$ transition metals,” *J. Phys. Soc. Jpn.* **68**, 620–624.
- Sakuma, Akimasa, 2000, “First-principles study on the non-collinear magnetic structures of disordered alloys,” *J. Phys. Soc. Jpn.* **69**, 3072–3083.
- Salpeter, E. E., and H. A. Bethe, 1951, “A relativistic equation for bound-state problems,” *Phys. Rev.* **84**, 1232–1242.
- Sandratskii, L. M., 1991, “Symmetry analysis of electronic states for crystals with spiral magnetic order. II. Connection with limiting cases,” *J. Phys. Condens. Matter* **3**, 8587–8596.
- Sandratskii, L. M., 1998, “Noncollinear magnetism in itinerant-electron systems: Theory and applications,” *Adv. Phys.* **47**, 91–160.
- Sandratskii, L. M., and P. Bruno, 2002, “Exchange interactions and Curie temperature in $(\text{Ga}, \text{Mn})\text{As}$,” *Phys. Rev. B* **66**, 134435.
- Sangiovanni, G., M. Capone, C. Castellani, and M. Grilli, 2005, “Electron-Phonon Interaction close to a Mott Transition,” *Phys. Rev. Lett.* **94**, 026401.
- Santini, Paolo, Stefano Carretta, Giuseppe Amoretti, Roberto Caciuffo, Nicola Magnani, and Gerard H. Lander, 2009, “Multipolar interactions in f -electron systems: The paradigm of actinide dioxides,” *Rev. Mod. Phys.* **81**, 807–863.
- Sanyal, B., L. Bergqvist, and O. Eriksson, 2003, “Ferromagnetic materials in the zinc-blende structure,” *Phys. Rev. B* **68**, 054417.
- Sato, K., *et al.*, 2010, “First-principles theory of dilute magnetic semiconductors,” *Rev. Mod. Phys.* **82**, 1633–1690.
- Sato, Masahiro, 2007, “Four-spin-exchange- and magnetic-field-induced chiral order in two-leg spin ladders,” *Phys. Rev. B* **76**, 054427.
- Savrasov, S. Y., 1998, “Linear Response Calculations of Spin Fluctuations,” *Phys. Rev. Lett.* **81**, 2570–2573.
- Sayad, Mohammad, and Michael Potthoff, 2015, “Spin dynamics and relaxation in the classical-spin Kondo-impurity model beyond the Landau-Lifschitz-Gilbert equation,” *New J. Phys.* **17**, 113058.
- Sayad, Mohammad, Roman Rausch, and Michael Potthoff, 2016, “Relaxation of a Classical Spin Coupled to a Strongly Correlated Electron System,” *Phys. Rev. Lett.* **117**, 127201.
- Scalmani, Giovanni, and Michael J. Frisch, 2012, “A new approach to noncollinear spin density functional theory beyond the local density approximation,” *J. Chem. Theory Comput.* **8**, 2193–2196.
- Schäfer, Thomas, *et al.*, 2021, “Tracking the Footprints of Spin Fluctuations: A MultiMethod, MultiMessenger Study of the Two-Dimensional Hubbard Model,” *Phys. Rev. X* **11**, 011058.
- Schapere, A., and F. Wilczek, 1989, *Geometric Phases in Physics* (World Scientific, Singapore).
- Scheurer, Mathias S, Shubhayu Chatterjee, Wei Wu, Michel Ferrero, Antoine Georges, and Subir Sachdev, 2018, “Topological order in the pseudogap metal,” *Proc. Natl. Acad. Sci. U.S.A.* **115**, E3665–E3672.
- Schiffer, P., A. P. Ramirez, W. Bao, and S.-W. Cheong, 1995, “Low Temperature Magnetoresistance and the Magnetic Phase Diagram of $\text{La}_{1-x}\text{Ca}_x\text{MnO}_3$,” *Phys. Rev. Lett.* **75**, 3336–3339.
- Schlenker, C., and M. Marezio, 1980, “The order-disorder transition of $\text{Ti}^{3+}\text{-Ti}^{3+}$ pairs in Ti_4O_7 and $(\text{Ti}_{1-x}\text{V}_x)_4\text{O}_7$,” *Philos. Mag.* **B 42**, 453–472.
- Schrieffer, J. R., 1999, *Theory of Superconductivity* (Avalon Publishing, New York).

- Schüler, M., M. Rösner, T. O. Wehling, A. I. Lichtenstein, and M. I. Katsnelson, 2013, “Optimal Hubbard Models for Materials with Nonlocal Coulomb Interactions: Graphene, Silicene, and Benzene,” *Phys. Rev. Lett.* **111**, 036601.
- Schulz, H. J., 1990, “Effective Action for Strongly Correlated Fermions from Functional Integrals,” *Phys. Rev. Lett.* **65**, 2462–2465.
- Schuwalow, Sergej, Daniel Grieger, and Frank Lechermann, 2010, “Realistic modeling of the electronic structure and the effect of correlations for Sn/Si(111) and Sn/Ge(111) surfaces,” *Phys. Rev. B* **82**, 035116.
- Secchi, A., S. Brener, A. I. Lichtenstein, and M. I. Katsnelson, 2013, “Non-equilibrium magnetic interactions in strongly correlated systems,” *Ann. Phys. (Amsterdam)* **333**, 221–271.
- Secchi, A., A. I. Lichtenstein, and M. I. Katsnelson, 2016a, “Non-equilibrium itinerant-electron magnetism: A time-dependent mean-field theory,” *Phys. Rev. B* **94**, 085153.
- Secchi, A., A. I. Lichtenstein, and M. I. Katsnelson, 2016b, “Spin and orbital exchange interactions from dynamical mean field theory,” *J. Magn. Magn. Mater.* **400**, 112.
- Shallcross, S., A. E. Kissavos, V. Meded, and A. V. Ruban, 2005, “An *ab initio* effective Hamiltonian for magnetism including longitudinal spin fluctuations,” *Phys. Rev. B* **72**, 104437.
- Sharma, S., J. K. Dewhurst, C. Ambrosch-Draxl, S. Kurth, N. Helbig, S. Pittalis, S. Shallcross, L. Nordström, and E. K. U. Gross, 2007, “First-Principles Approach to Noncollinear Magnetism: Towards Spin Dynamics,” *Phys. Rev. Lett.* **98**, 196405.
- Sharma, S., E. K. U. Gross, A. Sanna, and J. K. Dewhurst, 2018, “Source-free exchange-correlation magnetic fields in density functional theory,” *J. Chem. Theory Comput.* **14**, 1247–1253.
- Shirane, G., V. J. Minkiewicz, and R. Nathans, 1968, “Spin waves in 3d metals,” *J. Appl. Phys.* **39**, 383–390.
- Shirinyan, Albert A., Valerii K. Kozin, Johan Hellsvik, Manuel Pereiro, Olle Eriksson, and Dmitry Yudin, 2019, “Self-organizing maps as a method for detecting phase transitions and phase identification,” *Phys. Rev. B* **99**, 041108.
- Simon, E., J. Gy. Vida, S. Khmelevskiy, and L. Szunyogh, 2015, “Magnetism of ordered and disordered Ni₂MnAl full Heusler compounds,” *Phys. Rev. B* **92**, 054438.
- Simon, E., L. Rózsa, K. Palotás, and L. Szunyogh, 2018, “Magnetism of a Co monolayer on Pt(111) capped by overlayers of 5d elements: A spin-model study,” *Phys. Rev. B* **97**, 134405.
- Singer, R., F. Dietermann, and M. Fähnle, 2011, “Spin Interactions in bcc and fcc Fe beyond the Heisenberg Model,” *Phys. Rev. Lett.* **107**, 017204.
- Singer, R., M. Fähnle, and G. Bihlmayer, 2005, “Constrained spin-density functional theory for excited magnetic configurations in an adiabatic approximation,” *Phys. Rev. B* **71**, 214435.
- Singh, N., P. Elliott, T. Nautiyal, J. K. Dewhurst, and S. Sharma, 2019, “Adiabatic generalized gradient approximation kernel in time-dependent density functional theory,” *Phys. Rev. B* **99**, 035151.
- Sivadas, Nikhil, Satoshi Okamoto, Xiaodong Xu, Craig J. Fennie, and Di Xiao, 2018, “Stacking-dependent magnetism in bilayer CrI₃,” *Nano Lett.* **18**, 7658–7664.
- Skomski, R., and J. M. D. Coey, 1999, *Permanent Magnetism* (CRC Press, Boca Raton).
- Skomski, Ralph, 2021, in *Handbook of Magnetism and Magnetic Materials*, edited by J. M. D. Coey and Stuart S. P. Parkin (Springer International Publishing, Cham, Switzerland).
- Skomski, Ralph, and J. M. D. Coey, 1993, “Giant energy product in nanostructured two-phase magnets,” *Phys. Rev. B* **48**, 15812–15816.
- Slater, J. C., 1951, “Magnetic effects and the Hartree-Fock equation,” *Phys. Rev.* **82**, 538–541.
- Slezák, J., P. Mutombo, and V. Cháb, 1999, “STM study of a Pb/Si(111) interface at room and low temperatures,” *Phys. Rev. B* **60**, 13328–13330.
- Snowball, Ian, Lovisa Zillén, and Per Sandgren, 2002, “Bacterial magnetite in Swedish varved lake-sediments: A potential biomarker of environmental change,” *Quat. Int.* **88**, 13–19.
- Söderlind, P., A. Landa, I. L. M. Locht, D. Åberg, Y. Kvashnin, M. Pereiro, M. Däne, P. E. A. Turchi, V. P. Antropov, and O. Eriksson, 2017, “Prediction of the new efficient permanent magnet SmCoNiFe₃,” *Phys. Rev. B* **96**, 100404.
- Solovyev, I. V., 2002, “Electronic structure and stability of the ferromagnetic ordering in double perovskites,” *Phys. Rev. B* **65**, 144446.
- Solovyev, I. V., 2006, “Lattice distortion and magnetism of 3d – t_{2g} perovskite oxides,” *Phys. Rev. B* **74**, 054412.
- Solovyev, I. V., 2021, “Exchange interactions and magnetic force theorem,” *Phys. Rev. B* **103**, 104428.
- Solovyev, I. V., P. H. Dederichs, and I. Mertig, 1995, “Origin of orbital magnetization and magnetocrystalline anisotropy in TX ordered alloys (where T = Fe, Co and X = Pd, Pt),” *Phys. Rev. B* **52**, 13419–13428.
- Solovyev, I. V., I. V. Kashin, and V. V. Mazurenko, 2015, “Mechanisms and origins of half-metallic ferromagnetism in CrO₂,” *Phys. Rev. B* **92**, 144407.
- Solovyev, I. V., and K. Terakura, 1998, “Effective single-particle potentials for MnO in light of interatomic magnetic interactions: Existing theories and perspectives,” *Phys. Rev. B* **58**, 15496–15507.
- Solovyev, I. V., and K. Terakura, 1999a, “Magnetic Spin Origin of the Charge-Ordered Phase in Manganites,” *Phys. Rev. Lett.* **83**, 2825–2828.
- Solovyev, I. V., and K. Terakura, 1999b, “Zone Boundary Softening of the Spin-Wave Dispersion in Doped Ferromagnetic Manganites,” *Phys. Rev. Lett.* **82**, 2959–2962.
- Solovyev, Igor, 2009, “Long-range magnetic interactions induced by the lattice distortions and the origin of the E-type antiferromagnetic phase in the undoped orthorhombic manganites,” *J. Phys. Soc. Jpn.* **78**, 054710.
- Solovyev, Igor, Noriaki Hamada, and Kiyoyuki Terakura, 1996a, “Crucial Role of the Lattice Distortion in the Magnetism of LaMnO₃,” *Phys. Rev. Lett.* **76**, 4825–4828.
- Solovyev, Igor, Noriaki Hamada, and Kiyoyuki Terakura, 1996b, “t_{2g} versus all 3d localization in LaMO₃ perovskites (M = Ti – Cu): First-principles study,” *Phys. Rev. B* **53**, 7158–7170.
- Song, Tiancheng, *et al.*, 2019, “Switching 2D magnetic states via pressure tuning of layer stacking,” *Nat. Mater.* **18**, 1298–1302.
- Soriano, D., A. N. Rudenko, M. I. Katsnelson, and M. Rösner, 2021, “Environmental screening and ligand-field effects to magnetism in CrI₃ monolayer,” *npj Comput. Mater.* **7**, 162.
- Sotnikov, O. M., V. V. Mazurenko, J. Colbois, F. Mila, M. I. Katsnelson, and E. A. Stepanov, 2021, “Probing the topology of the quantum analog of a classical skyrmion,” *Phys. Rev. B* **103**, L060404.
- Souliou, Sofia-Michaela, Jiří Chaloupka, Giniyat Khaliullin, Gihun Ryu, Anil Jain, B. J. Kim, Matthieu Le Tacon, and Bernhard Keimer, 2017, “Raman Scattering from Higgs Mode Oscillations in the Two-Dimensional Antiferromagnet Ca₂RuO₄,” *Phys. Rev. Lett.* **119**, 067201.
- Soven, Paul, 1967, “Coherent-potential model of substitutional disordered alloys,” *Phys. Rev.* **156**, 809–813.

- Spalek, J., 2007, “*t*-*J* model then and now: A personal perspective from the pioneering times,” *Acta Phys. Pol. A* **111**, 409–424.
- Spišák, D., and J. Hafner, 1997, “Theory of bilinear and biquadratic exchange interactions in iron: Bulk and surface,” *J. Magn. Magn. Mater.* **168**, 257–268.
- Staub, U., M. Shi, C. Schulze-Briese, B. D. Patterson, F. Fauth, E. Dooryhee, L. Soderholm, J. O. Cross, D. Mannix, and A. Ochiai, 2005, “Temperature dependence of the crystal structure and charge ordering in Yb_4As_3 ,” *Phys. Rev. B* **71**, 075115.
- Staunton, J., B. L. Gyorffy, A. J. Pindor, G. M. Stocks, and H. Winter, 1984, “The ‘disordered local moment’ picture of itinerant magnetism at finite temperatures,” *J. Magn. Magn. Mater.* **45**, 15–22.
- Staunton, J., B. L. Gyorffy, A. J. Pindor, G. M. Stocks, and H. Winter, 1985, “Electronic structure of metallic ferromagnets above the Curie temperature,” *J. Phys. F* **15**, 1387–1404.
- Staunton, J., B. L. Gyorffy, G. M. Stocks, and J. Wadsworth, 1986, “The static, paramagnetic, spin susceptibility of metals at finite temperatures,” *J. Phys. F* **16**, 1761–1788.
- Staunton, J. B., and B. L. Gyorffy, 1992, “Onsager Cavity Fields in Itinerant-Electron Paramagnets,” *Phys. Rev. Lett.* **69**, 371–374.
- Staunton, J. B., L. Szunyogh, A. Buruzs, B. L. Gyorffy, S. Ostanin, and L. Udvardi, 2006, “Temperature dependence of magnetic anisotropy: An *ab initio* approach,” *Phys. Rev. B* **74**, 144411.
- Steenbock, Torben, Jos Tasche, Alexander I. Lichtenstein, and Carmen Herrmann, 2015, “A Green’s-function approach to exchange spin coupling as a new tool for quantum chemistry,” *J. Chem. Theory Comput.* **11**, 5651–5664.
- Stefanucci, Gianluca, and Robert van Leeuwen, 2013, *Nonequilibrium Many-Body Theory of Quantum Systems: A Modern Introduction* (Cambridge University Press, Cambridge, England).
- Stepanov, E. A., S. Brener, V. Harkov, M. I. Katsnelson, and A. I. Lichtenstein, 2022, “Spin dynamics of itinerant electrons: Local magnetic moment formation and Berry phase,” *Phys. Rev. B* **105**, 155151.
- Stepanov, E. A., S. Brener, F. Krien, M. Harland, A. I. Lichtenstein, and M. I. Katsnelson, 2018, “Effective Heisenberg Model and Exchange Interaction for Strongly Correlated Systems,” *Phys. Rev. Lett.* **121**, 037204.
- Stepanov, E. A., C. Dutreix, and M. I. Katsnelson, 2017, “Dynamical and Reversible Control of Topological Spin Textures,” *Phys. Rev. Lett.* **118**, 157201.
- Stepanov, E. A., V. Harkov, and A. I. Lichtenstein, 2019, “Consistent partial bosonization of the extended Hubbard model,” *Phys. Rev. B* **100**, 205115.
- Stepanov, E. A., V. Harkov, M. Rösner, A. I. Lichtenstein, M. I. Katsnelson, and A. N. Rudenko, 2022, “Coexisting charge density wave and ferromagnetic instabilities in monolayer InSe,” *npj Comput. Mater.* **8**, 118.
- Stepanov, E. A., A. Huber, A. I. Lichtenstein, and M. I. Katsnelson, 2019, “Effective Ising model for correlated systems with charge ordering,” *Phys. Rev. B* **99**, 115124.
- Stepanov, E. A., A. Huber, E. G. C. P. van Loon, A. I. Lichtenstein, and M. I. Katsnelson, 2016, “From local to nonlocal correlations: The dual boson perspective,” *Phys. Rev. B* **94**, 205110.
- Stepanov, E. A., S. A. Nikolaev, C. Dutreix, M. I. Katsnelson, and V. V. Mazurenko, 2019, “Heisenberg-exchange-free nanoskyrmion mosaic,” *J. Phys. Condens. Matter* **31**, 17LT01.
- Stepanov, E. A., E. G. C. P. van Loon, A. A. Katanin, A. I. Lichtenstein, M. I. Katsnelson, and A. N. Rubtsov, 2016, “Self-consistent dual boson approach to single-particle and collective excitations in correlated systems,” *Phys. Rev. B* **93**, 045107.
- Stöhr, J., and H. C. Siegmann, 2006, *Magnetism: From Fundamentals to Nanoscale Dynamics*, Springer Series in Solid-State Sciences Vol. 152 (Springer, New York).
- Stratonovich, R. L., 1957, “On a method of calculating quantum distribution functions,” *Sov. Phys. Dokl.*, **2**, 416, <https://ui.adsabs.harvard.edu/abs/1957SPhD...2..416S/abstract>.
- Streib, Simon, Ramon Cardias, Manuel Pereiro, Anders Bergman, Erik Sjöqvist, Cyrille Barreateau, Anna Delin, Olle Eriksson, and Danny Thonig, 2022, “Adiabatic spin dynamics and effective exchange interactions from constrained tight-binding electronic structure theory: Beyond the Heisenberg regime,” *Phys. Rev. B* **105**, 224408.
- Streib, Simon, Attila Szilva, Vladislav Borisov, Manuel Pereiro, Anders Bergman, Erik Sjöqvist, Anna Delin, Mikhail I. Katsnelson, Olle Eriksson, and Danny Thonig, 2021, “Exchange constants for local spin Hamiltonians from tight-binding models,” *Phys. Rev. B* **103**, 224413.
- Stringfellow, M. W., 1968, “Observation of spin-wave renormalization effects in iron and nickel,” *J. Phys. C* **1**, 950–965.
- Subkhangulov, R. R., A. B. Henriques, P. H. O. Rappl, E. Abramof, Th. Rasing, and A. V. Kimel, 2014, “All-optical manipulation and probing of the *d*-*f* exchange interaction in EuTe ,” *Sci. Rep.* **4**, 4368.
- Szczeczek, Yolande H., Michael A. Tusch, and David E. Logan, 1998, “Spin interactions in an Anderson-Hubbard model,” *J. Phys. Condens. Matter* **10**, 639–655.
- Szilva, A., M. Costa, A. Bergman, L. Szunyogh, L. Nordström, and O. Eriksson, 2013, “Interatomic Exchange Interactions for Finite-Temperature Magnetism and Nonequilibrium Spin Dynamics,” *Phys. Rev. Lett.* **111**, 127204.
- Szilva, A., *et al.*, 2017, “Theory of noncollinear interactions beyond Heisenberg exchange: Applications to bcc Fe,” *Phys. Rev. B* **96**, 144413.
- Tegus, O., E. Brück, K. H. J. Buschow, and F. R. De Boer, 2002, “Transition-metal-based magnetic refrigerants for room-temperature applications,” *Nature (London)* **415**, 150–152.
- Temmerman, W. M., A. Svane, L. Petit, M. Lüders, P. Strange, and Z. Szotek, 2007, “Pressure induced valence transitions in *f*-electron systems,” *Phase Transitions* **80**, 415–443.
- Temmerman, W. M., Z. Szotek, and H. Winter, 1993, “Band-structure method for 4*f* electrons in elemental Pr metal,” *Phys. Rev. B* **47**, 1184–1189.
- Terletska, H., T. Chen, and E. Gull, 2017, “Charge ordering and correlation effects in the extended Hubbard model,” *Phys. Rev. B* **95**, 115149.
- Terletska, Hanna, Tianran Chen, Joseph Paki, and Emanuel Gull, 2018, “Charge ordering and nonlocal correlations in the doped extended Hubbard model,” *Phys. Rev. B* **97**, 115117.
- Thiele, M., E. K. U. Gross, and S. Kümmel, 2008, “Adiabatic Approximation in Nonperturbative Time-Dependent Density-Functional Theory,” *Phys. Rev. Lett.* **100**, 153004.
- Thoene, Jan, Stanislav Chadov, Gerhard Fecher, Claudia Felser, and Jürgen Kübler, 2009, “Exchange energies, Curie temperatures and magnons in Heusler compounds,” *J. Phys. D* **42**, 084013.
- Thomson, Alex, and Subir Sachdev, 2018, “Fermionic Spinon Theory of Square Lattice Spin Liquids near the Néel State,” *Phys. Rev. X* **8**, 011012.
- Turner, Stefan, Rudolf Hanel, and Peter Klimek, 2018, *Introduction to the Theory of Complex Systems* (Oxford University Press, New York).
- Tiablukov, S. V., 2013, *Methods in the Quantum Theory of Magnetism* (Springer, New York).

- Tie-song, Zhao, Jin Han-min, Guo Guang-hua, Han Xiu-feng, and Chen Hong, 1991, "Magnetic properties of R ions in RCO_5 compounds ($R = \text{Pr, Nd, Sm, Gd, Tb, Dy, Ho, and Er}$)," *Phys. Rev. B* **43**, 8593–8598.
- Toschi, A., R. Arita, P. Hansmann, G. Sangiovanni, and K. Held, 2012, "Quantum dynamical screening of the local magnetic moment in Fe-based superconductors," *Phys. Rev. B* **86**, 064411.
- Toth, S., and B. Lake, 2015, "Linear spin wave theory for single- Q incommensurate magnetic structures," *J. Phys. Condens. Matter* **27**, 166002.
- Treglia, G., F. Ducastelle, and F. Gautier, 1978, "Generalised perturbation theory in disordered transition metal alloys: Application to the self-consistent calculation of ordering energies," *J. Phys. F* **8**, 1437–1456.
- Tresca, C., *et al.*, 2018, "Chiral Spin Texture in the Charge-Density-Wave Phase of the Correlated Metallic Pb/Si(111) Monolayer," *Phys. Rev. Lett.* **120**, 196402.
- Tresca, Cesare, and Matteo Calandra, 2021, "Charge density wave in single-layer Pb/Ge(111) driven by Pb-substrate exchange interaction," *Phys. Rev. B* **104**, 045126.
- Tsubokawa, Ichiro., 1960, "On the magnetic properties of a CrBr₃ single crystal," *J. Phys. Soc. Jpn.* **15**, 1664–1668.
- Turek, I., J. Kudrnovský, G. Bihlmayer, and S. Blügel, 2003, "Ab initio theory of exchange interactions and the Curie temperature of bulk Gd," *J. Phys. Condens. Matter* **15**, 2771–2782.
- Turek, I., J. Kudrnovský, M. Diviš, P. Franek, G. Bihlmayer, and S. Blügel, 2003, "First-principles study of the electronic structure and exchange interactions in bcc europium," *Phys. Rev. B* **68**, 224431.
- Turek, I., J. Kudrnovský, V. Drchal, and P. Bruno, 2006, "Exchange interactions, spin waves, and transition temperatures in itinerant magnets," *Philos. Mag.* **86**, 1713–1752.
- Turek, I., J. Kudrnovský, V. Drchal, P. Bruno, and S. Blügel, 2003, "Ab initio theory of exchange interactions in itinerant magnets," *Phys. Status Solidi (b)* **236**, 318–324.
- Turzhenskii, S., A. I. Liechtenstein, and M. I. Katsnelson, 1990, "Degree of localization of magnetic moments and the non-Heisenberg nature of exchange interactions in metals and alloys," *Sov. Phys. Solid State* **32**, 1138–1142, <https://www.mathnet.ru/eng/ftt/v32/i7/p1952>.
- Udvardi, L., and L. Szunyogh, 2009, "Chiral Asymmetry of the Spin-Wave Spectra in Ultrathin Magnetic Films," *Phys. Rev. Lett.* **102**, 207204.
- Udvardi, L., L. Szunyogh, K. Palotás, and P. Weinberger, 2003, "First-principles relativistic study of spin waves in thin magnetic films," *Phys. Rev. B* **68**, 104436.
- Ugeda, M. M., *et al.*, 2016, "Characterization of collective ground states in single-layer NbSe₂," *Nat. Phys.* **12**, 92.
- Ullrich, Carsten A., 2018, "Density-functional theory for systems with noncollinear spin: Orbital-dependent exchange-correlation functionals and their application to the Hubbard dimer," *Phys. Rev. B* **98**, 035140.
- Upton, M. H., T. Miller, and T.-C. Chiang, 2005, "Unusual band dispersion in Pb films on Si(111)," *Phys. Rev. B* **71**, 033403.
- Valmispild, V. N., C. Dutreix, M. Eckstein, M. I. Katsnelson, A. I. Lichtenstein, and E. A. Stepanov, 2020, "Dynamically induced doublon repulsion in the Fermi-Hubbard model probed by a single-particle density of states," *Phys. Rev. B* **102**, 220301.
- Vandelli, M., V. Harkov, E. A. Stepanov, J. Gukelberger, E. Kozik, A. Rubio, and A. I. Lichtenstein, 2020, "Dual boson diagrammatic Monte Carlo approach applied to the extended Hubbard model," *Phys. Rev. B* **102**, 195109.
- Vandelli, Matteo, Anna Galler, Angel Rubio, Alexander I. Lichtenstein, Silke Biermann, and Evgeny A. Stepanov, 2023, "Doping-dependent charge- and spin-density wave orderings in a monolayer of Pb adatoms on Si(111)," [arXiv:2301.07162](https://arxiv.org/abs/2301.07162).
- Vandelli, Matteo, Josef Kaufmann, Mohammed El-Nabulsi, Viktor Harkov, Alexander I. Lichtenstein, and Evgeny A. Stepanov, 2022, "Multi-band D-TRILEX approach to materials with strong electronic correlations," *SciPost Phys.* **13**, 036.
- van Loon, E. G. C. P., M. Schüler, M. I. Katsnelson, and T. O. Wehling, 2016, "Capturing nonlocal interaction effects in the Hubbard model: Optimal mappings and limits of applicability," *Phys. Rev. B* **94**, 165141.
- van Loon, Erik G. C. P., Alexander I. Lichtenstein, Mikhail I. Katsnelson, Olivier Parcollet, and Hartmut Hafermann, 2014, "Beyond extended dynamical mean-field theory: Dual boson approach to the two-dimensional extended Hubbard model," *Phys. Rev. B* **90**, 235135.
- van Loon, Erik G. C. P., Malte Rösner, Mikhail I. Katsnelson, and Tim O. Wehling, 2021, "Random phase approximation for gapped systems: Role of vertex corrections and applicability of the constrained random phase approximation," *Phys. Rev. B* **104**, 045134.
- van Loon, Erik G. C. P., Malte Rösner, Gunnar Schönhoff, Mikhail I. Katsnelson, and Tim O. Wehling, 2018, "Competing Coulomb and electron-phonon interactions in NbS₂," *npj Quantum Mater.* **3**, 1–8.
- van Schilfgaarde, M., and V. P. Antropov, 1999, "First-principles exchange interactions in Fe, Ni, and Co," *J. Appl. Phys.* **85**, 4827–4829.
- van Schilfgaarde, Mark, I. A. Abrikosov, and B. Johansson, 1999, "Origin of the Invar effect in iron-nickel alloys," *Nature (London)* **400**, 46–49.
- Vaz, C. A. F., J. A. C. Bland, and G. Lauhoff, 2008, "Magnetism in ultrathin film structures," *Rep. Prog. Phys.* **71**, 056501.
- Verlhac, B., *et al.*, 2022, "Thermally induced magnetic order from glassiness in elemental neodymium," *Nat. Phys.* **18**, 905–911.
- Verschuur, Gerrit L., 1996, *Hidden Attraction: The History and Mystery of Magnetism* (Oxford University Press, New York).
- Verwey, E. J. W., and P. W. Haayman, 1941, "Electronic conductivity and transition point of magnetite Fe₃O₄," *Physica (Amsterdam)* **8**, 979–987.
- Verwey, E. J. W., P. W. Haayman, and F. C. Romeijn, 1947, "Physical properties and cation arrangement of oxides with spinel structures II. Electronic conductivity," *J. Chem. Phys.* **15**, 181–187.
- Vida, Gy. J., E. Simon, L. Rózsa, K. Palotás, and L. Szunyogh, 2016, "Domain-wall profiles in Co/Ir_n/Pt(111) ultrathin films: Influence of the Dzyaloshinskii-Moriya interaction," *Phys. Rev. B* **94**, 214422.
- Vishina, Alena, Olle Eriksson, Olga Yu. Vekilova, Anders Bergman, and Heike C. Herper, 2021, "Ab-initio study of the electronic structure and magnetic properties of Ce₂Fe₁₇," *J. Alloys Compd.* **888**, 161521.
- Vollmer, R., M. Etzkorn, P. S. Anil Kumar, H. Ibach, and J. Kirschner, 2003, "Spin-Polarized Electron Energy Loss Spectroscopy of High Energy, Large Wave Vector Spin Waves in Ultrathin fcc Co Films on Cu(001)," *Phys. Rev. Lett.* **91**, 147201.
- Vollmer, R., M. Etzkorn, P. S. Anil Kumar, H. Ibach, and J. Kirschner, 2004, "Spin-wave excitation in ultrathin Co and Fe films on Cu(001) by spin-polarized electron energy loss spectroscopy," *J. Appl. Phys.* **95**, 7435–7440.
- Vonsovskii, S. V., 1974, *Magnetism*, Vol. 2 (John Wiley & Sons, New York).
- Vonsovsky, S. V., Yu. A. Izyumov, and E. Z. Kurmaev, 1982, *Superconductivity of Transition Metals, Their Alloys and Compounds* (Springer-Verlag, Berlin).
- Wachter, P., 1980, "Physics of Eu₃S₄ and Sm₃S₄," *Philos. Mag.* **B 42**, 497–498.

- Wan, Xiangang, Jinming Dong, and Sergej Y. Savrasov, 2011, “Mechanism of magnetic exchange interactions in europium monochalcogenides,” *Phys. Rev. B* **83**, 205201.
- Wan, Xiangang, Quan Yin, and Sergej Y. Savrasov, 2006, “Calculation of Magnetic Exchange Interactions in Mott-Hubbard Systems,” *Phys. Rev. Lett.* **97**, 266403.
- Wang, C. S., R. E. Prange, and V. Korenman, 1982, “Magnetism in iron and nickel,” *Phys. Rev. B* **25**, 5766–5777.
- Wang, Duo, and Biplab Sanyal, 2021, “Systematic study of monolayer to trilayer CrI₃: Stacking sequence dependence of electronic structure and magnetism,” *J. Phys. Chem. C* **125**, 18467–18473.
- Wang, Kangying, Sergey Nikolaev, Wei Ren, and Igor Solovyev, 2019, “Giant contribution of the ligand states to the magnetic properties of the Cr₂Ge₂Te₆ monolayer,” *Phys. Chem. Chem. Phys.* **21**, 9597–9604.
- Watzenböck, C., M. Edelmann, D. Springer, G. Sangiovanni, and A. Toschi, 2020, “Characteristic Timescales of the Local Moment Dynamics in Hund’s Metals,” *Phys. Rev. Lett.* **125**, 086402.
- Webster, Lucas, and Jia-An Yan, 2018, “Strain-tunable magnetic anisotropy in monolayer CrCl₃, CrBr₃, and CrI₃,” *Phys. Rev. B* **98**, 144411.
- Weng, Z. Y., C. S. Ting, and T. K. Lee, 1991, “Path-integral approach to the Hubbard model,” *Phys. Rev. B* **43**, 3790–3793.
- Werner, Philipp, Armin Comanac, Luca de’ Medici, Matthias Troyer, and Andrew J. Millis, 2006, “Continuous-Time Solver for Quantum Impurity Models,” *Phys. Rev. Lett.* **97**, 076405.
- Werner, Philipp, and Andrew J. Millis, 2007, “Efficient Dynamical Mean Field Simulation of the Holstein-Hubbard Model,” *Phys. Rev. Lett.* **99**, 146404.
- Werner, Philipp, and Andrew J. Millis, 2010, “Dynamical Screening in Correlated Electron Materials,” *Phys. Rev. Lett.* **104**, 146401.
- White, Robert M., and Bradford Bayne, 1983, *Quantum Theory of Magnetism*, Vol. 1 (Springer, New York).
- Wiltschko, Wolfgang, Ursula Munro, Hugh Ford, and Roswitha Wiltschko, 2006, “Bird navigation: What type of information does the magnetite-based receptor provide?,” *Proc. R. Soc. B* **273**, 2815–2820.
- Wolf, S. A., D. D. Awschalom, R. A. Buhrman, J. M. Daughton, S. von Molnár, M. L. Roukes, A. Y. Chtchelkanova, and D. M. Treger, 2001, “Spintronics: A spin-based electronics vision for the future,” *Science* **294**, 1488–1495.
- Wolf, Yuri I., Mikhail I. Katsnelson, and Eugene V. Koonin, 2018, “Physical foundations of biological complexity,” *Proc. Natl. Acad. Sci. U.S.A.* **115**, E8678–E8687.
- Wollmann, Lukas, Stanislav Chadov, Jürgen Kübler, and Claudia Felser, 2014, “Magnetism in cubic manganese-rich Heusler compounds,” *Phys. Rev. B* **90**, 214420.
- Wu, Wei, Mathias S. Scheurer, Shubhayu Chatterjee, Subir Sachdev, Antoine Georges, and Michel Ferrero, 2018, “Pseudogap and Fermi-Surface Topology in the Two-Dimensional Hubbard Model,” *Phys. Rev. X* **8**, 021048.
- Wu, Wei, and A.-M. S. Tremblay, 2014, “Phase diagram and Fermi liquid properties of the extended Hubbard model on the honeycomb lattice,” *Phys. Rev. B* **89**, 205128.
- Wysocki, A. L., J. K. Glasbrenner, and K. D. Belashchenko, 2008, “Thermodynamics of itinerant magnets in a classical spin-fluctuation model,” *Phys. Rev. B* **78**, 184419.
- Wysocki, Aleksander L., Kirill D. Belashchenko, and Vladimir P. Antropov, 2011, “Consistent model of magnetism in ferropnictides,” *Nat. Phys.* **7**, 485–489.
- Yang, Hongxin, Jinghua Liang, and Qirui Cui, 2023, “First-principles calculations for Dzyaloshinskii-Moriya interaction,” *Nat. Rev. Phys.* **5**, 43–61.
- Yildirim, T., A. B. Harris, Amnon Aharony, and O. Entin-Wohlman, 1995, “Anisotropic spin Hamiltonians due to spin-orbit and Coulomb exchange interactions,” *Phys. Rev. B* **52**, 10239–10267.
- Ying, T., K. P. Schmidt, and S. Wessel, 2019, “Higgs Mode of Planar Coupled Spin Ladders and Its Observation in C₉H₁₈N₂CuBr₄,” *Phys. Rev. Lett.* **122**, 127201.
- Yoon, Hongkee, Seung Woo Jang, Jae-Hoon Sim, Takao Kotani, and Myung Joon Han, 2019, “Magnetic force theory combined with quasi-particle self-consistent GW method,” *J. Phys. Condens. Matter* **31**, 405503.
- Yoon, Hongkee, Taek Jung Kim, Jae-Hoon Sim, and Myung Joon Han, 2020, “Jx: An open-source software for calculating magnetic interactions based on magnetic force theory,” *Comput. Phys. Commun.* **247**, 106927.
- Yoon, Hongkee, Taek Jung Kim, Jae-Hoon Sim, Seung Woo Jang, Taisuke Ozaki, and Myung Joon Han, 2018, “Reliability and applicability of magnetic-force linear response theory: Numerical parameters, predictability, and orbital resolution,” *Phys. Rev. B* **97**, 125132.
- Yosida, K., 1996, *Theory of Magnetism* (Springer-Verlag, Berlin).
- You, M. V., V. Heine, A. J. Holden, and P. J. Lin-Chung, 1980, “Magnetism in Iron at High Temperatures,” *Phys. Rev. Lett.* **44**, 1282–1284.
- Zabala-Lekuona, Andoni, José Manuel Seco, and Enrique Colacio, 2021, “Single-molecule magnets: From Mn12-ac to dysprosium metallocenes, a travel in time,” *Coord. Chem. Rev.* **441**, 213984.
- Zakeri, Kh., T.-H. Chuang, A. Ernst, L. M. Sandratskii, P. Buczek, H. J. Qin, Y. Zhang, and J. Kirschner, 2013, “Direct probing of the exchange interaction at buried interfaces,” *Nat. Nanotechnol.* **8**, 853–858.
- Zakeri, Kh., Y. Zhang, J. Prokop, T.-H. Chuang, N. Sakr, W. X. Tang, and J. Kirschner, 2010, “Asymmetric Spin-Wave Dispersion on Fe(110): Direct Evidence of the Dzyaloshinskii-Moriya Interaction,” *Phys. Rev. Lett.* **104**, 137203.
- Zakeri, Khalil, Huajun Qin, and Arthur Ernst, 2021, “Unconventional magnonic surface and interface states in layered ferromagnets,” *Commun. Phys.* **4**, 18.
- Zein, N. E., 1984, “Density functional calculations of crystal elastic moduli and phonon spectra,” *Fiz. Tverd. Tela (Leningrad)* **26**, 3028–3034 [*Sov. Phys. Solid State* **26**, 1825 (1984)], <https://www.mathnet.ru/eng/ftt/v26/i10/p3028>.
- Zener, Clarence, 1951, “Interaction between the *d*-shells in the transition metals. II. Ferromagnetic compounds of manganese with perovskite structure,” *Phys. Rev.* **82**, 403–405.
- Zhang, Li-chuan, Dongwook Go, Jan-Philipp Hanke, Patrick M. Buhl, Sergii Grytsiuk, Stefan Blügel, Fabian R. Lux, and Yuriy Mokrousov, 2020, “Imprinting and driving electronic orbital magnetism using magnons,” *Commun. Phys.* **3**, 1–8.
- Zhang, Tong, *et al.*, 2010, “Superconductivity in one-atomic-layer metal films grown on Si(111),” *Nat. Phys.* **6**, 104–108.
- Zheng, Fawei, and Ping Zhang, 2021, “MagGene: A genetic evolution program for magnetic structure prediction,” *Comput. Phys. Commun.* **259**, 107659.
- Zhu, Xiangzhou, Alexander Edström, and Claude Ederer, 2020, “Magnetic exchange interactions in SrMnO₃,” *Phys. Rev. B* **101**, 064410.
- Zimmermann, Bernd, Gustav Bihlmayer, Marie Böttcher, Mohammed Bouhassoune, Samir Lounis, Jairo Sinova, Stefan Heinze, Stefan Blügel, and Bertrand Dupé, 2019, “Comparison of first-principles methods to extract magnetic parameters in ultrathin films: Co/Pt(111),” *Phys. Rev. B* **99**, 214426.